Biosynthesis and biological relevance of herbivore-induced nitrogenous defense compounds in maize

Dissertation

To Fulfill the

Requirements for the Degree of

„doctor rerum naturalium" (Dr. rer. nat.)

Submitted to the Council of the Faculty

of Biology and Pharmacy

of the Friedrich Schiller University Jena

by Diplom-Biochemiker Vinzenz Handrick

born on November 10, 1985 in Bautzen

Reviewers

1. **Prof. Dr. Jonathan Gershenzon**
   MAX-PLANCK-INSTITUT FOR CHEMICAL ECOLOGY, JENA,
   BIOCHEMISTRY DEPARTMENT

2. **Prof. Dr. Günter Theißen**
   FRIEDRICH-SCHILLER-UNIVERSITÄT JENA, DEPARTMENT OF
   GENETICS

3. **Dr. Monika Frey**
   TECHNISCHE UNIVERSITÄT MÜNCHEN, DEPARTMENT OF
   GENETICS

Date of public defense: **December 21, 2016**

Table of Contents

1 Introduction

1.1 Natural product formation in plants

Plants are the nutritional basis for a large number of living organisms including vertebrates, invertebrates, fungi and bacteria. Plants are therefore continuously subjected to biotic stresses, which are parried by different defense mechanisms. To protect themselves against attackers, plants, for example, synthesize specialized metabolites, also known as natural products or secondary metabolites.

In contrast to primary metabolites, which are synthetized by all plant species, specialized metabolites are non-essential for the basic processes of growth and development. According to estimates, plants synthesize over 200,000 natural products, which had initially been considered as 'by-products'. Specialized metabolites derive mostly from amino acid, isoprenoid, fatty acid/polyketide and phenylpropanoid pathways (Dixon, 2001; Dixon and Strack, 2003).

The ability to synthesize certain specialized metabolites is the consequence of specific ecological situations. Appropriate for its environment, each plant lineage synthesizes a distinct set of compounds (Pichersky and Lewinsohn, 2011). Some adaptions are common across taxa e.g. the formation of phenylpropanoid derivatives or terpenes, while other metabolites are specific to a number of plant families or species, such as glucosinolates, which occur almost exclusively in plants of the order Brassicales (Halkier and Gershenzon, 2006).

In plants, 10–20% of the genes in the genome encode for enzymes involved in the formation of specialized metabolites (Somerville and Somerville, 1999). Oxidases including cytochrome P450s and dioxygenases are by far the largest enzyme families (Dixon and Strack, 2003; Nelson and Werck-Reichhart, 2011) followed by glucosyltransferases, terpene synthases, and *O*-methyltransferases (Dixon and Strack, 2003).

The diversification of biosynthetic pathways due to selective pressure results in an abundance of products, which are considered to have an advantage for the plant. The functions of many of these products have been elucidated. Nearly all classes of specialized metabolites contain compounds that are known to serve as a barrier for plant pathogens and/or herbivores (Mithöfer and Boland, 2012).

1.2 Direct and indirect plant defenses

The interaction between plants and their attackers entails an arms race involving reciprocal development of defense mechanisms and counter adaptations. Plants have evolved sophisticated defense systems that can be categorized in several ways. Defenses can have direct effects on the attacking organism, or influence it indirectly by altering its ecological environment. Both, direct and indirect plant defenses can either be permanently present (constitutive) or inducible upon attack.

Direct defenses act by themselves on the attacker. This category includes morphological structures such as thorns and prickles, and lignification (Mithöfer and Boland, 2012). Inside plant tissues or deposited on the surface, specialized metabolites and proteins can act as feeding deterrents, anti-digestive compounds, and toxins (Mithöfer and Boland, 2012). Indirect defenses, e.g. emission of volatiles or secretion of extrafloral nectar, attract enemies of attackers, thus also reducing damage to plant tissues (Heil, 2008). In maize, for instance, root damage caused by the larvae of the western corn rootworm (*Diabrotica virgifera virgifera*) induces the formation of (E)-β-caryophyllene (Rasmann et al., 2005). The sesquiterpene (E)-β-caryophyllene strongly attracts an entomopathogenic nematode, which in consequence diminishes the emergence of adult *D. v. virgifera* (Rasmann et al., 2005).

Defensive specialized metabolites belong to diverse chemical classes including isoprene-derived terpenoids, nitrogen-containing alkaloids, phenolic compounds such as flavonoids or coumarins, and others (Mithöfer and Boland, 2012). Their location in the plant is often critical for their action against enemies. Location is also critical for plants themselves. To avoid intoxication active compounds are often stored in the vacuole, in specialized cell compartments or as inactivated derivatives, which become activated upon attack (Bones and Rossiter, 1996; Weinhold and Baldwin, 2011). This is especially true for permanent, constitutive defense compounds which are in many cases highly concentrated within cells. Other defense compounds are also produced 'on demand' after attack, such as many volatile organic compounds (VOCs) (Kessler and Baldwin, 2001). Frequently plants defend themselves with both constitutive and condensed metabolites.

1.3 Induced defense mechanisms

Beside avoidance of intoxication, inducible defenses have been shown to be of further benefit to plants. (1) Elevated levels of defenses often have more detrimental consequences on herbivore fitness and behavior than low concentrations. The induction of defense compounds may prevent the adaptation of attacking insects and thus retard the arms race (Karban et al, 1997). (2) When the constitutive synthesis of defensive compounds requires a limited resource, such as nitrogen, induction again is advantageous as it reduces the metabolic load and enables the use of nitrogen for growth and development (Preisser et al, 2007). However, the costs and benefits of induced and constitutive defenses in a given case depend on the specific ecological environment.

A prerequisite for all induced plant defense mechanisms is the recognition of the herbivore or pathogen. To detect an attacking herbivore or an infesting pathogen, plants use a variety of environmental cues or internal factors, including physical and chemical signals (Rivas, 2011; Jayaraman et al., 2014).

Chemical signals (elicitors) form a group of structurally non-related molecules. They originate from the attacker or are released as endogenous compounds from the plant itself. The molecular pattern of elicitors can be recognized by plant receptors. Molecular patterns are classified by the originating organisms and are divided into microbe-associated molecular patterns (MAMPs), herbivore-associated molecular patterns, and damage-associated molecular patterns (DAMPs) (Maffei et al., 2012). The membrane-bound pattern recognition receptors (PRRs) interact with molecular patterns such as MAMPs and initiate the response to several stresses to provide the first line of inducible defense (Tena et al., 2011).

PRRs trigger downstream signaling networks. The pattern recognition receptors initiate membrane depolarization caused by the influx of Ca^{2+} into the cytoplasm (Jeworutzki et al., 2010). Ca^{2+}-activated protein kinases and mitogen-activated protein kinase (MAPK) cascades mediate subsequently the formation of phytohormones including abscisic acid (ABA), ethylene (ET), jasmonic acid and its derivatives (JA), and salicylic acid (SA) (Tena et al., 2011).

Signaling pathways that are activated by phytohormones can influence one another and specify responses to abiotic and biotic challenges (Koornneef and Pieterse, 2008). Jasmonates, especially (+)-7-*iso*-jasmonic acid (hereafter jasmonic acid), are critical for the plant response to herbivore damage. JA biosynthesis is regulated by jasmonate ZIM-domain proteins (JAZ) (Wasternack and Hause, 2013). JAZ inhibits the expression of the key transcriptional activator, MYC2, which also controls JA biosynthesis (Chini et al., 2007). Elevated JA levels,

mediated e.g. by MAPK cascades, lead to the proteasomal degradation of JAZ proteins. With the degradation of JAZ, MYC2 becomes active and promotes the biosynthesis of JA, and the expression of genes encoding for enzymes involved in the formation of defense compounds (Xu et al., 2002; Wasternack and Hause, 2013).
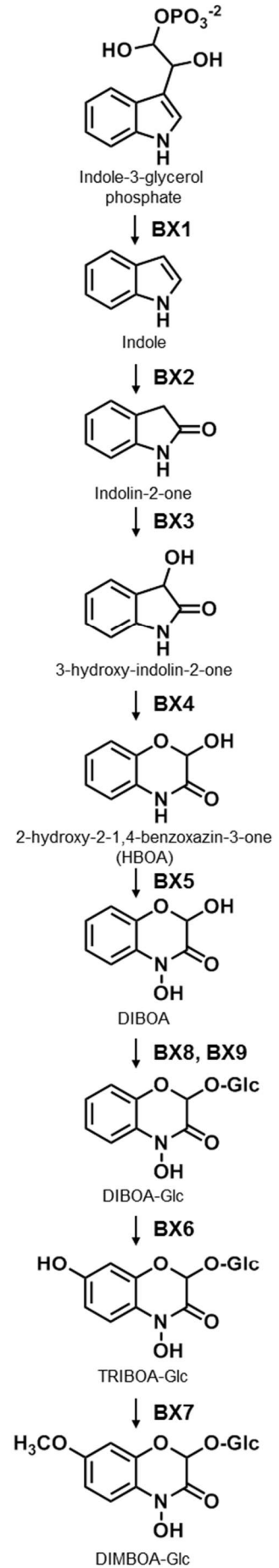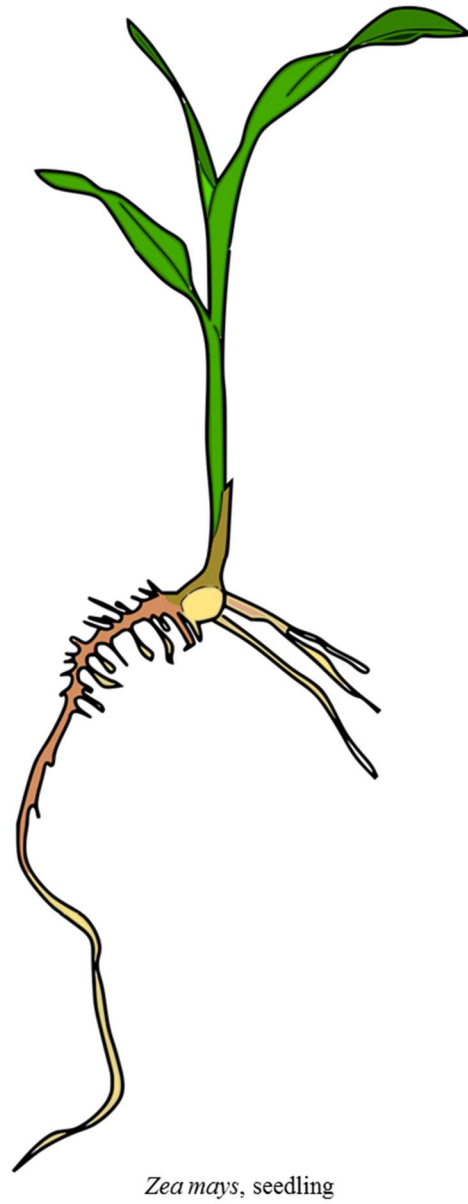
1.4 Maize defense against insect herbivores

Maize is one of the world's most important crops and has become a model organism for basic research investigating monocotyledonous plants (Strable and Scanlon, 2009). With the comprehensive research resources available for maize, surveys can be conducted to study e.g. the plant defense against insect herbivores in detail.

Among the best studied maize defense compounds are the benzoxazinoids (Figure 1), which are found predominantly in grasses (Niemeyer, 2009). The biosynthesis and regulation will be described in detail in the following section. The effects of benzoxazinoids are multi-faceted. For instance, maize cultivars with high benzoxazinoid levels are more resistant to larvae of the European corn borer and aphids (Klun et al., 1970; Beck et al. 1983). The biological activity is due to intermediates of benzoxazinoid breakdown. This breakdown is initiated by maceration of maize tissues, and intermediates of this process have been described to react with a range of nucleophiles including amino acid residues in active sites of enzymes (Cuevas et al., 1990). For example, the benzoxazinoid DIMBOA was found to inhibit digestive and detoxifying proteins such as trypsin and α-chymotrypsin, esterase, and glutathione-S-transferase (Cuevas et al., 1990; Houseman et al., 1992; Mukanganyama et al., 2003).

Figure 1. Core pathway of the benzoxazinoid biosynthesis elucidated in *Zea mays* (A). The biosynthetic products are highly concentrated in young seedlings. In maize, biosynthetic genes of the core pathway cluster on the short arm of chromosome 4 (B).The physical location on the chromosome is indicated in brackets. ▶

A

Indole-3-glycerol phosphate

↓ **BX1**

Indole

↓ **BX2**

Indolin-2-one

↓ **BX3**

3-hydroxy-indolin-2-one

↓ **BX4**

2-hydroxy-2-1,4-benzoxazin-3-one (HBOA)

↓ **BX5**

DIBOA

↓ **BX8, BX9**

DIBOA-Glc

↓ **BX6**

TRIBOA-Glc

↓ **BX7**

DIMBOA-Glc

Zea mays, seedling

B

Bx6 (1.1 Mbp)
Bx3 (3.0)
Bx4, Bx5 (3.1)
Bx8 (3.2)
Bx1, Bx2 (3.3)

Bx7 (18.2)

Zea mays chromosome 4
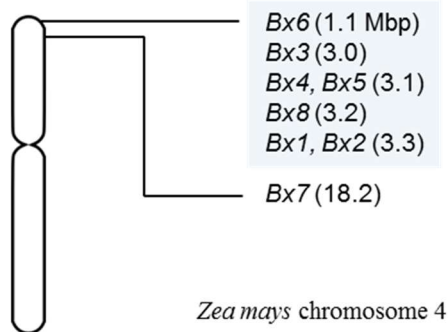
Other well studied natural products protecting maize against insect herbivores are maysin and chlorogenic acid. Maysin, a C-glucoside of the flavone luteolin, is highly concentrated in silks. Depending on the cultivar, maysin constitutes up to 0.9% of the silk fresh weight (Snook et al., 1993). High levels of maysin in silks have been considered responsible for the slower growth and arrested development of corn earworm larvae (Elliger et al., 1980; Rector et al., 2003). Chlorogenic acid, 3-caffeoyl-quinic acid, is induced in leaf tissues and silk
in response to herbivory (Bushman et al, 2002). The maize fruit-worm *Heliothis zea* has been found to be sensitive to chlorogenic acid (Isman and Duffey, 1982).

Besides defense by specialized metabolites, proteases, protease inhibitors, elicitor peptides, and ribosome-inactivating proteins are known to contribute to resistance against insect herbivores in maize (Pechan et al., 2000; Tamayo et al., 2000; Huffaker et al., 2011; Lawrence et al., 2012). For example, the maize proteinase inhibitor MPI accumulates adjacent to feeding sites of the Egyptian cotton leafworm (*Spodoptera littoralis*) and effectively inhibits elastase and chymotrypsin-like activities in the larval midgut (Tamayo et al., 2000). The expression of defense proteins in maize has been demonstrated to be influenced by a 23 amino acid peptide named ZmPep1 (Huffaker et al., 2011). ZmPep1 is induced by jasmonic acid (Huffaker et al., 2011), which as described earlier signals plant attack. ZmPep1 reinforces the immune response and leads to the *de novo* biosynthesis of jasmonic acid (Huffaker et al., 2011). The gene *Benzoxazinless*1, encoding the initial enzyme of benzoxazinoid biosynthesis, is also induced by the application of ZmPep1 (Huffaker et al., 2011).

The genetic variation of maize germplasm has been used to map quantitative trait loci (QTLs) associated with resistance against insect herbivores (Meihls et al., 2012). The basis for such approaches are high-resolution physical and genetic maps of the 10 maize chromosomes (Gardiner et al., 1993, Wei et al., 2009; Zhou et al., 2009; Ganal et al., 2011). Each chromosome is divided into 8 to 12 'bins' (100 bins in total), which derive from DNA restriction (Gardiner et al., 1993). Bins are characterized by specific molecular markers (Ganal et al., 2011). The genotyped nested-association mapping (NAM) population, which represents the genetic variation of maize germplasm (Flint-Garcia et al., 2005; Yu et al., 2008; McMullen et al., 2009) and the sequenced genome of the maize inbred line B73 (Schnable et al., 2009) allow, for instance, the mapping of genes responsible for differences in specialized metabolite biosynthesis and regulation. I attempted to identify and characterize biosynthetic genes underlying maize herbivore resistance QTLs, which has rarely been done in the past (Meihls et al., 2012).

1.5 Cyclic hydroxamic acids: Major defense chemicals in grasses

The major defense compounds in graminaceous plants including maize, wheat and rye are benzoxazinoid derivatives, which share the 2-hydroxy-2*H*-1,4-benzoxazin-3(4*H*)-one (HBOA) skeleton (Figure 1). As for many other defense compounds, benzoxazinoids are predominantly stored as glycosides in the vacuoles and are enzymatically hydrolyzed into the respective aglucone and the sugar moiety upon tissue injury (Niemeyer, 2009). A subsequent non-enzymatic breakdown of the liberated, unstable aglucones leads to the formation of highly reactive metabolites. The stability and reactivity of such compounds is determined by functional groups on the benzoxazinone skeleton (Atkinson et al., 1992; Glauser et al., 2011). The reactivity of these compounds towards nucleophilic moieties of proteins and nucleic acids is thought to be the basis of benzoxazinoid toxicity against a wide range of insect herbivores and plant pathogens (Niemeyer, 2009).

1.6 The benzoxazinoid pathway

The biosynthesis of benzoxazinoids in maize has been extensively studied since the 1990s (Gierl and Frey, 2001; Frey et al., 2009). The first reaction takes place in the plastids. Indole-3-glycerol phosphate, which derives from the shikimate pathway, is converted to indole catalyzed by the indole-3-glycerol phosphate lyase BENZOXAZINLESS1 (BX1). A subsequent stepwise introduction of four oxygen atoms by the P450 monooxygenases BX2, BX3, BX4, and BX5 leads to the formation of 2,4-dihydroxy-1,4-benzoxazin-3-one (DIBOA), the core-structure of the benzoxazinoid hydroxamic acids. DIBOA acts as substrate for the UDP-glucosyltransferases, BX8 and BX9, which transform the compound into the stable glucoside DIBOA-Glc (Rad et al., 2001). A hydroxylation of DIBOA-Glc at C7 catalyzed by the 2-oxoglutarate/Fe(II)-dependent dioxygenase BX6 and a subsequent methylation of the introduced hydroxyl group catalyzed by the *O*-methyltransferase BX7 lead to the production of 2-(2,4-dihydroxy-7-methoxy-1,4-benzoxazin-3-one)-β-D-glucopyranose (DIMBOA-Glc) in the cytosol (Jonczyk et al., 2008). The entire pathway is depicted in Figure 1.

Besides DIMBOA-Glc, many maize lines produce significant amounts of further benzoxazinoid derivatives such as 2-(2-hydroxy-4,7-dimethoxy-1,4-benzoxazin-3-one)-β-D-glucopyranose (HDMBOA-Glc), 2-(2,4-dihydroxy-7,8-dimethoxy-1,4-benzoxazin-3-one)-β-D-glucopyranose (DIM$_2$BOA-Glc), and 2-(2-hydroxy-4,7,8-trimethoxy-1,4-benzoxazin-3-one)-β-D-glucopyranose (HDM$_2$BOA-Glc) (Makowska et al., 2015).

Upon jasmonic acid treatment, insect herbivory or fungal infestation, HDMBOA-Glc accumulates and becomes the dominant benzoxazinoid in maize (Oikawa et al., 2002; Oikawa et al., 2004; Glauser et al., 2011; Dafoe et al., 2011; Marti et al., 2013). The biosynthesis of HDMBOA-Glc has been investigated in wheat (Oikawa et al., 2002). Feeding of wheat leaf protein extracts with DIMBOA-Glc and the methyltransferase co-factor *S*-adenosyl-L-methionine resulted in the formation of HDMBOA-Glc, indicating a 4-*O*-methyltransferase activity (Oikawa et al., 2002). However, the responsible *O*-methyltransferase enzymes in wheat and maize were unknown. Analogous to the formation of HDMBOA-Glc, HDM$_2$BOA-Glc is likely derived from DIM$_2$BOA-Glc by a methylation of the hydroxamic group (Glauser et al., 2011) (Figure 4). The synthesis of DIM$_2$BOA-Glc was assumed to include similar catalytic steps as already described for the conversion of DIBOA-Glc to DIMBOA-Glc catalyzed by the 2-oxoglutarate/Fe(II)-dependent dioxygenase BX6 and the 7-*O*-methyltransferase BX7 (Jonczyk et al., 2008) (Figure 1 and 4). Uncovering the enzymes involved in the biosynthesis of HDMBOA-Glc, DIM$_2$BOA-Glc, and HDM$_2$BOA-Glc and their role in plant defense was a major objective of this work.

1.7 *Bx* gene cluster and the regulation of benzoxazinoid formation

It has been shown that genes of the core benzoxazinoid pathway including *Bx*1, *Bx*2, *Bx*3, *Bx*4, *Bx*5, *Bx*6, and *Bx*8 are located in close proximity to each other on the short arm of maize chromosome 4 (Frey et al., 2009) (Figure 1). In general, such an organization of functionally related genes in 'operon-like' gene clusters in plants is considered to synchronize the regulation of gene expression and thus reduce the regulatory flexibility on the single gene level (Jonczyk et al., 2008; Osbourn, 2010).

Enzymes competing for substrates at branch points between primary and secondary metabolism often have dramatic effects on the velocity of downstream reactions and thus determine the concentration of the respective end products (LaPorte et al., 1984; Sato et al., 1999). In addition to BX1, indole-3-glycerol phosphate lyase (IGL) and tryptophan synthase (TS) also utilize indole-3-glycerol phosphate as substrate, yielding volatile indole and tryptophan, respectively. Sequence polymorphisms at *Bx*1 and differences in *Bx*1 expression in a diverse panel of maize inbred lines dominantly affected the formation of the end product DIMBOA-Glc (Butrón et al., 2010; Zheng et al., 2015). The expression of *Bx*1 has been shown to be controlled by distal cis-acting regulatory elements (Zheng et al., 2015).

DIMBOA-Glc as the most abundant BXD in maize is mainly produced in young seedlings 4–6 days after germination and declines thereafter (Cambier et al., 2000). In contrast, DIBOA-Glc, the DIMBOA-Glc precursor, is continuously synthesized and accumulates in older vegetative stages (Köhler et al., 2015). HDMBOA-Glc and HDM_2BOA-Glc also accumulate in older tissues (Cambier et al., 2000; Köhler et al., 2015) and their formation can be induced upon insect herbivory and fungus infection (Oikawa et al., 2004; Glauser et al., 2011; Köhler et al., 2015). Interestingly, the magnitude of HDMBOA-Glc induction declines with the age of the plant, indicating that HDMBOA-Glc formation is primarily controlled by the level of DIMBOA-Glc (Köhler et al., 2015). Thus, the regulation of the entire BXD pathway, which is strongly connected to the developmental stage of the maize plant, seems to be regulated by the first enzymes and supports the theory of gene-regulation in 'operon-like' clusters (Osbourn, 2010; Köhler et al., 2015).

1.8 Plant 2-oxoglutarate/Fe(II)-dependent dioxygenases

2-oxoglutarate/Fe(II)-dependent dioxygenases (2-ODDs) catalyze a wide array of different reactions such as hydroxylations, demethylations, desaturations, ring closures, ring cleavage, epimerizations, rearrangements, halogenations, and demethylenations (Farrow and Facchini, 2014). More than 0.4% of maize genes encode 2-ODDs; however, only a few of them have been cloned and characterized.

2-ODDs depend on ferrous iron as a co-factor, which is essential for the binding of molecular oxygen and the subsequent oxidative reactions (Figure 2). This co-factor is complexed by two histidine residues and a glutamate / aspartate residue as part of the highly conserved $HX(D/E)X_nH$ triad motif (Hegg and Que, 1997; Hewitson et al., 2005). For almost all reactions catalyzed by 2-ODDs, the oxidation of the substrate is coupled to the oxidation and subsequent decarboxylation of the co-substrate 2-oxoglutarate, resulting in the formation of the product, succinate, and carbon dioxide (Hangasky et al., 2013) (Figure 2).

Along the evolutionary line from algae to angiosperms, the number of 2-ODDs involved in specialized metabolite biosynthesis has increased steadily, which is thought to be the result of adaptation to new environmental stresses caused by the migration to land (Kawai et al., 2014). 2-ODDs catalyze e.g. the formation of flavones (FSN1) (Britsch, 1990; Falcone Ferreyra et al., 2015), the modification of the methylsulfinylalkyl glucosinolate side chain (AOP2 and AOP3) (Kliebenstein et al, 2001; Hansen et al., 2008), the synthesis of alkaloids such as scopolamine (H6H) (Hashimoto and Yamada, 1987), and the formation of the
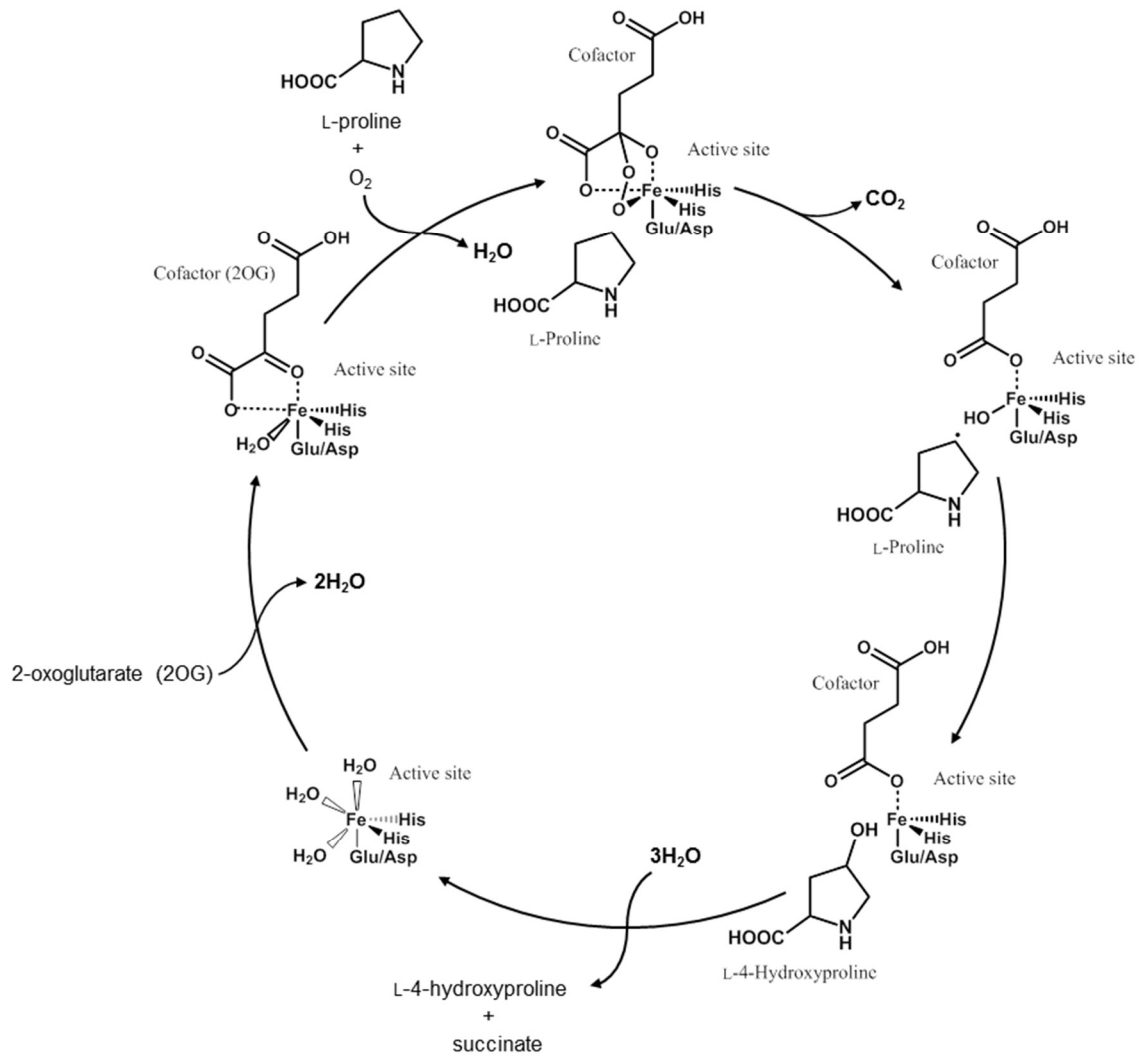
Figure 2. Catalytic cycle of prolyl hydroxylase, which belongs to the enzymatic class of 2-oxoglutarate/Fe(II)-dependent dioxygenases. Modified from Smirnova et al., 2012.

core structure of coumarins (F6'H1) (Kai et al., 2008). In contrast to their role in secondary metabolism, 2-ODDs also play essential roles in primary metabolism (Kawai et al., 2014). Posttranscriptional modifications of amino acid side chains by 2-ODDs, e.g. the hydroxylation of peptidyl-proline leading to peptidyl-4-hydroxyproline (Hutton et al., 1967), are crucial for structural proteins and can as well function as sensors for hypoxia (Vigani et al., 2013). 2-ODDs have been further shown to redundantly demethylate repressive histone methylations enabling subsequent transcription (Cho et al., 2012), and to contribute to the homeostasis

of phytohormones by synthesizing or inactivating intermediates in the auxin, ethylene, gibberellin, and salicylic acid metabolism (Farrow and Facchini, 2014).

The benzoxazinoid pathway as described so far comprises a single characterized 2-ODD, the DIBOA-Glc hydroxylase BX6. However, the formation of DIM$_2$BOA-Glc includes a further hydroxylation step, which again could be catalyzed by a 2-ODD enzyme.

1.9 Plant *O*-methyltransferases

O-Methyltransferases (OMTs) catalyze the transfer of a methyl group from the co-factor *S*-adenosyl-L-methionine (SAM) to the hydroxyl group of an acceptor molecule, resulting in the formation of the respective methyl ether and *S*-adenosyl-L-homocysteine (SAH). Many OMTs are characterized by a high degree of specificity towards their substrate molecules and regioselectivity of the methylation site (Ibrahim, 1997; Ibrahim et al., 1998), although they often share a high amino acid sequence similarity. Only a few OMTs have been shown to accept multiple structurally related compounds such as phenylpropanoids and flavonoids (Gauthier et al., 1996; Chiron et al., 2000).

The majority of plant OMTs (≥92%) possesses five highly conserved regions, rich in glycine, in the C-terminal part of the protein sequence (Ibrahim, 1997, Ibrahim et al., 1998). Region I (VDVGGG), II (GINFDLPH), and III (EHVGGDMF) have been identified to be involved in SAM binding (Zubieta et al, 2001). Region IV (GKVI) and V (GGERT), which flank the substrate binding site, are involved in metal ion binding and contain the catalytic residues (Vidgren et al., 1994, Zubieta et al, 2001). A second unique feature of plant *O*-methyltransferases is an N-terminal domain. This domain is responsible for the dimerization of OMTs, which appears to be common to plant *O*-methyltransferases (Zubieta et al, 2001). The interface between homodimers forms the back wall of the substrate binding site, which determines the substrate specificity of OMTs (Zubieta et al, 2001). The formation of non-native heterodimers of four highly similar OMTs (93 – 99%) involved in the berberine biosynthesis led to changes in substrate specificity profiles and in some cases the different isoforms accept new substrates (Frick and Kutchan, 1999).

SAM-dependent *O*-methyltransferase products play many roles in plant growth and development, defense against microbes, seed germination, and the interaction with the environment (Hahlbrock and Scheel, 1989; Siqueira et al., 1991). Furthermore, *O*-methylation of specialized metabolites has been shown to increase the specific activity of these compounds (Ibrahim et al., 1987; Preisig et al., 1989; Dixon and Palva, 1995).

Based on phylogenetic analysis and substrate specificities, plant OMTs have been divided into two major groups (Lam et al., 2007). Enzymes of group I methylate CoA esters of phenylpropanoids, which are essential for lignin biosynthesis, and a variety of smaller organic acids such as benzoic acid, jasmonic acid, or salicylic acid (Lam et al., 2007). Group I OMTs have been found to be mostly involved in the biosynthesis of guaiacyl-like lignin (Lam et al., 2007). Lignin of primitive land plants consists almost entirely of guaiacyl (Boerjan et al., 2003), suggesting that OMTs from group I may have evolved early in the evolution of vascular plants (Lam et al., 2007). Subsequent evolutionary forces including convergent and divergent processes may have given rise to functionalization, the high substrate specificity, and the strong regioselectivity of group II OMTs (Lam et al., 2007).

Substrates of group II OMTs in the subordinate phylogenetic clusters are in the majority of cases structurally related (Lam et al., 2007). For instance, benzoxazinoids and flavonoids have common structural features and it has been shown that the benzoxazinoid 7-*O*-methyltransferase *Bx7* clusters with a flavonoid 7-*O*-methyltransferase from *Hordeum vulgare* (HvF7Omt) (Jonczyk et al., 2008). Therefore *O*-methyltransferases synthesising the benzoxazinoids DIM$_2$BOA-Glc, HDMBOA-Glc, and HDM$_2$BOA-Glc are very likely similar to BX7.

1.10 The formation of aldoximes by cytochrome P450 enzymes: An entry point to natural product biosynthesis

Aldoximes are known as precursors for a variety of specialized metabolites such as glucosinolates, cyanogenic glycosides, and camalexin (Halkier and Gershenzon, 2006; Bak et al., 2006; Nafisi et al., 2006; Bjarnholt and Møller, 2008; Jørgensen et al., 2011). Aldoximes are produced from their corresponding amino acids by P450 enzymes of the CYP79 family (Figure 3; Hamberger and Bak, 2013). The first reported CYP79 enzyme (CYP79A1) was characterized in Sorghum, a plant species closely related to maize. CYP79A1 catalyzes the conversion of L-tyrosine to p-hydroxyphenylacetaldoxime (Figure 3), which is subsequently converted to the cyanogenic glycoside dhurrin (Koch et al., 1995; Sibbesen et al., 1995).

CYP79s are unique among cytochrome P450 enzymes by not accepting lipophilic substrates, but utilizing exclusively amino acids (Hamberger and Bak, 2013). However consistently, the amino acid substrates identified so far, L-tyrosine, L-phenylalanine, L-tryptophan, L-alanine, L-leucine and L-isoleucine, all have lipophilic side chains. As a result of *N*-hydroxylation, dehydration, decarboxylation,

and a final isomerization, the amino acid substrate is converted to its appropriate aldoxime (Figure 3) (Koch et al., 1995; Sibbesen et al., 1995).
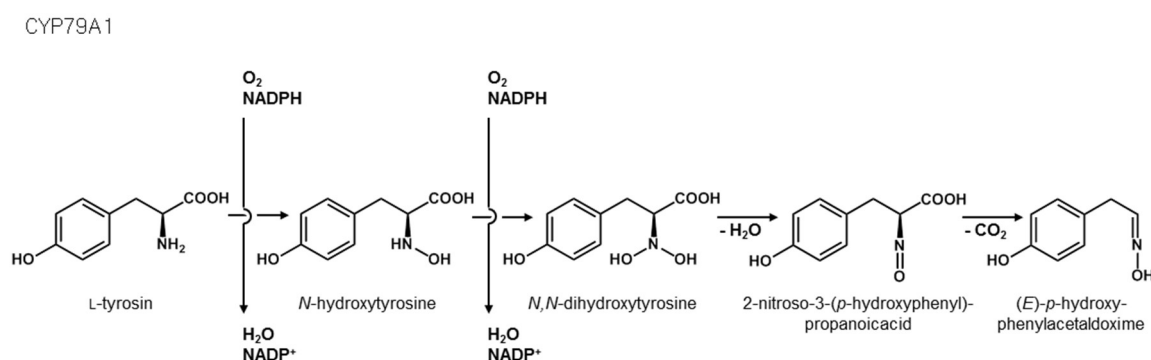
CYP79A1

Figure 3. The multifunctional P450 enzyme CYP79A1 catalyzes the conversion of L-tyrosine into (*E*)-*p*-hydroxy-phenylacetaldoxime. In sorghum, (*E*)-*p*-hydroxy-phenylacetaldoxime is further converted to the cyanogenic glucoside dhurrin. Modified from Sibbessen et al.,1995.

The formation of activated oxygen species, needed for the biosynthesis of aldoximes, is common to all cytochrome P450 enzymes (Werck-Reichart and Feyereisen, 2000). The active center of CYPs is composed of the iron-protoporphyrin IX (heme) with a thiolate of a conserved cysteine residue as fifth ligand (Werck-Reichart and Feyereisen, 2000). In the first step, water as the sixth iron-ligand is replaced by the substrate. Supported by the increase in redox potential, the ferrous state of the complex is decreased in a one-electron reduction. Further, molecular oxygen is bound, which results in a superoxide complex. Then a second reduction step yields an activated oxygen species (Werck-Reichart and Feyereisen, 2000).

Members of the CYP79 family are found in all so far sequenced plant genomes, including monocotyledons and dicotyledons (Irmisch et at., 2013). In poplar which produces no aldoxime-derived defense compounds, two CYP79 paralogues, CYP79D6v3 and CYP79D7v2, have been characterized (Irmisch et at., 2013). Both enzymes accept L-tyrosine, L-phenylalanine, L-tryptophan, L-leucine and L-isoleucine and yield the corresponding aldoxime (Irmisch et at., 2013). The enzymatic products are particularly formed subsequent to herbivory (Irmisch et at., 2013; McCormick et al., 2014). The major aldoximes in the volatile blend, phenylacetaldoxime, 3-methylbutyraldoxime, and 2-methylbutyraldoxime have been shown to contribute to direct as well indirect plant defense (Irmisch et at., 2013; McCormick et al., 2014). Indole-3-acetaldoxime (IAOx), only present in trace amounts in poplar leaf extracts (Irmisch et at., 2013), is discussed to be a precursor for the biosynthesis of indole-3-acetic acid (IAA), which is widely known to be involved in many aspects of plant growth and development (Sugawara et al., 2009;

Novák et al, 2012). IAOx is suggested to be metabolized to indole-3-acetonitrile (IAN) (Normanly et al., 1997; Sugawara et al., 2009). IAN itself is again found to contribute to chemical defense in crucifers (Pedras et al., 2002). Nitrilases identified in Arabidopsis and maize are thought to convert IAN subsequently to IAA (Normanly et al., 1997, Park et al., 2003).

The maize genome comprises four putative CYP79 sequences with unknown function (Irmisch et at., 2013). In contrast to Sorghum, maize is not known to produce cyanogenic glycosides, suggesting that the putative CYP79 enzymes are involved in volatile aldoxime formation or IAA biosynthesis. The role of CYP79 enzymes in maize became another objective of this work.

2 Overview of Manuscripts

2.1 Manuscript I

Natural Variation in Maize Aphid Resistance is Associated with 2,4-Dihydroxy-7-Methoxy-1,4-Benzoxazin-3-One Glucoside Methyltransferase Activity

Lisa N. Meihls*, Vinzenz Handrick*, Gaétan Glauser, Hugues Barbier, Harleen Kaur, Meena M. Haribal, Alexander E. Lipka, Jonathan Gershenzon, Edward S. Buckler, Matthias Erb, Tobias G. Köllner and Georg Jander. (2013). THE PLANT CELL, 25: 2341-2355.

SUMMARY

Maize cultivars differ greatly in their susceptibility towards insect herbivores. Genetic mapping of maize leaf aphid susceptibility and the formation of *O*-methylated benzoxazinoids, well known as plant defense compounds in grasses, revealed the same quantitative trait locus on chromosome 1. The metabolic QTL on chromosome 1 comprises three *O*-methyltransferases (OMTs) methylating the most abundant benzoxazinoid DIMBOA-Glc. DIMBOA-Glc levels, determined by the mapped OMTs on chromosome 1, positively correlated with callose deposition in response to leaf aphid infestation, suggesting additional signaling properties of DIMBOA-Glc or its aglucone.

AUTHOR CONTRIBUTION

Based on ideas of LNM, VH, ME, TGK, and GJ
Designed Experiments: LNM, VH (10%), JG, ME, TGK, and GJ
Conducted experiments: LNM, VH (40%), GG, HB, HK, and MMH
Performed data analyses: LNM, VH (40%), JG, HK, AEL, ESB, ME, TGK, and GJ
Wrote the manuscript: ME, TGK, and GJ

* LNM and VH share first authorship.

2.2 Manuscript II

The maize cytochrome P450 CYP79A61 produces phenylacetaldoxime and indole-3-acetaldoxime in heterologous systems and might contribute to plant defense and auxin formation

Sandra Irmisch, Philipp Zeltner, Vinzenz Handrick, Jonathan Gershenzon and Tobias G. Köllner. (2015). BMC PLANT BIOLOGY, 15: 128.

SUMMARY

From amino acids, plants produce a group of aldoxime compounds, which are known as volatiles and as precursors in cyanogenic glycoside, glucosinolate, and presumably plant hormone biosynthesis. A maize cytochrome P450 enzyme of the CYP79 family catalyzes the formation of (*E/Z*)-phenylacetaldoxime and (*E/Z*)-indole-3-acetaldoxime. The accumulation of (*E/Z*)-phenylacetaldoxime in leaves upon simulated herbivory is linked with a role in plant defense and both aldoximes are suggested as precursors of the induced plant hormones phenylacetic acid and indole-3-acetic acid.

AUTHOR CONTRIBUTION

Based on ideas of SI, PZ, and TGK
Designed Experiments: SI, PZ, and TGK
Conducted experiments: SI, PZ, VH (10%), and TGK
Performed data analyses: SI, PZ, VH (10%), and TGK
Wrote the manuscript: SI, VH (10%), JG, and TGK

2.3 Manuscript III

Biosynthesis of 8-*O*-Methylated Benzoxazinoid Defense Compounds in Maize

Vinzenz Handrick*, Christelle A. M. Robert*, Kevin R. Ahern, Simon Zhou, Ricardo A. R. Machado, Daniel Maag, Gaétan Glauser, Felix E. Fernandez-Penny, Jima N. Chandran, Eli Rodgers-Melnik, Bernd Schneider, Edward S. Buckler, Wilhelm Boland, Jonathan Gershenzon, Georg Jander, Matthias Erb, and Tobias G. Köllner. THE PLANT CELL: In Revision.

SUMMARY

Benzoxazinoids are major defense compounds in maize and other grasses. A genome-wide association mapping strategy was used to identify quantitative trait loci comprising the dioxygenase and two *O*-methyltransferases that catalyze the conversion of DIMBOA-Glc into the 8-*O*-methylated benzoxazinoids, DIM_2BOA-Glc and HDM_2BOA-Glc. This branch of the pathway specifically increases maize resistance against aphids.

AUTHOR CONTRIBUTION

Based on ideas of VH, CAMR, JG, WB, GJ, ME, and TGK
Designed Experiments: VH (40%), CAMR, ESB, JG, GJ, ME, and TGK
Conducted experiments: VH (60%), CAMR, RARM, ME, ERM, and JNC
Performed data analyses: VH (60%), CAMR, RARM, WB, ERM, GJ, BS, and ME
Wrote the manuscript: VH (60%), CAMR, GJ, ME, and TGK

* VH and CAMR share first authorship.

3 Manuscripts

3.1 Manuscript I

Natural Variation in Maize Aphid Resistance is Associated with 2,4-Dihydroxy-7-Methoxy-1,4-Benzoxazin-3-One Glucoside Methyltransferase Activity°

Natural Variation in Maize Aphid Resistance Is Associated with 2,4-Dihydroxy-7-Methoxy-1,4-Benzoxazin-3-One Glucoside Methyltransferase Activity[C][W]

Lisa N. Meihls,[a,1] Vinzenz Handrick,[b,1] Gaetan Glauser,[c] Hugues Barbier,[a,2] Harleen Kaur,[a,3] Meena M. Haribal,[a] Alexander E. Lipka,[d] Jonathan Gershenzon,[b] Edward S. Buckler,[d,e] Matthias Erb,[b,1] Tobias G. Köllner,[b,1] and Georg Jander[a,1,4]

[a] Boyce Thompson Institute for Plant Research, Ithaca, New York 14853
[b] Max Planck Institute for Chemical Ecology, 07745 Jena, Germany
[c] Institute of Biology, University of Neuchâtel, 2009 Neuchatel, Switzerland
[d] U.S. Department of Agriculture–Agricultural Research Service, Robert W. Holley Center for Agriculture and Health, Ithaca, New York 14853
[e] Department of Plant Breeding and Genetics, Institute for Genomic Diversity, Cornell University, Ithaca, New York 14853

Plants differ greatly in their susceptibility to insect herbivory, suggesting both local adaptation and resistance tradeoffs. We used maize (*Zea mays*) recombinant inbred lines to map a quantitative trait locus (QTL) for the maize leaf aphid (*Rhopalosiphum maidis*) susceptibility to maize Chromosome 1. Phytochemical analysis revealed that the same locus was also associated with high levels of 2-hydroxy-4,7-dimethoxy-1,4-benzoxazin-3-one glucoside (HDMBOA-Glc) and low levels of 2,4-dihydroxy-7-methoxy-1,4-benzoxazin-3-one glucoside (DIMBOA-Glc). In vitro enzyme assays with candidate genes from the region of the QTL identified three O-methyltransferases (*Bx10a-c*) that convert DIMBOA-Glc to HDMBOA-Glc. Variation in HDMBOA-Glc production was attributed to a natural CACTA family transposon insertion that inactivates *Bx10c* in maize lines with low HDMBOA-Glc accumulation. When tested with a population of 26 diverse maize inbred lines, *R. maidis* produced more progeny on those with high HDMBOA-Glc and low DIMBOA-Glc. Although HDMBOA-Glc was more toxic to *R. maidis* than DIMBOA-Glc in vitro, BX10c activity and the resulting decline of DIMBOA-Glc upon methylation to HDMBOA-Glc were associated with reduced callose deposition as an aphid defense response in vivo. Thus, a natural transposon insertion appears to mediate an ecologically relevant trade-off between the direct toxicity and defense-inducing properties of maize benzoxazinoids.

INTRODUCTION

Plants in natural and agricultural ecosystems are constantly attacked by a multitude of insect herbivores, including leaf and root chewers, stem borers, leaf miners, gall formers, and phloem feeders. Most of these herbivores have distinct geographical distributions, resulting in divergent herbivore communities across latitudinal (Züst et al., 2012), longitudinal (Kozlov, 2008), and altitudinal gradients (Pélissier et al., 2008). The pronounced geographical heterogeneity of herbivore communities coincides with considerable variation in herbivore resistance and expression of defensive traits in many plants (Johnson, 2011). In some natural ecosystems, the geographical distribution of herbivores has been shown to covary with specific defensive phenotypes (Prasad et al., 2012; Züst et al., 2012). However, similar associations have rarely been described for crop species, and the extent to which pest occurrence may have shaped the defensive makeup of crops remains unknown.

Independent of geographical patterns, the high genetic diversity of plants provides an opportunity to map quantitative trait loci (QTL) conferring insect resistance (Kroymann et al., 2003; Klingler et al., 2009; Qiu et al., 2010). QTL mapping exploits genetically heritable within-species differences that can statistically be associated with a specific part of the genome. QTL mapping is often limited by the relatively high cost of genotyping and the difficulty of repeating experiments with a segregating population. To overcome these limitations, large sets of recombinant inbred lines have been created for several plant species, including *Arabidopsis thaliana* (Keurentjes et al., 2011) and maize (*Zea mays*) (Flint-Garcia et al., 2005; Yu et al., 2008; McMullen et al., 2009a). Once such recombinant inbred lines have been genotyped, they represent a permanent resource that can be used to genetically map loci that influence any phenotypic trait that varies in the population.

As a productive food crop that is attacked by more than 90 insect species (Steffey et al., 1999), maize is an attractive model

for the identification of resistance factors. Geographical variation in the abundance of insect herbivores suggests that there may be associated variation in the level of pest resistance among different commercial maize lines. For instance, the western maize rootworm (*Diabrotica virgifera virgifera*) is a major pest in the midwestern US but has not been present in Europe until recently (Miller et al., 2005). The maize leaf aphid (*Rhopalosiphum maidis*) does not survive winters in North America but migrates north each summer from warmer areas, resulting in periodic outbreaks of this species (Steiner et al., 1985).

Recent genome sequencing of the maize inbred line B73 (Schnable et al., 2009) and the development of high-resolution physical and genetic maps (Wei et al., 2009; Zhou et al., 2009; Ganal et al., 2011) has opened up new research opportunities. A nested association mapping (NAM) population of ~5000 recombinant inbred lines was generated by crossing a genetically diverse population of 25 maize inbred lines to B73 (Flint-Garcia et al., 2005; Yu et al., 2008; McMullen et al., 2009a). The NAM population has been used to map numerous maize traits, including resistance to northern leaf blight (*Setosphaeria turcica*; Poland et al., 2011) and southern leaf blight (*Bipolaris maidis*; Kump et al., 2011). In both cases, genome-wide association mapping revealed numerous QTL with relatively small additive

effects. To date, the NAM population has not been employed to identify alleles involved in insect resistance.

Insect resistance factors in maize as well as other plants have been identified not only by genetic mapping approaches but also by phytochemical screening. Known maize antiherbivore defenses include protease inhibitors (Lawrence et al., 2012), the Maize insect resistance1 (Mir1) Cys protease (Pechan et al., 2000), ribosome-inactivating proteins (Walsh et al., 1991; Bass et al., 1995), and other protein-mediated defenses, as well as secondary metabolites such as chlorogenic acid (Cortés-Cruz et al., 2003), maysin (Rector et al., 2003), and benzoxazinoids (Frey et al., 1997). Benzoxazinoids have been demonstrated to confer resistance to aphids (Ahmad et al., 2011), chewing herbivores (Glauser et al., 2011), and a wide range of other pests, pathogens, and weeds (Niemeyer, 2009). They are found abundantly in many Poaceae, including maize, wheat (*Triticum aestivum*), and rye (*Secale cereale*) (Zuniga et al., 1983), as well as in several dicot species in the Plantaginaceae and Ranunculaceae (Schullehner et al., 2008). In maize seedlings, the predominant benzoxazinoid is 2,4-dihydroxy-7-methoxy-1,4-benzoxazin-3-one (DIMBOA; Figure 1), which is stored as an inactive glucoside (DIMBOA-Glc). Constitutive benzoxazinoid levels tend to decline as the plants age (Cambier et al., 2000). In addition to DIMBOA-Glc,
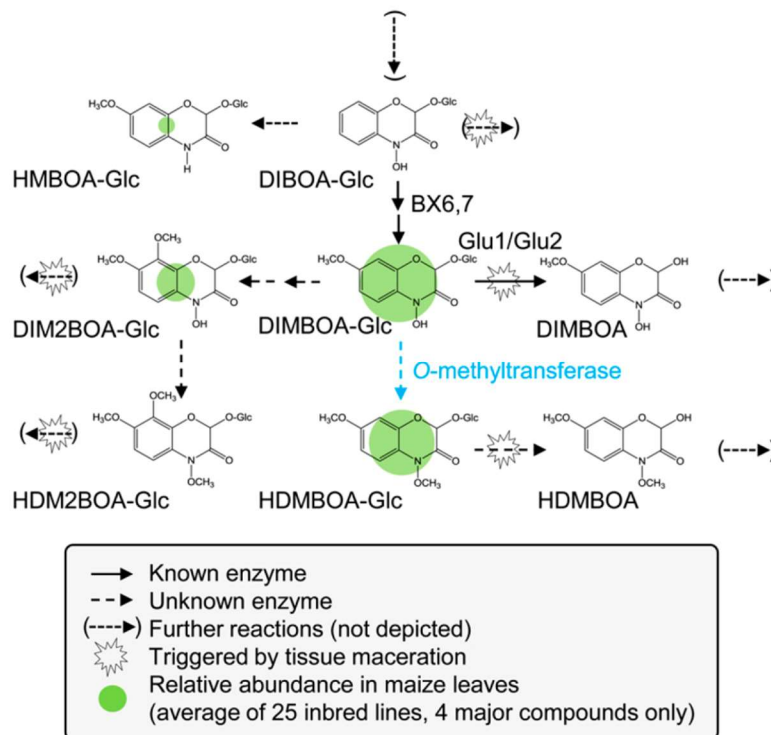
Figure 1. Selected Steps of Benzoxazinoid Metabolism in Maize.

The major benzoxazinoids detected in the leaves of maize seedlings are DIMBOA-Glc, HDMBOA-Glc, DIM2BOA-Glc, and HMBOA-Glc. In contrast with DIMBOA-Glc, the biosynthetic steps leading to HDMBOA-Glc, DIM2BOA-Glc, and HMBOA-Glc are unknown. Upon tissue disruption by herbivores, the different glucosides are cleaved by β-glucosidases (Glu), leading to the release of active aglucones. The *N*-methoxyl group of HDMBOA decreases its stability and renders it more reactive than DIMBOA.
[See online article for color version of this figure.]
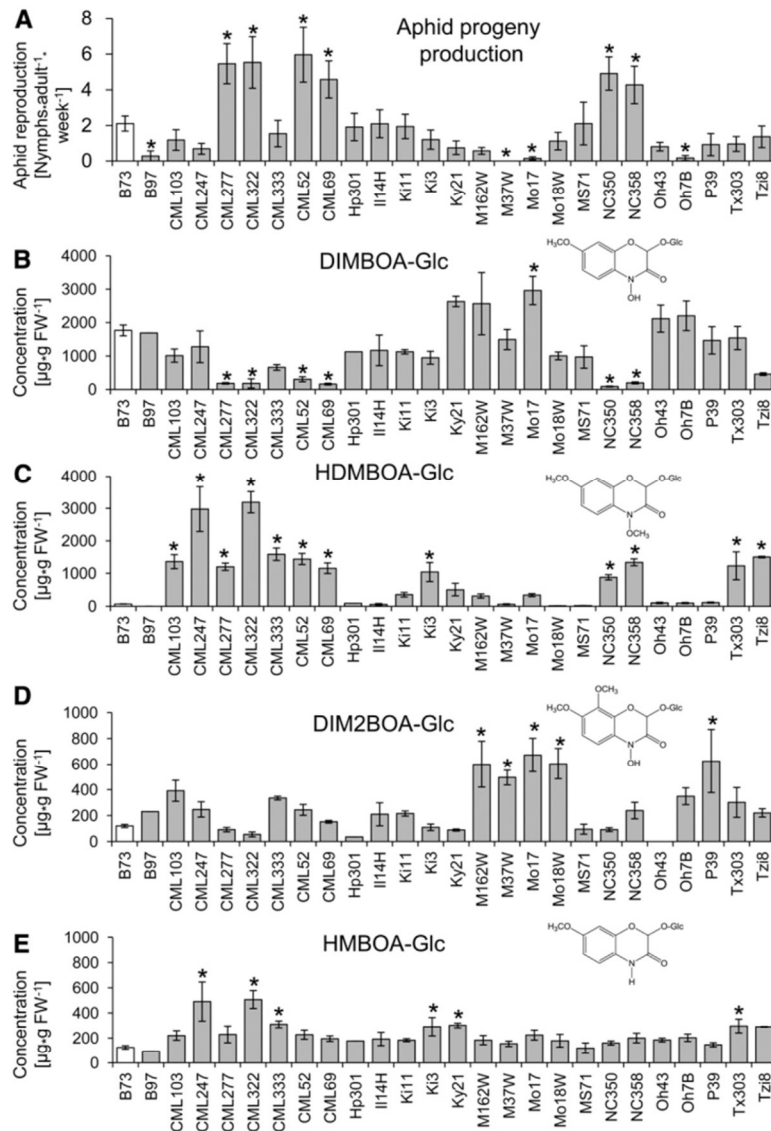
Figure 2. Aphid Reproduction on and Benzoxazinoid Content in Parental Lines of the Maize NAM Population.

(A) The number of *R. maidis* progeny produced per adult aphid over 7 d is shown (mean ± se; *n* = 8; *n* = 18 for B73). Asterisks indicate significant differences relative to B73 (*P < 0.05, Dunnett's test).

(B) to **(E)** DIMBOA-Glc, HDMBOA-Glc, DIM2BOA-Glc, and HMBOA-Glc abundance (mean ± se; *n* = 3 to 7, with the exception of single measurements for B97 and Hp301, for which no statistical calculations were done). Asterisks indicate significant differences relative to B73 (*P < 0.05, Dunnett's test). FW, fresh weight.

2-hydroxy-4,7-dimethoxy-1,4-benzoxazin-3-one glucoside (HDMBOA-Glc), 2,4-dihydroxy-7,8-dimethoxy-1,4-benzoxazin-3-one glucoside (DIM2BOA-Glc), and 2-hydroxy-7-methoxy-1,4-benzoxazin-3-one glucoside (HMBOA-Glc) are commonly found in maize leaves.

Benzoxazinoids are predominantly stored as glucosides in the cell vacuole. Tissue maceration by chewing herbivores results in the release of active aglucones by the action of endogenous β-glucosidases (Figure 1). The nonenzymatic breakdown of the major aglucone DIMBOA results in the formation of 6-methoxybenzoxalin-3-one, which is insect deterrent (Grambow et al., 1986). Insect feeding also induces enzymatic conversion of DIMBOA-Glc to HDMBOA-Glc (Oikawa et al., 2004; Dafoe et al., 2011; Glauser et al., 2011). While HDMBOA-Glc is also activated by glucosidases during tissue maceration, further nonenzymatic breakdown is faster for HDMBOA than DIMBOA (Maresh et al., 2006). The conversion of DIMBOA-Glc to HDMBOA-Glc has been associated with increased resistance to both pathogens and herbivores (Oikawa et al., 2004; Dafoe et al., 2011;
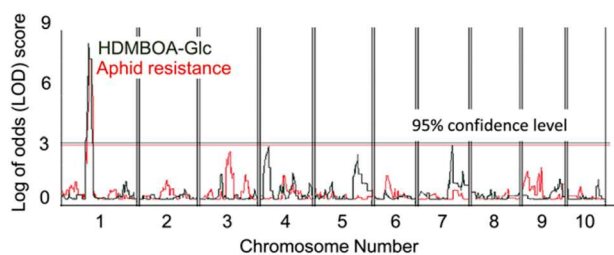
Figure 3. QTL for Aphid Resistance and HDMBOA-Glc Content Colocalize on Maize Chromosome 1 in the B73 × CML322 Recombinant Inbred Line Population.
[See online article for color version of this figure.]

Glauser et al., 2011). Thus, herbivory-induced HDMBOA-Glc accumulation creates a pool of reactive defense compounds that allows maize plants to respond more rapidly to subsequent herbivore attack. Although DIMBOA-Glc methyltransferase activity has been demonstrated enzymatically (Oikawa et al., 2002), it was unclear which genes encode this activity.

Unlike chewing herbivores, such as caterpillars, aphids feed by inserting their stylets into phloem sieve elements. Analysis of aphid honeydew and sap collected by stylectomy shows that DIMBOA-Glc, but not DIMBOA, is found in the phloem (Givovich et al., 1992, 1994; Caillaud and Niemeyer, 1996). Additionally, aphid feeding does not increase overall DIMBOA accumulation (Cambier et al., 2001), suggesting that glucosidase-mediated activation of DIMBOA-Glc does not occur in response to insects that feed exclusively from the phloem sieve elements. However, a recent study shows that DIMBOA is secreted into the apoplast upon aphid infestation (Ahmad et al., 2011).

In artificial diet experiments, DIMBOA-Glc and DIMBOA reduced feeding by five monocot-feeding aphid species (Givovich and Niemeyer, 1995). In the case of the rose-grain aphid (*Metopolophium dirhodum*) feeding from artificial diet, the HDMBOA-Glc LD_{50} (concentration to reduce aphid survival by 50%) was fivefold lower than the DIMBOA-Glc LD_{50} (Cambier et al., 2001), suggesting that, as in the case of chewing herbivores, conversion of DIMBOA-Glc to HDMBOA-Glc could provide a defensive benefit to the plants. Benzoxazinoids may also function to elicit the production of other plant defensive metabolites or proteins. The maize *benzoxazinoneless1* (*bx1*) *indole glycerol phosphate lyase1* (*igl1*) double mutant, which is blocked in the first step of benzoxazinoid biosynthesis, has reduced callose accumulation as a defense response (Ahmad et al., 2011). Infiltration of DIMBOA, but not HDMBOA-glucoside, into the maize apoplastic space induced callose formation, suggesting that differences in the structure or reactivity of benzoxazinoids leads to differential regulation of maize callose accumulation.

As chewing herbivores rather than aphids have been the focus of most prior research on natural variation in maize herbivore resistance (McMullen et al., 2009a; Meihls et al., 2012), we initiated experiments using *R. maidis* and recombinant inbred lines of the NAM population to identify resistance mechanisms. Concerted mapping of loci associated with aphid resistance, benzoxazinoid production, and callose deposition was followed by the molecular and biochemical characterization of candidate

genes. Our results show that dominant aphid susceptibility in several NAM parental lines is associated with a DIMBOA-Glc methyltransferase that is inactivated by a transposon insertion in other inbred lines.

RESULTS

Mapping of *R. maidis* Resistance and HDMBOA-Glc QTL to the Same Interval on Maize Chromosome 1

To explore natural variation in maize aphid resistance, we measured *R. maidis* reproduction on 2-week-old seedlings of the NAM population parental lines (Figure 2). Reproduction was low on the inbred lines B97, M37W, Mo17, and Oh7B, intermediate on B73, and high on CML52, CML69, CML277, CML322, NC350, and NC358. Aphid progeny production varied more than 100-fold, suggesting that it should be possible to map aphid resistance as a quantitative trait using the recombinant inbred lines of the NAM population. Analysis of aphid reproduction on 124 recombinant inbred lines derived from B73 × CML322 identified a single significant QTL on maize Chromosome 1 (bin 1.04; see Supplemental Figure 1A online). On average, the CML322 allele increased aphid progeny production by approximately three nymphs per adult aphid per week (see Supplemental Figure 1B online), and aphid susceptibility was dominant in F1 progeny of crosses between B73 and CML322 (see Supplemental Figure 1C online). Measurement of *R. maidis* reproduction on recombinant inbred lines derived from B73 crossed to CML52, CML69, and CML277 also identified a significant aphid resistance QTL in maize bin 1.04 (see Supplemental Figure 2 online). Going on the assumption that aphid resistance is influenced by the same locus in all four of these inbred lines, we combined the data sets in an association mapping approach. This narrowed the genomic interval containing the aphid resistance QTL to ~4 Mb containing 31 annotated genes (see Supplemental Table 1 online).

Since benzoxazinoids are known to have a profound effect on maize resistance to insect herbivores (Cambier et al., 2001; Oikawa et al., 2004; Dafoe et al., 2011; Glauser et al., 2011), we measured benzoxazinoid concentration in 2-week-old seedlings of the NAM parental lines as a possible explanatory factor for the observed aphid performance differences (Figure 2A). All of the detected benzoxazinoids showed considerable variation in the NAM parental lines (Figure 2). DIMBOA-Glc and HDMBOA-Glc concentrations were negatively correlated (P < 0.01, $r = -0.51$, $n = 27$; see Supplemental Figure 3A online), DIMBOA-Glc and DIM2-BOA-Glc were positively correlated (P < 0.05, $r = 0.39$, $n = 27$; see Supplemental Figure 3B online), and no significant correlation was observed between DIMBOA-Glc and HMBOA-Glc concentrations (P > 0.05, $r = 0.18$, $n = 27$; see Supplemental Figure 3C online). Aphid reproduction was negatively correlated with DIMBOA-Glc (P < 0.01, $r = -0.76$, $n = 27$; see Supplemental Figure 4A online) and positively with HDMBOA-Glc (P < 0.05, $r = 0.45$, $n = 27$; see Supplemental Figure 4B online) across the NAM parental lines. In particular, the six NAM parental lines that were most suitable for aphid reproduction (CML52, CML69, CML277, CML322, NC350, and NC358; Figure 2A) had the lowest DIMBOA-Glc content (Figure 2B) and relatively high HDMBOA-Glc levels (Figure 2C).
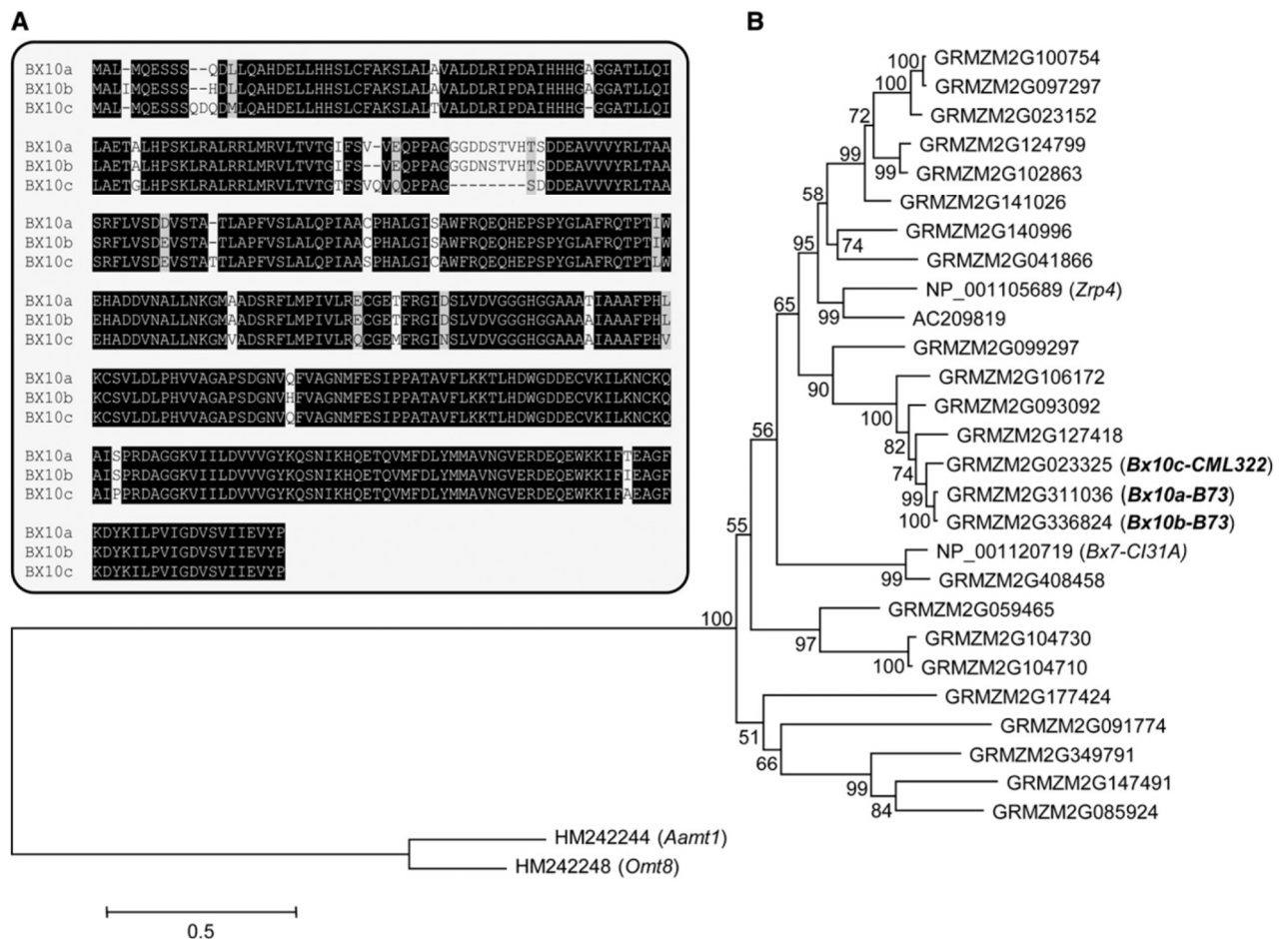
Figure 4. Sequence Alignment and Rooted Phylogenetic Tree with the Three Maize *O*-Methyltransferases Contained within the HDMBOA-Glc QTL.

(A) Protein sequence alignment (ClustalW) of the three *O*-methyltransferase homologs GRMZM2G311036, GRMZM2G336824, and GRMZM2G023325 (*Bx10a-c*).

(B) Rooted phylogenetic tree of putative maize *Omt* genes similar to *Bx10a-c*. The tree was inferred using the maximum likelihood method and $n = 1000$ replicates for bootstrapping. Bootstrap values are shown next to each node. The tree is drawn to scale, with branch lengths measured in the number of substitutions per site. The maize genes *Aamt1* and *Omt8* were used as an outgroup. Sequences used for the alignment are shown in Supplemental Data Set 1 online.

To test whether a QTL for HDMBOA-Glc production colocalizes with the identified aphid resistance QTL, we quantified benzoxazinoids in B73 × CML322 recombinant inbred lines that had previously been used for aphid resistance mapping. The identified HDMBOA-Glc QTL coincided with the aphid resistance QTL (Figure 3). The hypothesis that CML322 has constitutively higher DIMBOA-Glc methyltransferase activity than B73 is supported by the observations that (1) the CML322 allele in bin 1.04 increased HDMBOA-Glc content by ~1200 μg/g fresh weight relative to the B73 allele (see Supplemental Figure 5A online); (2) high HDMBOA-Glc content is dominant in F1 progeny from a B73 × CML322 cross (see Supplemental Figure 5B online); (3) a QTL for DIMBOA-Glc content is located on Chromosome 1 in the B73 × CML322 recombinant inbred population (see Supplemental Figure 5C online); and (4) DIMBOA-

Glc and HDMBOA-Glc concentrations are negatively correlated in these lines (see Supplemental Figure 5D online).

Three Putative Methyltransferase Genes with Homology to Benzoxazinoneless7 Are Located in the Aphid Resistance/HDMBOA-Glc QTL

Given the colocalization of the aphid resistance and HDMBOA-Glc QTL (Figure 3), we hypothesized that variation in a DIMBOA-Glc methyltransferase would constitute the underlying genetic basis of these phenotypes. Three adjacent genes in the QTL interval (GRMZM2G311036, GRMZM2G336824, and GRMZM2G023325) cluster closely together in a phylogenetic tree of predicted maize *O*-methyltransferase sequences (Figure 4). These three genes showed >40% amino acid sequence identity to Benzoxazinoneless7 (BX7)

(GenBank ID NP_001120719; TRIBOA-Glc *O*-methyltransferase), a known enzyme in the DIMBOA-Glc biosynthesis pathway (Jonczyk et al., 2008). Thus, the enzymes encoded by GRMZM2G311036, GRMZM2G336824, and GRMZM2G023325 were likely candidates for catalyzing the conversion of DIMBOA-Glc to HDMBOA-Glc. Following the convention used for the other nine known maize benzoxazinoid biosynthesis genes, we named the identified genes *Benzoxazinoneless10a* (*Bx10a*; GRMZM2G311036), *Bx10b* (GRMZM2G336824), and *Bx10c* (GRMZM2G023325).

A Transposon Insertion in *Bx10c* Correlates with Low Levels of HDMBOA-Glc and Lower Aphid Reproduction

The *Bx10c* gene in inbred line B73 was found to contain an inserted CACTA family transposon (base pairs 66,501,488 to 66,509,673 on Chromosome 1 in the maize genome assembly v2), with ~73% DNA sequence identity to the previously described *Doppia4* transposon (GenBank ID AF187822.1; Bercury et al., 2001). The >8000-bp insertion in the first exon of *Bx10c* is likely to be a knockout mutation. Although *Bx10a* and/or *Bx10b* transcripts could be detected using quantitative RT-PCR (qRT-PCR) analysis, *Bx10c* was not expressed in B73 (Figure 5). Due to the 98% DNA sequence identity of *Bx10a* and *Bx10b*, attempts to design primers that would reliably amplify one but not the other were unsuccessful. Analysis of DNA sequence data from the maize HapMap2 project (Chia et al., 2012) showed that the *Bx10c* gene in CML322 does not contain the *Doppia4*-like transposon insertion. This observation was confirmed by PCR amplification and DNA sequencing of the complete gene (GenBank ID = KC754964). Consistent with this finding, *Bx10c* transcription was detectable by qRT-PCR in CML322 seedlings (Figure 5). To investigate the *Bx10c* transposon insertion presence or absence in all NAM parental lines, a PCR approach with gene-specific and transposon insertion-specific primers was conducted as shown in Figure 6A. Whereas 10 of the maize lines contained an insertion in *Bx10c*, the other 17 did not (Figure 6B). On average, NAM parental lines with the transposon insertion had significantly higher DIMBOA-Glc content (Figure 6C), lower HDMBOA-Glc content (Figure 6D), and lower aphid reproduction (Figure 6E) than lines without the insertion. However, due to reduced genetic recombination resulting from the proximity of *Bx10c* to the pericentromeric region of Chromosome 1 (Gore et al., 2009), we cannot rule out possible effects of other nearby genes on the observed phenotypes.

The *Bx10a*, *Bx10b*, and *Bx10c* Genes Encode DIMBOA-Glc *O*-Methyltransferases and Are Differentially Expressed in the NAM Lines

Gene cloning and in vitro enzyme assays showed that the B73 alleles of *Bx10a* and *Bx10b* encode an enzyme with DIMBOA-Glc *O*-methyltransferase activity (Figure 7). Enzyme activity depended on the presence of *S*-adenosyl-L-Met as a methyl donor in the reaction mixture. As *Bx10c* is interrupted by a transposon insertion in inbred line B73, we cloned this gene from CML322, which does not have an insertion (Figure 6B). Enzyme assays showed that BX10c from CML322 also has DIMBOA-Glc *O*-methyltransferase activity (Figure 7).
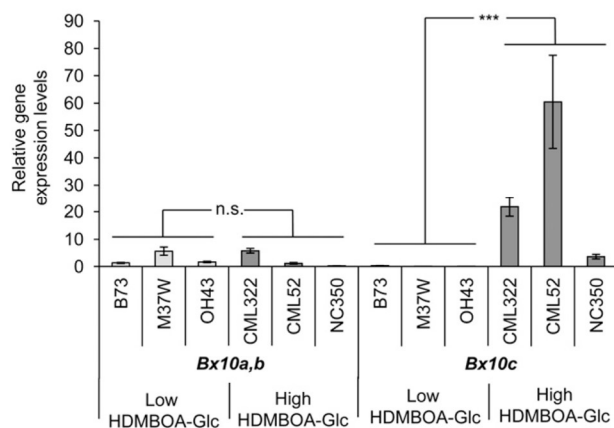
Figure 5. *Bx10c* Is Expressed in the High HDMBOA-Glc Lines CML322, CML52, and NC350 but Not in the Low HDMBOA-Glc Lines B73, M37W, and Oh43.

Gene expression of uninfested plants was measured using qRT-PCR relative to *actin* (means ± SE; *n* = 6). Asterisks indicate significant differences in expression levels between high and low HDMBOA-Glc genotypes (*t* test, ***P < 0.001; n.s., not significant).

To test whether differences in *Bx10* gene expression can explain the different HDMBOA-Glc levels in the NAM lines, we compared transcript abundance of *Bx10a/b* and *Bx10c* in three high HDMBOA-Glc lines (CML322, CML52, and NC350) and three low HDMBOA-Glc lines (B73, M37W, and Oh43). Whereas *Bx10a/b* transcripts could be detected in nearly all lines at low levels, *Bx10c* showed a strong transcript accumulation exclusively in the high HDMBOA-Glc lines (Figure 5). These results indicate that the constitutive conversion of DIMBOA-Glc to HDMBOA-Glc is mainly regulated by *Bx10c* gene expression.

Maize Lines Containing Less DIMBOA-Glc, Form Less Callose and Are More Susceptible to Aphids

To obtain a more detailed understanding of the contrasting roles of DIMBOA-Glc and HDMBOA-Glc in aphid resistance, we conducted in vitro feeding assays with purified compounds. DIMBOA-Glc and HDMBOA-Glc were added to aphid artificial diet at concentrations similar to those observed in whole maize leaves (Figures 2B and 2C). Contrary to the positive correlation between DIMBOA-Glc and aphid resistance in planta (Figure 5), but similar to what has been observed with other herbivores and pathogens (Cambier et al., 2001; Oikawa et al., 2004; Dafoe et al., 2011; Glauser et al., 2011), artificial diet assays showed that HDMBOA-Glc is more toxic for *R. maidis* than DIMBOA-Glc; whereas 2 mM HDMBOA-Glc significantly reduced aphid progeny production (Figure 8A) and survival (Figure 8B), 2 mM DIMBOA-Glc did not. Benzoxazinoid assays conducted with the remaining aphid diet showed intact benzoxazinoids and no breakdown products, suggesting that DIMBOA-Glc and HDMBOA-Glc remained intact over the course of the experiment.

Although experiments with fungal pathogens and caterpillar feeding found induced conversion of DIMBOA-Glc to HDMBOA-Glc
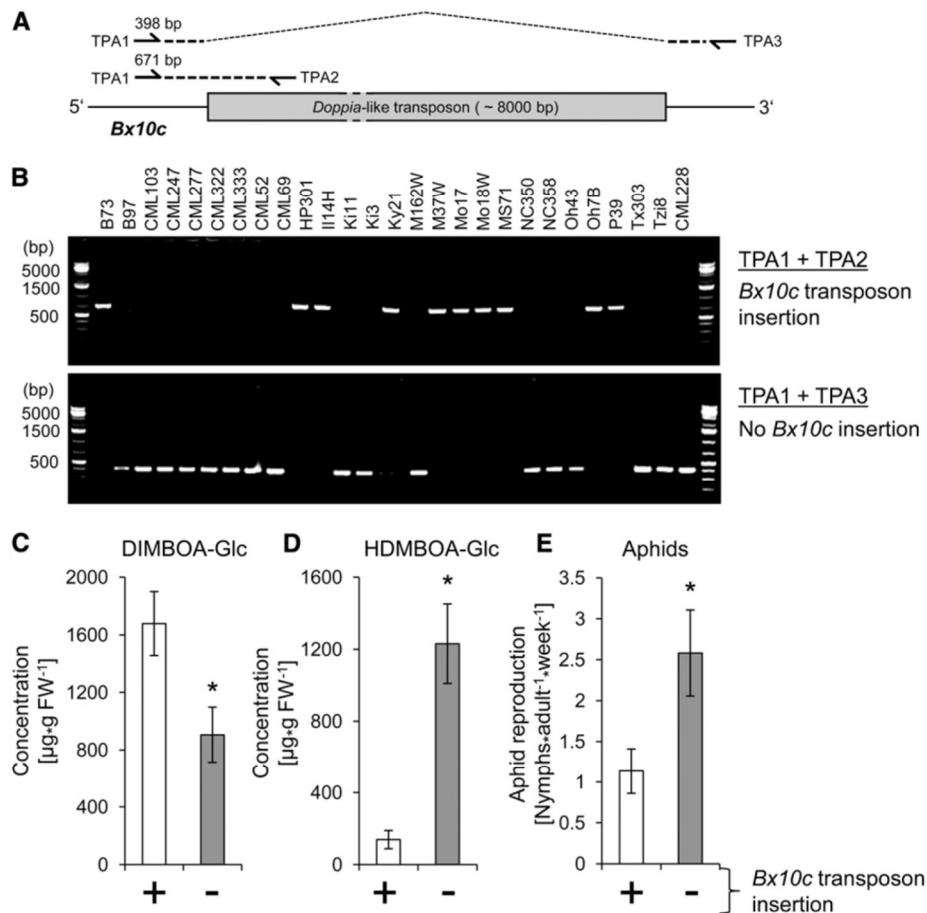
Figure 6. A *Doppia*-Like Transposon in *Bx10c* Is Associated with Reduced HDMBOA-Glc Production and Increased Aphid Resistance in the NAM Parental Lines.

(A) Strategy for PCR analysis to amplify fragments that are specific for either the insertion or the deletion allele.

(B) Detection of the transposon knockout and functional alleles of *Bx10c* by PCR using primers TPA1, TPA2, and TPA3 (described in Supplemental Table 2 online).

(C) to **(E)** Comparison of DIMBOA-Glc content, HDMBOA-Glc content, and aphid reproduction in NAM parental lines, with and without the transposon insertion (mean ± SE; *n* = 10 or 17). Asterisks indicate significant differences (*P < 0.05; two-tailed Student's *t* test). FW, fresh weight.

(Oikawa et al., 2004; Dafoe et al., 2011; Glauser et al., 2011), this was not the case with *R. maidis* feeding (Figure 9), thus ruling out differential induction as a possible explanation for the above discrepancy. As an alternative hypothesis, we tested whether other defenses are induced by DIMBOA-Glc but not HDMBOA-Glc. Ahmad et al. (2011) demonstrated that infiltration of DIMBOA, but not HDMBOA-Glc, into maize leaves induced accumulation of callose, a common plant defense against aphid feeding (Dreyer and Campbell, 1987; Walling, 2000; Botha and Matsiliza, 2004). To determine whether similar effects can result from natural variation in maize benzoxazinoid content, we measured constitutive and aphid-induced callose accumulation in B73, CML52, CML69, CML277, CML322, NC350, and NC358. Aphid feeding increased callose formation on all seven tested maize lines (Figure 10A). However, both control and aphid-treated

samples from the six maize inbred lines with low DIMBOA-Glc content had much lower callose levels than the corresponding B73 reference samples (P < 0.05, Tukey's HSD test; Figure 10A). As in the case of aphids that were able to roam freely on whole maize seedlings (Figure 2A), aphids that were caged on individual leaves in this experiment produced more progeny on inbred lines with low DIMBOA-Glc content than on B73 (Figure 10B). Taken together, this suggests that DIMBOA-Glc increases aphid resistance by promoting callose deposition and that the increased production of HDMBOA-Glc by methylation of DIMBOA-Glc leads to aphid susceptibility via a reduction in callose defenses.

When aphids were given a choice of host plants, there was no significant difference in their settling on B73 relative to NC350 or NC358 (see Supplemental Figure 6 online). In the case of pairwise comparisons with CML277 and CML52, aphids actually

Figure 7. BX10a-c Are Functional DIMBOA-Glc O-Methyltransferases That Produce HDMBOA-Glc.

(A) Equal amounts of purified recombinant BX10a, BX10b, and BX10c as well as a control without enzyme were incubated with the substrate DIMBOA-Glc and the cosubstrate S-adenosyl-ʟ-Met. Products were extracted with methanol and analyzed by HPLC-UV. mAU: milli absorbance unit.
(B) Schematic representation of the reaction catalyzed by BX10 in the presence of the cosubstrate S-adenosyl-ʟ-Met (SAM).
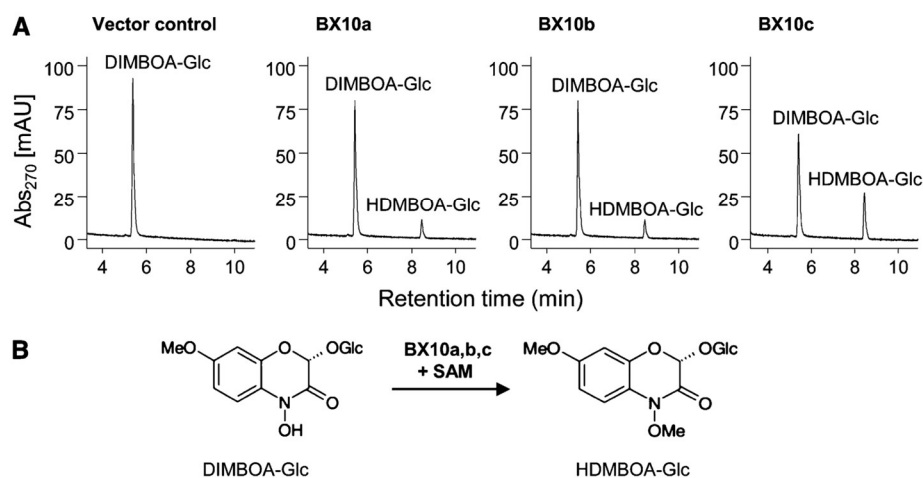
preferred the less suitable host, B73. Thus, it appears that different plant factors mediate *R. maidis* host plant choice and reproductive success on maize.

DISCUSSION

By mapping a QTL for natural variation in maize resistance to *R. maidis*, we identified a DIMBOA-Glc methyltransferase maize gene family representing important catalysts in the formation of plant defenses. Although several studies have demonstrated that herbivory and pathogen infection induce DIMBOA-Glc to HDMBOA-Glc conversion in maize (Oikawa et al., 2004; Dafoe et al., 2011; Glauser et al., 2011; Huffaker et al., 2011), it was unclear which genes encode this enzyme activity. In addition to *Bx10a*, *Bx10b*, and *Bx10c*, other genes that are in the same cluster of the phylogenetic tree (Figure 4; GRMZM2G099297, GRMZM2G106172, GRMZM2G093092, and GRMZM2G127418) may also encode DIMBOA-Glc methyltransferases. Given the currently available DNA sequence data, it is not possible to determine whether the size of this gene family varies among the inbred lines of the NAM population.

The presence of multiple genes encoding the same DIMBOA-Glc methyltransferase activity may allow variable defense activation in different plant tissues or in response to different pests and pathogens. Whereas DIMBOA-Glc is produced constitutively in most maize lines studied so far, the conversion to HDMBOA-Glc can be both constitutive (as shown here) or induced by insect feeding and pathogen attack (Oikawa et al., 2004; Dafoe et al., 2011; Glauser et al., 2011; Huffaker et al., 2011). In the maize hybrid Delprim, HMDBOA-Glc is strongly inducible in the leaves, but produced constitutively in the roots (Marti et al., 2013). Across the maize inbred lines of the NAM population, the *Bx10c* transposon insertion strongly influences the relative constitutive abundance of DIMBOA-Glc and HDMBOA-

Glc (Figures 6C and 6D). However, the lack of *Bx10c* transcripts in Oh43 (Figure 5), an inbred line which does not contain a *Bx10c* transposon insertion, suggests another regulatory mechanism for *Bx10c* downregulation in this line. Additionally, it is quite likely that the transcriptional regulation of other members of the DIMBOA-Glc methyltransferase gene family affects the constitutive or induced accumulation of HDMBOA-Glc. Such biochemical redundancy in key regulated steps of defense pathways may occur commonly in plants. For instance, although most reactions in *Arabidopsis* indole glucosinolate biosynthesis are encoded by single genes, induced indole glucosinolate methoxylation is encoded by multiple genes with the same enzymatic functions (Pfalz et al., 2009, 2011).

In addition to having toxic effects on herbivores and pathogens, DIMBOA has a further function in the induction of callose as a plant defense response. This was previously demonstrated by reduced callose accumulation in a *bx1 igl1* maize double mutant, as well as by callose formation in response to infiltration of DIMBOA into the apoplastic space (Ahmad et al., 2011). Our results show that natural variation in this pathway has a significant effect on maize aphid resistance. Even though HDMBOA-Glc is more deleterious than DIMBOA-Glc to *R. maidis* in artificial diet assays (Figure 8), aphids grow better on maize with low DIMBOA-Glc and elevated HDMBOA-Glc (see Supplemental Figure 4 online). This can be explained by the observation that callose, which provides defense against aphids (Dreyer and Campbell, 1987; Walling, 2000; Botha and Matsiliza, 2004), is more abundant in B73 than in maize lines with low DIMBOA-Glc content (Figure 10A). Further research will be needed to identify the mechanisms by which DIMBOA and/or one of its breakdown products induces callose formation. It is quite possible that DIMBOA acts early in a pathway that induces not only callose formation, but also other plant defenses that provide protection against aphids.
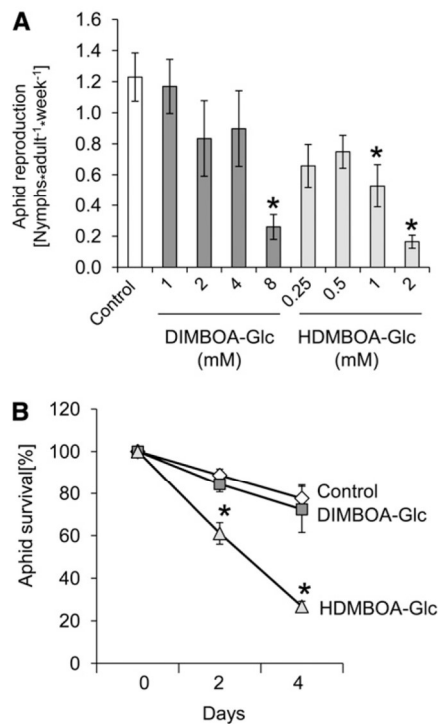
Figure 8. HDMBOA-Glc Reduces Aphid Performance in Vitro More Strongly Than DIMBOA-Glc.

(A) Aphid progeny production on diet with benzoxazinoids. Progeny per adult aphid were counted after 2 d on diet containing the indicated concentrations of DIMBOA-Glc and HDMBOA-Glc (mean ± se; $n = 6$; $n = 12$ for controls). Asterisks indicate significant differences (*$P < 0.05$, Dunnett's test relative to control samples).
(B) Adult aphid survival on diet with benzoxazinoids. Diet contained no benzoxazinoids (control; diamonds), 2 mM DIMBOA-Glc (squares), or 2 mM HDMBOA-Glc (triangles) (mean ± se; $n = 6$; $n = 12$ for controls). Asterisks indicate significant differences (*$P < 0.05$, Dunnett's test relative to control samples).

Callose induction by benzoxazinoids in maize is similar to previously reported callose induction by indole glucosinolate breakdown in *Arabidopsis* (Clay et al., 2009). Specificity of these pathways is demonstrated by the fact that chemically similar transformations lead to opposite effects on callose formation. Whereas DIMBOA induces callose formation in maize, and *O*-methylation to HDMBOA abolishes this effect (Ahmad et al., 2011), hydrolysis of indol-3-ylmethylglucosnolate (or 1-methoxyindol-3-ylmethylglucosinolate) in *Arabidopsis* does not trigger callose formation but hydrolysis of the *O*-methylated product 4-methoxyindole-3-ylmethylglucosinolate creates an inducer of callose formation (Clay et al., 2009). For both plant species, activation of existing defense products, benzoxazinoids (maize) or glucosinolates (*Arabidopsis*) is an indicator of enemy attack and thus provides a reliable signal for inducing other defenses. It is likely that future research with other plant systems will provide additional examples of defensive metabolites that have a secondary function as signals in activating other defenses.

Although aphids produce more progeny on plants with low DIMBOA-Glc content (Figure 2), this was not reflected as a preference for these plants in aphid choice assays (see Supplemental Figure 6 online). In two cases, the aphids actually settled preferentially on inbred lines that are less suitable host plants. This suggests that different plant factors affect host plant choice and reproduction in the case of *R. maidis*. It is not known what plant cues affect host plant choice in this species. However, similar situations, where choices made by adult insects do not identify the best host plants for developing progeny have been reported in other plant–insect interactions (Mayhew, 2001).

The parental lines of the NAM population, which were chosen based on their high level of genetic diversity (Flint-Garcia et al., 2005; McMullen et al., 2009b; Chia et al., 2012), vary considerably in their accumulation of defense-related benzoxazinoids (Figure 2). The negative correlation between DIMBOA-Glc and HDMBOA-Glc content (see Supplemental Figure 3A online) suggests that there are divergent defense strategies in maize. B73 and other maize lines with constitutively high DIMBOA-Glc and low HDMBOA-Glc levels likely rely on inducible responses to increase HDMBOA-Glc accumulation when there is an herbivore or pathogen attack. Conversely, maize seedlings with high levels of HDMBOA-Glc are already provisioned to be more resistant to attack by chewing herbivores. However, such lines might also be more prone to false alarms and the production of phytotoxic benzoxazinoid breakdown products in the absence of attack. Thus, depending on the particular environment in which a plant is located, either constitutive or inducible HDMBOA-Glc production may be the better strategy.

Previous studies have mapped QTL for resistance to lepidopteran herbivores, the southwestern maize borer (*Diatraea grandiosella*) and the maize earworm (*Helicoverpa zea*), to bin 1.04 of the maize genome (Byrne et al., 1998; Groh et al., 1998; Brooks et al., 2005). This variation in chewing herbivore resistance may also be mediated by regulation of DIMBOA-Glc methyltransferase. A previously reported bin 1.04 QTL for
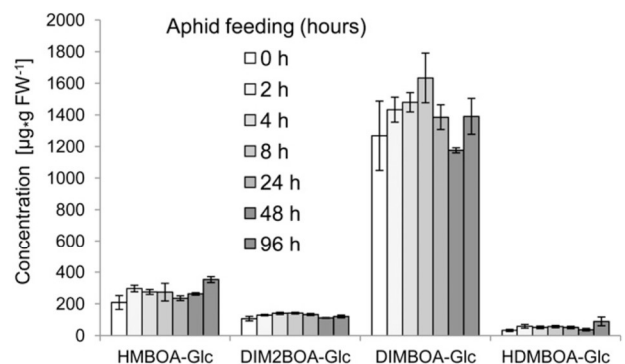

Figure 9. Aphids Do Not Induce Benzoxazinoid Biosynthesis in Maize.

Accumulation of benzoxazinoids in B73 after 0, 2, 4, 8, 24, 48, and 96 h of aphid feeding (mean ± se; $n = 5$). No significant differences were detected (*$P > 0.05$; Dunnett's test relative to 0-h control time point). FW, fresh weight.
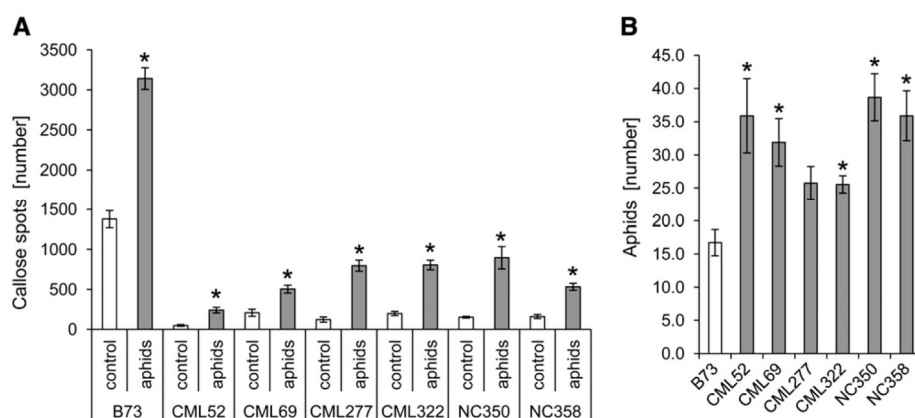
Figure 10. Aphid-Induced Callose Formation Is Reduced in Maize Inbred Lines with Low DIMBOA-Glc and High HDMBOA-Glc Concentrations.

(A) Number of callose spots in maize leaves with and without aphid feeding (mean ± SE; $n = 4$ [controls], $n = 18$ [B73 + aphids], and $n = 9$ [other inbred lines + aphids]). Asterisks indicate significant differences relative to control for each genotype ($P < 0.05$; two-tailed Student's t tests).
(B) Number of aphids present 3 d after 10 aphids were caged on a leaf blade (mean ± SE; $n = 18$ [B73], and $n = 9$ [other inbred lines]). Asterisks indicate significant differences (*$P < 0.06$; two-tailed t test compared with B73 control, with Bonferroni correction for multiple comparisons).

DIMBOA-Glc abundance (Butrón et al., 2010) likely also reflects variation in DIMBOA-Glc methyltransferase activity. However, as HDMBOA-Glc was not measured in this assay, it is not possible to determine whether there was a concomitant increase in this metabolite. Since B73 × CML322 recombinant inbred lines, which we used in our study (Figure 3A), also were used by Butrón et al. (2010), it is quite likely that the same QTL was mapped.

It is perhaps significant that the six NAM parental lines with the highest constitutive HDMBOA-Glc/DIMBOA-Glc ratio (CML52, CML69, CML277, CML322, CML350, and CML358; Figure 2) represent tropical germplasm. Since pressure from insect herbivores and pathogens tends to be higher in tropical habitats (Rasmann and Agrawal, 2011), maize breeding in such regions may have selected for plants with constitutively elevated HDMBOA-Glc accumulation. The Egyptian cotton leafworm (*Spodoptera littoralis*) and the fall armyworm (*Spodoptera frugiperda*) are able to reglycosylate DIMBOA to DIMBOA-Glc (Glauser et al., 2011), which may render this compound ineffective as a defense. However, HDMBOA is highly unstable and immediately degrades into active catabolites, which may make it impossible for caterpillars to detoxify it effectively. The ability of maize plants to produce high amounts of HDMBOA-Glc may therefore be an important prerequisite for stable yields under heavy pressure by chewing arthropods. Aphids, on the other hand, tend to be a lesser problem than chewing herbivores at the maize seedling stage. Thus, the concomitant selection for aphid susceptibility due to a reduction in callose accumulation and perhaps other aphid-specific defenses may not be a significant problem for tropical maize farmers. It remains to be determined whether defenses elicited by DIMBOA are beneficial in temperate agroecosystems, which are characterized by a distinct pathogen community (Ullstrup and Renfro, 1976) and a few dominating herbivore pests, many of which are resistant to benzoxazinoids (Dafoe et al., 2011; Glauser et al., 2011; Robert et al., 2012).

The distinct induction patterns, phytochemical properties, and potential defense elicitation roles of benzoxazinoids suggest that they may have divergent functions in plant defenses against different herbivores and pathogens. Alternatively, benzoxazinoids may act synergistically at different biological levels to protect the plant against its enemies (Glauser et al., 2011). Deciphering the individual contribution of the different benzoxazinoid derivatives to insect resistance has remained difficult because of their unknown biochemical and genetic origins and the lack of genetic resources to study them in vivo. Data presented here will permit identification of additional genes involved in maize benzoxazinoid metabolism. For instance, investigation of natural variation in DIM2BOA-Glc accumulation (Figure 2D) may lead to the identification of the as yet unknown enzymes for the biosynthesis of this benzoxazinoid. GRMZM2G408458 for instance, which is similar to *Bx7* (Figure 4), may also be part of the core DIMBOA-Glc biosynthesis pathway.

A single large-effect benzoxazinoid QTL causes most of the aphid resistance variation in our experiments (Figure 6E). However, it is likely that more extensive analysis of all recombinant inbred lines in the NAM population would identify additional aphid resistance mechanisms. For instance, other QTL may function in maize inbred lines that are more resistant to *R. maidis* than B73 (Figure 2A). Similarly, genetic mapping of resistance to chewing herbivores has identified QTL that are not linked to known benzoxazinoid-related genes (McMullen et al., 2009a; Meihls et al., 2012). Our results demonstrate that newly available maize genetic and genomic resources make it straightforward to proceed from the observation of such natural variation in insect resistance to elucidating the genetic and biochemical basis of this variation. The identification of these and other herbivore resistance QTL will open up new opportunities for improving maize through classical breeding and transgenic approaches.

METHODS

Plants and Growth Conditions

To grow maize (*Zea mays*) plants for experiments, single seeds were buried ~1.5 cm deep in a 7.6 × 7.6-cm plastic pot (~200 cm³) filled with moistened maize mix (produced by mixing 0.16 m³ Metro-Mix 360 [Scotts], 0.45 kg finely ground lime, 0.45 kg Peters Unimix [Scotts], 68 kg Turface MVP [Profile Products], 23 kg coarse quartz sand, and 0.018 m³ pasteurized field soil). Plants were grown in Conviron growth chambers under 16-h-light/8-h-dark photoperiod and 180 μmol photons m^{-2} s^{-1} light at constant 23°C and 60% humidity and were watered from below as needed.

Aphids and Growth Conditions

A maize leaf aphid (*Rhopalosiphum maidis*) colony was started with insects obtained from S. Gray (USDA Plant Soil and Nutrition Laboratory, Ithaca, NY), from a colony that was originally collected in New York State and had been maintained on barley (*Hordeum vulgare*). Aphids were reared on 4- to 8-week-old maize plants (variety B73) under 16-h-light/8-h-dark photoperiod at constant 23°C. Plants were watered from below as needed. Adult aphids were used for all experiments.

Whole-Plant Aphid Bioassays

NAM population parental lines, F1 progeny, and B73 × CML322, B73 × CML277, B73 × CML69, and B73 × CML52 recombinant inbred lines were screened for resistance to *R. maidis* infestation. Plants were used for aphid bioassays at the age of 2 weeks (V2-V3 stage). Ten adult aphids were confined on 2-week-old seedling plants using microperforated polypropylene bags (15.25 cm × 61 cm; PJP Marketplace). Seven days after infestation, the surviving adults and progeny were counted.

Aphid choice assays were performed under conditions similar to the whole-plant aphid bioassays. Seeds of the two inbred lines used for comparisons were planted in opposite corners of individual pots. Ten aphids were released in the center of the pots between the plants. The pots were covered with perforated bags in a manner that allowed contact between the leaves of the two plants. Pots were placed in the growth chamber in randomized orientation. After 24 h, the surviving aphids were counted, and the plant from which they were feeding was recorded.

Artificial Diet Assays

A previously described benzoxazinoid artificial diet assay (Cambier et al., 2001) was modified to measure the effects of benzoxazinoids on *R. maidis* reproduction and survival. DIMBOA-Glc and HDMBOA-Glc were purified from maize as described previously (Glauser et al., 2011). All other chemicals were purchased from Sigma-Aldrich.

Aphid artificial diet was adapted from Prosser and Douglas (1992). Five stock solutions were prepared as follows: Solution A, 4.1 mM FeCl$_3$·6H$_2$O, 1 mM CuCl$_2$·4H$_2$O, 2 mM MnCl$_2$·6H$_2$O, and 10.5 mM ZnSO$_4$; Solution B, 0.1 mM biotin, 4.2 mM pantothenate, 0.9 mM folic acid, 16 mM nicotinic acid, 2.4 mM pyridoxine, 1.5 mM thiamine, 72 mM choline, and 56 mM *myo*-inositol; Solution C, 11 mM Ala, 19 mM Arg, 29 mM Asn, 29 mM Asp, 5 mM Cys, 33 mM Gln, 17 mM Glu, 2.4 mM Gly, 17 mM His, 17 mM Ile, 17 mM Leu, 17 mM Lys, 5.7 mM Met, 5.7 mM Phe, 11 mM Pro, 11 mM Ser, 17 mM Thr, 5.7 mM Trp, 1.2 mM Tyr, and 17 mM Val; Solution D, 19 mM ascorbic acid, 1.7 mM citric acid, 8.1 mM MgSO$_4$·7H$_2$O, and 1660 mM Suc; and Solution E, 660 mM K$_2$HPO$_4$. Diet for aphid bioassays was prepared by mixing 1 mL Solution A, 5 mL Solution B, 50 mL Solution C, 30 mL Solution D, 10 mL Solution E, and 4 mL water. DIMBOA-Glc was added to the diet at 1, 2, 4, and 8 mM concentrations. HDMBOA-Glc was added to the diet at 0.25, 0.5, 1, and 2 mM concentrations.

Fifteen to 20 adult *R. maidis* were added to 30-mL plastic cups, a sheet of Parafilm (Pechiney Packaging Company) was stretched across the 3-cm diameter opening, 80 μL of artificial diet, with and without benzoxazinoids, was pipetted onto the Parafilm, and another sheet of Parafilm was stretched across the top to keep the diet in place. The number of nymphs produced by the adult aphids was counted after 2 d on control diet, diet containing DIMBOA-Glc (1, 2, 4, or 8 mM), or diet containing HDMBOA-Glc (0.25, 0.5, 1, or 2 mM). The number of surviving adult aphids was counted after 2 and 4 d on control diet and diet with 2 mM DIMBOA-Glc or 2 mM HDMBOA-Glc. The continued presence of intact benzoxazinoids and absence of breakdown products in the aphid diet was confirmed at the end of the experiment.

Tissue Collection for Benzoxazinoid Assays

For measurement of leaf benzoxazinoid content, NAM parental lines, B73 × CML322 recombinant inbred lines, and B73 × CML322 F1 progeny were grown in the same manner as for aphid bioassays. When the plants were 2 weeks old, the distal half of the second leaf was harvested and snap-frozen in liquid nitrogen for benzoxazinoid assays.

For measuring benzoxazinoid changes induced by aphid feeding, cages were placed 1 cm away from the leaf tip on the dorsal side of the third leaf of 2-week-old maize seedlings. Ten aphids were added to each cage and, at the end of the feeding period, the ~1-cm leaf segment contained within the cage was harvested for benzoxazinoid assays. To avoid the influence of diurnal cycles on benzoxazinoid abundance, aphids were added to the cages in a staggered manner (0, 2, 4, 8, 24, 48, and 96 h after the start of the experiment), and all tissue samples were harvested at noon, 96 h after the start of the experiment. The harvested tissue samples were snap-frozen in liquid nitrogen and stored at −80°C for later analysis of benzoxazinoids.

Extraction and Analysis of Benzoxazinoids

Benzoxazinoid concentrations were determined according to a previously described protocol (Glauser et al., 2011) with some modifications. Extraction solvents were HPLC-grade methanol (VWR), Milli-Q water (Millipore), and analytical-grade formic acid (Sigma-Aldrich). Fresh plant leaves were frozen in liquid nitrogen, stored at −80°C, and ground to a powder with a mortar and pestle under liquid nitrogen. Twenty milligrams of frozen powder were weighed in a 1.5-mL microcentrifuge tube, and 1 mL of extraction solvent (methanol/water/formic acid, 50:49.5:0.5, v/v) was added. The tubes were vortexed for ~10 s, and five to 10 glass beads (2 mm diameter) were added to each tube. The samples were then extracted in a tissue lyser (Retsch MM300) at 30 Hz for 3 min and centrifuged at 14,000g for 3 min, and the supernatant was transferred to an HPLC vial and stored at −80°C before analysis.

Benzoxazinoid analysis was performed on an Acquity UPLC system (Waters) equipped with an eλ photodiode array detector and coupled to a Synapt G2 quadrupole time-of-flight mass spectrometer (Waters) through an electrospray interface. An Acquity BEH C18 column from Waters (2.1 × 50 mm, 1.7-μm particle size) was used. The following gradient program was employed at a flow rate of 400 μL/min: solvent A = water + formic acid 0.05%, solvent B = acetonitrile + formic acid 0.05%; 2 to 27.2% B in 3.5 min, 27.2 to 100% B in 1.0 min, holding at 100% B for 1.0 min, and reequilibration at 2% B for 1.0 min. The temperatures of the column and autosampler were maintained at 40 and 15°C, respectively. The injection volume was 2.5 μL. UV spectra were acquired over the range 210 to 400 nm at a frequency of 20 Hz and a resolution of 1.2 nm. The extracted trace at 264 nm was used for quantification of benzoxazinoids. The quadrupole time-of-flight mass spectrometer was operated in positive ion mode over a range of 85 to 600 D using a scan time of 0.4 s. Source parameters were as follows: capillary and cone voltages 2800 and 25 V, respectively, source temperature 120°C, desolvation gas flow and

temperature 800 L/h and 330°C, respectively, cone gas flow 20 L/h. Accurate mass measurements were provided by infusing a solution of the synthetic peptide Leu enkephalin through the Lockspray ESI probe. The mobile phase was directed to waste before the mass spectrometry from 0.0 to 1.0 min and 4.0 to 6.5 min. The following extracted ion chromatograms were used with a mass window of ±0.01 D for quantification: mass-to-charge ratio (m/z) 194.045 for DIMBOA-Glc (retention time [RT] 2.14 min) and DIMBOA (RT 2.38 min), m/z 166.050 for HDMBOA–Glc (RT 2.71 min) and HDMBOA (RT 3.22 min), m/z 224.056 for DIM2BOA-Glc (RT 2.18 min), and m/z 178.051 for HMBOA-Glc (RT 2.07 min). Absolute concentrations of benzoxazinoids were determined using external calibration curves obtained from purified DIMBOA, DIMBOA-Glc, and HDMBOA-Glc standards (Glauser et al., 2011). The concentrations of the calibration points were 0.2, 1, 2, 5, 20, and 50 μg/mL for the three benzoxazinoids. Whenever benzoxazinoid concentrations in plant samples were equal to or <5 μg/mL, mass spectrometry traces were used for quantification. For concentrations above 5 μg/mL, the UV trace was employed since the signal exceeded the linear domain of the mass spectrometry. We verified that similar values were obtained with both detection modes for a signal corresponding to a concentration of 5 μg/mL.

Callose Assays

Maize inbred lines B73, CML52, CML69, CML277, CML322, NC350, and NC358 were grown in a growth chamber for 10 d. Callose formation was induced by caging 10 *R. maidis* 1 cm from the leaf tip on the dorsal side of the third leaf for 3 d. Control leaves received cages without aphids for 3 d. After 3 d, the number of aphid offspring in each cage was counted, and the portion of the leaf contained in the cage was stained according to a previously described protocol (Luna et al., 2011). Each leaf segment was decolorized for 48 h in 98% ethanol and stained for 2 h with 0.01% aniline-blue in 0.07 M, pH 9.0, phosphate buffer. Callose spots were counted by microscopy on both sides of the 14-mm leaf segment that was contained within the aphid cage.

Data Analysis

QTL analysis using individual sets of recombinant inbred lines was done by composite interval mapping using the Windows QTL Cartographer software version 2.5 (Wang et al., 2012). The experimental LOD threshold was determined by permutation tests with 500 repetitions at the significance level of 0.05. All analyses were performed using the default settings in the WinQTL program. The program settings were as follows: the CIM program module = Model 6: Standard Model, walking speed = 2 centimorgans, control marker numbers = 5, window size = 10 centimorgans, regression method = backward regression method. Maize genetic marker data were downloaded from www.panzea.org and were used for association mapping using multiple sets of recombinant lines from the NAM population. Statistical tests were conducted using JMP (www.jmp.com) and SAS (www.sas.com).

Preparation of Genomic DNA, RNA, and cDNA

Leaf material was harvested from 14-d-old seedlings, flash-frozen in liquid nitrogen, and stored at −80°C until sample preparation. After grinding of the frozen leaf material to a fine powder in a mortar filled with liquid nitrogen, DNA and RNA were extracted using the DNeasy plant mini kit (Qiagen) and RNeasy plant mini kit (Qiagen), respectively, according to the manufacturer's instructions. Nucleic acid concentration, purity, and quality were assessed using a spectrophotometer (NanoDrop 2000c; Thermo Scientific) and an Agilent 2100 Bioanalyzer (Agilent Technologies). Prior to cDNA synthesis, 0.75 μg RNA was DNase treated using 1 μL DNase (Fermentas). Single-stranded cDNA was prepared from the DNase-treated RNA using SuperScript III reverse transcriptase and oligo(dT$_{20}$) primers (Invitrogen).

Cloning and Expression of *O*-Methyltransferase Genes

The complete open reading frames of *Bx10a-B73*, *Bx10b-B73*, and *Bx10c-CML322* were amplified from cDNA with the primer pairs listed in Supplemental Table 1 online. PCR products were cloned as blunt fragments into the sequencing vector pCR-Blunt II-TOPO (Invitrogen) and both strands were fully sequenced. For heterologous expression with an N-terminal His-tag, the genes were inserted as *Bsa*I fragments into the expression vector pASK-IBA37 plus (IBA). The constructs were introduced into the *Escherichia coli* strain TOP10 (Invitrogen). Liquid cultures of the bacteria harboring the expression constructs were grown at 37°C to an OD$_{600}$ of 0.6 to 0.8. Anhydrotetracycline (IBA) was added to a final concentration of 200 μg L^{-1}, and the cultures were incubated for 20 h at 18°C. The cells were sedimented for 5 min at 5000g and 4°C. For breaking up the cells, the pellet was resuspended in ice-cold 4 mL 50 mM Tris-HCl, pH 8.0, containing 0.5 M NaCl, 20 mM imidazole, 50 mM mercaptoethanol, and 10% glycerol and subsequently exposed to ultrasonication (4 × 20 s; Bandelin UW2070). The debris was separated by centrifugation for 20 min at 16,100g and 4°C. N-terminal His-tagged proteins were purified using nickel-nitrilotriacetic acid spin columns (Qiagen) according to the manufacturer's instructions. The purified proteins were eluted with 50 mM Tris-HCl, pH 8.0, containing 0.5 M NaCl, 250 mM imidazole, and 10% glycerol. The salt was removed by gel filtration using Illustra NAP-10 columns (GE Healthcare), and the proteins were redissolved in 50 mM MOPS, pH 7.0, containing 50% glycerol.

O-Methyltransferase Assays

The in vitro *O*-methyltransferase activity of BX10a-B73, BX10b-B73, and BX10c-CML322 was proven using enzyme assays containing purified recombinant protein, the substrate DIMBOA-Glc, and the cosubstrate S-adenosyl-L-Met. The assays were performed with 4 mM DTT, 0.4 mM S-adenosyl-L-Met, 0.2 mM DIMBOA-Glc, and 0.5 μg desalted enzyme buffered by 50 μM MOPS, pH 7.0, in a volume of 50 μL. The assays were performed in glass vials and incubated for 20 min at 25°C at 400 rpm using a ThermoMixer comfort 5355 (Eppendorf). The reaction was stopped by adding 1 volume of methanol, and the mixture was centrifuged for 10 min at 4200g and 4°C. HDMBOA-Glc formation was determined by reversed phase liquid chromatography using an Agilent 1200 HPLC system (Agilent Technologies). For separation, a Kinetex 2.6 μm C18 100 × 4.6-mm column was used (Phenomenex). Formic acid (0.05%) and acetonitrile were used as eluents A and B, respectively. Elution was initiated isocratically for 0.5 min at 10% eluent B and continued with linear gradients to 40 and 100% eluent B in 30 min and 1 min, respectively. The column was reequilibrated for 4 min. The flow rate was set to 1.1 mL/min. Five microliters of the sample was injected, and the absorbance was measured at the maximum of 270 nm. Metabolite identities were confirmed using authentic standard compounds.

Sequence Analysis and Phylogenetic Tree Reconstruction

A nucleotide sequence alignment of maize methyltransferase genes similar to *Bx10a*, *Bx10b*, and *Bx10c* was computed using the MUSCLE (codon) algorithm (see Supplemental Data Set 1 online; gap open, −2.9; gap extend, 0; hydrophobicity multiplier, 1.2; clustering method, UPGMB) implemented in MEGA5 (Tamura et al., 2011). Based on the MUSCLE alignment, a phylogenetic tree was reconstructed with MEGA5 using a maximum likelihood algorithm (general time-reversible model, gamma distributed rates among sites). Codon positions included were 1st+2nd +3rd+Noncoding. All positions with <90% site coverage were eliminated. Ambiguous bases were allowed at any position. A bootstrap resampling analysis with 1000 replicates was performed to evaluate the tree topology. Two recently described maize methyltransferase genes, *Anthranilic acid methyltransferase1* (*Aamt1*) and *O-Methyltransferase8* (*Omt8*), which both

belong to a different class of *O*-methyltransferases, were included as an outgroup.

Transposon Analysis

To test for the presence of a *Doppia*-like transposon in the first exon of *Bx10c* alleles, PCR was performed with genomic DNA as template and the gene specific primer TPA1 located on exon 1 and the transposon specific primer TPA2 (Supplemental Table 2 online). Conversely, the absence of the transposon was analyzed using two gene specific primers (TPA1 and TPA3) binding on gene regions upstream and downstream, respectively, of the transposon insertion site. The resulting PCR products (671 bp and 398 bp, respectively) were cloned as blunt fragments into the sequencing vector pCR®-Blunt II-TOPO® and both strands were fully sequenced.

qRT-PCR Analysis

For the amplification of *Bx10* gene fragments with a length of ~150 bp, primer pairs specific for *Bx10a/b* and *Bx10c* were designed having a Tm $\geq$ 58°C, a GC content between 35 and 55%, and a primer length in the range of 20 to 25 nucleotides (see Supplemental Table 2 online for primer information). Primer specificity was confirmed by agarose gel electrophoresis, melting curve analysis, and sequence verification of cloned PCR amplicons. Primer pair efficiency was determined using the standard curve method with fivefold serial dilution of cDNA and found to be between 90 and 105%. The actin gene Zm-*Actin1* (accession number MZEACT1G) was used as a reference gene. The cDNA was prepared as described above, and 1 µL cDNA was used in all 20-µL reactions. Samples were run in triplicates using Brilliant III SYBR Green QPCR Master Mix (Stratagene) with ROX as the reference dye. The following PCR conditions were applied for all reactions: initial incubation at 95°C for 3 min followed by 40 cycles of amplification (95°C for 20 s and 60°C for 20 s). Plate reads were taken during the annealing and the extension step of each cycle. Data for the melting curves were gathered at the end of cycling from 55 to 95°C.

All samples were run on the same PCR machine (MxPro Mx3000P; Stratagene, Agilent Technologies) in an optical 96-well plate. Five biological replicates were analyzed as triplicates in the quantitative PCR for each of the two inbred lines. Data for the relative quantity to calibrator average (dRn) were exported from the MXPro Software.

Accession Numbers

Sequence data from this article can be found in GenBank/EMBL data libraries under the following accession numbers: *Aamt1*, HM242244; *Omt8*, HM242248; *Zrp4*, NP_001105689; *Bx7-Cl31A*, NP_001120719; *Bx10a-B73*, KC754962; *Bx10b-B73*, KC754963; *Bx10c-CML322*, KC754964; GRMZM2G100754, AFW64970; GRMZM2G097297, AFW64969; GRMZM2G023152, AFW60893; GRMZM2G124799, AFW78713; GRMZM 2G102863, AFW78712; GRMZM2G141026, AFW78711; GRMZM2G140996, AFW78710; GRMZM2G041866, AFW65591; GRMZM2G099297, AFW64033; GRMZM2G106172, AFW87991; GRMZM2G093092, AFW87990; GRMZM 2G127418, DAA39165; GRMZM2G408458, AFW60754; GRMZM2G059465, DAA48819; GRMZM2G104730, AFW55836; GRMZM2G104710, AFW55834; GRMZM2G177424, DAA60533; GRMZM2G091774, AFW56785; GRMZM 2G349791, AFW60116; GRMZM2G147491, DAA38843; and GRMZM2G 085924, DAA38899.

Supplemental Data

The following materials are available in the online version of this article.

Supplemental Figure 1. Aphid Susceptibility Is Caused by a Dominant Allele on CML322 Chromosome 1.

Supplemental Figure 2. Maize Chromosome LOD Plots Showing Location of Aphid Resistance QTL.

Supplemental Figure 3. Correlation of DIMBOA-Glc Content with Other Benzoxazinoids in Parental Lines of the NAM Population.

Supplemental Figure 4. Correlation of Aphid Resistance and Benzoxazinoid Content of Maize Leaves.

Supplemental Figure 5. High HDMBOA-Glc Accumulation Is Caused by a Dominant Allele on CML322 Chromosome 1.

Supplemental Figure 6. Aphid Choice Experiments, Comparing B73 to More Susceptible Inbred Lines.

Supplemental Table 1. Predicted B73 Genes in the Area of the Bin 1.04 *R. maidis* Resistance QTL.

Supplemental Table 2. Primers Used in This Study.

Supplemental Data Set 1. Nucleotide Sequence Alignment of Putative Methyltransferase Genes Similar to *Bx10a*, *Bx10b*, and *Bx10c*.

AUTHOR CONTRIBUTIONS

L.N.M., V.H., J.G., M.E., T.G.K., and G.J. designed the research. L.N.M., V.H., G.G., H.B., H.K., and M.M.H. performed research. L.N.M., V.H., J.G., H.K., A.E.L., E.S.B., M.E., T.G.K., and G.J. analyzed data. M.E., T.G.K., and G.J. wrote the article. L.N.M. and V.H. contributed equally to the study and share first authorship. M.E., T.G.K. and G.J. contributed equally to the study and share senior authorship.

REFERENCES

Ahmad, S., Veyrat, N., Gordon-Weeks, R., Zhang, Y.H., Martin, J., Smart, L., Glauser, G., Erb, M., Flors, V., Frey, M., and Ton, J. (2011). Benzoxazinoid metabolites regulate innate immunity against aphids and fungi in maize. Plant Physiol. **157:** 317–327.

Bass, H.W., OBrian, G.R., and Boston, R.S. (1995). Cloning and sequencing of a second ribosome-inactivating protein gene from maize (*Zea mays* L.). Plant Physiol. **107:** 661–662.

Bercury, S.D., Panavas, T., Irenze, K., and Walker, E.L. (2001). Molecular analysis of the *Doppia* transposable element of maize. Plant Mol. Biol. **47:** 341–351.

Botha, C.E.J., and Matsiliza, B. (2004). Reduction in transport in wheat (*Triticum aestivum*) is caused by sustained phloem feeding by the Russian wheat aphid (*Diuraphis noxia*). S. Afr. J. Bot. **70:** 249–254.

Brooks, T.D., Willcox, M.C., Williams, W.P., and Buckley, P.M. (2005). Quantitative trait loci conferring resistance to fall armyworm and southwestern corn borer leaf feeding damage. Crop Sci. **45:** 2430–2434.

Butrón, A., Chen, Y.C., Rottinghaus, G.E., and McMullen, M.D. (2010). Genetic variation at *bx1* controls DIMBOA content in maize. Theor. Appl. Genet. **120:** 721–734.

Byrne, P.F., McMullen, M.D., Wiseman, B.R., Snook, M.E., Musket, T.A., Theuri, J.M., Widstrom, N.W., and Coe, E.H. (1998). Maize silk maysin concentration and corn earworm antibiosis: QTLs and genetic mechanisms. Crop Sci. **38:** 461–471.

Caillaud, C.M., and Niemeyer, H.M. (1996). Possible involvement of the phloem sealing system in the acceptance of a plant as host by an aphid. Experientia **52:** 927–931.

Cambier, V., Hance, T., and de Hoffmann, E. (2000). Variation of DIMBOA and related compounds content in relation to the age and plant organ in maize. Phytochemistry **53:** 223–229.

Cambier, V., Hance, T., and De Hoffmann, E. (2001). Effects of 1,4-benzoxazin-3-one derivatives from maize on survival and fecundity of *Metopolophium dirhodum* (Walker) on artificial diet. J. Chem. Ecol. **27:** 359–370.

Chia, J.M., et al. (2012). Maize HapMap2 identifies extant variation from a genome in flux. Nat. Genet. **44:** 803–807.

Clay, N.K., Adio, A.M., Denoux, C., Jander, G., and Ausubel, F.M. (2009). Glucosinolate metabolites required for an *Arabidopsis* innate immune response. Science **323:** 95–101.

Cortés-Cruz, M., Snook, M., and McMullen, M.D. (2003). The genetic basis of C-glycosyl flavone B-ring modification in maize (*Zea mays* L.) silks. Genome **46:** 182–194.

Dafoe, N.J., Huffaker, A., Vaughan, M.M., Duehl, A.J., Teal, P.E., and Schmelz, E.A. (2011). Rapidly induced chemical defenses in maize stems and their effects on short-term growth of *Ostrinia nubilalis*. J. Chem. Ecol. **37:** 984–991.

Dreyer, D.L., and Campbell, B.C. (1987). Chemical basis of host-plant resistance to aphids. Plant Cell Environ. **10:** 353–361.

Flint-Garcia, S.A., Thuillet, A.C., Yu, J., Pressoir, G., Romero, S.M., Mitchell, S.E., Doebley, J., Kresovich, S., Goodman, M.M., and Buckler, E.S. (2005). Maize association population: A high-resolution platform for quantitative trait locus dissection. Plant J. **44:** 1054–1064.

Frey, M., Chomet, P., Glawischnig, E., Stettner, C., Grün, S., Winklmair, A., Eisenreich, W., Bacher, A., Meeley, R.B., Briggs, S.P., Simcox, K., and Gierl, A. (1997). Analysis of a chemical plant defense mechanism in grasses. Science **277:** 696–699.

Ganal, M.W., et al. (2011). A large maize (*Zea mays* L.) SNP genotyping array: development and germplasm genotyping, and genetic mapping to compare with the B73 reference genome. PLoS ONE **6:** e28334.

Givovich, A., and Niemeyer, H.M. (1995). Comparison of the effect of hydroxamic acids from wheat on 5 species of cereal aphids. Entomol. Exp. Appl. **74:** 115–119.

Givovich, A., Morse, S., Cerda, H., Niemeyer, H.M., Wratten, S.D., and Edwards, P.J. (1992). Hydroxamic acid glucosides in honeydew of aphids feeding on wheat. J. Chem. Ecol. **18:** 841–846.

Givovich, A., Sandstrom, J., Niemeyer, H.M., and Pettersson, J. (1994). Presence of a hydroxamic acid glucoside in wheat phloem sap, and its consequences for performance of *Rhopalosiphum padi* (L) (Homoptera, Aphididae). J. Chem. Ecol. **20:** 1923–1930.

Glauser, G., Marti, G., Villard, N., Doyen, G.A., Wolfender, J.L., Turlings, T.C., and Erb, M. (2011). Induction and detoxification of maize 1,4-benzoxazin-3-ones by insect herbivores. Plant J. **68:** 901–911.

Gore, M.A., Chia, J.M., Elshire, R.J., Sun, Q., Ersoz, E.S., Hurwitz, B.L., Peiffer, J.A., McMullen, M.D., Grills, G.S., Ross-Ibarra, J., Ware, D.H., and Buckler, E.S. (2009). A first-generation haplotype map of maize. Science **326:** 1115–1117.

Grambow, H.J., Luckge, J., Klausener, A., and Muller, E. (1986). Occurrence of 2-(2-hydroxy-4,7-dimethoxy-2h-1,4-benzoxazin-3-One)-beta-D-glucopyranoside in *Triticum aestivum* leaves and its conversion into 6-methoxy-benzoxazolinone. Zeitschrift für Naturforschung **41:** 684–690.

Groh, S., Khairallah, M.M., González-de-León, D., Willcox, M., Jiang, C., Hoisington, D.A., and Melchinger, A.E. (1998). Comparison of QTLs mapped in RILs and their test-cross progenies of tropical maize for insect resistance and agronomic traits. Plant Breed. **117:** 193–202.

Huffaker, A., Dafoe, N.J., and Schmelz, E.A. (2011). ZmPep1, an ortholog of *Arabidopsis* elicitor peptide 1, regulates maize innate immunity and enhances disease resistance. Plant Physiol. **155:** 1325–1338.

Johnson, M.T.J. (2011). Evolutionary ecology of plant defences against herbivores. Funct. Ecol. **25:** 305–311.

Jonczyk, R., Schmidt, H., Osterrieder, A., Fiesselmann, A., Schullehner, K., Haslbeck, M., Sicker, D., Hofmann, D., Yalpani, N., Simmons, C., Frey, M., and Gierl, A. (2008). Elucidation of the final reactions of DIMBOA-glucoside biosynthesis in maize: Characterization of Bx6 and Bx7. Plant Physiol. **146:** 1053–1063.

Keurentjes, J.J.B., Willems, G., van Eeuwijk, F., Nordborg, M., and Koornneef, M. (2011). A comparison of population types used for QTL mapping in *Arabidopsis thaliana*. Plant Gen. Res. **9:** 185–188.

Klingler, J.P., Nair, R.M., Edwards, O.R., and Singh, K.B. (2009). A single gene, *AIN*, in *Medicago truncatula* mediates a hypersensitive response to both bluegreen aphid and pea aphid, but confers resistance only to bluegreen aphid. J. Exp. Bot. **60:** 4115–4127.

Kozlov, M. (2008). Losses of birch foliage due to insect herbivory along geographical gradients in Europe: A climate-driven pattern? Clim. Change **87:** 107–117.

Kroymann, J., Donnerhacke, S., Schnabelrauch, D., and Mitchell-Olds, T. (2003). Evolutionary dynamics of an *Arabidopsis* insect resistance quantitative trait locus. Proc. Natl. Acad. Sci. USA **100** (suppl. 2)**:** 14587–14592.

Kump, K.L., Bradbury, P.J., Wisser, R.J., Buckler, E.S., Belcher, A.R., Oropeza-Rosas, M.A., Zwonitzer, J.C., Kresovich, S., McMullen, M.D., Ware, D., Balint-Kurti, P.J., and Holland, J.B. (2011). Genome-wide association study of quantitative resistance to southern leaf blight in the maize nested association mapping population. Nat. Genet. **43:** 163–168.

Lawrence, S.D., Novak, N.G., Kayal, W.E., Ju, C.J.T., and Cooke, J.E.K. (2012). Root herbivory: Molecular analysis of the maize transcriptome upon infestation by Southern corn rootworm, *Diabrotica undecimpunctata howardi*. Physiol. Plant. **144:** 303–319.

Luna, E., Pastor, V., Robert, J., Flors, V., Mauch-Mani, B., and Ton, J. (2011). Callose deposition: A multifaceted plant defense response. Mol. Plant Microbe Interact. **24:** 183–193.

Maresh, J., Zhang, J., and Lynn, D.G. (2006). The innate immunity of maize and the dynamic chemical strategies regulating two-component signal transduction in *Agrobacterium tumefaciens*. ACS Chem. Biol. **1:** 165–175.

Marti, G., Erb, M., Boccard, J., Glauser, G., Doyen, G.R., Villard, N., Robert, C.A., Turlings, T.C., Rudaz, S., and Wolfender, J.L. (2013). Metabolomics reveals herbivore-induced metabolites of resistance and susceptibility in maize leaves and roots. Plant Cell Environ. **36:** 621–639.

Mayhew, P.J. (2001). Herbivore host choice and optimal bad motherhood. Trends Ecol. Evol. (Amst.) **16:** 165–167.

McMullen, M., Frey, M., and Degenhardt, J. (2009a). Genetics and biochemistry of insect resistance in maize. In Handbook of Maize: Its Biology, J.L. Bennetzen and S. Hake, eds (New York: Springer), pp. 271–289.

McMullen, M.D., et al. (2009b). Genetic properties of the maize nested association mapping population. Science **325:** 737–740.

Meihls, L.N., Kaur, H., and Jander, G. (December 6, 2012). Natural variation in maize defense against insect herbivores. Cold Spring Harb. Symp. Quant. Biol. (online) doi/10.1101/sqb.2012.77.014662.

Miller, N., Estoup, A., Toepfer, S., Bourguet, D., Lapchin, L., Derridj, S., Kim, K.S., Reynaud, P., Furlan, L., and Guillemaud, T. (2005). Multiple transatlantic introductions of the western corn rootworm. Science **310:** 992.

Niemeyer, H.M. (2009). Hydroxamic acids derived from 2-hydroxy-2H-1,4-benzoxazin-3(4H)-one: Key defense chemicals of cereals. J. Agric. Food Chem. **57:** 1677–1696.

Oikawa, A., Ishihara, A., and Iwamura, H. (2002). Induction of HDMBOA-Glc accumulation and DIMBOA-Glc 4-O-methyltransferase by jasmonic acid in poaceous plants. Phytochemistry **61:** 331–337.

Oikawa, A., Ishihara, A., Tanaka, C., Mori, N., Tsuda, M., and Iwamura, H. (2004). Accumulation of HDMBOA-Glc is induced by biotic stresses prior to the release of MBOA in maize leaves. Phytochemistry **65:** 2995–3001.

Pechan, T., Ye, L.J., Chang, Y.M., Mitra, A., Lin, L., Davis, F.M., Williams, W.P., and Luthe, D.S. (2000). A unique 33-kD cysteine proteinase accumulates in response to larval feeding in maize genotypes resistant to fall armyworm and other Lepidoptera. Plant Cell **12:** 1031–1040.

Pélissier, H.C., Peters, W.S., Collier, R., van Bel, A.J., and Knoblauch, M. (2008). GFP tagging of sieve element occlusion (SEO) proteins results in green fluorescent forisomes. Plant Cell Physiol. **49:** 1699–1710.

Pfalz, M., Mikkelsen, M.D., Bednarek, P., Olsen, C.E., Halkier, B.A., and Kroymann, J. (2011). Metabolic engineering in *Nicotiana benthamiana* reveals key enzyme functions in *Arabidopsis* indole glucosinolate modification. Plant Cell **23:** 716–729.

Pfalz, M., Vogel, H., and Kroymann, J. (2009). The gene controlling the indole glucosinolate modifier1 quantitative trait locus alters indole glucosinolate structures and aphid resistance in *Arabidopsis*. Plant Cell **21:** 985–999.

Poland, J.A., Bradbury, P.J., Buckler, E.S., and Nelson, R.J. (2011). Genome-wide nested association mapping of quantitative resistance to northern leaf blight in maize. Proc. Natl. Acad. Sci. USA **108:** 6893–6898.

Prasad, K.V., et al. (2012). A gain-of-function polymorphism controlling complex traits and fitness in nature. Science **337:** 1081–1084.

Prosser, W.A., and Douglas, A.E. (1992). A test of the hypotheses that nitrogen is upgraded and recycled in an aphid *Acyrthosiphon pisum* symbiosis. J. Insect Physiol. **38:** 93–99.

Qiu, Y.F., Guo, J.P., Jing, S.L., Zhu, L.L., and He, G.C. (2010). High-resolution mapping of the brown planthopper resistance gene *Bph6* in rice and characterizing its resistance in the 9311 and Nipponbare near isogenic backgrounds. Theor. Appl. Genet. **121:** 1601–1611.

Rasmann, S., and Agrawal, A.A. (2011). Latitudinal patterns in plant defense: Evolution of cardenolides, their toxicity and induction following herbivory. Ecol. Lett. **14:** 476–483.

Rector, B.G., Liang, G.M., and Guo, Y. (2003). Effect of maysin on wild-type, deltamethrin-resistant, and Bt-resistant *Helicoverpa armigera* (Lepidoptera: Noctuidae). J. Econ. Entomol. **96:** 909–913.

Robert, C.A., et al. (2012). A specialist root herbivore exploits defensive metabolites to locate nutritious tissues. Ecol. Lett. **15:** 55–64.

Schnable, P.S., et al. (2009). The B73 maize genome: Complexity, diversity, and dynamics. Science **326:** 1112–1115.

Schullehner, K., Dick, R., Vitzthum, F., Schwab, W., Brandt, W., Frey, M., and Gierl, A. (2008). Benzoxazinoid biosynthesis in dicot plants. Phytochemistry **69:** 2668–2677.

Steffey, K., Rice, M.E., All, J., Andrew, D.A., Gray, M.E., and Van Duyn, J.W. (1999). Handbook of Corn Insects. (Lanham, MD: Entomological Society of America).

Steiner, W.W.M., Voegtlin, D.J., and Irwin, M.E. (1985). Genetic differentiation and its bearing on migration in North-American populations of the corn leaf aphid, *Rhopalosiphum maidis* (Fitch) (Homoptera, Aphididae). Ann. Entomol. Soc. Am. **78:** 518–525.

Tamura, K., Peterson, D., Peterson, N., Stecher, G., Nei, M., and Kumar, S. (2011). MEGA5: Molecular evolutionary genetics analysis using maximum likelihood, evolutionary distance, and maximum parsimony methods. Mol. Biol. Evol. **28:** 2731–2739.

Ullstrup, A.J., and Renfro, B.L. (1976). A comparison of maize diseases in temperate and in tropical environments. Int. J. Pest Manage. **22:** 491–498.

Walling, L.L. (2000). The myriad plant responses to herbivores. J. Plant Growth Regul. **19:** 195–216.

Walsh, T.A., Morgan, A.E., and Hey, T.D. (1991). Characterization and molecular cloning of a proenzyme form of a ribosome-inactivating protein from maize. Novel mechanism of proenzyme activation by proteolytic removal of a 2.8-kilodalton internal peptide segment. J. Biol. Chem. **266:** 23422–23427.

Wang, S.M., Basten, C.J., and Zeng, Z.B. (2012). Windows QTL Cartographer 2.5. (Raleigh, NC: North Carolina State University).

Wei, F., et al. (2009). The physical and genetic framework of the maize B73 genome. PLoS Genet. **5:** e1000715.

Yu, J., Holland, J.B., McMullen, M.D., and Buckler, E.S. (2008). Genetic design and statistical power of nested association mapping in maize. Genetics **178:** 539–551.

Zhou, S., et al. (2009). A single molecule scaffold for the maize genome. PLoS Genet. **5:** e1000711.

Zuniga, G.E., Argandona, V.H., Niemeyer, H.M., and Corcuera, L.J. (1983). Hydroxamic acid content in wild and cultivated Gramineae. Phytochemistry **22:** 2665–2668.

Züst, T., Heichinger, C., Grossniklaus, U., Harrington, R., Kliebenstein, D.J., and Turnbull, L.A. (2012). Natural enemies drive geographic variation in plant defenses. Science **338:** 116–119.

3.2 Manuscript II

The maize cytochrome P450 CYP79A61 produces
phenylacetaldoxime and indole-3-acetaldoxime in heterologous
systems and might contribute to plant defense and auxin formation

**BMC
Plant Biology**

RESEARCH ARTICLE

Open Access

The maize cytochrome P450 CYP79A61 produces phenylacetaldoxime and indole-3-acetaldoxime in heterologous systems and might contribute to plant defense and auxin formation

Sandra Irmisch, Philipp Zeltner, Vinzenz Handrick, Jonathan Gershenzon and Tobias G. Köllner[*]

Abstract

Background: Plants produce a group of aldoxime metabolites that are well known as volatiles and as intermediates in cyanogenic glycoside and glucosinolate biosynthesis in particular plant families. Recently it has been demonstrated that aldoximes can also accumulate as part of direct plant defense in poplar. Cytochrome P450 enzymes of the CYP79 family were shown to be responsible for the formation of aldoximes from their amino acid precursors.

Results: Here we describe the identification and characterization of maize CYP79A61 which was heterologously expressed in yeast and *Nicotiana benthamiana* and shown to catalyze the formation of (*E/Z*)-phenylacetaldoxime and (*E/Z*)-indole-3-acetaldoxime from L-phenylalanine and L-tryptophan, respectively. Simulated herbivory on maize leaves resulted in an increased *CYP79A61* transcript accumulation and in elevated levels of L-phenylalanine and (*E/Z*)-phenylacetaldoxime. Although L-tryptophan levels were also increased after the treatment, (*E/Z*)-indole-3-acetaldoxime could not be detected in the damaged leaves. However, simulated herbivory caused a significant increase in auxin concentration.

Conclusions: Our data suggest that CYP79A61 might contribute to the formation of (*E/Z*)-phenylacetaldoxime in maize. Since aldoximes have been described as toxic compounds for insect herbivores and pathogens, the increased accumulation of (*E/Z*)-phenylacetaldoxime after simulated herbivory indicates that this compound plays a role in plant defense. In addition, it is conceivable that (*E/Z*)-indole-3-acetaldoxime produced by recombinant CYP79A61 could be further converted into the plant hormone indole-3-acetic acid after herbivore feeding in maize.

Keywords: Maize, P450, CYP79, Herbivory, Aldoxime, Auxin, Cyanogenic glycoside

Background

Aldoximes, a group of nitrogen-containing plant secondary metabolites, have been intensively studied as key intermediates in the biosynthesis of plant defense compounds such as glucosinolates, cyanogenic glycosides, and various phytoalexins [1–3]. Moreover, these compounds are known to be released as volatiles from flowers and vegetative organs of a multitude of plant species [4]. In general, aldoximes are produced from their corresponding amino acid precursors through the action of cytochrome P450 monooxygenases (CYPs) of the CYP79 family (recently reviewed in [5]). Members of this family have been identified from several plant species and the presence of putative *CYP79* genes in all angiosperm genomes sequenced so far suggests a widespread distribution of CYP79s in higher plants [6]. The first reported CYP79 enzyme, CYP79A1, was isolated from sorghum (*Sorghum bicolor*) and catalyzes the conversion of L-tyrosine to *p*-hydroxy-phenylacetaldoxime which is the precursor of dhurrin, the major cyanogenic glycoside in sorghum [7]. CYP79B2 and CYP79B3 from Arabidopsis are two examples of CYP79

* Correspondence: koellner@ice.mpg.de
Department of Biochemistry, Max Planck Institute for Chemical Ecology, Hans-Knöll Straße 8, 07745 Jena, Germany

M a n u s c r i p t   I I

Irmisch *et al. BMC Plant Biology* (2015) 15:128

Page 2 of 14

enzymes involved in glucosinolate and phytoalexin formation. Both enzymes accept L-tryptophan as substrate and produce indole-3-acetaldoxime which is further converted into indole glucosinolates and camalexin in Arabidopsis [8, 9]. The aldoxime intermediates produced by CYP79 enzymes do not accumulate in the plant but are channeled within a large protein complex called a metabolon [10].

Recently, it has been shown that CYP79 enzymes are also responsible for the production of volatile aldoximes. The two enzymes CYP79D6v3 and CYP79D7v2 from *Populus trichocarpa* catalyze the formation of (*E/Z*)-2-methylbutyraldoxime, (*E/Z*)-3-methylbutyraldoxime, and (*E/Z*)-isobutyraldoxime from L-isoleucine, L-leucine, and L-valine, respectively [6]. The aldoximes produced are characteristic components of the herbivore-induced volatile blend of poplar and it has been demonstrated that they are involved in the attraction of natural enemies of herbivores [11]. In addition to the volatile aliphatic aldoximes which are released from poplar without detectable accumulation in the plant, CYP79D6v3 and CYP79D7v2 also produce the less volatile (*E/Z*)-phenylacetaldoxime. This compound was found to accumulate in poplar leaves after herbivore feeding and bioassays using pure (*E/Z*)-phenylacetaldoxime revealed a toxic effect against a generalist lepidopteran herbivore, suggesting that aldoxime accumulation may contribute to direct plant defense against insects [6].

During the last two decades, maize (*Zea mays*) has become an important model species for studying plant-insect interactions on a physiological and molecular level. As many other plants, maize responds to caterpillar feeding by the expression of a complex arsenal of defense reactions such as the accumulation of secondary compounds [12, 13], the formation of defensive proteins [14, 15], and the release of volatiles [16]. Despite the intensive research on maize, there is little information about the occurrence of aldoximes and aldoxime-derived defense compounds in this plant species. A few early papers reported maize as a cyanogenic species. However, the measured hydrogen cyanide content was rather low in comparison to sorghum and other cyanogenic plants, and a cyanogenic glycoside could not be identified in maize so far [17–19]. The emission of aliphatic aldoximes from herbivore-damaged maize has been reported for two different cultivars [20, 21] but it seems that the majority of maize germplasm is not able to generate such compounds [22, 23]. However, a recent survey of all available plant genomes revealed the presence of four putative *CYP79* genes in the maize genome [6]. We have now begun to study these enzymes and their contribution to aldoxime production in maize.

This paper reports the characterization of CYP79A61, an enzyme able to convert L-phenylalanine and L-tryptophan into phenylacetaldoxime and indole-3-acetaldoxime, respectively. Simulated herbivory on maize leaves resulted in the upregulation of *CYP79A61* gene expression and in an increase in amino acid substrate accumulation, corresponding to higher levels of phenylacetaldoxime in treated plants in comparison to undamaged control plants. Since indole-3-acetic acid (IAA) was also significantly upregulated after the treatment, we propose that CYP79A61 plays a role in herbivore-induced auxin formation.

Results
Maize possesses four *CYP79* genes
In a previous study on poplar CYP79 enzymes [6], we performed a BLAST analysis with all available angiosperm genomes to study the distribution of *CYP79* genes in higher plants. Among others this analysis revealed the presence of four putative *CYP79* sequences in the genome of the maize inbred line B73. The open reading frames of the four genes GRMZM2G138248, GRMZM2G011156, GRMZM2G105185, and GRMZM2G178351 encode for proteins with 552, 546, 559, and 550 amino acids, respectively (Fig. 1). Motifs reported to be conserved in CYP79 proteins such as the heme binding site (SFSxGRRxCxA/G), the PERH motif, and the NP motif in one of the substrate binding sites were also found in the identified maize CYP79 sequences (Fig. 1). A phylogenetic analysis using these sequences and already characterized CYP79s from other plant species showed that GRMZM2G138248 clustered together with sorghum CYP79A1 (72 % amino acid identity) while the other three maize proteins GRMZM2G011156, GRMZM2G105185, and GRMZM2G178351 formed a separate clade in the basal part of the phylogenetic tree (Fig. 2). A synteny analysis of the maize and sorghum genomes revealed that GRMZM2G138248 and sorghum *CYP79A1* seem not to represent orthologous genes since they were found to be located in non-syntenic genomic regions (Additional file 1: Figure S1). However, the putative sorghum *CYP79* gene Sb10g022470 which encodes a protein with 83.3 % amino acid sequence similarity to GRMZM2G138248 could be identified as a likely orthologue of GRMZM2G138248 (Additional file 1: Figures S2 and S3).

We tried to amplify the maize *CYP79* genes from cDNA made from herbivore-damaged seedlings of the commercial hybrid line Delprim, a cultivar commonly used in maize-insect interaction studies. While the complete open reading frame of GRMZM2G138248 could be isolated from the cDNA, the amplification of GRMZM2G011156, GRMZM2G105185, and GRMZM2G178351 failed, suggesting that these genes were not present in Delprim or not expressed in seedlings under the experimental conditions. The GRMZM2G138248 gene obtained was designated *CYP79A61* following the standard P450 nomenclature (D.R. Nelson, P450 Nomenclature Committee).

```
SbCYP79A1      MATMEVEAAAATV--LAAPLLSSSAILKLLLFVVTLSYLARALR--RPRKSTTKCSSTTCASPPAGVGNP  66
GRMZM2G138248  -MVSSPQANKFPLRKQISSPSSSCMTPHVLLVLVILLYLVRTLRPWRSRRNSTCCT-------------P  56
GRMZM2G105185  -MALAPSHAHASL--AVAPFTVLCTFLALVALLLLHRYRRSNARPSKKTRQLHRR---------------  52
GRMZM2G178351  -MALAPSHAHASL--AVAPFTVLCTFLALVALLFLHRYRRSNARPSKKTRQ-----------------   48
GRMZM2G011156  -MALAPSHA---L--VVAPFTALCAFLAL-ALLFL--YSKATS-SSKKTQQL----------------   42

SbCYP79A1      PLPPGPVPWPVVGNLPEMLL-NKPAFRWIHQMMREMGTDIACVKLGGVHVVSITCPEIAREVLRKQDANF  135
GRMZM2G138248  SLPPGPVPWPVVGNLPEMMLSDKPAFHWIHHIMKEAGTDIACIKLGGVHVIPISCPKIALEVLSNQDANF  126
GRMZM2G105185  -LPPGPAGLPIIGSM-HCLVSKKPVFRWVHGLLKDMNTKILCLRFGAVHVVVVACPEIAREVFRTNDAAL  120
GRMZM2G178351  -LPPGPAGLPIIGSL-HCLVSKKPVFRWVHGLLKDMNTKILCLRFGAVHVVVVACPEIAREVLRTNDAAL  116
GRMZM2G011156  -LPPGPAGLPIIGSL-HCVSKRPVFRWIHGLLKDMDTNVLCLRFGAVHVVVACPETAREVLRTNDAVL  110

SbCYP79A1      ISRPLTFASETFSGGYRNAVLSPYGDQWKKMRRVLTSEIICPSRHAWLHDKRTDEADNLTRYVYNLATKA  205
GRMZM2G138248  ASRPLTFASKTFSTGYRDAAMSHCGDHWKKMGRVLASEIVCPSRHRWLHDKRADEADNLTRYVYNLATKA  196
GRMZM2G105185  ASRPETDACELFSLGYKGASLSPYGEQWRKMRRVLTSEILSASMEQRQQRRAQEADYLVRSLYSQCCSS  190
GRMZM2G178351  ASRPETDACELFSLGYKGAILSPYGEQWRKMRRVLTSEILSASMEQRQQRRAQEADYLVASLYSQCCSS  186
GRMZM2G011156  ASRPETVASALFSFGYKGSILTPYGEQWKKMRRVLSSEILSASMEQRLQRRAQEADYLVGFLYSQCSAS  180

SbCYP79A1      ATGDV-------AVDVRHVARHYCGNVIRRLMFNRRYFGEPQADGGPGPMEVLHMDAVFTSLGLLYAFCV  268
GRMZM2G138248  GSSG--------AVDVRHIARHYCGNVVRRLMFNTRYFGKPQPDSGPGPLEVQHVDAVFTSLGLLYSFCV  258
GRMZM2G105185  ASAAASS-ASSAVVDIRHVARHFSSNMIRSLVFGKRHFG---GGAGPGAEEVAHVDALFALLNYVYIFSV  256
GRMZM2G178351  ASAAASSAASSAVVDIRHVARHFSCNMIRSLVFGKRHFG---AGAGPGPEEVAHVDTLFALLNYIYIFSV  253
GRMZM2G011156  AAACCCS-----AVDVRHVARHFCGNMIRTLVFGKRHFSGGGGGGGPGPEEVTHMDALFTLLNYVYCFSV  245

SbCYP79A1      SDYLP----WIR-GLDLDGHEKIVKEANVAVNRLHDTVIDDRWRQWKS----GERQEMEDFLDVLITLKD  329
GRMZM2G138248  SDYLP----WIL-GLDLDGHEKMVKEANERVTRLHDAVIDERWRLWKS----GERRELEDFLDVLIMLKD  319
GRMZM2G105185  SDYVPAAWRWMVAGLDLGGDREAGRSVMRTLSRLHDPIIRERIHEWDGLRERGEKREVRDFLDALVSLVD  326
GRMZM2G178351  SDYVPAAWRWMVAGLDLGGDREAGRSVMRTLSRLHDPIIRERIREWDGLRERGEKREVRDFLDALVSLVD  323
GRMZM2G011156  SDYVPAAWTWMVAG----DHKKVAESVMETLSRLHDPIIRERIREWEGLRERGDRREARDFLDALVSLED  311

                                          NP
SbCYP79A1      AQ-GNPLLTIEEVKAQSQDITFAAVDNPSNAVEWALAEMVNNPEVMAKAMEELDRVVGRERLVQESDIPK  398
GRMZM2G138248  AEAGRPVLSIEEVKALLMDITFASMDNPSNAVEWALAEMVNNPTMLKKAVDEIDSVVGQERLVQEHDIPR  389
GRMZM2G105185  SQ-GRPFLSFDEIKAQTAEMMFATIDNPSNAVEWALAEMMNRPEVMQKAMEELDAVVGKDRLVQESDISG  395
GRMZM2G178351  SQ-GRPFLSFDEIKAQTAEMMFATIDNPSNAVEWALAEMMNRPEVMKKAMEELDAVVGKDRLVQESDIPG  392
GRMZM2G011156  AE-GQPFLSFDEIKAQTAEMMFATIDNPSNTVEWALAEMMNRPEVMHKAMEELDTVVGKDRLVQEPDIPR  380

                                                                        E
                                                                      FxPDRHL
SbCYP79A1      LNYVKACIREAFRLHPVAPFNVPHVALADTTIAGYRVPKGSHVILSRTGLGRNPRVWDEPLRFYPDRHLA  468
GRMZM2G138248  LNYTKACIREAFRLHPVAPFNVPHVAVADATVAGYRIPKGSHVILSRTGLGRNPDVWDDPLRFDPERHIP  459
GRMZM2G105185  LNYLKACVREAFRLHPYHALNLPHVAMEDTVVSGYLVPKGSHVLLSRLALGRNPDVWDAPLRFRPERHLV  465
GRMZM2G178351  LNYLKACVREAFRLHPYHALNLPHVAMEDTVVSGYLVPKGSHVLLSRLALGRNPDVWDEPLQFRPERHLV  462
GRMZM2G011156  LNYLKACVREAFRLHPYHAFNPPHVATEDAVVSGYLIPKGSHVILSRVGLGRNPDVWDAPLQFRPERHLM  450

                                               A
                                           SFSxGRRxCxG
SbCYP79A1      TAASD--------VALTENDLRFISFSTGRRGCIAASLGTAMSVMLFGRLLQGFTWSKPAGVEAVDLSES  530
GRMZM2G138248  LSPEME-------VSLVERDLRFISFSTGRRGCIAALGTDMTIMLFARLLQGFSWSKMTGVAAIDLSES  522
GRMZM2G105185  NDDDGG---DNHHVVLTEPDLRFISFSAGRRGCPGVSLGSSITMMLFARLLQGFAWTKPPGVRAIRLEES  532
GRMZM2G178351  NDGD---------VVLTEPDLRFISFSAGRRGCPGVSLGSSITMMLFARLLQGFAWSKPPGVRAIRLEES  523
GRMZM2G011156  MNENDDVDDRYHHVVLTEPDLRFISFSAGRRGCPGVSLGSSVTMMLFARLLQGFTWTKPPGVRAIRLQES  520

SbCYP79A1      KSDTFMATPLVLHAEPRLPAHLYPSISI*--  559
GRMZM2G138248  RHNTFMARPLVLQAKPRLPAHLYPGILLCK*  553
GRMZM2G105185  SASLALAEPLLLQAQPRLPVHLYAASG*---  560
GRMZM2G178351  SASLALAEPLLLQAQPRLPVHLYAASG*---  551
GRMZM2G011156  STSLALAEPLLLQAQPRLPVHLYASG*----  547
```
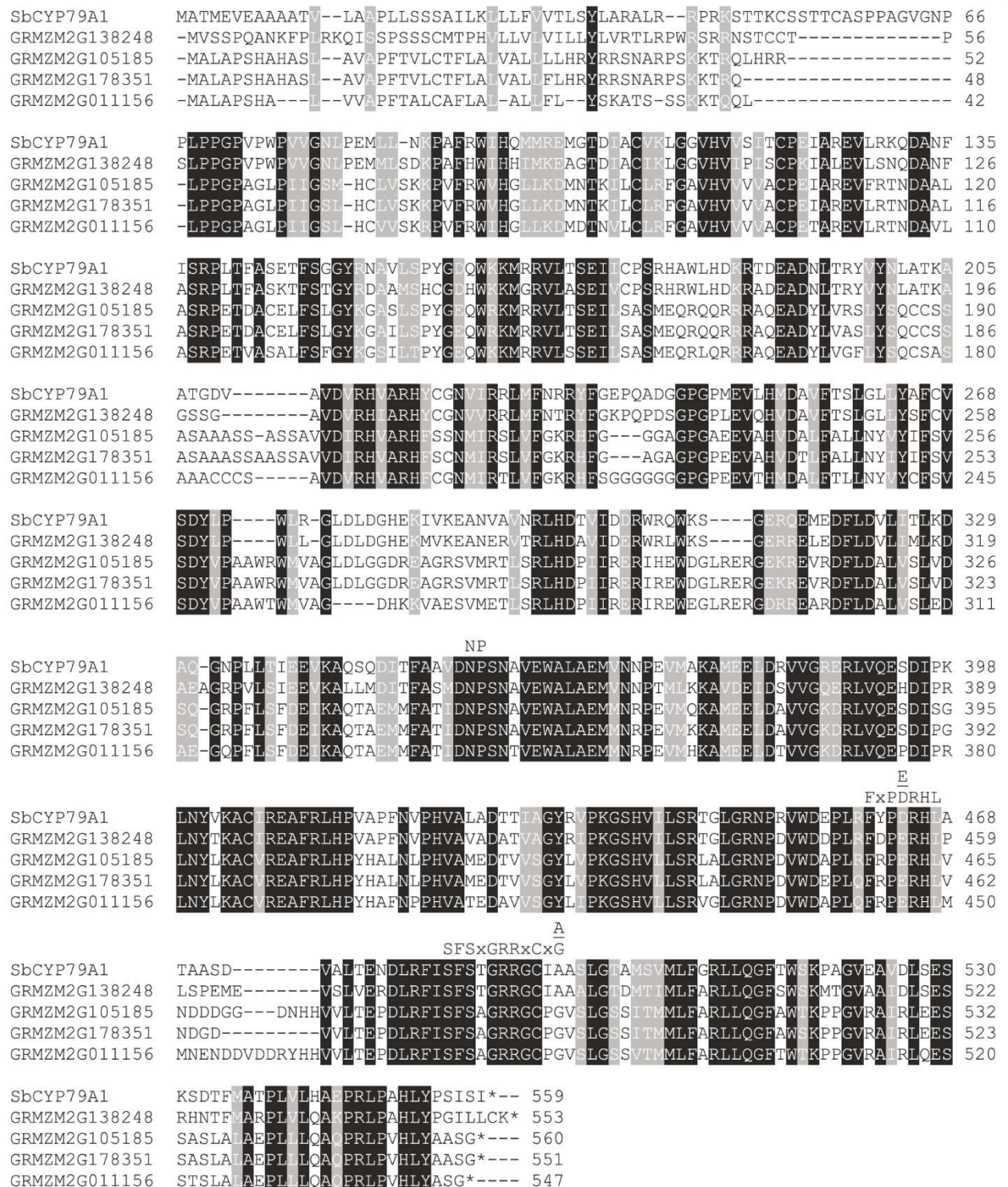
Fig. 1 Comparison of the amino acid sequences of putative maize CYP79s with sorghum CYP79A1. Amino acids identical in all five sequences are marked by black boxes and amino acids with similar side chains are marked by gray boxes. Sequence motifs characteristic for CYP79 proteins are labeled
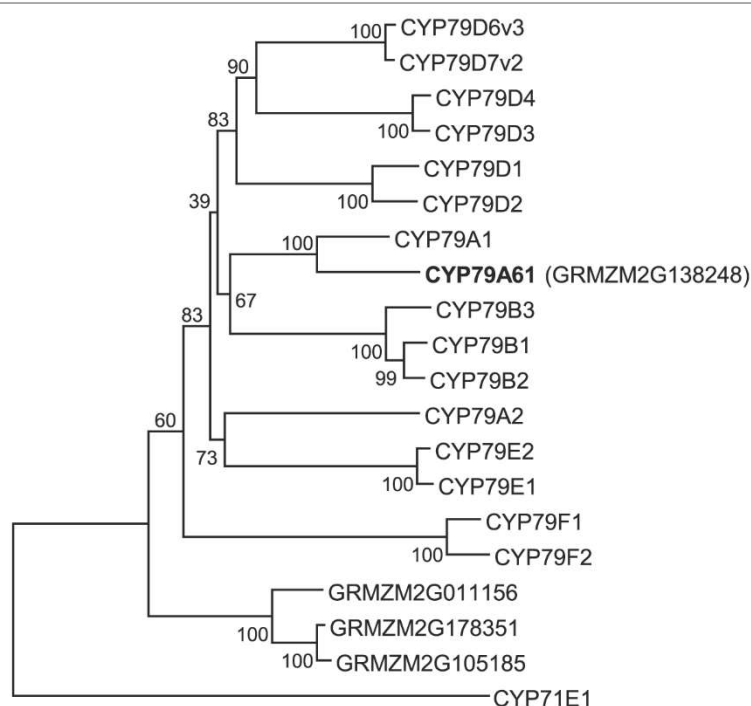
Manuscript II

Irmisch *et al. BMC Plant Biology* (2015) 15:128

Page 4 of 14

Fig. 2 Phylogenetic tree of CYP79 sequences from maize and previously characterized CYP79 enzymes from other plant species. The rooted tree was inferred with the neighbor-joining method and *n* = 1000 replicates for bootstrapping. Bootstrap values are shown next to each node. As an outgroup, CYP71E1 from *Sorghum bicolor* was chosen. Accession numbers are given in the Methods section
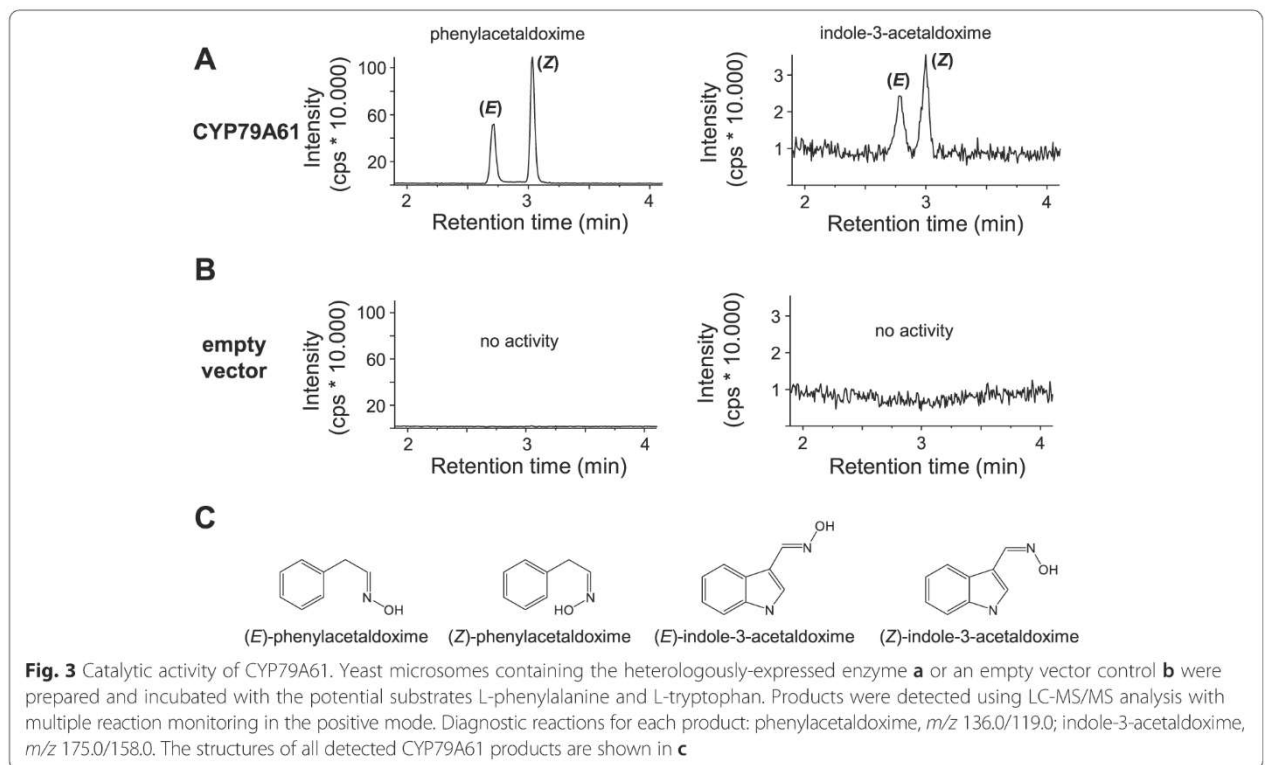
CYP79A61 produces *(E)*- and *(Z)*-isomers of phenylacetaldoxime and indole-3-acetaldoxime after yeast expression

For heterologous expression in yeast (*Saccharomyces cerevisiae*), the complete open reading frame of *CYP79A61* was cloned into the vector pESC-Leu2d [24] and the resulting construct was transferred into the *S. cerevisiae* strain WAT11 which carries the Arabidopsis cytochrome P450 reductase 1 (CPR1) [25]. Prepared microsomes containing recombinant CYP79A61 and CPR1 were incubated with the potential amino acid substrates L-phenylalanine, L-tyrosine, L-tryptophan, L-isoleucine, and L-leucine in the presence of the electron donor NADPH. Enzyme products were detected using liquid chromatography-tandem mass spectrometry (LC-MS/MS) analysis and verified by the use of authentic standards prepared as described in the Methods section. CYP79A61 accepted L-phenylalanine and L-tryptophan as substrates and converted them into mixtures of the *(E)*- and *(Z)*-isomers of phenylacetaldoxime and indole-3-acetaldoxime, respectively (Fig. 3). No activity could be observed with L-tyrosine, L-isoleucine, and L-leucine. The pH optima for the formation of phenylacetaldoxime and indole-3-acetaldoxime were 7.0 and 7.2, respectively, and the substrate affinity for L-phenylalanine (K_m = 117.2 ± 6.0 μM) was slightly higher than that for L-tryptophan (K_m = 150.2 ± 9.2 μM) (Fig. 4). Since measurements of

carbon monoxide difference spectra were inconclusive, we were not able to determine the protein concentrations in the microsomes and thus to calculate the turnover numbers for the different substrates. However, the large difference between the maximal velocities (V_{max}) for 1 mM L-phenylalanine (118.3 ± 3.7 ng *(E/Z)*-phenylacetaldoxime*h^{-1}*assay^{-1}) and 1 mM L-tryptophan (4.7 ± 0.1 ng *(E/Z)*-indole-3-acetaldoxime*h^{-1}*assay^{-1}) (Fig. 4b) suggests a higher turnover number for L-phenylalanine than for L-tryptophan.

Nicotiana benthamiana expressing CYP79A61 produces phenylacetaldoxime, indole-3-acetaldoxime and phenylacetaldoxime-derived metabolites

To verify the biochemical properties of the recombinant protein in an *in vivo* plant system, *CYP79A61* was transferred into *Nicotiana benthamiana* using *Agrobacterium tumefaciens* and transiently expressed under control of the 35S promoter. As a negative control, a vector carrying the *35S::eGFP* fusion was used. A construct encoding the suppressor of silencing protein p19 [26] was coinfiltrated to increase transient protein expression. The *eGFP*-expressing plants showed a bright fluorescence on the 3rd day after infiltration. Thus, CYP79A61 products were analyzed 3 days after infiltration. To analyze potential volatile aldoxime products, a volatile collection was performed. Plants expressing the maize *CYP79A61* gene

Biosynthesis of induced defense compounds

Irmisch *et al. BMC Plant Biology* (2015) 15:128

Page 5 of 14

Fig. 3 Catalytic activity of CYP79A61. Yeast microsomes containing the heterologously-expressed enzyme **a** or an empty vector control **b** were prepared and incubated with the potential substrates L-phenylalanine and L-tryptophan. Products were detected using LC-MS/MS analysis with multiple reaction monitoring in the positive mode. Diagnostic reactions for each product: phenylacetaldoxime, *m/z* 136.0/119.0; indole-3-acetaldoxime, *m/z* 175.0/158.0. The structures of all detected CYP79A61 products are shown in **c**

were found to release (*E/Z*)-phenylacetaldoxime in small amounts (Fig. 5b). In addition, some structurally related volatiles including 2-phenylacetaldehyde, 2-phenylethanol, benzyl cyanide, and 2-phenylnitroethane could be detected in the headspace of these plants (Fig. 5b, Additional file 1: Figure S4). In contrast, control plants expressing *eGFP* released none of the above-mentioned compounds. LC-MS/MS analysis of methanol extracts made from leaf material harvested right after the volatile collection revealed a strong accumulation of (*E/Z*)-phenylacetaldoxime and a moderate accumulation of (*E/Z*)-indole-3-acetaldoxime in leaves harboring the *35S::CYP79A61* construct, while no aldoximes could be detected in leaf material harvested from *eGFP*-expressing control plants (Fig. 5a).

Caterpillar oral secretion induces *CYP79A61* gene expression as well as amino acid substrate accumulation and phenylacetaldoxime formation
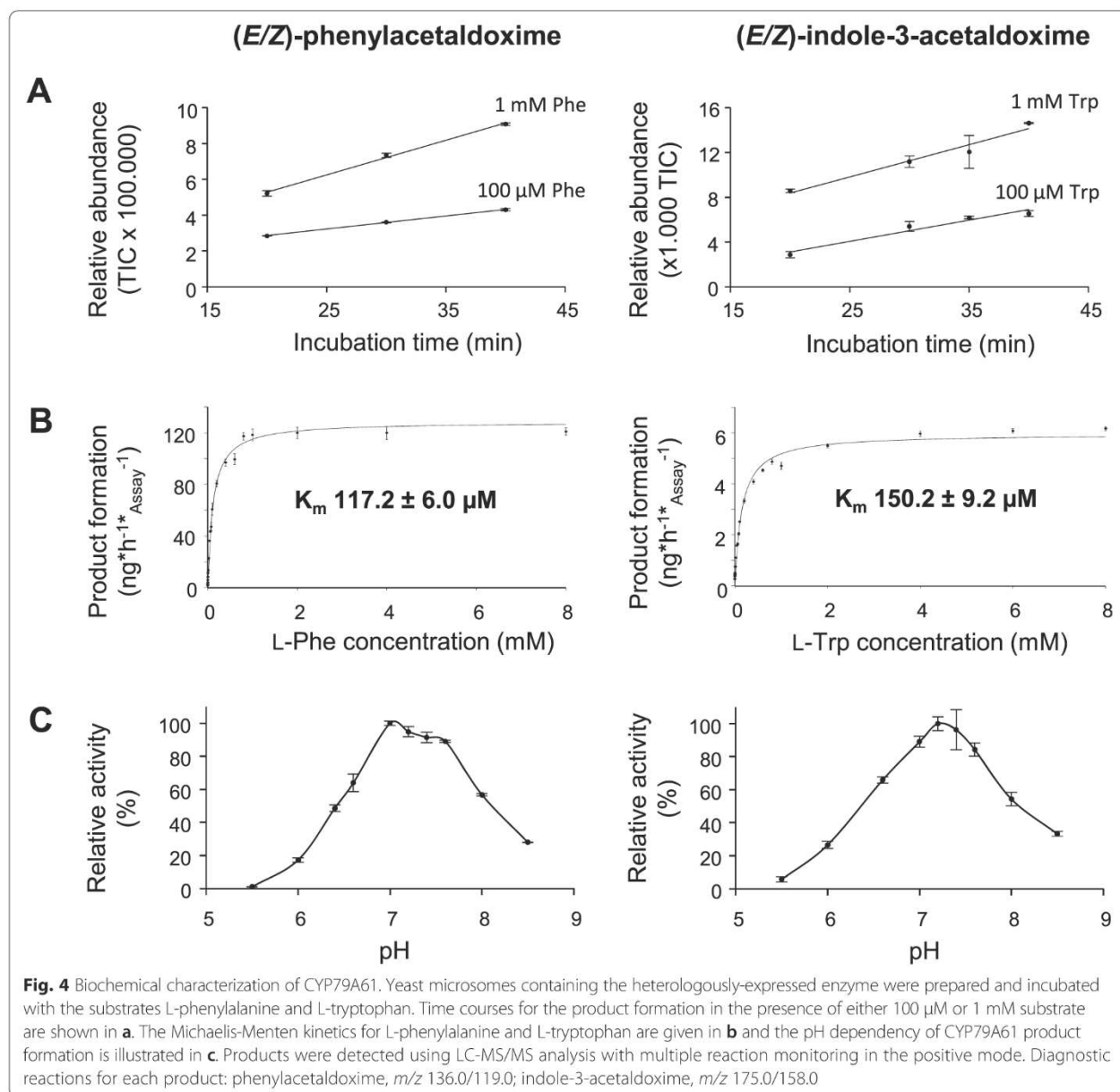
To test whether the expression of *CYP79A61* is influenced by herbivory, young maize plants of the cultivar Delprim were treated with oral secretion collected from Egyptian cotton leafworm (*Spodoptera littoralis*) larvae and *CYP79A61* transcript accumulation was analyzed in the leaves using quantitative (q)RT-PCR. While undamaged control plants showed a basal *CYP79A61* expression, simulated herbivory led to a significant increase in transcript accumulation (Fig. 6a). In contrast, *Spi1*, a member of the *YUCCA*-like gene family in maize which

has been reported to be involved in indole-3-acetic acid formation [27], was not expressed in damaged and undamaged maize leaves (c_q values >39). LC-MS/MS analysis of L-phenylalanine and L-tryptophan in methanol extracts made from the same samples revealed a significant upregulation of both CYP79A61 substrates in response to the oral secretion treatment (Fig. 6b and c). (*E/Z*)-Phenylacetaldoxime showed a similar accumulation pattern with significantly higher amounts in damaged leaves than in undamaged controls (Fig. 6d). Indole-3-acetaldoxime, however, could not be detected in these leaf extracts.

Caterpillar secretion induces the formation of the auxins indole-3-acetic acid and phenylacetic acid as potential aldoxime-derived metabolites

To investigate whether the maize cultivar Delprim is able to produce volatile aldoximes after herbivory, we conducted a volatile collection on plants treated with caterpillar oral secretions. Despite the accumulation of (*E/Z*)-phenylacetaldoxime in leaves, no aldoximes or aldoxime-derived nitriles or nitro compounds could be detected as volatiles (Additional file 1: Figure S5). However, several mono- and sesquiterpenes, green leaf volatiles and esters could be identified which have already been described in the literature [22, 23].
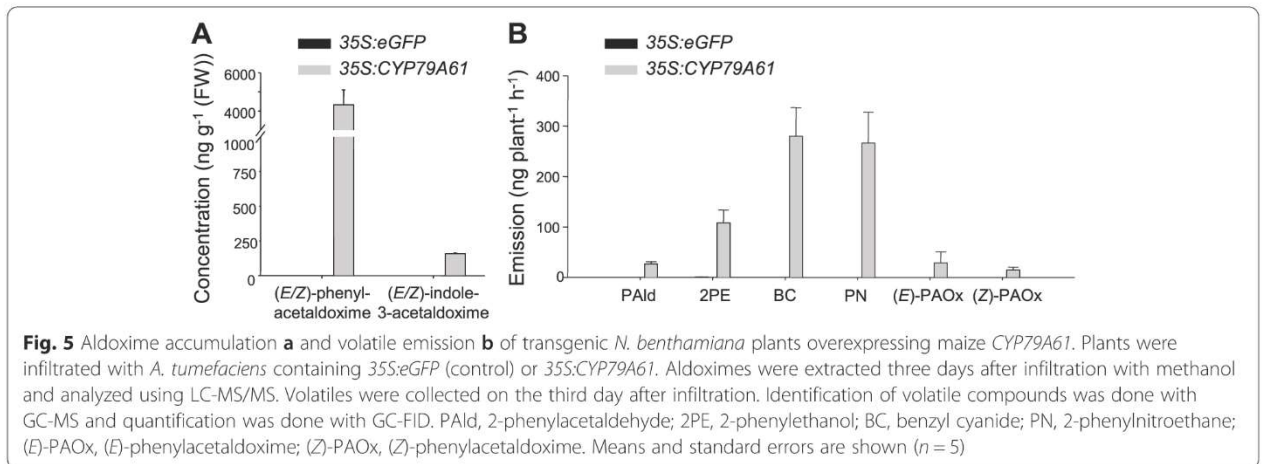
We then looked for potential metabolites of indole-3-acetaldoxime and phenylacetaldoxime since both are thought to be potential precursors for the biosynthesis

Manuscript II

Irmisch *et al. BMC Plant Biology* (2015) 15:128

Page 6 of 14

Fig. 4 Biochemical characterization of CYP79A61. Yeast microsomes containing the heterologously-expressed enzyme were prepared and incubated with the substrates L-phenylalanine and L-tryptophan. Time courses for the product formation in the presence of either 100 μM or 1 mM substrate are shown in **a**. The Michaelis-Menten kinetics for L-phenylalanine and L-tryptophan are given in **b** and the pH dependency of CYP79A61 product formation is illustrated in **c**. Products were detected using LC-MS/MS analysis with multiple reaction monitoring in the positive mode. Diagnostic reactions for each product: phenylacetaldoxime, *m/z* 136.0/119.0; indole-3-acetaldoxime, *m/z* 175.0/158.0

of the auxins indole-3-acetic acid and phenylacetic acid (PAA), respectively [28], we searched for these metabolites in leaves of undamaged and oral secretion-treated maize plants. The accumulation of indole-3-acetic acid as well as the accumulation of phenylacetic acid was significantly increased in treated leaves in comparison to undamaged control leaves (Fig. 6e and f).

Since aldoximes are intermediates in the biosynthesis of cyanogenic glycosides, we also searched for these compounds in maize leaves. Maize has been reported as a cyanogenic plant species [17–19], but no cyanogenic glycosides have been identified so far. We used LC-MS/

MS analysis to measure potential phenylacetaldoxime-derived cyanogenic glycosides, such as prunasin and amygdalin, as well as the *p*-hydroxyphenylacetaldoxime-derived cyanogenic glycoside dhurrin in oral secretion-treated maize leaves and in coleoptiles of maize and sorghum. As already reported in the literature [29, 30], dhurrin was found in large amounts in sorghum coleoptiles. However, none of the above mentioned cyanogenic glycosides could be detected in maize (Additional file 1: Figure S6), suggesting that at least the tested cultivar Delprim is not able to accumulate these compounds in significant amounts.

Irmisch *et al. BMC Plant Biology* (2015) 15:128

Page 7 of 14

Fig. 5 Aldoxime accumulation **a** and volatile emission **b** of transgenic *N. benthamiana* plants overexpressing maize *CYP79A61*. Plants were infiltrated with *A. tumefaciens* containing *35S:eGFP* (control) or *35S:CYP79A61*. Aldoximes were extracted three days after infiltration with methanol and analyzed using LC-MS/MS. Volatiles were collected on the third day after infiltration. Identification of volatile compounds was done with GC-MS and quantification was done with GC-FID. PAld, 2-phenylacetaldehyde; 2PE, 2-phenylethanol; BC, benzyl cyanide; PN, 2-phenylnitroethane; (*E*)-PAOx, (*E*)-phenylacetaldoxime; (*Z*)-PAOx, (*Z*)-phenylacetaldoxime. Means and standard errors are shown (*n* = 5)

Discussion

Aldoximes and aldoxime-derived compounds such as nitriles and cyanogenic glycosides are widespread secondary plant metabolites. They play important roles in plant defense against insects and pathogens [1, 3, 6, 11, 31] and are discussed to be involved in plant-pollinator interactions [32]. Although maize as one of the most important crop species has been intensively investigated during the last decades, little is known about the occurrence and role of aldoximes in this plant.

In this paper, we identified and characterized the P450 enzyme CYP79A61, one member of a small gene family comprising four genes with similarity to plant *CYP79*s. Like other CYP79 enzymes from the A- and B-subfamilies, recombinant CYP79A61 was shown to accept only aromatic amino acids as substrates. However, in contrast to most other CYP79 enzymes which have very high substrate specificity [5], both *in vitro* and *in vivo* experiments revealed that the recombinant maize enzyme was able to convert L-phenylalanine and L-tryptophan to phenylacetaldoxime and indole-3-acetaldoxime, respectively (Figs. 3 and 5). The conversion of a broader range of amino acids into aldoximes has only been reported for two poplar CYP79D enzymes [6]. The K_m values of CYP79A61 for L-phenylalanine and L-tryptophan were relatively high ($K_{m \text{ (Phe)}} = 117.2$ μM; $K_{m \text{ (Trp)}} = 150.2$ μM), but in the range reported for other CYP79 enzymes. It has been suggested that the low substrate affinity of these enzymes has evolved to avoid possible depletion of the free amino acid pool in plants [33].

The analysis of aldoximes in maize revealed a significant increase in phenylacetaldoxime accumulation in leaves treated with caterpillar oral secretion in comparison to leaves from undamaged control plants (Fig. 6d), suggesting a role of this compound in plant defense. Phenylacetaldoxime was previously shown to accumulate in poplar leaves after herbivory by gypsy moth (*Lymantria dispar*) caterpillars and feeding of pure phenylacetaldoxime to *L.*

dispar larvae had negative effects on caterpillar survival, growth, and time until pupation [6]. Although the overall concentration of phenylacetaldoxime in maize leaves subjected to simulated herbivory (Fig. 6d) was relatively low compared to that found in poplar leaves, local formation of this compound giving higher concentrations around the wound site as already reported for defensive sesquiterpenes in maize [34] is conceivable. In addition, aldoximes have been suggested to play a role in plant defense against pathogens [10] and the accumulation of phenylacetaldoxime in treated maize leaves might thus represent a defense barrier against pathogen attack following insect herbivore damage. Apart from accumulating in plant tissue, aldoximes can serve as precursors for other defensive compounds [1–3, 35]. In the Japanese apricot (*Prunus mume*), for example, phenylacetaldoxime is converted into the cyanogenic glycosides prunasin and amygdalin [36]. This is unlikely to occur in maize since we could not detect these compounds neither in regurgitant-treated leaves nor in maize coleoptiles (Additional file 1: Figure S6), the developmental stage reported to possess the highest cyanogenic potential [19]. However, we cannot rule out that phenylacetaldoxime acts as a precursor for other so far unknown maize defense compounds.

Since CYP79A61 had similar K_m values for L-phenylalanine and L-tryptophan and both amino acids were found to accumulate in the same order of magnitude in maize leaves (Fig. 6b and c), one would expect that the enzyme produces equal amounts of phenylacetaldoxime and indole-3-acetaldoxime in planta. However, while phenylacetaldoxime was detected in maize leaves, no accumulation of indole-3-acetaldoxime could be observed (Fig. 6). Local differences in amino acid substrate concentrations caused, for example, by specific substrate channeling processes might be an explanation for this observation. However, it is far more likely that the lack of indole-3-acetaldoxime detection is due to the aldoxime being further converted into
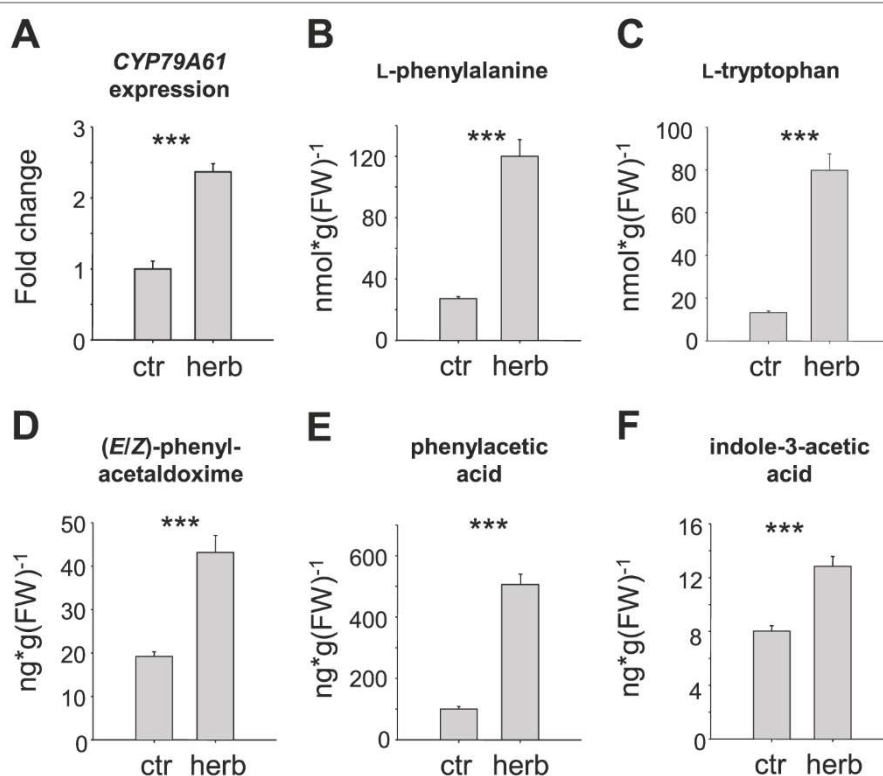
Manuscript II

Irmisch *et al. BMC Plant Biology* (2015) 15:128

Page 8 of 14

Fig. 6 The response of maize leaves to simulated herbivory. *CYP79A61* gene expression **a**, L-phenylalanine **b** and L-tryptophan **c** accumulation, (*E/Z*)-phenylacetaldoxime content **d**, and phenylacetic acid **e** and indole-3-acetic acid **f** levels were measured in undamaged leaves (ctr) and leaves subjected to simulated herbivory (herb). (*E/Z*)-phenylacetaldoxime, L-phenylalanine, L-tryptophan, and the auxins phenylacetic acid and indole-3-acetic acid were extracted with methanol and analyzed by LC-MS/MS. Gene expression was determined by qRT-PCR. Means and standard errors are shown ($n = 5$). Asterisks indicate statistical significance in Student's t-test. Gene expression: $p < 0.001$; $t = -4.99$; L-phenylalanine: $p < 0.001$, $t = 15.242$; L-tryptophan: $p < 0.001$, $t = 16.293$; phenylacetaldoxime: $p = < 0.001$, $t = 6.934$; phenylacetic acid: $p = < 0.001$, $t = -18.259$; indole-3-acetic acid: $p = < 0.001$, $t = -5.644$

other compounds. In various plant species, including maize, the conversion of indole-3-acetaldoxime into the corresponding acid is thought to serve as an alternative route for the formation of the essential plant growth hormone indole-3-acetic acid [37–40], presumably involving indole-3-acetonitrile as an intermediate [37, 38]. The analysis of *CYP79A61* transcript accumulation in maize leaves revealed that the gene was significantly upregulated after herbivore feeding, matching an increased accumulation of IAA in the same tissues (Fig. 6a and f). Moreover, overexpression of *CYP79A61* in *N. benthamiana* revealed that the enzyme is able to produce indole-3-acetaldoxime under natural conditions in planta (Fig. 5a). Thus it is conceivable that CYP79A61 might produce indole-3-acetaldoxime as a specific substrate for herbivory-induced IAA formation in maize leaves. The conversion of indole-3-acetaldoxime to indole-3-acetonitrile is likely catalyzed by a P450 enzyme similar to the recently described poplar enzymes CYP71B40 and CYP71B41 which were shown to produce benzyl cyanide from phenylacetaldoxime after herbivory [35]. Indole-3-acetonitrile could then be further converted into IAA by maize nitrilase 2, an enzyme already implicated in auxin formation in maize [41]. In future experiments, the overexpression of maize *CYP79A61* in an Arabidopsis *cyp79b2 cyp79b3* double mutant which has been described to lack the accumulation of indole-3-acetaldoxime [40] would allow the analysis of *CYP79A61*-mediated formation of indole-3-acetaldoxime and its metabolism in a clean and sensitive background in planta. Since IAA can be formed via different biosynthetic pathways [28], it is possible that other enzymes rather than CYP79A61 are responsible for the observed IAA accumulation after simulated herbivory. Thus, a comprehensive expression analysis of candidate genes such as *TAA* and *YUCCA* might help to understand the biochemical origin of herbivore-induced IAA formation in maize. However, we have already shown that *Spi1*, a member of the YUCCA-like gene family in maize [27], was not expressed in damaged and undamaged maize leaves.

It is well established that herbivore feeding can cause changes in auxin levels in plants. For example, feeding

Biosynthesis of induced defense compounds

Irmisch *et al. BMC Plant Biology* (2015) 15:128

Page 9 of 14

of gall-inducing insects on wheat and late goldenrod (*Solidago altissima*) leads to increased IAA levels in the damaged tissues [42, 43] while simulated herbivory on wild tobacco (*Nicotiana attenuata*) resulted in decreased IAA accumulation [44]. Since auxins are potent modifiers of plant defense reactions [45], it is likely that the elevated IAA and PAA levels in herbivore-damaged maize also mediate defense responses. The presence of aldoxime-producing *CYP79* genes in all so far sequenced angiosperm genomes might indicate a broader occurrence of aldoxime-mediated auxin formation, especially under biotic stresses such as herbivory or pathogen attack.

A sequence comparison with already characterized CYP79s from other plants showed that CYP79A61 was most similar to CYP79A1, an enzyme known to catalyze the key reaction of dhurrin formation in sorghum [7]. However, despite an amino acid identity of 72 %, both enzymes have different substrate specificities with CYP79A1 solely converting tyrosine to *p*-hydroxyphenylacetaldoxime [46]. A comparative analysis of the maize and the sorghum genome revealed that *CYP79A61* and *CYP79A1* are not located on syntenic chromosomal regions and are therefore not orthologues (Additional file 1: Figure S1). Interestingly, no gene with orthology to sorghum *CYP79A1* could be found in the maize genome (Additional file 1: Figure S2), suggesting a recent loss of the *CYP79A1* orthologue in the maize lineage after diversification of the common ancestor of maize and sorghum. This gene loss might explain the absence of dhurrin formation in maize (Additional file 1: Figure S6). A so far uncharacterized sorghum *CYP79* gene (Sb10g022470) could be identified as the orthologue of *CYP79A61* (Additional file 1: Figures S2 and S3). However, whether this gene encodes for a protein with the same substrate specificity as CYP79A61 remains unknown.

Like dhurrin, we also could not detect the cyanogenic glycosides prunasin or amygdalin in the maize cultivar Delprim, neither in coleoptiles nor in undamaged or damaged leaves of young plants (Additional file 1: Figure S6). Moreover, a volatile collection experiment showed that Delprim did not release aldoximes after herbivory (Additional file 1: Figure S5). However, in the literature there is evidence that maize is cyanogenic [17–19], and a few maize lines have been reported to produce aliphatic volatile aldoximes after herbivore feeding [20, 21]. It is conceivable that the three putative *CYP79* genes GRMZM2G011156, GRMZM2G105185, and GRMZM2G178351, which could not be amplified from Delprim cDNA, are expressed in other maize cultivars or under different experimental conditions and contribute to volatile aldoxime and/or cyanogenic glycoside formation. Thus, a comprehensive characterization and gene expression analysis of different *CYP79* alleles from diverse maize cultivars will help to further understand the formation

and function of these nitrogenous defense compounds and their variability among maize cultivars.

Conclusions
We showed that maize produces aldoximes in response to simulated herbivory. A P450 enzyme of the CYP79 family, CYP79A61, could be identified able to catalyze the formation of phenylacetaldoxime and indole-3-acetaldoxime in two different heterologous systems. Since the expression of *CYP79A61* was upregulated after simulated herbivory, we hypothesize that the enzyme contributes to herbivore-induced aldoxime formation in maize. While phenylacetaldoxime accumulated in herbivore-damaged leaves and might play a role in maize defense against herbivores or pathogens, indole-3-acetaldoxime could not be detected in the plant. However, it is conceivable that this aldoxime is rapidly converted to indole-3-acetic acid which has been described as a mediator of various plant defense responses [45].

Methods
Plant and insect material
Seeds of the maize (*Zea mays* L.) hybrid line Delprim from Delley Samen und Pflanzen (Delley, Switzerland) were grown in commercially available potting soil in a climate-controlled chamber with a 16 h photoperiod (1 mmol $(m^2)^{-1} s^{-1}$ of photosynthetically-active radiation, temperature cycle 24/20 °C (day/night) and 60 % relative humidity). Twelve day old-plants (15–25 cm high, 4 expanded leaves) were used in the experiment. Eggs of *Spodoptera littoralis* Boisd. (Lepidoptera: Noctuidae) were obtained from Aventis (Frankfurt, Germany) and were reared on an artificial wheat germ diet (Heliothis mix, Stonefly Industries, Bryan, TX, USA) for about 10 days at 22 °C under an illumination of 750 μmol $(m^2)^{-1} s^{-1}$. Larvae were reared for another week on Delprim leaves and oral secretions were collected every day with a pipette and frozen at –20 °C until further usage. For the caterpillar secretion treatment (4 pm), 2 maize leaves per plant were cut with a razor blade and 15 μL oral secretion (1:2 diluted in water) were applied to the wound site. This treatment was repeated the next morning at 9 am prior to volatile collection.

Volatile collection and analysis
For volatile collection, plants were separately placed in airtight 3 L glass desiccators. Charcoal-filtered air was pumped into the desiccators at a flow rate of 2 L min^{-1} and left the desiccators through a filter packed with 30 mg Porapaq Q (ARS, Inc., Gainesville, FL, USA). Volatiles were collected for 5 h (10 am – 3 pm). After collection the volatiles were desorbed by eluting the filter twice with 100 μL dichloromethane containing

Manuscript II

Irmisch *et al. BMC Plant Biology* (2015) 15:128

Page 10 of 14

nonyl acetate as an internal standard (10 ng μL^{-1}). Qualitative and quantitative analysis of maize volatiles was conducted using an Agilent 6890 Series gas chromatograph coupled to an Agilent 5973 quadrupole mass selective detector (interface temp.: 270 °C; quadrupole temp.: 150 °C, source temp.: 230 °C, electron energy: 70 eV) or a flame ionization detector (FID) operated at 300 °C, respectively. The constituents of the volatile bouquet were separated with a DB-5MS column (Agilent, Santa Clara, CA, USA, 30 m × 0.25 mm × 0.25 μm) and He (MS) or H$_2$ (FID) as carrier gas. One microliters of the sample was injected without split at an initial oven temperature of 40 °C. The temperature was held for 2 min and then increased to 155 °C with a gradient of 7 °C min^{-1}, followed by a further increase to 300 °C with 60 °C min^{-1} and a hold for 3 min.

Compounds were identified by comparison of retention times and mass spectra to those of authentic standards obtained from Fluka (Seelze, Germany), Roth (Karlsruhe, Germany), Sigma (St, Louis, MO, USA) or Bedoukian (Danbury, CT, USA), or by reference spectra in the Wiley and National Institute of Standards and Technology libraries and in the literature [47].

Plant tissue sampling, RNA extraction and reverse transcription

Treated maize leaves were harvested immediately after the volatile collection (3 pm), flash-frozen in liquid nitrogen and stored at −80 °C until further processing. After grinding the frozen leaf material in liquid nitrogen to a fine powder, total RNA was isolated using the "RNeasy Plant Mini Kit" (Quiagen GmbH, Hilden, Germany) according to manufacturer's instructions. RNA concentration, purity and quality were assessed using a spectrophotometer (NanoDrop 2000c, Thermo Scientific, Wilmington, DE, USA) and an Agilent 2100 Bioanalyzer (Agilent Technologies GmbH, Waldbronn, Germany). Prior to cDNA synthesis, 0.75 μg RNA was DNase-treated using 1 μL DNase (Fermentas GmbH, St. Leon Roth, Germany). Single-stranded cDNA was prepared from the DNase-treated RNA using SuperScript^{TM} III reverse transcriptase and oligo (dT$_{12-18}$) primers (Invitrogen, Carlsbad, CA, USA).

Identification and isolation of *CYP79* genes

To identify putative maize *CYP79* genes, a BLAST search against the *Z. maize* genome database (http://www.phytozome.net/poplar) was conducted using the amino acid sequence of CYP79A1 from *Sorghum bicolor* (L.) Moench (Genbank Q43135) as input sequence. Four sequences representing putative P450 enzymes of the CYP79 family were identified. One of these sequences could be amplified from cDNA attained from herbivore-induced leaves of *Z. mays*. Primer sequence information

is available in Additional file 1: Table S1. The PCR product was cloned into the sequencing vector pCR$^{®-}$Blunt II-TOPO$^{®}$ (Invitrogen) and both strands were fully sequenced.

Heterologous expression of CYP79A61 in Saccharomyces cerevisiae

The complete open reading frame of *CYP79A61* was cloned into the pESC-Leu2d vector [24] as a *Not*I/*Bgl*II fragment and the resulting construct was transferred into the *S. cerevisiae* strain WAT11 [25]. For gene expression, a single yeast colony was picked to inoculate a starting culture which contained 30 mL SC minimal medium lacking leucine (6.7 g L^{-1} yeast nitrogen base without amino acids, but with ammonium sulfate). Other components: 100 mg L^{-1} of L-adenine, L-arginine, L-cysteine, L-lysine, L-threonine, L-tryptophan and uracil; 50 mg L^{-1} of the amino acids L-aspartic acid, L-histidine, L-isoleucine, L-methionine, L-phenylalanine, L-proline, L-serine, L-tyrosine, L-valine; 20 g L^{-1} D-glucose. The culture was grown overnight at 28 °C and 180 rpm. One OD of this culture (approx. 2×10^7 cells mL^{-1}) was used to inoculate 100 mL YPGA full medium (10 g L^{-1} yeast extract, 20 g L^{-1} bactopeptone, 74 mg L^{-1} adenine hemisulfate, 20 g L^{-1} D-glucose) which was grown for 32–35 h (until OD about 5), induced by the addition of galactose and cultured for another 15–18 h. Cells were harvested and yeast microsomes were isolated according to the procedures described by Pompon et al. [25] and Urban et al. [48] with minor modifications. Briefly, the culture was centrifuged (7500 g, 10 min, 4 °C), the supernatant was decanted, the pellet was resuspended in 30 mL TEK buffer (50 mM Tris-HCl pH 7.5, 1 mM EDTA, 100 mM KCl) and then centrifuged again. Then the cell pellet was carefully resuspended in 2 mL of TES buffer (50 mM Tris-HCl pH 7.5, 1 mM EDTA, 600 mM sorbitol, 10 g L^{-1} bovine serum fraction V protein and 1.5 mM β-mercaptoethanol) and transferred to a 50 mL conical tube. Glass beads (0.45–0.50 mm diameter, Sigma-Aldrich Chemicals, Steinheim, Germany) were added so that they filled the full volume of the cell suspension. Yeast cell walls were disrupted by 5 cycles of 1 min shaking by hand and subsequent cooling down on ice for 1 min. The crude extract was recovered by washing the glass beads 4 times with 5 mL TES. The combined washing fractions were centrifuged (7500 g, 10 min, 4 °C), and the supernatant was transferred into another tube and centrifuged again (100,000 g , 60 min, 4 °C). The resulting microsomal protein fraction was homogenized in 2 mL TEG buffer (50 mM Tris–HCl, 1 mM EDTA, 30 % w/v glycerol) using a glass homogenizer (Potter-Elvehjem, Fisher Scientific, Schwerte, Germany). Aliquots were stored at −20 °C and used for protein assays.

Analysis of recombinant CYP79A61

To determine the substrate specificity of CYP79A61, yeast microsomes harboring recombinant protein were incubated for 30 min at 25 °C and 300 rpm individually with the potential substrates L-phenylalanine, L-valine, L-leucine, L-isoleucine, L-tyrosine and L-tryptophan in glass vials containing 300 μL of the reaction mixture (75 mM sodium phosphate buffer (pH 7.0), 1 mM substrate (concentration was variable for Km determination), 1 mM NADPH and 10 μL of the prepared microsomes). Reaction mixtures containing microsomes prepared from WAT11 transformed with the empty vector served as negative controls. Assays were stopped by placing on ice after 300 μL MeOH were added. Reaction products were analyzed using LC-MS/MS as described below. Product accumulation was measured after different incubation times (20–40 min) and under different pH conditions (pH 5.5–8.5). For the determination of the K_m values, assays were carried out as triplicates and enzyme concentrations and incubation times (30 min) were chosen so that the reaction velocity was linear during the incubation time period.

qRT-PCR analysis of *CYP79A61* and *Spi1* expression

cDNA was prepared as described above and diluted 1:3 with water. For the amplification of the *CYP79A61* gene fragment (146 bp) and the *Spi1* gene fragment (99 bp), primer pairs were designed having a Tm ≥ 56 °C, a GC content between 52 and 56 % and a primer length in the range of 18–21 nt (see Additional file 1: Table S1 online for primer information). Primer specificity was confirmed by agarose gel electrophoresis, melting curve analysis, standard curve analysis, and sequence verification of cloned PCR amplicons. The transcription repressor Leunig (LUG) [49] was used as a reference gene. Samples were run in triplicates using Brilliant® III SYBR® Green QPCR Master Mix (Stratagene, Carlsbad, CA, USA) with ROX as reference dye. The following PCR conditions were applied for all reactions: Initial incubation at 95 °C for 3 min followed by 40 cycles of amplification (95 °C for 20 s, 60 °C for 20 s). Plate reads were taken during the annealing and the extension steps of each cycle. Data for the melting curves were recorded at the end of cycling from 55 to 95 °C.

All samples were run on the same PCR machine (Mx3000P, Agilent Technologies, Santa Clara, CA, USA) in an optical 96-well plate. Five biological replicates were analyzed as triplicates in the qRT-PCR for each of the three treatments. Data for the relative quantity to calibrator average (dRn) were exported from the MXPro Software.

Transient expression of *CYP79A61* in *N. benthamiana*

For gene expression in *N. benthamiana*, the coding region of *CYP79A61* was cloned into the pCAMBiA2300U

vector. After verification of the sequence integrity, pCAMBiA vectors carrying the *CYP79A61* or *eGFP* construct and the construct *pBIN::p19* were separately transferred into *Agrobacterium tumefaciens* strain LBA4404. The transformation was confirmed by PCR. Five milliliters of an overnight culture (220 rpm, 28 °C) were used to inoculate 50 mL LB medium (50 μg mL⁻¹ kanamycin, 25 μg mL⁻¹ rifampicin and 25 μg mL⁻¹ gentamicin) for overnight growth. The following day, the cultures were centrifuged (4000 *g*, 5 min) and the cells were resuspended in infiltration buffer (10 mM MES, 10 mM MgCl₂, 100 μM acetosyringone, pH 5.6) to reach a final OD of 0.5. After shaking for at least 1 h at RT, the cultures carrying *CYP79A61* or *eGFP* were mixed with an equal volume of cultures carrying *pBIN:p19*. Since p19 functions as a suppressor of silencing, it enhances the expression of the desired coexpressed protein in planta [26].

For transformation, 3–4 week-old *N. benthamiana* plants were dipped upside down in an *A. tumefaciens* solution and vacuum was applied to infiltrate the leaves. Infiltrated plants were shaded with cotton tissue to protect them from direct irradiation. Volatiles were measured on the 3rd day after transformation as described above.

LC-MS/MS analysis of aldoximes, amino acids, auxins, and cyanogenic glycosides

For determining amino acid and aldoxime concentration, 100 mg of plant powder was extracted with 1 mL MeOH. For the measurement of amino acids, the MeOH extract was diluted 1:10 with water and spiked with ¹³C, ¹⁵N abeled amino acids (algal amino acids ¹³C,¹⁵N, Isotec, Miamisburg, OH, USA) at a concentration of 10 μg of the mix per mL. The concentration of the individual labeled amino acids in the mix had been previously determined by classical HPLC-fluorescence detection analysis after pre-column derivatization with *o*-phthaldialdehyde-mercaptoethanol using external standard curves made from standard mixtures (amino acid standard mix and Gln, Asn and Trp, Fluka). Amino acids in the diluted MeOH extract were directly analyzed by LC-MS/MS. The method described by Jander et al. [50] was used with some modifications. Briefly, chromatography was performed on an Agilent 1200 HPLC system (Agilent Technologies, Boeblingen, Germany). Separation was achieved on a Zorbax Eclipse XDB-C18 column (50 × 4.6 mm, 1.8 μm, Agilent Technologies) with aqueous formic acid (0.05 %) and acetonitrile employed as mobile phases A and B, respectively. The elution profile was: 0–1 min, 97 % A; 1–2.7 min, 3–100 % B in A; 2.7–3 min 100 % B and 3.1–6 min 97 % A. The mobile phase flow rate was 1.1 mL min⁻¹ and the column temperature was maintained at 25 °C. The liquid chromatography was coupled to an API 5000 tandem mass

Manuscript II

Irmisch *et al. BMC Plant Biology* (2015) 15:128

Page 12 of 14

spectrometer (Applied Biosystems, Darmstadt, Germany) equipped with a Turbospray ion source operated in positive ionization mode (ion spray voltage, 5500 eV; turbo gas temp, 700 °C; nebulizing gas, 70 psi; curtain gas, 35 psi; heating gas, 70 psi; collision gas, 2 psi). Multiple reaction monitoring (MRM) was used to monitor a parent ion → product ion reaction for each analyte. MRMs were chosen as described in Jander et al. [50] except for Arg (m/z 175 → 70), and Lys (m/z 147 → 84). Both Q1 and Q3 quadrupoles were maintained at unit resolution. Analyst 1.5 software (Applied Biosystems) was used for data acquisition and processing. Individual amino acids in the sample were quantified from corresponding peaks in the $^{13}C,^{15}N$ labeled amino acid internal standard, except for tryptophan which was quantified using $^{13}C,^{15}N$-Phe applying a response factor of 0.42.

Aldoximes were measured from MeOH extracts as described in Irmisch et al. [6] using the same LC-MS/MS system as described above. Formic acid (0.2 %) in water and acetonitrile were employed as mobile phases A and B, respectively, on a Zorbax Eclipse XDB-C18 column (50 × 4.6 mm, 1.8 µm). The elution profile (gradient 1) was: 0–0.5 min, 30 % B; 0.5–3 min, 30–66 % B; 3–3.1 min, 66–100 % B; 3.1–4 min 100 % B and 4.1–6 min 30 % B at a flow rate of 0.8 mL min^{-1} at 25 °C. The API 5000 tandem mass spectrometer was operated in positive ionization mode (ion spray voltage, 5500 eV; turbo gas temp, 700 °C; nebulizing gas, 60 psi; curtain gas, 30 psi; heating gas, 50 psi; collision gas, 6 psi). MRM was used to monitor parent ion → product ion reactions for each analyte as follows: m/z 136.0 → 119.0 (collision energy (CE), 17 V; declustering potential (DP), 56 V) for phenylacetaldoxime; m/z 102.0 → 69.0 (CE, 13 V; DP, 31 V) for 2-methylbutyraldoxime; m/z 102.0 → 46.0 (CE, 15 V; DP, 31 V) for 3-methylbutyraldoxime; m/z 175.0 → 158.0 (CE, 17 V; DP, 56 V) for indole-3-acetaldoxime and m/z 152.0 → 107.0 (CE, 27 V; DP, 100 V) for *p*-hydroxyphenylacetaldoxime. The concentration of aldoximes was determined using external standard curves made with authentic standards synthesized as described in Irmisch et al. [6].

The auxins IAA and PAA were analyzed based on the protocol of Balcke et al. [51]. 100 mg of plant powder were extracted with 300 µL MeOH. Two hundred microliters of the extract was diluted 1:10 with water containing 0.1 % formic acid and loaded to equilibrated Chromabond® HR-X polypropylene columns (45 µm, Macherey Nagel, Düren, Germany). The columns were washed with acidified water. The fraction containing the auxins was eluted with 1 mL acetonitrile, which was then dried under a stream of nitrogen gas. The samples were redissolved in 30 µL MeOH and subsequently analyzed by the same LC-MS/MS system as described above. Separations were performed on an Agilent XDB-

C18 column (50 × 4.6 mm, 1.8 µm). Eluents A and B were water containing 0.05 % formic acid and acetonitrile, respectively. The elution profile was: 0–0.5 min, 5 % B in A; 0.5–4.0 min, 5–50 % B; 4.1–4.5 min 100 % B and 4.6–7 min 5 % B. The flow rate was set to 1.1 mL min^{-1}. For IAA analysis, the API 5000 tandem mass spectrometer was operated in positive ionization mode (ion spray voltage, 5500 eV; turbo gas temp, 700 °C; nebulizing gas, 60 psi; curtain gas, 30 psi; heating gas, 50 psi; collision gas, 6 psi). The MRM transition and parameter settings for IAA were as follows: m/z 176 → 130 (CE, 19 V; DP, 31 V). PAA was detected separately by mass spectrometer operated in negative ionization mode (ion spray voltage, –4500 eV; turbo gas temp, 700 °C; nebulizing gas, 60 psi; curtain gas, 30 psi; heating gas, 50 psi; collision gas, 6 psi). The MRM transition and parameter settings for PAA were as follows: m/z 135 → 91 (CE, –10 V; DP, –25 V). The concentration of PAA was determined using external standard curves made with authentic standard (Sigma-Aldrich). IAA concentration was determined internally by spiking the plant extracts with $^{2}H_5$-IAA (OlChemIm Ltd., Olomouc, Czech Republic).

For the analysis of cyanogenic glycosides (dhurrin, prunasin, linamarin, and lotaustralin), 100 mg plant powder was extracted with 300 µL MeOH and 200 µL of the extract was diluted 1:10 with water containing 0.1 % formic acid. Ten microliters of the extracts were directly injected and analyzed by LC-MS/MS. The column and eluents used for the separation were the same as already described for the auxins. The elution profile was: 0–0.5 min, 5 % B in A; 0.5–6.0 min, 5–50 % B; 6.1–7.5 min 100 % B and 7.6–10.5 min 5 % B. The flow rate was set to 1.1 mL min^{-1}. The tandem mass spectrometer was operated in negative ionization mode (ion spray voltage, –4500 eV; turbo gas temp, 700 °C; nebulizing gas, 60 psi; curtain gas, 30 psi; heating gas, 50 psi; collision gas, 6 psi). MRM was used to monitor parent ion → product ion reactions for each analyte as follows: m/z 310.0 → 179.0 for dhurrin, m/z 294.0 → 89.0 (CE, –22; DP, –15) for prunasin, m/z 260.0 → 179.0 for lotaustralin, m/z 246.0 → 179.0 for linamarin, and m/z 456.0 → 179.0 for amygdalin. If not stated above, the transition parameter settings for the cyanogenic glycosides were as follows: CE, –10 V; DP, –15 V.

Sequence analysis and phylogenetic tree reconstruction

An alignment of maize CYP79 enzymes and CYP79A1 from *S. bicolor* was constructed and visualized using BioEdit (http://www.mbio.ncsu.edu/bioedit/bioedit.html) and the ClustalW algorithm. For the estimation of a phylogenetic tree, we used the ClustalW algorithm (gap open, 10; gap extend, 0.1; Gonnet; penalties, on; gap separation, 4; cut off, 30 %) implemented in MEGA5

Biosynthesis of induced defense compounds

Irmisch *et al. BMC Plant Biology* (2015) 15:128

Page 13 of 14

[52] to compute an amino acid alignment of the maize CYP79 sequences and other already characterized CYP79 enzymes. The tree was reconstructed with MEGA5 using a neighbor-joining algorithm (Poisson model). A bootstrap resampling analysis with 1000 replicates was performed to evaluate the tree topology.

The synteny analysis was done using the Ensembl-Plants web service (http://www.plants.ensembl.org).

Statistical analysis

To test for statistical significance, data were log transformed whenever necessary and analyzed using the Student's t-test implemented in SigmaPlot 11.0 for Windows (Systat Software Inc. 2008).

Accession numbers

Sequence data for genes and proteins discussed in this article can be found in the GenBank under the following identifiers: CYP79A61 (KP297890), CYP79D6v3 (KF56 2515), CYP79D7v2 (KF562516), CYP79D3 (AAT11920), CYP79D4 (AAT11921), CYP79D1 (AAF27289), CYP 79D2 (AAF27290), CYP79A1 (Q43135), CYP79B3 (AEC 07294), CYP79B1 (AAD03415), CYP79B2 (AEE87143), CYP79A2 (AAF70255), CYP79E1 (AF140609), CYP79E2 (AF140610), CYP79F2 (AAG24796), CYP79F1 (AEE29 448), CYP71E1 (AAC39318).

Additional file

Additional file 1: Figure S1. Comparative genomic analysis of *Sorghum bicolor* chromosome 1 with maize chromosomes 1, 2, 5, and 9. The analysis was done using the web server http://www.plants.ensembl.org. **Figure S2.** Comparative genomic analysis of *Zea mays* chromosome 9 with *Sorghum bicolor* chromosomes 1 and 10. The analysis was done using the web server http://www.plants.ensembl.org. **Figure S3.** Phylogenetic tree of CYP79 sequences from maize and *Sorghum bicolor*. The rooted tree was inferred with the neighbor-joining method and *n* = 1000 replicates for bootstrapping. Bootstrap values are shown next to each node. As an outgroup, CYP71A13 from *Arabidopsis thaliana* was chosen. **Figure S4.** Volatiles released from transgenic *Nicotiana benthamiana* plants transiently overexpressing either a *35S::eGFP* construct or a *35S::CYP79A61* construct. Volatiles were collected 3 days after *Agrobacterium tumefaciens* infiltration and analyzed using GC-MS. 1, 5-*epi*-aristolochene; 2, 2-phenylethanol; 3, benzyl cyanide; 4, 2-phenylnitroethane; 5, phenylacetaldoxime; IS, internal standard. **Figure S5.** Volatiles released from undamaged 10 day-old *Zea mays* (cultivar Delprim) seedlings (control) and seedlings treated with caterpillar oral secretion (herbivory). Volatiles were collected and analyzed using GC-MS. 1, β-myrcene; 2, 3-hexen-1-ol acetate; 3, limonene; 4, linalool; 5, (*E*)-4,8-dimethyl-1,3,7-nonatriene; 6, phenylmethyl acetate; 7, 2-phenylethyl acetate; 8, indole; 9, geranyl acetate; 10, (*E*)-β-caryophyllene; 11, (*E*)-α-bergamotene; 12, (*E*)-β-farnesene; 13, β-sesquiphellandrene; 14, 4,8,12-trimethyltrideca-1,3,7,11-tetraene; IS, internal standard. **Figure S6.** Accumulation of cyanogenic glycosides in maize and sorghum. Maize and sorghum coleoptiles were harvested 3 days after germination. Undamaged maize leaves and caterpillar oral secretion-treated maize leaves were obtained as described in the Methods section. Glycosylated compounds were extracted with methanol and cyanogenic glycosides were analyzed using LC-MS/MS with multiple reaction monitoring (MRM). MRMs for dhurrin, prunasin, and amygdalin were established using authentic standards obtained from SIGMA-Aldrich (http://www.sigmaaldrich.com) (dhurrin) or prepared from bitter almonds (prunasin, amygdalin) and MRMs for lotaustralin and linamarin were calculated from those of dhurrin and prunasin. Amygdalin, lotaustralin and linamarin could not be detected in maize and sorghum (data not shown). **Table S1.** Oligonucleotides used in this study.

Abbreviations

CYP: Cytochrome P450 monooxygenase; LC-MS/MS: Liquid chromatography-tandem mass spectrometry; IAA: Indole-3-acetic acid; PAA: Phenylacetic acid; FID: Flame ionization detector; MRM: Multiple reaction monitoring.

Competing interests

The authors declare that they have no competing interests.

Authors' contributions

SI, PZ and VH carried out the experimental work. SI, JG, and TGK participated in the design of the study and improved the manuscript. SI and TGK conceived of the study and drafted the manuscript. All authors read and approved the final manuscript.

References

1. Halkier BA, Gershenzon J. Biology and biochemistry of glucosinolates. Annu Rev Plant Biol. 2006;57:303–33.
2. Bak S, Paquette SM, Morant M, Morant AV, Saito S, Bjarnholt N, et al. Cyanogenic glycosides: a case study for evolution and application of cytochromes P450. Phytochem Rev. 2006;5(2–3):309–29.
3. Glawischnig E. Camalexin. Phytochemistry. 2007;68(4):401–6.
4. Knudsen JT, Eriksson R, Gershenzon J, Stahl B. Diversity and distribution of floral scent. Bot Rev. 2006;72(1):1–120.
5. Hamberger B, Bak S. Plant P450s as versatile drivers for evolution of species-specific chemical diversity. Philos Trans R Soc Lond B Biol Sci. 2013;368(1612):20120426.
6. Irmisch S, McCormick AC, Boeckler GA, Schmidt A, Reichelt M, Schneider B, et al. Two herbivore-induced cytochrome P450 enzymes CYP79D6 and CYP79D7 catalyze the formation of volatile aldoximes involved in poplar defense. Plant Cell. 2013;25(11):4737–54.
7. Sibbesen O, Koch B, Halkier BA, Moller BL. Cytochrome P-450TYR is a multifunctional heme-thiolate enzyme catalyzing the conversion of L-tyrosine to p-hydroxyphenylacetaldehyde oxime in the biosynthesis of the cyanogenic glucoside dhurrin in *Sorghum bicolor* (L.) Moench. J Biol Chem. 1995;270(8):3506–11.
8. Hull AK, Vij R, Celenza JL. Arabidopsis cytochrome P450s that catalyze the first step of tryptophan-dependent indole-3-acetic acid biosynthesis. Proc Natl Acad Sci U S A. 2000;97(5):2379–84.
9. Rauhut T, Glawischnig E. Evolution of camalexin and structurally related indolic compounds. Phytochemistry. 2009;70(15–16):1638–44.
10. Moller BL. Plant science. Dynamic metabolons. Science. 2010;330(6009):1328–9.
11. Clavijo McCormick A, Irmisch S, Reinecke A, Boeckler GA, Veit D, Reichelt M, et al. Herbivore-induced volatile emission in black poplar: regulation and role in attracting herbivore enemies. Plant Cell Environ. 2014;37(8):1909–23.
12. Glauser G, Marti G, Villard N, Doyen GA, Wolfender JL, Turlings TCJ, et al. Induction and detoxification of maize 1,4-benzoxazin-3-ones by insect herbivores. Plant J. 2011;68(5):901–11.
13. Marti G, Erb M, Boccard J, Glauser G, Doyen GR, Villard N, et al. Metabolomics reveals herbivore-induced metabolites of resistance and susceptibility in maize leaves and roots. Plant Cell Environ. 2013;36(3):621–39.
14. Pechan T, Cohen A, Williams WP, Luthe DS. Insect feeding mobilizes a unique plant defense protease that disrupts the peritrophic matrix of caterpillars. Proc Natl Acad Sci U S A. 2002;99(20):13319–23.

Manuscript II

Irmisch *et al. BMC Plant Biology* (2015) 15:128

Page 14 of 14

15. Rohrmeier T, Lehle L. Wip1, a wound-inducible gene from Maize with homology to Bowman-Birk Proteinase-Inhibitors. Plant Mol Biol. 1993;22(5):783–92.
16. Turlings TCJ, Tumlinson JH, Lewis WJ. Exploitation of herbivore-induced plant odors by host-seeking parasitic Wasps. Science. 1990;250(4985):1251–3.
17. Brunnich JC. Hydrocyanic acid in fodder-plants. J Chem Soc. 1903;83:788–96.
18. Lehmann G, Zinsmeister HD, Erb N, Neunhoeffer O. Content of hydrocyanic acid in corn and cereal products. Z Ernahrungswiss. 1979;18(1):16–22.
19. Erb N, Zinsmeister H, Lehmann G, Michely D. Der blausäuregehalt von getreidearten gemässigter klimazonen. Z Lebensm Unters Forsch. 1981;173(3):176–9.
20. Takabayashi J, Takahashi S, Dicke M, Posthumus MA. Developmental stage of herbivore *Pseudaletia-Separata* affects production of herbivore-induced synomone by corn plants. J Chem Ecol. 1995;21(3):273–87.
21. Turlings TCJ, Bernasconi M, Bertossa R, Bigler F, Caloz G, Dorn S. The induction of volatile emissions in maize by three herbivore species with different feeding habits: possible consequences for their natural enemies. Biol Control. 1998;11(2):122–9.
22. Degen T, Dillmann C, Marion-Poll F, Turlings TCJ. High genetic variability of herbivore-induced volatile emission within a broad range of maize inbred lines. Plant Physiol. 2004;135(4):1928–38.
23. Köllner TG, Schnee C, Gershenzon J, Degenhardt J. The sesquiterpene hydrocarbons of maize (*Zea mays*) form five groups with distinct developmental and organ-specific distributions. Phytochemistry. 2004;65(13):1895–902.
24. Ro DK, Ouellet M, Paradise EM, Burd H, Eng D, Paddon CJ, et al. Induction of multiple pleiotropic drug resistance genes in yeast engineered to produce an increased level of anti-malarial drug precursor, artemisinic acid. BMC Biotechnol. 2008;8:83.
25. Pompon D, Louerat B, Bronine A, Urban P. Yeast expression of animal and plant P450s in optimized redox environments. Methods Enzymol. 1996;272:51–64.
26. Voinnet O, Rivas S, Mestre P, Baulcombe D. An enhanced transient expression system in plants based on suppression of gene silencing by the p19 protein of tomato bushy stunt virus. Plant J. 2003;33(5):949–56.
27. Gallavotti A, Barazesh S, Malcomber S, Hall D, Jackson D, Schmidt RJ, et al. *Sparse inflorescence1* encodes a monocot-specific *YUCCA*-like gene required for vegetative and reproductive development in maize. Proc Natl Acad Sci U S A. 2008;105(39):15190–5.
28. Pollmann S, Muller A, Weiler EW. Many roads lead to "auxin": of nitrilases, synthases, and amidases. Plant Biol (Stuttg). 2006;8(3):326–33.
29. Akazawa T, Miljanich P, Conn EE. Studies on cyanogenic glycoside of *Sorghum vulgare*. Plant Physiol. 1960;35(4):535–8.
30. Halkier BA, Olsen CE, Moller BL. The biosynthesis of cyanogenic glucosides in higher-plants - the (*E*)-Isomers and (*Z*)-Isomers of *Para*-Hydroxyphenylacetaldehyde Oxime as intermediates in the biosynthesis of Dhurrin in *Sorghum-Bicolor* (L) Moench. J Biol Chem. 1989;264(33):19487–94.
31. Gleadow RM, Moller BL. Cyanogenic glycosides: synthesis, physiology, and phenotypic plasticity. Annu Rev Plant Biol. 2014;65:155–85.
32. Raguso RA. Wake up and smell the roses: the ecology and evolution of floral scent. Annu Rev Ecol Evol Syst. 2008;39:549–69.
33. Moller BL, Andersen MD, Busk PK, Svendsen I. Cytochromes P450 from cassava (*Manihot esculenta* Crantz) catalyzing the first steps in the biosynthesis of the cyanogenic glucosides linamarin and lotaustralin - Cloning, functional expression in *Pichia pastoris*, and substrate specificity of the isolated recombinant enzymes. J Biol Chem. 2000;275(3):1966–75.
34. Kollner TG, Lenk C, Schnee C, Kopke S, Lindemann P, Gershenzon J, et al. Localization of sesquiterpene formation and emission in maize leaves after herbivore damage. BMC Plant Biol. 2013;13:15.
35. Irmisch S, Clavijo McCormick A, Gunther J, Schmidt A, Boeckler GA, Gershenzon J, et al. Herbivore-induced poplar cytochrome P450 enzymes of the CYP71 family convert aldoximes to nitriles which repel a generalist caterpillar. Plant J. 2014;80(6):1095–107.
36. Yamaguchi T, Yamamoto K, Asano Y. Identification and characterization of CYP79D16 and CYP71AN24 catalyzing the first and second steps in L-phenylalanine-derived cyanogenic glycoside biosynthesis in the Japanese apricot, *Prunus mume* Sieb. et Zucc. Plant Mol Biol. 2014;86(1–2):215–23.
37. Rajagopal R, Larsen P. Metabolism of indole-3-acetaldoxime in plants. Planta. 1972;103(1):45–54.

38. Bak S, Feyereisen R. The involvement of two P450 enzymes, CYP83B1 and CYP83A1, in auxin homeostasis and glucosinolate biosynthesis. Plant Physiol. 2001;127(1):108–18.
39. Zhao YD, Hull AK, Gupta NR, Goss KA, Alonso J, Ecker JR, et al. Trp-dependent auxin biosynthesis in Arabidopsis: involvement of cytochrome P450s CYP79B2 and CYP79B3. Genes Dev. 2002;16(23):3100–12.
40. Sugawara S, Hishiyama S, Jikumaru Y, Hanada A, Nishimura T, Koshiba T, et al. Biochemical analyses of indole-3-acetaldoxime-dependent auxin biosynthesis in Arabidopsis. Proc Natl Acad Sci U S A. 2009;106(13):5430–5.
41. Park WJ, Kriechbaumer V, Muller A, Piotrowski M, Meeley RB, Gierl A, et al. The nitrilase ZmNIT2 converts indole-3-acetonitrile to indole-3-acetic acid. Plant Physiol. 2003;133(2):794–802.
42. Onkokesung N, Galis I, von Dahl CC, Matsuoka K, Saluz HP, Baldwin IT. Jasmonic acid and ethylene modulate local responses to wounding and simulated herbivory in *Nicotiana attenuata* leaves. Plant Physiol. 2010;153(2):785–98.
43. Tooker JF, De Moraes CM. Feeding by a gall-inducing caterpillar species alters levels of indole-3-acetic and abscisic acid in *Solidago altissima* (Asteraceae) stems. Arthropod Plant Interact. 2011;5(2):115–24.
44. Tooker J, De Moraes C. Feeding by Hessian fly (*Mayetiola destructor* [Say]) larvae on wheat increases levels of fatty acids and indole-3-acetic acid but not hormones involved in plant-defense signaling. J Plant Growth Regul. 2011;30(2):158–65.
45. Erb M, Meldau S, Howe GA. Role of phytohormones in insect-specific plant reactions. Trends Plant Sci. 2012;17(5):250–9.
46. Moller BL, Kahn RA, Fahrendorf T, Halkier BA. Substrate specificity of the cytochrome P450 enzymes CYP79A1 and CYP71E1 involved in the biosynthesis of the cyanogenic glucoside dhurrin in *Sorghum bicolor* (L.) Moench. Arch Biochem Biophys. 1999;363(1):9–18.
47. Joulain D, König WA. The Atlas of Spectral Data of Sesquiterpene Hydrocarbons. Hamburg, Germany: E.B.-Verlag; 1998.
48. Urban P, Werckreichhart D, Teutsch HG, Durst F, Regnier S, Kazmaier M, et al. Characterization of recombinant plant cinnamate 4-hydroxylase produced in yeast - kinetic and spectral properties of the major plant P450 of the Phenylpropanoid pathway. Eur J Biochem. 1994;222(3):843–50.
49. Manoli A, Sturaro A, Trevisan S, Quaggiotti S, Nonis A. Evaluation of candidate reference genes for qPCR in maize. J Plant Physiol. 2012;169(8):807–15.
50. Jander G, Norris SR, Joshi V, Fraga M, Rugg A, Yu S, et al. Application of a high-throughput HPLC-MS/MS assay to Arabidopsis mutant screening; evidence that threonine aldolase plays a role in seed nutritional quality. Plant J. 2004;39(3):465–75.
51. Balcke GU, Handrick V, Bergau N, Fichtner M, Henning A, Stellmach H, et al. An UPLC-MS/MS method for highly sensitive high-throughput analysis of phytohormones in plant tissues. Plant Methods. 2012;8(1):47.
52. Tamura K, Peterson D, Peterson N, Stecher G, Nei M, Kumar S. MEGA5: molecular evolutionary genetics analysis using maximum likelihood, evolutionary distance, and maximum parsimony methods. Mol Biol Evol. 2011;28(10):2731–9.

3.3 Manuscript III

Biosynthesis of 8-*O*-Methylated Benzoxazinoid Defense Compounds in Maize°

Running head: The late steps of benzoxazinoid formation in maize

Biosynthesis of 8-*O*-methylated benzoxazinoid defense compounds in maize

Vinzenz Handrick[a,1], Christelle A. M. Robert[b,1], Kevin R. Ahern[c], Shaoqun Zhou[c], Ricardo A. R. Machado[b], Daniel Maag[d], Gaetan Glauser[d], Felix E. Fernandez-Penny[c], Jima N. Chandran[a], Eli Rodgers-Melnik[e], Bernd Schneider[a], Edward S. Buckler[e], Wilhelm Boland[a], Jonathan Gershenzon[a], Georg Jander[c,2], Matthias Erb[b,2], and Tobias G. Köllner[a,2,3]

[a]Max Planck Institute for Chemical Ecology, 07745 Jena, Germany
[b]Institute of Plant Sciences, University of Bern, 3013 Bern, Switzerland
[c]Boyce Thompson Institute for Plant Research, Ithaca, New York 14853, USA
[d]Institute of Biology, University of Neuchatel, 2009 Neuchatel, Switzerland
[e]Institute for Genomic Diversity, Cornell University, Ithaca, New York 14853, USA

[1]These authors contributed equally to this work and share first authorship
[2] These authors contributed equally to this work and share senior authorship
[3] Address for correspondence: koellner@ice.mpg.de

Estimated length of the published article from the page calculator: xx pages

The author responsible for distribution of materials integral to the findings presented in this article in accordance with the policy described in the Instructions for Authors (www.plantcell.org) is: Tobias G. Köllner (koellner@ice.mpg.de).

SYNOPSIS

Benzoxazinoids are major defense compounds in maize and other grasses. We used a genome-wide quantitative trait mapping strategy to identify a dioxygenase and two *O*-methyltransferases that catalyze the conversion of DIMBOA-Glc into the 8-*O*-methylated benzoxazinoids, DIM$_2$BOA-Glc and HDM$_2$BOA-Glc. We further show that this branch of the pathway specifically increases maize resistance against aphids.

ABSTRACT

Benzoxazinoids are important defense compounds in grasses. Here, we investigated the biosynthesis and biological roles of the 8-*O*-methylated benzoxazinoids, DIM_2BOA-Glc and HDM_2BOA-Glc. Using quantitative trait locus mapping and heterologous expression, we identified a 2-oxoglutarate-dependent dioxygenase (BX13) which catalyzes the conversion of DIMBOA-Glc into a new benzoxazinoid intermediate (TRIMBOA-Glc) by an uncommon reaction involving a hydroxylation and a likely ortho-rearrangement of a methoxy group. TRIMBOA-Glc is then converted to DIM_2BOA-Glc by a previously described *O*-methyltransferase BX7. Furthermore, we identified a new *O*-methyltransferase (BX14) that converts DIM_2BOA-Glc to HDM_2BOA-Glc. The role of these enzymes in vivo was demonstrated by characterization of recombinant inbred lines, including Oh43, which has a point mutation in the start codon of *Bx13* and lacks both DIM_2BOA-Glc and HDM_2BOA-Glc, and Il14h, which has an inactive *Bx14* allele and lacks HDM_2BOA-Glc in leaves. Experiments with near-isogenic maize lines (NILs) derived from crosses between B73 and Oh43 revealed that the absence of DIM_2BOA-Glc and HDM_2BOA-Glc does not alter the constitutive accumulation or deglucosylation of other benzoxazinoids. The growth of various chewing herbivores was not significantly affected by the absence of BX13-dependent metabolites, while aphid performance increased, suggesting that DIM_2BOA-Glc and/or HDM_2BOA-Glc provide specific protection against phloem feeding insects.

INTRODUCTION

To protect themselves from herbivores, plants synthesize diverse arrays of toxic metabolites. Benzoxazinoids are among the most important plant defense compounds in many grasses, including wheat and maize (Niemeyer, 2009). They are predominantly stored as glucosides in the vacuoles and are enzymatically hydrolyzed into the respective aglucones and sugars upon tissue injury (reviewed in Niemeyer, 2009). Subsequent non-enzymatic breakdown of the unstable aglucones leads to the formation of highly reactive metabolites that are toxic to a wide range of chewing and phloem-feeding insect herbivores and plant pathogens (Niemeyer, 2009). However, certain herbivores can circumvent benzoxazinoid toxicity by re-glucosylating the aglucones (Glauser et al., 2011; Wouters et al., 2014) and their breakdown products (Maag et al., 2014). Specialized maize feeders like the western corn rootworm (*Diabrotica virgifera virgifera*) and the fall armyworm (*Spodoptera frugiperda*) even use benzoxazinoids as foraging cues (Köhler et al., 2015; Robert et al., 2012).

The core biosynthetic pathway of the major maize benzoxazinoid 2-(2,4-di-hydroxy-7-methoxy-1,4-benzoxazin-3-one)-β-D-glucopyranose (DIMBOA-Glc) has been extensively studied (Gierl and Frey, 2001; Jonczyk et al., 2008; reviewed in Frey et al., 2009). The biosynthesis starts in the plastids with the conversion of the shikimate pathway-derived indole-3-glycerol phosphate into indole, catalyzed by the indole-3-glycerol phosphate lyase benzoxazinoneless 1 (BX1). A subsequent stepwise introduction of four oxygen atoms by the P450 monooxygenases BX2, BX3, BX4, and BX5 leads to the formation of 2,4-dihydroxy-1,4-benzoxazin-3-one (DIBOA), the core structure of the benzoxazinoids. DIBOA acts as substrate for the UDP-glucosyltransferases BX8 and BX9, which transform the toxic compound into the stable glucoside DIBOA-Glc (von Rad et al., 2001). A hydroxylation of DIBOA-Glc at C-7, catalyzed by the 2-oxoglutarate-dependent dioxygenase (2ODD) BX6, and a subsequent methylation of the introduced hydroxyl group, catalyzed by the *O*-methyltransferase BX7, lead to the production of DIMBOA-Glc in the cytosol (Jonczyk et al., 2008).

DIMBOA-Glc is the most abundant benzoxazinoid in young and undamaged leaves of many maize lines, reaching levels up to 3 mg g^{-1} fresh weight (Meihls et al., 2013). However, upon insect herbivory or fungal infestation, its derivative 2-(2-

hydroxy-4,7-dimethoxy-1,4-benzoxazin-3-one)-β-D-glucopyranose (HDMBOA-Glc) accumulates and becomes the dominant benzoxazinoid (Oikawa et al., 2004; Glauser et al., 2011; Dafoe et al., 2011; Marti et al., 2013). Three homologous *O*-methyltransferases (BX10, BX11, and BX12; formerly designated BX10a, BX10b, and BX10c) convert DIMBOA-Glc into HDMBOA-Glc by *S*-adenosyl-L-methionine-dependent methylation of the hydroxamic group of DIMBOA-Glc (Meihls et al., 2013). After tissue maceration caused, for example, by chewing herbivores, DIMBOA-Glc and HDMBOA-Glc are hydrolyzed by endogenous β-glucosidases, resulting in the liberation of 2,4-dihydroxy-7-methoxy-1,4-benzoxazin-3-one (DIMBOA) and 2-hydroxy-4,7-dimethoxy-1,4-benzoxazin-3-one (HDMBOA), respectively (Babcock and Esen, 1994; Czjzek et al., 2000). Although both aglucones are unstable, non-enzymatic breakdown is faster for HDMBOA than for DIMBOA and HDMBOA has been associated with increased resistance against leaf-chewing herbivores (Oikawa et al., 2004; Maresh et al., 2006; Glauser et al., 2011; Meihls et al., 2013). On the other hand, the decline in DIMBOA-Glc as a result of increased HDMBOA-Glc production has been shown to be associated with a reduction in callose deposition, which increases the plant's susceptibility to phloem feeding aphids (Ahmad et al, 2011; Meihls et al, 2013; Tzin et al, 2015).

Besides DIMBOA-Glc and HDMBOA-Glc, many maize lines produce significant amounts of other benzoxazinoid derivatives such as the 8-*O*-methylated compounds, 2-(2,4-dihydroxy-7,8-dimethoxy-1,4-benzoxazin-3-one)-β-D-glucopyranose (DIM$_2$BOA-Glc) and 2-(2-hydroxy-4,7,8-trimethoxy-1,4-benzoxazin-3-one)-β-D-glucopyranose (HDM$_2$BOA-Glc) (Cambier et al., 1999; Glauser et al., 2011). DIM$_2$BOA-Glc is most likely formed through the addition of a methoxy group to DIMBOA-Glc. HDM$_2$BOA-Glc, on the other hand, is likely derived from DIM$_2$BOA-Glc by a methylation of the hydroxamic group and is also induced after herbivory (Glauser et al., 2011). In contrast to the other major benzoxazinoids, the biosynthesis and biological relevance of DIM$_2$BOA-Glc and HDM$_2$BOA-Glc are unknown.

To elucidate the biosynthesis of DIM$_2$BOA-Glc and HDM$_2$BOA-Glc, we took advantage of the sequenced genome of the maize inbred line B73 (Schnable et al., 2009), the availability of high-resolution physical and genetic maps (Wei et al., 2009; Zhou et al., 2009; Ganal et al., 2011) and the nested association mapping (NAM) population generated from 25 diverse maize inbred lines (Flint-Garcia et al., 2005; Yu et al., 2008; McMullen et al., 2009). Using quantitative trait locus (QTL)

mapping combined with heterologous expression, we were able to identify enzymes involved in DIM_2BOA-Glc and HDM_2BOA-Glc formation. To understand the importance of the identified enzymes in benzoxazinoid biosynthesis, we analyzed the genetic basis of natural variation in constitutive and herbivore-induced DIM_2BOA-Glc and HDM_2BOA-Glc levels. Finally, the generation of near-isogenic maize lines that differ in their capacity to produce DIM_2BOA-Glc and HDM_2BOA-Glc allowed us to study the importance of these compounds for the interaction between maize and different herbivores. Our experiments show that DIM_2BOA-Glc and HDM_2BOA-Glc are produced through an unexpected intermediate and specifically increase maize resistance to aphids.

RESULTS

Natural variation in constitutive and induced DIM_2BOA-Glc and HDM_2BOA-Glc

To identify genes responsible for the formation of DIM_2BOA-Glc and HDM_2BOA-Glc in maize, we first profiled their abundance in the leaves and roots of different NAM parental maize lines. In the leaves, DIM_2BOA-Glc levels varied substantially, ranging from 18 µg g^{-1} FW in the inbred line CML277 to 600 µg/g FW in the inbred line P39 (Figure 1A). This pattern is consistent with earlier findings (Meihls et al., 2013). In the roots, concentrations varied between 42 µg g^{-1} FW in CML322 and 1000 µg g^{-1} FW in Mo18W. One inbred line, Oh43, produced no detectable amounts of DIM_2BOA-Glc in either leaves or roots. The constitutive concentrations of HDM_2BOA-Glc were lower than those of DIM_2BOA-Glc, with the highest concentrations being found in the leaves of HP301 (27 µg g^{-1} FW) and the roots of CML277 (339 µg g^{-1} FW). Again, Oh43 contained no detectable amounts of HDM_2BOA-Glc in both tissues (Figure 1A). Several other lines produced no detectable amounts of HDM_2BOA-Glc. Apart from their consistent absence in Oh43, no clear correlations between leaf- and root DIM_2BOA-Glc and HDM_2BOA-Glc levels were found across the different parental lines (Pearson Product Moment Correlations, $P > 0.05$).
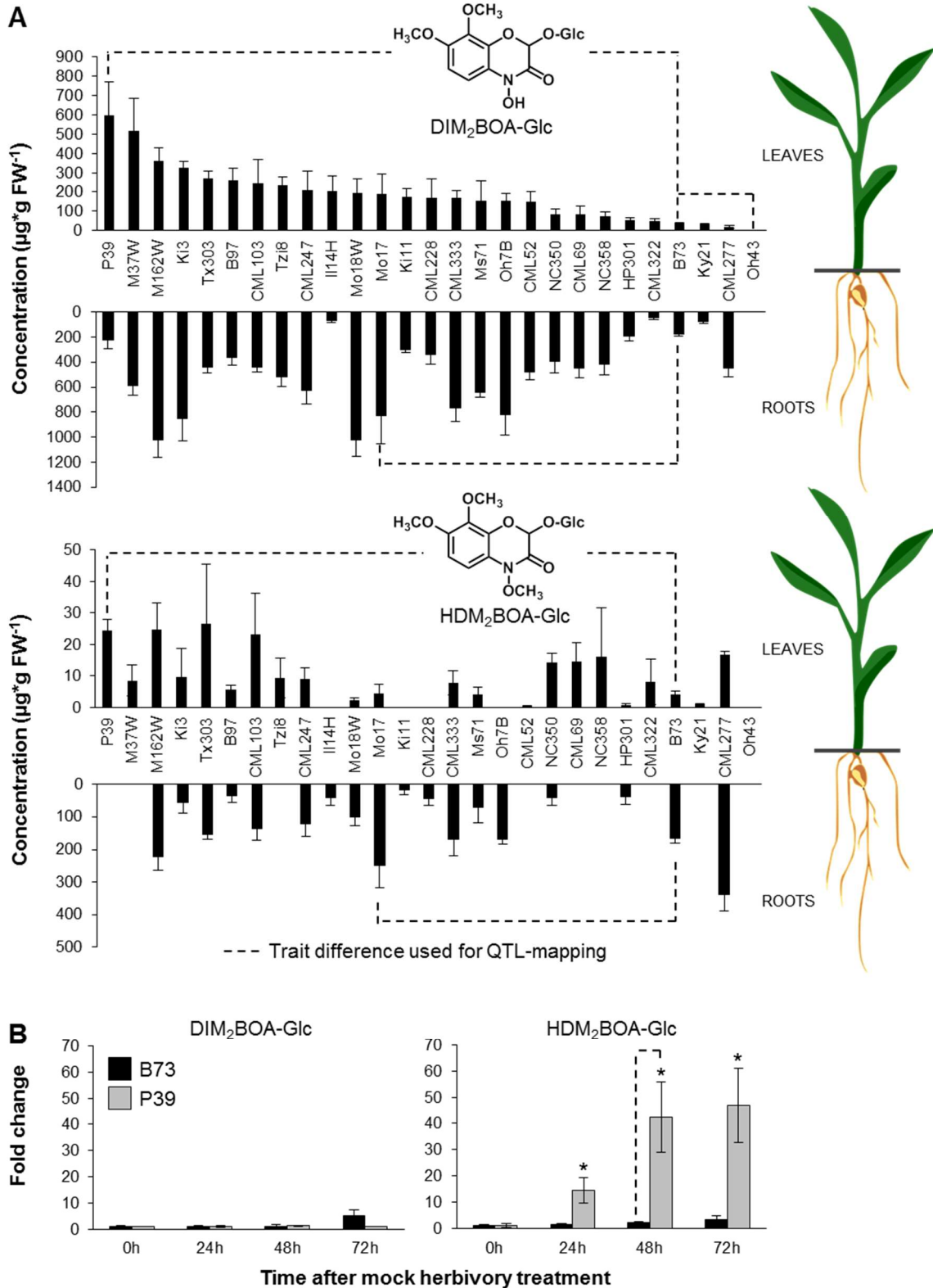
Figure 1. Benzoxazinoid abundance in leaves and roots of the nested association mapping (NAM) parental lines. (A) DIM$_2$BOA-Glc (top) and HDM$_2$BOA-Glc (bottom) concentrations in the leaves and roots of the NAM parental lines. Lines are sorted by average leaf-concentrations. DIM$_2$BOA-Glc was not detectable in the line Oh43. n = 3 - 6. (B) Induction of DIM$_2$BOA-Glc and HDM$_2$BOA-Glc in the leaves of the lines B73 and P39 at different time points. Herbivory was mimicked by wounding and application of *Spodoptera exigua* regurgitant. Fold changes compared to non-elicited controls are shown. Stars indicate significant differences in inducibility between B73 and P39 (n = 5, Student's *t*-test, *P* < 0.05). Dashed lines indicate trait differences that were used for QTL-mapping.

HDM$_2$BOA-Glc is known to be induced by biotic stresses such as pathogen infestation and insect feeding (Oikawa, 2004; Ahmad et al., 2011; Marti et al., 2013). Preliminary screens indicated that different NAM parental lines also differ in their inducibility (Supplemental Tables 1 and 2). We therefore profiled herbivore-induced changes in two NAM lines, B73 and P39, in detail. Leaves were wounded on one side of the midrib and treated with regurgitant of the generalist beet armyworm (*Spodoptera exigua*) to mimic herbivory (Erb et al., 2009). In both lines, DIM$_2$BOA-Glc concentrations did not significantly change upon this mock herbivory treatment. However, we observed a significant local accumulation of HDM$_2$BOA-Glc after application of insect regurgitant, which was more than 40-fold greater in P39 than in B73 (Figure 1B). No changes in DIM$_2$BOA-Glc or HDM$_2$BOA-Glc were observed on the other side of the midrib of the induced leaves (Supplemental Figure 0).

Mapping of constitutive and induced DIM$_2$BOA-Glc and HDM$_2$BOA-Glc production revealed three QTLs on chromosomes 2 and 4

Based on our initial screening, we performed several QTL mapping experiments using recombinant inbred lines derived from crosses between B73 and the other NAM lines. Due to the significant differences between constitutive DIM$_2$BOA-Glc and HDM$_2$BOA-Glc content in leaves of the inbred lines P39 and B73 (Figure 1A; DIM$_2$BOA-Glc, n ≥ 4, *P* < 0.05; HDM$_2$BOA-Glc, n ≥ 4, *P* < 0.05), we first mapped constitutive production of both compounds in the recombinant inbred population B73 x P39. Mapping of DIM$_2$BOA-Glc revealed three QTLs, *Bb1*, *Bb2*, and *Bb3* (*benzoxazinoid biosynthesis 1 – 3*), located on chromosomes 2 and 4 (bins 2.05, 2.09 and 4.03, respectively, Figure 2A, Supplemental Table 3). In contrast, the HDM$_2$BOA-Glc mapping resulted in two QTLs on chromosome 2 which were identical to *Bb1* and *Bb2* (Figure 2B). On average, each of the identified QTLs covered about 900 putative coding DNA sequences.

In contrast to inbred line P39, which produced the largest leaf amounts of DIM$_2$BOA-Glc among all the tested NAM parental lines, inbred line Oh43 accumulated no detectable amounts of this compound (Figure 1A). We therefore mapped the constitutive production of DIM$_2$BOA-Glc in the B73 x Oh43 recombinant inbred population. The mapping identified one QTL on chromosome 2 that was identical to *Bb2* (Figure 2C, Supplemental Table 3).
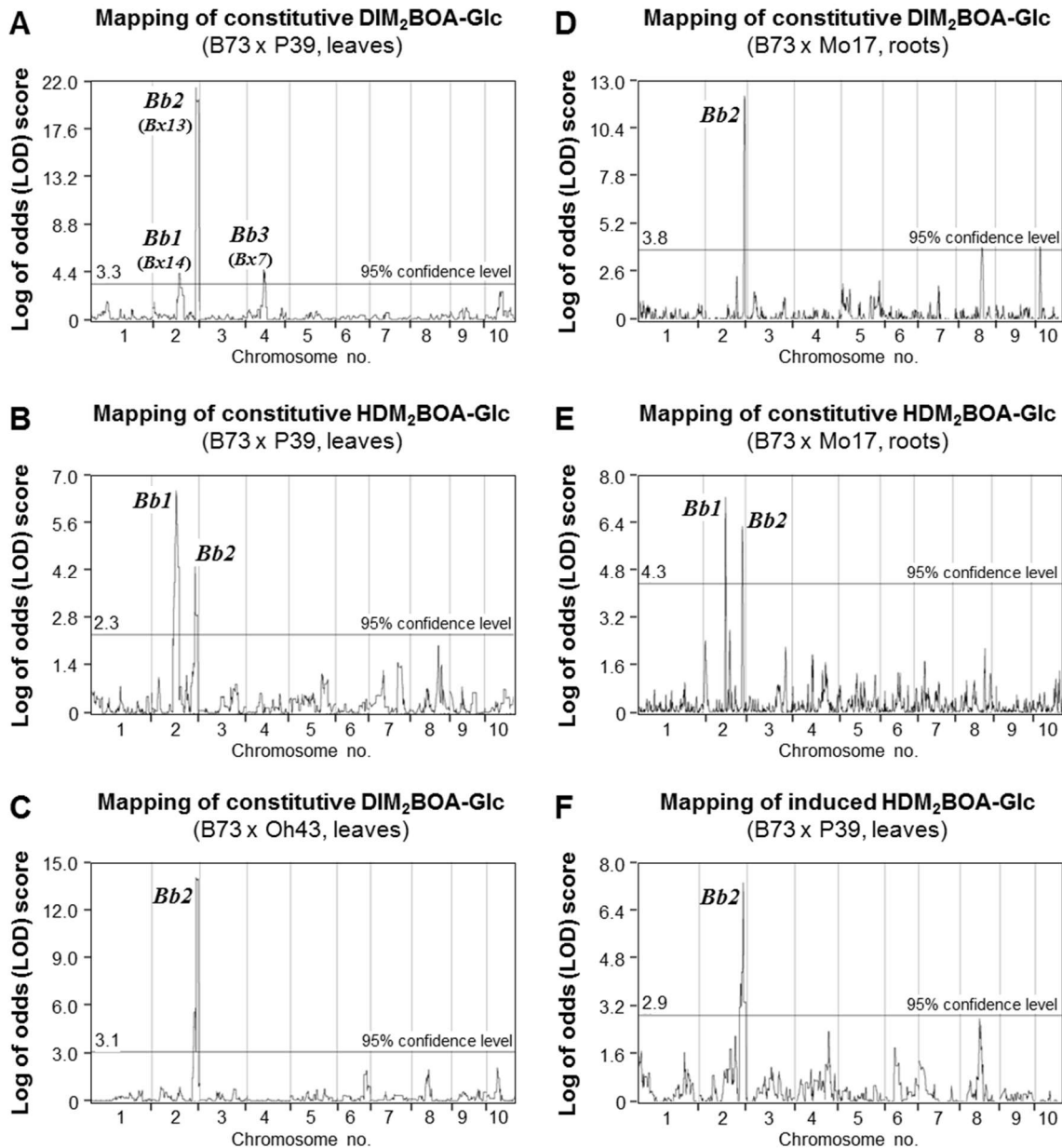
Figure 2. QTL mapping of constitutive and herbivore-induced content of DIM$_2$BOA-Glc and HDM$_2$BOA-Glc in different recombinant inbred line (RIL) populations. Constitutive DIM$_2$BOA-Glc content was mapped using the B73 x P39 (A), B73 x Oh43 (C), and B73 x Mo17 (D) RIL populations and resulted in three *benzoxazinoid biosynthesis* QTLs, *Bb1 – 3*, on chromosomes 2 and 4. Mapping of constitutive HDM$_2$BOA-Glc levels using the B73 x P39 RIL population (B) and B73 x Mo17 population (E) resulted in *Bb1* and *Bb2*. Mapping of HDM$_2$BOA-Glc abundance (F) in herbivory-induced leaves also resulted in *Bb2*.

Differences in root DIM$_2$BOA-Glc content between the B73 and Mo17 NAM lines (Figure 1A) allowed us to use the Mo17 x B73 population for mapping DIM$_2$BOA-Glc concentration in the roots. This experiment also revealed the QTL *Bb2* on chromosome 2 (Figure 2D, Supplemental Table 3). Although HDM$_2$BOA-Glc concentrations in B73 and Mo17 roots were not significantly different (Figure 1A), there is transgressive segregation for this trait and genetic mapping with the Mo17 x B73 population identified the *Bb1* and *Bb2* loci (Figure 2E), as in the case

of the B73 x P39 mapping population (Figure 2B). To gain insight into the genetic control of herbivore-induced formation of HDM$_2$BOA-Glc, we mapped the concentration of this compound in *S. exigua*-induced leaf sections of the B73 x P39 population. Again, as in all previous mapping experiments, a major QTL identical to *Bb2* was mapped (Figure 2F, Supplemental Table 3), suggesting that *Bb2* is required for the formation of both constitutive DIM$_2$BOA-Glc and herbivore-induced HDM$_2$BOA-Glc.

The QTL *Bb2* contains a candidate dioxygenase gene *Bx13*

Given that the formation of the core benzoxazinoid, DIMBOA-Glc, might follow a linear pathway (Frey et al., 2009; Meihls et al., 2013), we hypothesized that DIM$_2$BOA-Glc is produced from DIMBOA-Glc via hydroxylation of the aromatic ring at C-8 and subsequent methylation of the hydroxyl group. Such a reaction sequence is analogous to the formation of DIMBOA-Glc from DIBOA-Glc, which has been shown to involve the hydroxylation of the aromatic ring at C-7 and the methylation of the resulting hydroxyl group, catalyzed by the 2-oxoglutarate-dependent dioxygenase (2ODD) BX6 and the *O*-methyltransferase (OMT) BX7, respectively (Jonczyk et al., 2008). While two of the identified QTLs, *Bb1 and Bb3,* contain at least one putative OMT gene, only one QTL, *Bb2,* contained a putative 2ODD gene (AC148152.3_FG005). Since a sequence comparison with maize 2ODDs similar to AC148152.3_FG005 revealed that the mapped 2ODD gene clustered with *Bx6* (Figure 3A), we hypothesized that AC148152.3_FG005 encode the first enzymatic step in the formation of DIM$_2$BOA-Glc from DIMBOA-Glc.

BX13 catalyzes the oxidation of DIMBOA-Glc to TRIMBOA-Glc

To test the enzymatic activity of AC148152.3_FG005*,* we heterologously expressed the P39 allele in *Escherichia coli.* Enzyme assays containing the purified protein, the potential substrate DIMBOA-Glc, and the co-substrate 2-oxoglutarate resulted in the formation of a single product, while a control assay containing the nickel affinity-purified protein fraction from *E. coli* expressing the empty vector showed no product formation (Figure 3B). Liquid chromatography-mass spectro-
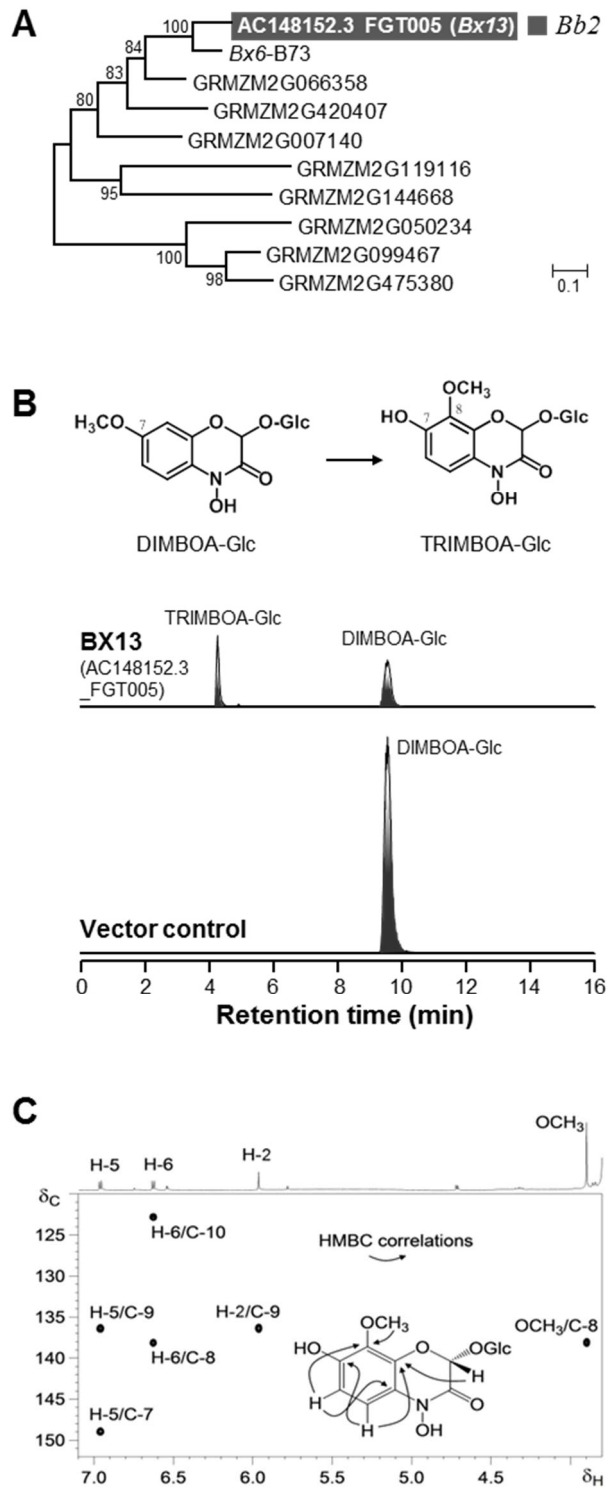
Figure 3. Identification, characterization and product identification of BX13. (A) Dendrogram analysis (unrooted tree) of maize *2ODD* genes similar to *Bx6*-B73. The tree was inferred using the maximum likelihood method and N = 1000 replicates for bootstrapping. Bootstrap values are shown next to each node. The tree is drawn to scale, with branch lengths measured in the number of substitutions per site. The candidate gene that has been mapped on chromosome 2 (QTL *Bb2*) is marked in grey. The alignment is available in Supplemental Data Set 1 online. (B) Purified recombinant BX13 as well as the empty vector control were incubated with DIMBOA-Glc and the co-factors Fe(II) and 2-oxoglutarate. Product formation was analyzed by LC-MS/MS. The relative intensities of the LC-MS/MS transitions are shown. (C) Partial HMBC spectrum (500 MHz) of TRIMBOA-Glc displaying correlation signals between protons and carbon atoms of the aglucone through three-bonds. The OC$\underline{H}_3$/C-8 cross signal verifies the position of the *O*-methyl group at C-8.

metry (LC-MS/MS) analysis of the enzyme product revealed a fragmentation pattern consistent with an oxidized DIMBOA-Glc (Supplemental Figure 1). Activity assays with HDMBOA-Glc showed that AC148152.3_FG005 was not able to accept this compound as substrate (Supplemental Figure 2). Notably, BX6, which shares 77% identity at the amino acid level to AC148152.3_FG005, showed no activity with DIMBOA-Glc (Supplemental Figure 2). Due to the catalytic activity of AC148152.3_FG005, we renamed the enzyme BX13, following the nomenclature for enzymes involved in benzoxazinoid biosynthesis (Frey et al., 2009).

In order to isolate the DIMBOA-Glc oxidation product for NMR analysis, 300 enzyme assays were performed and pooled. Product purification was done using semi-preparative HPLC, resulting in approximately 100 µg of pure compound. While the NMR measurements confirmed the known structure of the BX13 substrate DIMBOA-Glc, containing a methoxy group at C-7 of the aromatic ring, NMR analysis of the enzyme product revealed an unexpected structure, 2-(2,4,7-trihydroxy-8-methoxy-1,4-benzoxazin-3-one)-β-D-glucopyranose (TRIMBOA-Glc, Supplemental Table 5) with a hydroxyl group at C-7 and a methoxy group at C-8 of the aromatic ring (Figure 3C).

The DIM$_2$BOA-Glc-free inbred line Oh43 possesses a mutated allele of *Bx13*

In the NAM parental population, Oh43 was the only inbred line lacking any detectable amounts of DIM$_2$BOA-Glc and HDM$_2$BOA-Glc (Figure 1). A nucleotide sequence alignment of *Bx13*-P39 with genomic Oh43 Illumina sequences (SRX119503, http://blast.ncbi.nlm.nih.gov) revealed allelic variation within the *Bx13* start codon (*Bx13*-P39, ATG; *Bx13*-Oh43, TTG; Figure 4A). To verify this mutation, we sequenced the complete *Bx13*-B73 open reading frame amplified from Oh43 cDNA. Since there was a second in-frame start codon 41 codons downstream from the first ATG, the mutation of the Oh43 allele presumably results in a shorter open reading frame encoding a protein that lacks the first 41 amino acids (Supplemental Figures 3 and 4). Although alignments with crystallized plant 2ODD sequences revealed that the putative active site was unaffected by the truncation (Supplemental Figure 4), truncated recombinant BX13-Oh43 showed no enzymatic activity with DIMBOA-Glc (Figure 4B).
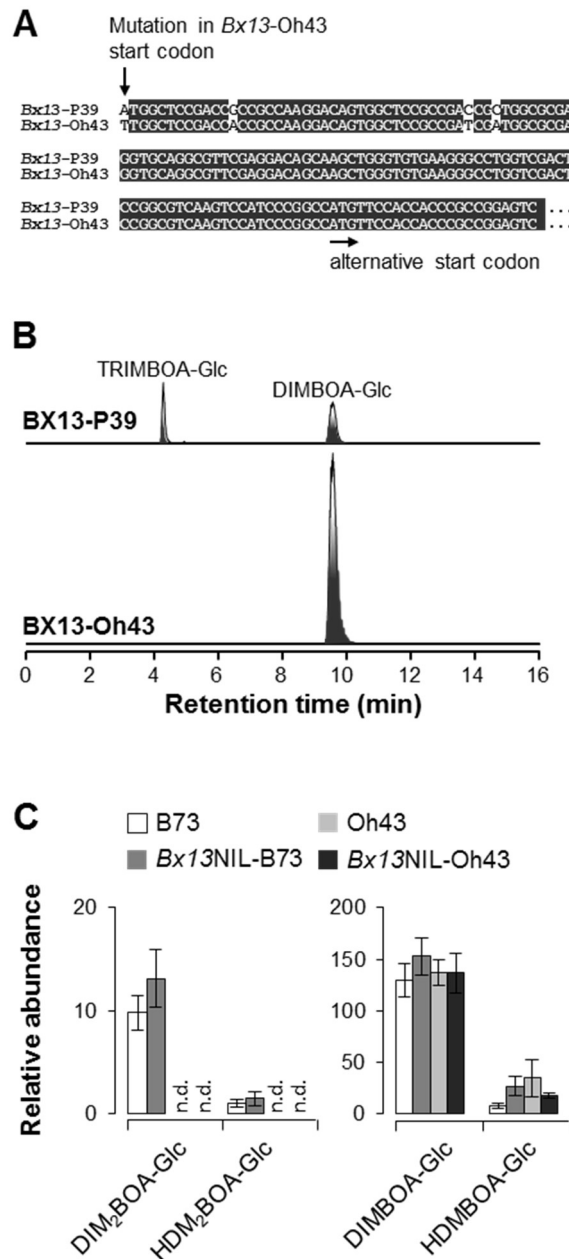
Figure 4. A mutation in the *Bx13* allele from the inbred line Oh43 causes loss of enzyme activity in vitro and in vivo. (A) Sequence alignment of *Bx13*-P39 and *Bx13*-Oh43. The two arrows indicate the start codon mutation of the Oh43 allele and the alternative start-codon, respectively. The complete alignment is shown in Supplemental Figure 3. (B) Activity assays of purified enzymes incubated with DIMBOA-Glc, the co-factors Fe(II), and 2-oxoglutarate. Shown are the relative intensities of the specific LC-MS/MS transitions. (C) Relative benzoxazinoid content in leaf extracts of the maize inbred lines B73 and Oh43, as well as of near isogenic lines possessing either the B73 allele of *Bx13* (*Bx13*NIL-B73) or the Oh43 allele of *Bx13* (*Bx13*NIL-Oh43). DIM$_2$BOA-Glc and HDM$_2$BOA-Glc could not be detected (n.d.) in leaves of the inbred Oh43 and the near isogenic line *Bx13*NIL-Oh43 (n = 5).

In order to discover other naturally-occurring *Bx13* knockout variants, we performed sensitive re-mapping of Illumina reads from 916 diverse maize lines in HapMap 3.1 (Bukowski et al., 2015). This approach, in combination with PCR amplification and re-sequencing, revealed that two inbred lines, LH38 and LH39, con-

tain the same start codon mutation as *Bx13*-Oh43 (Supplemental Figure 5). Benzoxazinoid analysis confirmed that LH38 and LH39 do not accumulate DIM_2BOA-Glc and HDM_2BOA-Glc (Supplemental Figure 5).

Near isogenic maize lines differing in the *Bx13* locus vary in DIM_2BOA-Glc and HDM_2BOA-Glc levels

To test the activity of BX13 in planta, we generated near isogenic lines (NILs) possessing either the B73 allele or the Oh43 allele of *Bx13.* Line Z022E0081 from the B73 x Oh43 RIL population, which is heterozygous for *Bx13* was selfed, 37 F2 progeny plants were genotyped at *Bx13* and other previously heterozygous genomic loci (Supplemental Table 4, Supplemental Figure 6), and homozygous, near-isogenic *Bx13*-B73 and *Bx13*-Oh43 lines were identified. The variable segment in this NIL pair constitutes less than 0.5% of the maize genome (approximately 4.7 Mbp and 185 genes). Constitutive and herbivore-induced formation of benzoxazinoids was measured in the identified homozygous lines. While the NIL carrying *Bx13*-B73 (*Bx13*NIL-B73) produced DIM_2BOA-Glc and HDM_2BOA-Glc in comparable amounts to B73, the NIL carrying *Bx13*-Oh43 (*Bx14*NIL-Oh43) contained no detectable DIM_2BOA-Glc and HDM_2BOA-Glc (Figure 4C). In contrast, DIMBOA-Glc and HDMBOA-Glc showed no significant differences between the parental lines and the NILs (Figure 4C).

The QTL *Bb3* comprises the *O*-methyltransferase gene *Bx7* which encodes an enzyme accepting TRIMBOA-Glc as substrate

The formation of DIM_2BOA-Glc from TRIMBOA-Glc requires a methylation of the C7 hydroxyl group, likely catalyzed by an *O*-methyltransferase. The QTLs *Bb1 and Bb3,* which appeared in the DIM_2BOA-Glc mapping (Figure 2A), contain seven sequences annotated as OMT, including *Bx7* (Figure 5A). Since BX7 methylates the C-7 hydroxyl group of TRIBOA-Glc (Jonczyk et al., 2008), we hypothesized that it could also catalyze the methylation of the corresponding hydroxyl group of TRIMBOA-Glc. To test this hypothesis, *Bx7* was heterologously expressed in *E. coli* and the purified recombinant protein was assayed with TRIMBOA-Glc as substrate and *S*-adenosyl-L-methionine (SAM) as co-substrate. While an empty vector control showed no product formation, recombinant BX7 produced significant amounts of DIM_2BOA-Glc (Figure 5B and Supplemental Figure 7).
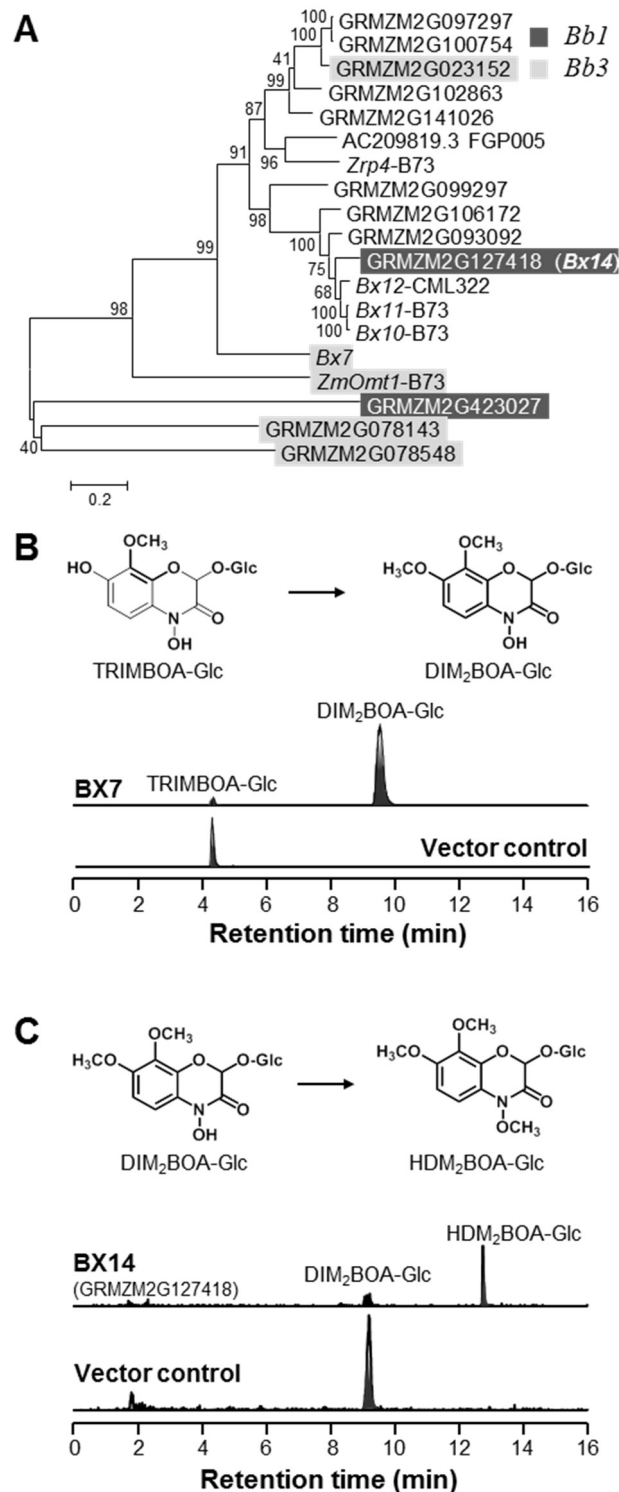
Figure 5. The *O*-methyltransferases BX7 and BX14 were identified by QTL mapping and accept benzoxazinoids as substrates. (A) Dendrogram analysis (unrooted tree) of mapped *OMTs* and maize *OMTs* with high sequence similarity to these candidates. The tree was inferred using the maximum likelihood method and n = 1000 replicates for bootstrapping. Bootstrap values are shown next to each node. The tree is drawn to scale, with branch lengths measured in the number of substitutions per site. Genes that have been mapped on chromosome 2 (QTL *Bb1*) are marked in dark grey, genes located in the QTL *Bb3* on chromosome 4 are highlighted in light grey. The alignment is available in Supplemental Data Set 2 online. (B-C) Activity assays of purified recombinant enzymes as well as the empty vector control incubated with the respective substrate and the co-substrate *S*-adenosyl-L-methionine. The relative intensities of the specific LC-MS/MS transitions (see Material and Methods) are shown.

Dendrogram analysis of the seven putative OMT genes located in the QTLs *Bb1* and *Bb3* showed that two sequences, GRMZM2G127418 and GRMZM2G023152, were similar to BX7 (Figure 5A). We therefore expressed these genes in *E. coli* to test whether they also methylate TRIMBOA-Glc. However, GRMZM2G127418 and GRMZM2G023152 showed no activity with this substrate (Supplemental Figure 7). Four other OMT genes including the previously characterized *ZmOmt1,* which encodes for tricetin *O*-methyltransferase (Zhou et al., 2008), belong to other OMT families and were thus not considered as benzoxazinoid-producing candidates.

Since *Bx7* is part of a small gene family consisting of 15 members with high sequence similarity to each other (Figure 5A), we tried to amplify all remaining potential *OMT* candidates and tested them for TRIMBOA-Glc OMT activity. However, only GRMZM2G097297, GRMZM2G100754, AC209819.3 FG005, *ZRP4*, *Bx10*, *Bx11*, and *Bx12* could be obtained from cDNA and none of them catalyzed the conversion of TRIMBOA-Glc into DIM_2BOA-Glc (Supplemental Figure 7).

BX14, an *O*-methyltransferase from the QTL *Bb1*, converts DIM_2BOA-Glc into HDM_2BOA-Glc

Two putative OMT genes could be identified in the confidence interval of *Bb1*, the QTL with the highest LOD score for constitutive HDM_2BOA-Glc production (Figure 5A). A dendrogram analysis revealed that one of them, GRMZM2G127418, showed high nucleotide identity to *Bx10* (87.5%), *Bx11* (87.4%), and *Bx12* (86.9%), which have been shown to encode for enzymes that catalyze the conversion of DIMBOA-Glc into HDMBOA-Glc (Meihls et al., 2013). The second OMT candidate in the *Bb1* QTL interval, GRMZM2G078548, clustered separately from the benzoxazinoid-specific OMT genes and showed only about 35% nucleotide identity to *Bx10-12* and 34% nucleotide identity to *Bx7* (Figure 5A).

To test for benzoxazinoid-specific OMT activity, GRMZM2G127418 was amplified from B73 leaf cDNA and heterologously expressed in *E. coli*. The enzyme was purified and incubated with the potential substrate DIM_2BOA-Glc and the co-substrate SAM. Subsequent LC-MS/MS analysis revealed the formation of HDM_2BOA-Glc, while the empty vector control showed no substrate turnover (Figure 5C). Therefore, GRMZM2G127418 was designated as BX14. In addition to DIM_2BOA-Glc, recombinant BX14 also accepted DIMBOA-Glc and produced

HDMBOA-Glc, while it showed no activity with TRIMBOA-Glc (Supplemental Figure 7). Other OMT with high similarity to BX14, including BX7, BX10, BX11, BX12, ZRP4, AC209819.3_FG005, GRMZM2G099297, GRMZM2G106172, and GRMZM2G093092 (Figure 5A), were not able to convert DIM_2BOA-Glc into HDM_2BOA-Glc (Supplemental Figure 8).

The inbred line Il14H possesses an inactive *Bx14* allele and is not able to produce HDM_2BOA-Glc in the leaves

Analysis of benzoxazinoids in the NAM parental lines showed that four of the tested lines produced no detectable amounts of HDM_2BOA-Glc but accumulated its potential precursor DIM_2BOA-Glc (Figure 1B). Since such a phenotype might be explained by an inactive *Bx14* allele, we performed a sequence comparison of *Bx14*-P39 with genomic Illumina sequences from the HDM_2BOA-Glc non-producing inbred line Il14H (SRP011907, http://blast.ncbi.nlm.nih.gov). In addition to several single nucleotide polymorphisms, the resulting alignment showed an in-frame insertion of 30 base pairs in the *Bx14*-Il14H allele leading to an extended open reading frame (Supplemental Figure 9). These mutations could be confirmed by sequencing of *Bx14*-Il14H amplified from cDNA. Activity assays with purified recombinant BX14-Il14H revealed that the enzyme did not accept DIM_2BOA-Glc as substrate (Supplemental Figure 10). PCR analysis of genomic DNA prepared from the 25 NAM parental inbred lines showed that the 30 bp insertion occurred in multiple *Bx14* alleles but was not correlated with the presence or absence of HDM_2BOA-Glc (Supplemental Figure 10). This indicates that most likely other point mutations, rather than the 30 bp insertion, caused the inactivity of the Il14H allele. Interestingly, we detected small amounts of HDM_2BOA-Glc in the roots of Il14H (Figure 1B). It is therefore likely that an additional OMT contributes to the production of this metabolite in Il14H roots.

The inducibility of HDM_2BOA-Glc is associated with a stronger induction of *Bx13* and *Bx14* in P39

Compared to B73, the inbred line P39 produced higher constitutive levels of DIM_2BOA-Glc and accumulated higher levels of HDM_2BOA-Glc after simulated herbivory (Figures 1A and 1C). To test whether variation in gene expression can explain these differences, we analyzed transcript accumulation of *Bx7*, *Bx13*, and

Bx14 in undamaged and damaged (mechanical damage + *S. exigua* oral secretion) leaves of P39 and B73 seedlings. *Bx7* was constitutively expressed in both lines and showed no significant increase in transcript accumulation after simulated herbivory. Notably, constitutive *Bx7* expression was significantly higher in P39 than in B73 (Figure 6A). *Bx13* and *Bx14* were significantly upregulated upon simulated herbivory in both inbred lines and showed significantly higher constitutive transcript accumulation in P39 in comparison to B73 (Figure 6B and C).
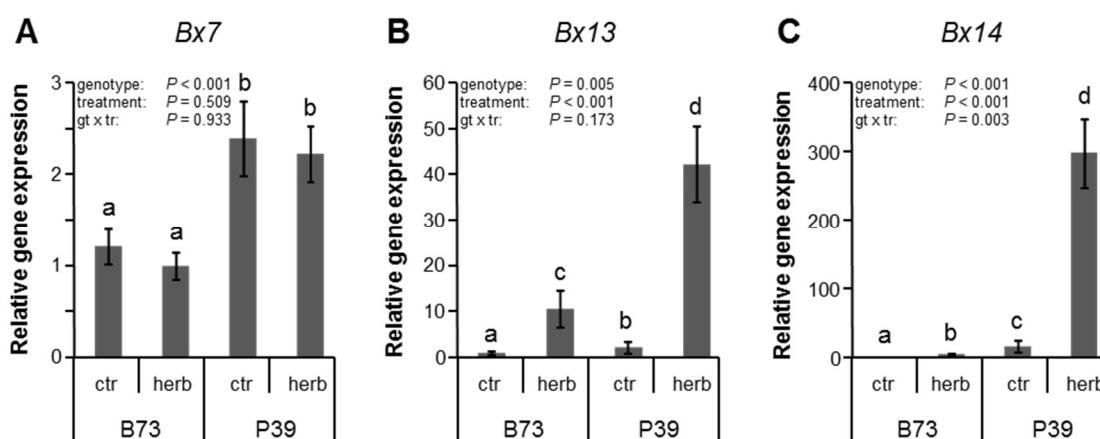
Figure 6. Transcript accumulation of Bx7, Bx13, and Bx14 in maize leaves upon simulated herbivory. Gene expression of Bx7, Bx13, and Bx14 in undamaged (ctr) and wounded (mechanical damage + S. exigua oral secretion (herb)) leaves of the maize inbred lines B73 and P39 was measured using qRT-PCR relative to actin1 (means ± SE; n = 7 biological replicates). Significance levels of a Two-way ANOVA are shown for the factors 'genotype', 'treatment', and the interaction term (genotype x treatment). Different letters indicate significant differences between genotypes and treatments.

BX13 activity has weak effects on the induction and activation of other benzoxazinoids

To assess the suitability of the two *Bx13* NILs (Figure 4C) for biological experiments, we first verified whether the inactivation of *Bx13* affects the constitutive and herbivore-induced biosynthesis and deglycosylation of benzoxazinoids in the leaves (Supplemental Figure 11). For this purpose, we incubated ground maize leaves at room temperature for 0 - 10 minutes and measured benzoxazinoid glucosides and aglucones. As expected, DIM_2BOA-Glc and HDM_2BOA-Glc were only present in the *Bx13*NIL-B73. Repeated measures analysis of variance showed no significant genotype or genotype*time effects for the other benzoxazinoids (Supplemental Table 6). Pairwise comparisons revealed slightly elevated levels of HBOA-Glc and DIMBOA-Glc in *S. frugiperda* attacked *Bx13*NIL-B73 compared to

*Bx13*NIL-Oh43 plants (Supplemental Figure 11). Furthermore, three to 10 min after tissue disruption, elevated levels of DIMBOA and MBOA were observed. These data suggest that *Bx13* inactivation has weak negative feedback effects on benzoxazinoid abundance and activation in herbivore attacked plants. Alternatively, the differential accumulation may be the result of changes in *S. frugiperda* behavior (see below).

The performance of chewing herbivores is not affected by *Bx13*

To understand the impact of HDM$_2$BOA-Glc and DIM$_2$BOA-Glc on the interaction between maize and chewing herbivores, we conducted several experiments. First, we offered pairs of *Bx13*NIL-Oh43 and *Bx13*NIL-B73 to fall armyworm larvae and recorded their feeding patterns. Surprisingly, the larvae caused more damage on *Bx13*NIL-B73 (Figure 7A) and were more often found on this genotype (Figure 7B). Larval weight gain did not differ between the two NILs in a no-choice experiment (Figure 7C). As the fall armyworm is well adapted to maize defenses and is known to use benzoxazinoids as foraging cues (Glauser et al., 2011; Köhler et al., 2015), we performed additional experiments with two generalist leaf feeders, the beet armyworm (*S. exigua*) and the Egyptian cotton leafworm. As HDM$_2$BOA-Glc and DIM$_2$BOA-Glc levels are higher in B73 roots than the leaves (Figure 1), we also tested the effect of *Bx13* inactivation on the banded cucumber beetle *Diabrotica balteata*. All tested herbivores gained the same amount of weight on *Bx13*NIL-B73 and *Bx13*NIL-Oh43 (Figure 7D), suggesting that HDM$_2$BOA-Glc and DIM$_2$BOA-Glc do not increase plant resistance against these chewing insects.
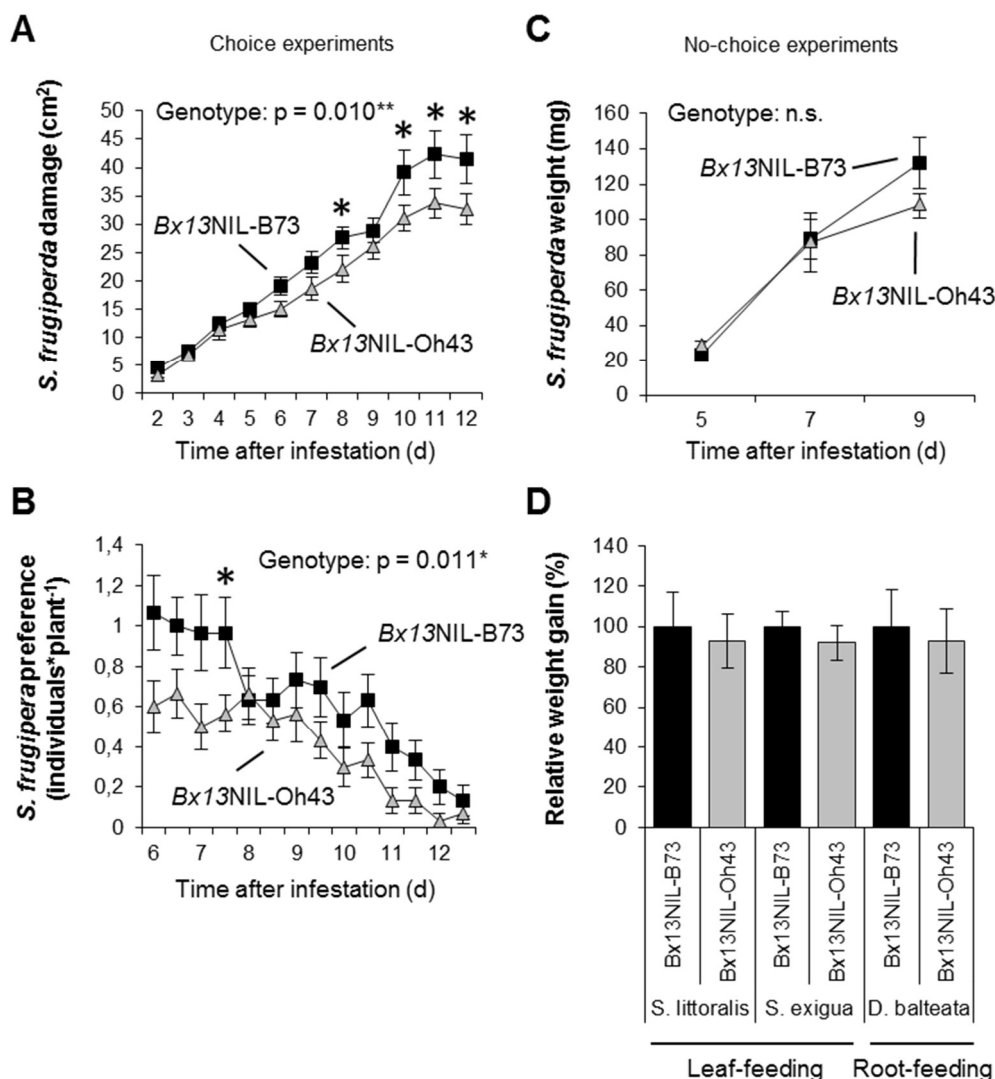
Figure 7. BX13 increases the attractiveness of maize plants to *Spodoptera frugiperda*, but does not affect the performance of *S. frugiperda* and other insects. Damage (A) and distribution (B) of *S. frugiperda* caterpillars on the *Bx13* mutant (*Bx13*NIL-Oh43) and its near-isogenic wild type line (*Bx13*NIL-B73) in choice experiments. Caterpillars were released into pots containing one plant of each genotype and left to feed for 12 days (n = 30). (C) *S. frugiperda* weight gain in a no-choice experiment (n = 18). Caterpillars were left to feed on individual plants for 9 days. Stars indicate significant differences between genotypes at individual time points. Significant p-values for overall genotype effects from analyses of variance (ANOVA) are shown. (D) Relative weight gain of three generalist herbivores feeding between 6 and 10 days on the leaves or roots of the two genotypes. For comparative purposes, weight gains are expressed in % relative to weight gain on *Bx13*NIL-B73 (*S. littoralis*, n = 7 - 9*; S. exigua*, n = 38 - 52; *D. balteata*, n = 8).

Bx13 decreases aphid reproduction

To test whether HDM_2BOA-Glc and DIM_2BOA-Glc affect the performance of phloem feeders, we conducted a performance experiment with corn leaf aphids (*Rhopalosiphum maidis*). Seven days after the start of the experiment, the survival of adult aphids was not significantly different on *Bx13*NIL-B73 and *Bx13*NIL-Oh43 maize seedlings (P = 0.3 and P = 0.65, Student's *t*-test of two independent experiments). However, aphids feeding on *Bx13*NIL-Oh43 produced 50% more progeny

than aphids feeding on *Bx13*NIL-B73 (Figure 8, Supplemental Figure 12), suggesting that HDM$_2$BOA-Glc and/or DIM$_2$BOA-Glc accumulation increases aphid resistance.
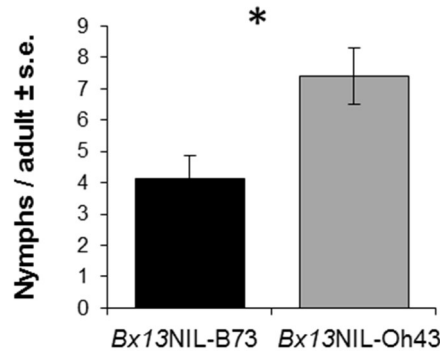

Figure 8. BX13 decreases aphid performance. The number of nymphs per adult on the *Bx13* mutant (*Bx13*NIL-Oh43) and its near-isogenic wild type line (*Bx13*NIL-B73) is shown (n = 20). The asterisk indicates significant differences between genotypes ($P < 0.05$, Student's *t*-test).

DISCUSSION

Maize produces a number of benzoxazinoids that defend the plant against insect herbivores and pathogens (Oikawa et al., 2004; Glauser et al., 2011; Ahmad et al., 2011; Meihls et al., 2013; Maag et al., 2014). The biosynthetic pathway leading to DIMBOA-Glc, the most abundant benzoxazinoid in maize, has been fully determined (Frey et al., 1997; von Rad et al., 2001; Jonczyk et al., 2008). However, how DIMBOA-Glc is converted into other benzoxazinoids is not well understood. Here, we investigated the biosynthesis and biological relevance of the 8-*O*-methylated benzoxazinoids, DIM$_2$BOA-Glc and HDM$_2$BOA-Glc.

The dioxygenase BX13 is the key enzyme for the formation of DIM$_2$BOA-Glc and HDM$_2$BOA-Glc

BX13 belongs to the 2-oxoglutarate-dependent dioxygenase superfamily and has been classified as a member of the recently defined DOXC class of 2ODDs, encompassing enzymes known to be involved in specialized metabolism (Kawai et al., 2014). Several lines of evidence indicated that BX13 acts as the key enzyme for the formation of DIM$_2$BOA-Glc and HDM$_2$BOA-Glc in planta: First, both constitutive DIM$_2$BOA-Glc levels and constitutive and herbivory-induced HDM$_2$BOA-Glc

levels mapped to the same major QTL (*Bb2*) on chromosome 2 that includes the *Bx13* gene, in experiments with several different RIL populations (Figure 2, Supplemental Table 3). Second, a natural knockout of *Bx13*, attributed to a mutated start codon in the inbred lines Oh43, LH38, and LH39, was correlated with a complete lack of DIM$_2$BOA-Glc and HDM$_2$BOA-Glc (Figure 1, Supplemental Figures 4 and 5) and analysis of near-isogenic lines differing mostly in the *Bx13* locus showed that a line carrying the mutated and inactive Oh43 allele produced no DIM$_2$BOA-Glc and HDM$_2$BOA-Glc (Figure 4C). Third, recombinant BX13 was able to convert DIMBOA-Glc to TRIMBOA-Glc (Figure 3B) while BX6 could not accept DIMBOA-Glc as substrate (Supplemental Figure 2A). Furthermore, we found no other *Bx6/13* homologues in the B73 genome that might catalyze this reaction (Figure 3A). Other routes to HDM$_2$BOA-Glc could be ruled out since neither BX13 nor BX6 accepted HDMBOA-Glc as substrate (Supplemental Figure 2B). Moreover, none of the tested OMT were able to methylate the hydroxyl group of the hydroxamic acid moiety of TRIMBOA-Glc (Supplemental Figure 7). Taken together, our findings demonstrate that the formation of DIM$_2$BOA-Glc and HDM$_2$BOA-Glc from DIMBOA-Glc most likely follows a linear pathway beginning with the conversion of DIMBOA-Glc into TRIMBOA-Glc catalyzed by BX13 (Figure 9).

BX13 catalyzes an unusual reaction that likely involves an ortho-rearrangement of the methoxy group

Contrary to our initial expectation that the BX13-catalyzed hydroxylation of DIMBOA-Glc would result in a compound possessing the hydroxyl group at C-8 next to the pre-existing methoxy group at C-7, NMR analysis of the enzyme product TRIMBOA-Glc revealed the opposite configuration with a hydroxyl group at C-7 and a methoxy group at C-8 (Figure 3C). This finding can be explained by a C-7 hydroxylation and a subsequent 1,2-shift of the methoxy group catalyzed by the enzyme. Indeed, 4-hydroxyphenylpyruvate dioxygenase (HPPD), a member of the 2ODD superfamily that does not use 2-oxoglutarate as a cofactor, is known to catalyze an oxidation of an aromatic ring and a subsequent ortho-rearrangement of an acetate side chain (Raspail et al., 2011). HPPD accepts 4-hydroxyphenylpyruvate as substrate and converts it into homogentisate, an essential intermediate in plastoquinone and tocopherol biosynthesis in plants (He
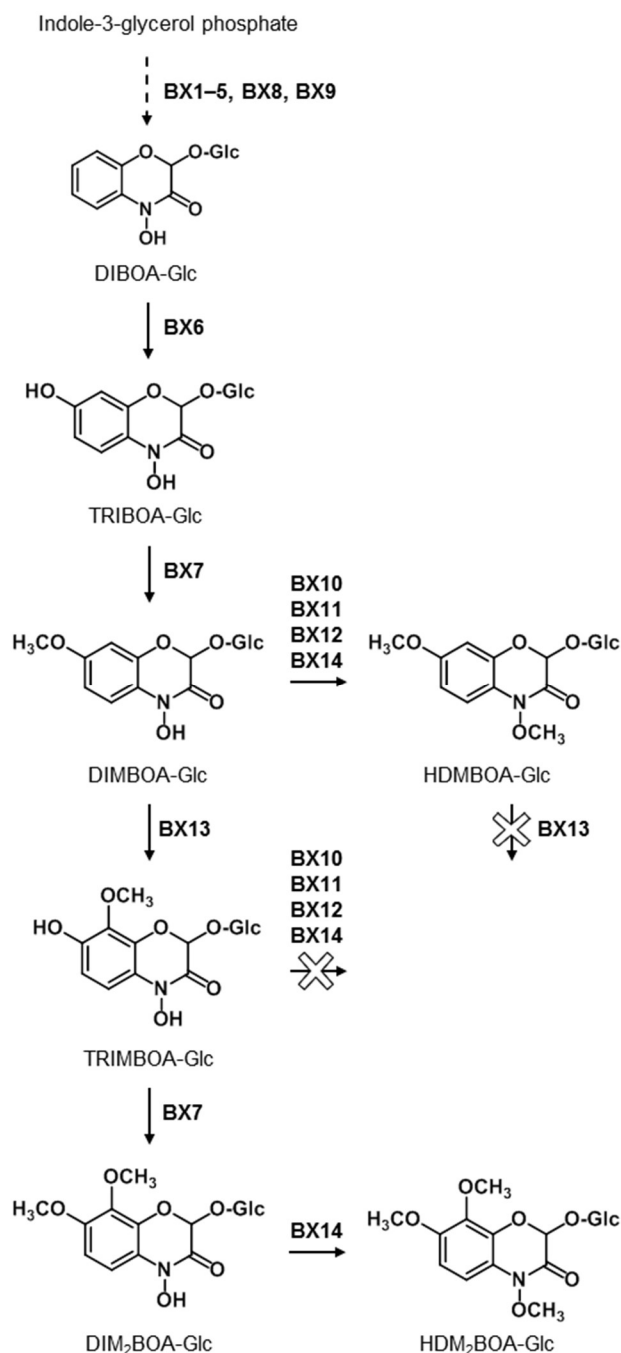
Figure 9. The later steps of benzoxazinoid formation in maize. The formation of DIMBOA-Glc (the major benzoxazinoid in maize) and HDMBOA-Glc originating from indole-3-glycerol phosphate have been reported earlier. The 8-O-methylated DIM_2BOA-Glc and HDM_2BOA-Glc are formed from DIMBOA-Glc by BX13, BX7, and BX14.

and Moran, 2009; Goodwin and Mercer, 1983). We propose that the formation of TRIMBOA-Glc by BX13 might follow a reaction mechanism similar to that described for HPPD (Figure 10). The active site of BX13 contains two highly conserved histidines and one aspartate residue (Supplemental Figure 4), that can form a complex with iron and 2-oxoglutarate (Schofield and Zhang, 1999). After binding

of molecular oxygen and DIMBOA-Glc, the activated dioxygen can attack the side chain of the 2-oxoglutarate leading to its decarboxylation. Then, C-7 hydroxylation of DIMBOA-Glc occurs via an electrophilic attack by an Fe-oxene. A subsequent 1,2-shift of the methoxy group favored by the positive charge at C-8 results in the formation of TRIMBOA-Glc (Figure 10). Although the proposed mechanism explains the production of TRIMBOA-Glc, we cannot rule out the possibility that hydroxylation of DIMBOA-Glc might alternatively occur at C-8 followed by a transfer of the methyl group from the methoxy group to the newly incorporated 8'-OH group. There are a few examples of plant 2ODDs possessing *O*-demethylation activity (Hagel and Facchini, 2010; Berim et al., 2014). However, a 2ODD-catalyzed transfer of a methyl group between two substrate OH groups has to our knowledge not been reported so far. To further study the reaction mechanism of BX13 and to discriminate between a methoxy group rearrangement and an alternative methyl group transfer, enzyme assays with either labeled DIMBOA-Glc or $^{18}O_2$, respectively, are planned for future experiments.
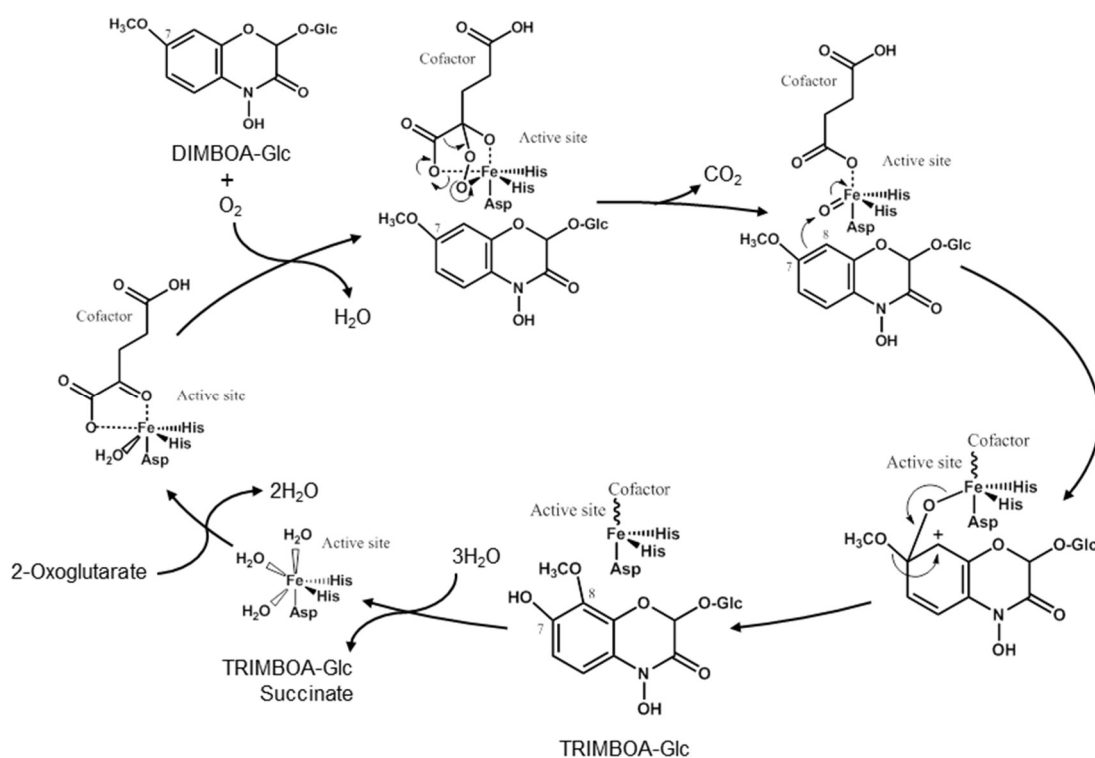

Figure 10. Proposed reaction mechanism for the formation of TRIMBOA-Glc from DIMBOA-Glc catalyzed by BX13. An initial oxidation of the C-7 methoxy group of DIMBOA-Glc might be followed by the elimination and simultaneous, aromatic ring substitution of the leaving moiety at position 8, resulting in TRIMBOA-Glc.

BX7 likely catalyzes two distinct steps in the benzoxazinoid metabolism

BX7 has been described to catalyze the methylation of the 7-OH group of TRIBOA-Glc (Jonczyk et al., 2008). As discussed above, the resulting DIMBOA-Glc can act as a substrate for BX13. Due to the unusual reaction of this 2ODD, the enzyme product TRIMBOA-Glc possesses a free hydroxyl group at C-7 similar to TRIBOA-Glc (Figure 3C). We showed that recombinant BX7 also accepted TRIMBOA-Glc as substrate and methylated the hydroxyl group at C-7 (Figure 5B). Since all other tested potential OMT candidates were not able to catalyze this reaction (Figure 5A, Supplemental Figure 7), we assume that BX7 catalyzes the *O*-methylations of both TRIBOA-Glc and TRIMBOA-Glc in planta. It is notable that both BX7 substrates, TRIBOA-Glc and TRIMBOA-Glc, were not found to accumulate in the plant, indicating a rapid turnover by the enzyme. A dendrogram analysis revealed that BX7 has a similar sequence to other plant OMT acting on polyhydroxylated small molecules such as phenylpropanoids and their derivatives (Figure 5A; Meihls et al., 2013; Zubieta et al., 2001). In general, the majority of enzymes belonging to this OMT group possess high substrate and positional specificity (Ibrahim et al., 1997; Zubieta et al., 2001). However, a few enzymes such as caffeic acid *O*-methyltransferase demonstrate greater substrate promiscuity (Zubieta et al., 2001). Although BX7 seems to have high positional specificity towards the hydroxyl group at C-7, catalytic activity is not influenced by the presence or absence of the neighboring methoxy group, indicating moderate spatial flexibility of the active site.

BX14 can accept DIMBOA-Glc and DIM$_2$BOA-Glc as substrates

The *O*-methyltransferase BX14 showed high similarity to the recently described DIMBOA-Glc *O*-methyltransferases BX10, BX11, and BX12 (Meihls et al., 2013) and catalyzed the same reaction as already described for BX10-12 (Supplemental Figure 8A). However, while BX10-12 possess high substrate specificity towards DIMBOA-Glc (Supplemental Figure 8A), BX14 also accepted DIM$_2$BOA-Glc as substrate and produced HDM$_2$BOA-Glc (Figure 5C). A dendrogram analysis suggests that *Bx10*, *Bx11*, and *Bx12* are likely derived by gene duplication of a *Bx14*-related ancestor (Figure 5A) and thus might have evolved their narrow substrate specificity after this gene duplication event.

Natural variation in *Bx7*, *Bx13*, and *Bx14* expression

It has been shown that genes of the core benzoxazinoid pathway including *Bx1*, *Bx2*, *Bx3*, *Bx4*, *Bx5*, *Bx6,* and *Bx8* are located in close proximity to each other on the short arm of maize chromosome 4 (Frey et al., 2009). In general, such an organization of functionally related genes in operon-like gene clusters in plants is considered to facilitate the co-regulation of gene expression (Jonczyk et al., 2008; Osbourn, 2010), which, however, would imply less regulatory flexibility at the single gene level. While DIMBOA-Glc is mainly produced in young seedlings 4–6 days after germination and declines thereafter, the production of HDMBOA-Glc and HDM_2BOA-Glc also occurs in older tissues (Cambier et al., 2000; Köhler et al., 2015). Moreover, HDMBOA-Glc and HDM_2BOA-Glc accumulate upon insect herbivory and fungus infection (Oikawa et al., 2004; Glauser et al., 2011; Köhler et al., 2015), indicating that genes involved in DIMBOA-Glc metabolism are differently regulated compared to genes of the core pathway. Indeed, *Bx10*, *Bx11*, *Bx12*, *Bx13*, and *Bx14* are located on different chromosomes and are not part of the core pathway gene cluster. The ability to regulate these genes independently of the core pathway might allow the plant to convert DIMBOA-Glc into distinct mixtures of metabolites in response to different biotic stresses and thus would help to adapt to different ecological niches.

DIM_2BOA-Glc and HDM_2BOA-Glc specifically increase plant resistance against aphids

Benzoxazinoid breakdown products are highly active and inhibit the growth of a variety of herbivores and pathogens (Niemeyer, 2009; Glauser et al., 2011; Ahmad et al., 2011; Meihls et al., 2013). Because of their capacity to be deglycosylated and form reactive hemiacetals like other benzoxazinoids, we hypothesized that the 8-*O*-methylated compounds, DIM_2BOA-Glc and HDM_2BOA-Glc, would also decrease the performance of chewing herbivores, but expected that the changes in polarity due to the additional methoxylation may result in changes in digestive stability (Glauser et al., 2011) and herbivore growth suppression. However, our experiments with NILs differing in their BX13 activity did not confirm these hypotheses: None of the four tested chewing herbivores showed a significant change in weight gain with variation in the content of the 8-*O*-methylated benzoxazinoids. Our benzoxazinoid profiling experiments revealed no negative feedback effects of BX13 on other benzoxazinoids, which allows us to rule out metabolic trade-offs as

an explanation for the absence of herbivore growth effects in the *BX13* NILs. Many chewing herbivores seem to be able to circumvent benzoxazinoid toxicity by reglycosylating the aglucones (Sasai et al., 2009; Glauser et al., 2011; Maag et al., 2014; Wouters et al., 2014). Because of this mechanism, even the generalist Egyptian cotton leafworm is able to tolerate DIMBOA concentrations of 200 µg g^{-1} FW (Glauser et al., 2011). It is therefore possible that the relatively low concentrations of DIM$_2$BOA-Glc and HDM$_2$BOA-Glc in *Bx13*NIL-B73 were within the range of benzoxazinoid tolerance of the different caterpillars tested.

Previous studies illustrated that benzoxazinoids can act as feeding stimulants and foraging cues for specialist maize feeders (Rostás, 2007; Robert et al., 2012; Köhler et al., 2015). The preference of the fall armyworm for young maize leaves for instance depends on the presence of benzoxazinoids (Köhler et al., 2015). Our choice experiments demonstrate that the fall armyworm prefers to feed on DIM$_2$BOA-Glc and HDM$_2$BOA-Glc-producing plants, which suggests that these compounds stimulate the feeding of this maize pest. Feeding stimulation by plant secondary metabolites is a general phenomenon among specialized insects and may help herbivores to recognize host plants and to use plant secondary metabolites for self-defense (Erb et al., 2013; Nishida, 2014). Whether the fall armyworm derives any benefits from feeding on DIM$_2$BOA-Glc and HDM$_2$BOA-Glc-containing plants remains to be elucidated.

In contrast to chewing herbivores, we observed that the presence of DIM$_2$BOA-Glc and HDM$_2$BOA-Glc was associated with a significant reduction of aphid reproduction (Figure 8). This observation suggests that BX13 products act as specific resistance factors in maize against aphids and possibly other phloem-feeding insects. However, although the *Bx13*-B73 and *Bx13*-Oh43 NILs vary at less than 0.5% of the maize genome, we cannot completely rule out the possibility that genes other than *Bx13* affect aphid reproduction on these inbred lines. Aphids seem to be more susceptible to benzoxazinoids than caterpillars, as their growth is more strongly affected by mutations in the core benzoxazinoid pathway (Ahmad et al., 2011; Köhler et al, 2015; Betsiashvili et al., 2015). It is therefore possible that small changes in benzoxazinoid patterns have more profound impacts on their physiology. Alternatively, DIM$_2$BOA-Glc and HDM$_2$BOA-Glc may have specific negative impacts on aphids. More detailed experiments would be necessary to test

this hypothesis. In earlier studies, we demonstrated that DIMBOA-Glc concentrations are positively associated with callose deposition and aphid resistance and that DIMBOA induces callose deposition (Ahmad et al., 2011; Meihls et al., 2013). In contrast, our DIM$_2$BOA-Glc and HDM$_2$BOA-Glc measurements across the NAM population show no clear correlation with aphid-induced callose deposition, as measured earlier (Meihls et al., 2013). We therefore propose that direct toxicity rather than indirect effects on callose deposition are responsible for the Bx13-dependent increase in aphid resistance.

Conclusions

Plant defense compounds are known for their astonishing variation in structure, biosynthesis and function. Here we show that even for a small family of defense compounds, the benzoxazinoids with about 20 members (Niemeyer, 2009), there is unexpected variability. For two maize benzoxazinoids with an additional methoxy function at C-8, biosynthesis involves the expected enzymes (2-oxoglutarate-dependent dioxygenases, *O*-methyltransferases), but proceeds via an unprecedented route. While other benzoxazinoids have been shown to act as direct defenses to chewing herbivores and as defense signaling compounds, the 8-*O*-methylated benzoxazinoids of maize appear to target phloem-feeding herbivores.

METHODS

Plant and insect material

Maize (*Zea mays*) plants were grown in commercially available potting soil (Tonsubstrat; Klasmann), in a climate-controlled chamber with a 16 h photoperiod, 1 mmol $(m^2)^{-1}$ s^{-1} of photosynthetically-active radiation, a temperature cycle of 22 ºC/18 ºC (day/night) and 65% relative humidity. Plants with three fully developed leaves were used in all experiments.

Caterpillars of Egyptian cotton leafworm (*Spodoptera littoralis*, Boisd.) and beet armyworm (*S. exigua*, Hübner), both obtained from Syngenta, were reared on an artificial diet based on white beans (Bergomaz et al., 1986) at 20°C and 22 °C, respectively, under natural light. Caterpillars of fall armyworm (*S. frugiperda* J.E. Smith) were kindly provided by Ted Turlings (FARCE laboratory, University of Neuchâtel, Switzerland) and reared on artificial diet. *Diabrotica balteata* larvae were

reared as described (Robert et al., 2012). Eggs of beet armyworm (*S. exigua*) for insect growth experiments were obtained from Benzon Research (Carlisle, PA, USA, www.benzonresearch.com) and were hatched at 23°C. A corn leaf aphid (*Rhopalosiphum maidis*) colony, initially collected in New York State by Stewart Gray (USDA-ARS, Ithaca, NY), was maintained on B73 seedlings in a growth chamber with a 16:8 h light:dark photoperiod at constant 23°C.

For artificial herbivory treatments, plants were scratched on the youngest leaf over 2 cm^2 with a razor blade and 5 µL of *S. exigua* spit were applied (n = 5). Damage was inflicted on one side of the midrib only to be able to distinguish local and systemic induction. Control plants remained undamaged (n = 5). Control leaves as well as the damaged and undamaged halves of the treated leaves were collected separately after 0, 24, 48 and 72 h.

Deglucosylation activity

*Bx13*NIL-Oh43 and *Bx13*NIL-B73 plants were infested with six first-instar *S. frugiperda* larvae or left uninfested as controls (n = 4).Three days later, leaf tissue was collected, ground to a fine powder in liquid nitrogen, aliquoted into 50 mg batches and incubated at 37°C for 1, 2, 3 or 10 min. Non-incubated samples were used as controls. After incubation, all reactions were stopped by adding 500 µl of H$_2$O:MeOH:FA (50:50:0.5 v/v, Methanol, LC-MS-grade, Merck; Milli-Q water, Millipore; formic acid, analytical-grade, Thermo Fischer Scientific, Spain), and BXDs were quantified as described below.

Generation of *Bx13* near isogenic lines

Using a previously described approach (Mijares et al., 2013; Tuinstra et al, 1997), near-isogenic lines (NILs) were made from RILs of B73 and Oh43, which contain a natural *Bx13* knockout mutation (Figure 4A). B73 x Oh43 RIL genotype data (www.panzea.org) were used to identify Z022E0081, a line that was still heterozygous in the region of the *Bx13* gene polymorphism after sixth generation of inbreeding (www.panzea.org; Supplemental Figure 6A). Line Z022E0081 was self-pollinated to produce progeny that were segregating at Bx13 and other remaining heterozygous loci. DNA from each of the predicted regions of heterozygosity was amplified by PCR using GoTaq Polymerase (www.promega.com), the primers listed in Supplemental Table 7, and the PCR cycle 94°C for 3 min, 34 cycles of 94°C for

30 sec, 57°C for 30 sec, and 72°C for 1 min, followed by 72°C extension for 10 min. Four predicted regions of heterozygosity were found to be already homozygous in our isolate of Z022E0081, which had been inbred for two generations after the original genotyping data (www.panzea.org) were generated. Among 37 tested progeny lines, we identified a pair of NILs that was (i) homozygous for either the B73 or the Oh43 allele of *Bx13* and (ii) homozygous with the same genotype at other loci that had been heterozygous in Z022E0081 (Supplemental Figure 6B). The variable region containing the *Bx13* in the genotyped NIL pair is 10 cM genetic distance, corresponding to 4.7 Mbp of DNA sequence and 185 predicted genes (www.maizgdb.org, RefGen v2). The two NILs were self-pollinated and progeny were used for subsequent experiments.

Extraction and analysis of benzoxazinoids

Plant material was ground to a fine powder under liquid nitrogen. For extraction, frozen powder was transferred to pre-cooled 2 mL microcentrifuge tubes, weighed, and three volumes of extraction solvent MeOH:H_2O:FA (50:50:0.5 v/v; Methanol, LC-MS-grade, Merck; Milli-Q water, Millipore; formic acid, analytical-grade, Thermo Fischer Scientific) were added. The tubes were immediately mixed until the powder was completely dispersed, and two chrome steel beads (4 mm diameter) were added to each tube. Plant tissues were subsequently extracted using a paint shaker, model S0-10 M (Fluid Management, Wheeling, IL, USA), at 10 Hz for 4 min and cell debris was sedimented at 13,000g for 30 min. The supernatant was stored at -20°C before analysis.

Plant extracts from the NAM screening, induction experiment (P39 and B73), and NIL screening were analyzed using liquid chromatography-tandem mass spectrometry (LC-MS/MS). Chromatography was performed on an Agilent 1200 HPLC system (Agilent Technologies). Separation was achieved on a Zorbax Eclipse XDB-C18 column (50 x 4.6 mm, 1.8 µm, Agilent Technologies) with aqueous formic acid (0.05%) and methanol employed as mobile phases A and B, respectively. The following elution profile was used: 0 – 0.5 min, 90% A; 0.5 – 1 min, 90 – 79% A; 1 – 10 min, 79 – 76% A; 10 – 11 min, 76 – 50% A; 11 – 13 min 50 – 0% A; 13 – 16 min 90% A. The mobile phase flow rate was 0.8 mL min^{-1} and the column temperature was maintained at 25°C. The injection volume was 5 µL. The liquid chromatography was coupled to an API 3200 tandem mass spectrometer

(Applied Biosystems) equipped with a Turbospray ion source operated in negative ionization mode (for detailed parameters see Supplemental Table 9). Multiple reaction monitoring (MRM) was used to monitor the parent ion > product ion transition for each analyte. Analyst 1.5 software (Applied Biosystems) was used for data acquisition and processing. Absolute concentrations of benzoxazinoids were determined using external calibration curves obtained from purified DIMBOA-Glc. For calibration, 31.3, 62.5, 125, 250, and 500 ng/mL solutions were analyzed prior to and after measurements. DIM_2BOA-Glc and HDM_2BOA were quantified using response factors of 0.9 and 8.9, respectively, compared to DIMBOA-Glc. Response factors were defined by determining the ratio of MRM intensities and intensities of the optical signal at 275 nm for these compounds.

*Bx13*NIL-B73 and *Bx13*NIL-Oh43 BXD profiles upon tissue disruption (deglucosylation activity) were analyzed as follows: Plant extracts were analyzed by liquid chromatography-tandem UV and mass spectrometry (LC-UV-MS) using an ACQUITY UPLC I-Class System equipped with an ACCQUITY UPLC photo diode array (PDa eλ) detector and an ACCQUITY UPLC mass detector (QDa). The chromatographic separation was achieved using a Waters ACQUITY UPLC BEH C18 (2.1 mm × 100 mm, 1.7 μm) at 40 °C using aqueous formic acid (0.05%) and acetonitrile (Fisher Chemicals) with 0.05% formic acid as mobile phases A and B, respectively. The injection volume was 2.5 μL and the flow rate was kept constant at 0.4 ml min^{-1}. The gradient system was as follows: 0-9.65 min: 97-83.6 % A; 9.65-11 min: 83.6-0 % A; 11-13 min: 0-0 % A; 13-13.10 min: 0-97% A; 13.10-15 min: 97-97 % A. UV spectra were monitored from 190 to 790 nm. The mass spectrometer was operated in negative mode to scan masses from 150 to 650 Da (ESI: 0.8 V, Cone voltage: 70 V) and for single ion recording in positive mode (SIR 194, ESI: 0.8 V) with a 5 Hz sampling frequency. Data were processed using MassLynx (Waters). Absolute concentrations of benzoxazinoids were calculated using external calibration curves of purified DIMBOA-Glc, HDMBOA-Glc and MBOA (Sigma Aldrich) at concentrations ranging from 3.125 to 50 μg mL^{-1}. HDM_2BOA-Glc, DIM_2BOA-Glc, HBOA-Glc, DIBOA-Glc and DIMBOA were quantified using response factors of 4.02, 0.85, 4.71, 1.02 and 0.36, respectively calculated as described above. Plant extracts from the recombinant inbred lines were analyzed as described elsewhere (Glauser et al., 2011).

Measurement of benzoxazinoids in roots of the intercrossed B73 x Mo17 population was done as follows: Maize seedling roots frozen in liquid nitrogen were manually ground in a mortar and pestle and transferred to 2 mL microcentrifuge tubes and weighed. Three microliters of extraction solvent (30:69.9:0.1 methanol, LC-MS-grade water (Sigma-Aldrich), formic acid) were added per mg of maize tissue. The extraction solvent was spiked with 0.075 mM 2-benzoxazolinone (BOA) as an internal standard. Ground tissue and extraction solvent were mixed by vortexing and incubated on a Labquake™ Rotisserie Shaker (Thermo Scientific) at 4°C for 40 min. Solid debris was separated from solvent by centrifuging at 11,000g for 10 minutes. For each sample, 200 µl extract were filtered through a 0.45 micron filter plate by centrifuging at 200g for 3 min. LC-MS/MS analysis was performed on an Ultimate 3000 UPLC system attached to a 3000 Ultimate diode array detector and a Thermo Q Exactive mass spectrometer (Thermo Scientific). The samples were separated on a Titan C18 7.5 cm x 2.1 mm x 1,9 µm Supelco Analytical Column (Sigma Aldrich) at the flow rate of 0.5 ml min^{-1}, using gradient flow of 0.1% formic acid in LC-MS-grade water (eluent A) and 0.1% formic acid in acetonitrile (eluent B) with conditions as follows: 0% B at 0 min, linear gradient to 100% B at 7 min, and linear gradient to 0% B at 11 min. Mass spectral parameters were set as follows: negative spray voltage 3500 V, capillary temperature 300°C, sheath gas 35 (arbitrary units), aux gas 10 (arbitrary units), probe heater temperature 200°C with an HESI probe. Full scan mass spectra were collected (R:35000 full width at half maximum, m/z 200; mass range: m/z 50 to 750) in negative mode. The quantification was done using a SIM chromatogram measured for m/z 240 using Excalibur 3.0 software. Relative DIM$_2$BOA content of each sample was estimated from the ratio of the DIM$_2$BOA peak area (mass range of m/z 240.0 – 240.2 and retention time 2.25 min) relative to BOA (mass range of m/z 134.0-134.2 and retention time 3.26 min), which was used as an internal standard. An annotation of benzoxazinoid derivatives by t_R and their fragmentation patterns is given in Supplemental Table 8.

Mapping analysis

Plants from individual sets of recombinant inbred lines (B73 x P39) were potted in 200 cm^3 volume plastic pots. The soil consisted of field soil (5/10, Ricoter Landerde Switzerland), peat (4/10, Ricoter) and sand (1/10, Migros Do It). Plants with three

fully developed leaves were induced as described above (n = 5). After 48 h, the induced half of the leaf (one side of the vein, "local") and the undamaged half ("systemic part") were collected. As induction changes benzoxazinoid levels in the local part but not in the systemic part of the leaves (Supplemental Figure 0), the systemic parts were used to map constitutive benzoxazinoids, while the local parts were used to map induced levels. Seeds of 80 maize RILs from the intercrossed B73 x Mo17 population (Lee et al., 2002) were germinated in moisturized rolls of germination paper (twelve seeds per RIL per roll). Germinated seedlings were transplanted to 10 cm x 10 cm plastic pots with Turface ® MVP ® calcined clay (Profile Products LLC) when their primary roots reach approximately 9 cm long. Transplanted seedlings were maintained in 16:8 light: dark growth conditions at 26°C and 70% relative humidity for six days. Seedling roots were harvested and frozen in liquid nitrogen.

The QTL analysis was done by composite interval mapping using the Windows QTL Cartographer software version 2.5 (Wang et al., 2012). The experimental LOD threshold was determined by permutation tests with 500 repetitions at the significance level of 0.05. All analyses were performed using the default settings in the WinQTL program as follows: the CIM program module = Model 6: Standard Model, walking speed = 2 centimorgans, control marker numbers = 5, window size = 10 centimorgans, regression method = backward regression method. Maize genetic marker data were downloaded from www.panzea.org and were used for linkage mapping using multiple sets of recombinant lines from the NAM population. A list of all RILs used for mapping in this study is given in Supplemental Table 10.

Preparation of RNA and cDNA

Frozen plant material was ground to a fine powder in a liquid nitrogen pre-cooled mortar and RNA was extracted using the RNeasy plant mini kit (Qiagen) according to the manufacturer's instructions. Nucleic acid concentration, purity, and quality were assessed using a spectrophotometer (NanoDrop 2000c; Thermo Scientific) and Agilent 2100 Bioanalyzer (Agilent Technologies). Prior to cDNA synthesis, 0.75 µg RNA was DNase treated using 1 U DNase (Fermentas). Single-stranded cDNA was prepared from the DNase-treated RNA using SuperScript III reverse transcriptase and oligo(dT20) primers (Invitrogen).

Gene synthesis

The complete open reading frames of *Bx6*-CI31A (AF540907) and *Bx7*-CI31A (NM_001127247) were synthesized after codon optimization for heterologous expression in *Escherichia coli* by Eurofins MWG Operon (for optimized sequences see Supplemental Figure 13). Synthetic genes were sub-cloned into the vector pUC57 and fully sequenced.

Cloning and heterologous expression

The complete open reading frames of *Bx10*-B73, *Bx11*-B73, *Bx12*-CML322, *Bx13*-P39, *Bx14*-B73, *Zrp4*-P39, AC209819.3_FG005, GRMZM2G100754, GRMZM2G097297, GRMZM2G023152, GRMZM2G102863, GRMZM2G141026, GRMZM2G106172, and GRMZM2G093092 were amplified from cDNA with the primer pairs listed in Supplemental Table 4 online. *Bx6*-CI31A and *Bx7*-CI31A were amplified from the plasmids containing the respective codon-optimized open reading frames as described above. The obtained PCR products were cloned as blunt fragments into the sequencing vector pCR-Blunt II-TOPO (Invitrogen) and both strands were fully sequenced. For heterologous expression with an N-terminal His-Tag, the genes were inserted into the expression vector pET100/D-TOPO (Invitrogen). The *O*-methyltransferase (OMT) genes *Bx10*-B73, *Bx11*-B73, *Bx12*-CML322, *Bx14*-B73, *Zrp4*-P39, AC209819.3_FG005, GRMZM2G100754, GRMZM2G097297, GRMZM2G023152, GRMZM2G102863, GRMZM2G141026, GRMZM2G106172, and GRMZM2G093092 were expressed in the *E. coli* strain BL21(DE3) (Invitrogen). For expression, liquid cultures of bacteria harboring the expression construct were grown at 37°C to an OD600 of 0.6 to 0.8. IPTG was added to a final concentration of 1 mM, and the cultures were incubated for 20 h at 18°C and 200 rpm. The two 2-oxoglutarate-dependent dioxygenase (2ODD) genes *Bx6*-CI31A and *Bx13*-P39 were introduced in the *E. coli* strain C41(DE3) pLysS (Lucigen), and heterologous expression was performed as described by Jaganaman and co-workers (2006). The cells were sedimented for 5 min at 5000g and 4 °C. For breaking-up the cells, the pellet was resuspended in ice-cold 4 mL 50 mM Tris-HCl (pH 8.0) containing 0.5 M NaCl, 20 mM imidazole, 50 mM 2-mercaptoethanol, and 10% glycerol and subsequently subjected to ultrasonication (4 x 20 sec, Bandelin UW2070). The debris was separated by centrifugation for 20

min at 16,100g and 4 °C. N-terminal His-tagged proteins were purified using Ni-NTA spin columns (Qiagen) according to the manufacturer's instructions. The purified proteins were eluted with 50 mM Tris-HCl (pH 8.0) containing 0.5 M NaCl, 250 mM imidazole and 10% glycerol. Eluates of the dioxygenases BX6 and BX13 were directly used for enzyme assays. For purified OMT, the salt was removed by gel filtration using illustraTM NAPTM-10 columns (GE Healthcare) and the proteins were redissolved in 50 mM Tris-HCL (pH 7.0) containing 50% glycerol.

In vitro characterization of recombinant enzymes

2ODD and OMT activities were tested using enzyme assays containing purified recombinant protein, benzoxazinoid substrates and the respective co-substrates. 2ODD assays with recombinant BX6 or BX13 were performed with 5 mM 2-mercaptoethanol, 5 mM 2-oxoglutarate, 0.5 mM ascorbate, 0.25 mM ferric chloride, 0.2 mg mL^{-1} substrate (DIMBOA-Glc or HDMBOA-Glc) and 0.5 µg desalted enzyme dissolved in 100 mM Tris-HCl, pH 7.0, in a total volume of 100 µL. OMT assays were performed with 0.2 mM dithiothreitol, 0.2 mM EDTA, 0.5 mM *S*-adenosyl-L-methionine, 0.2 mg mL^{-1} substrate, and 0.5 µg desalted enzyme solved in 100 mM Tris-HCl, pH 7.5, in a volume of 100 µL. For BX7 activity assays, TRIMBOA-Glc, which was purified as described below from 300 pooled BX13 enzyme assays, was used as substrate. BX14 activity was tested with DIMBOA-Glc, DIM$_2$BOA-Glc, and TRIMBOA-Glc. All assays were incubated in glass vials overnight at 25°C at 350 rpm using a ThermoMixer comfort 5355 (Eppendorf). The reaction was stopped with 5 µL formic acid, 99% pure (Sigma Aldrich), and centrifuged for 15 min at 13,000g. Product formation was monitored by the analytical methods described above. Metabolite identities were confirmed using authentic standard compounds.

Semi-preparative purification of DIMBOA-Glc and TRIMBOA-Glc

Supernatants of terminated BX13 assays were pooled (total volume of 30 mL) and chromatographically separated using an Agilent 1100 HPLC system (Agilent Technologies). The separation was achieved on a Nucleodur Sphinx RP column (250 x 4.6 mm, 5 µm, Macherey Nagel) with aqueous formic acid (0.1%) and acetonitrile (LC-MS grade, VWR chemicals) employed as mobile phases A and B, respectively with the following elution profile: 0 – 10 min, 10-70% B in A; 10 – 11 min 100% B; 11 – 14 min 10% B. The mobile phase flow rate was 1.1 mL min^{-1} and the column

temperature was maintained at 25°C. A volume of 100 μL was injected. Benzoxazinoids were traced at the absorption maximum of 270 nm and fractions between minutes 9.2 – 9.4 and 10.6 – 11.4 were collected with a SF-2120 Super Fraction collector (Advantec). Both fractions were concentrated with a Rotavapor R-114 rotary evaporation system (Büchi) and twice washed with aqueous methanol and subsequently verified by LC-MS/MS (see Extraction and analysis of benzoxazinoids). Collected and purified fractions containing 100 μg of the enzymatic product TRIMBOA-Glc and 700 μg DIMBOA-Glc, respectively, were dissolved in 50 μL Milli-Q water and freeze-dried for NMR analysis.

Nuclear magnetic resonance spectroscopy

^{1}H NMR, ^{1}H,^{1}H COSY, HMBC, and HSQC spectra were measured at 300 °K on a Bruker Avance III HD 700 NMR spectrometer (Bruker Biospin) using a cryogenically cooled 1.7 mm TCI ^{1}H{^{13}C} probe. The operating frequency was 700.45 MHz for ^{1}H and 176.13 MHz for ^{13}C. MeOH-d_4 was used as a solvent and tetramethylsilane as an internal standard. The residual HDO signal in the ^{1}H NMR spectra was suppressed using the NOESY solvent-presaturation (noesypr1d) pulse program.

Identification of TRIMBOA-Glc

The ^{1}H NMR spectrum of TRIMBOA-Glc displayed doublets of an AX spin system assignable to the aromatic protons H-5 (δ 6.96) and H-6 (δ 6.63) (J_{H5-H6} = 8.9 Hz), a singlet (1H) at a low field (δ 5.96) attributable to H-2 at the hydroxylated carbon atom of the 1,4-oxazin-3-one ring, and a singlet (integrating for three protons) with a chemical shift (δ 3.90) characteristic of a methoxy group on the aromatic ring. In addition, a complete set of ^{1}H NMR signals of the glucose unit were detected (see Supplemental Table 5 online). The signal of H-1' (δ 4.71) shows a spin-spin coupling $J_{H1'-H2'}$ = 7.9 Hz characteristic of β-configuration at the anomeric center of the glucose unit. The signal-to-noise ratio of this signal was reduced due to its proximity to the suppressed residual water signal. Attachment of the glucose to C-2 of the benzoxazinoid moiety was established by means of HMBC correlations of H-1' with C-2 (δ 98.1) and H-2 with C-1' (δ 104.3). The signal of H-2 also shows cross signals with C-3 (δ 157.1) and C-9 (δ 136.3), supporting its assignment to this particular

proton. HMBC correlations of H-5 and H-6 (Figure 3C) and the corresponding ^{13}C chemical shifts proved that the carbon atoms C-7 (δ 148.9) and C-8 (δ 138.1) in the aromatic ring were oxygenated. The question whether the oxygen functionality at C-7 or C-8 carries the *O*-methyl group was established by means of the correlation between the *O*-methyl signal and C-8 observed in the HMBC spectrum (Figure 3C). Thus, the structure of TRIMBOA-Glc was identified as 2-(2,4,7-trihydroxy-8-methoxy-1,4-benzoxazin-3-one)-β-D-glucopyranose. Further HMBC cross signals, together with HSQC correlations completed the assignment of the chemical shifts of the remaining carbon atoms (see Supplemental Table 5).

Sequence analysis and tree reconstruction

Multiple sequence alignments (MSA) of maize *OMT* and *2ODD* genes similar to *Bx7* and *Bx6*, respectively, were computed using the GUIDANCE2 server (http://guidance.tau.ac.il/ver2/) and the MAFFT (codon) MSA algorithm (see Supplemental Data Set 1 and Supplemental Data Set 2 online). Based on the MAFFT alignments, trees were reconstructed with MEGA5 (Tamura et al., 2011) using a maximum likelihood algorithm (general time-reversible model, gamma distributed rates among sites). Codon positions included were 1st+2nd+3rd+noncoding. All positions with <90% site coverage were eliminated. Ambiguous bases were allowed at any position. A bootstrap resampling analysis with 1000 replicates was performed to evaluate the topology of the generated trees.

qRT-PCR analysis

Relative quantification of *Bx7*, *Bx13*, and *Bx14* gene expression was carried out using qRT-PCR with the qPCR system MxPro Mx300P (Stratagene). For the amplification of gene fragments with a length of 150-250 bp, specific primer pairs were designed having a melting temperature equal or higher than 60°C, a GC content between 35 and 55%, and a primer length in the range of 20 to 25 nucleotides (Supplemental Table 7). Primer specificity was confirmed by agarose gel electrophoresis, melting point curve analysis, and sequence verification of cloned PCR amplicons. Primer pair efficiency was determined using the standard curve method with fivefold serial dilution of cDNA and was found to be between 90 and 105%. As reference, the actin gene *Zm-Actin1* (accession number MZEACT1G) was used.

cDNA was prepared as described above, and 1 μL cDNA was used in 20-μL reactions containing Brilliant III SYBR Green qPCR Master Mix (Stratagene) and ROX as the reference dye. Biological replicates were analyzed as triplicates. The PCR consisted of an initial incubation at 95°C for 3 min followed by 50 amplification cycles with 20 sec at 95°C and 20 sec at 60°C. For each cycle, reads were taken during the annealing and the extension step. At the end of cycling, the melting curves were gathered for 55 to 95°C. Data for the relative quantity of calibrator average (dRn) were exported from MxPro software.

Discovery of natural *Bx13* knockout variants in HapMap3 maize lines

In order to discover naturally-occurring knockout variants of *Bx13*, we performed sensitive re-mapping of Illumina reads from 916 diverse maize lines in HapMap 3.1 (Bukowski et al., 2015). Paired-end reads from each sample - previously aligned using BWA-MEM (Bukowski et al., 2015) were isolated from the existing BAM files within 10 kb of AC148152.3_FGT005 (*Bx13*; AGPv3 Chr2:231942642-231964277). These were then re-aligned to the same *Bx13*-proximal region of AGPv3 using Stampy (v. 1.0.23) with default options (Lunter and Goodson, 2011). Following alignment, we used Platypus to call variants, with option "assemble=1" (Rimmer et al., 2014). We then used SNPeff to infer the probable biochemical consequences of the variants (Cingolani et al., 2012). Samples containing putative frameshifts or start codon losses were candidates for knockout mutations. These mutations were confirmed by DNA sequencing.

Insect bioassays

To test caterpillar preference, *S. frugiperda* larvae were given the choice between one *Bx13*NIL-Oh43 and one *Bx13*NIL-B73 plant sown together in 11 cm height, 4 cm diameter plastic pots (n = 30). All plants were infested with three first instar *S. frugiperda* larvae. To prevent larvae from escaping, each pot was surrounded by a transparent plastic film (PPC-12.10A, Kodak). After two days, plant damage was recorded every day for ten days. After four days, the number of larvae feeding on each plant was recorded every 12 hours for six days.

   To measure *S. frugiperda* weight gain, individual *Bx13*NIL-Oh43 and *Bx13*NIL-B73 plants were infested with six first-instar *S. frugiperda* larvae (n = 18).

To prevent larvae from escaping, all plants were covered with 1.5 L polyethylene terephthalate (PET) bottles as described (Erb et al., 2011). Five, seven and nine days after infestation, larval mass was determined using a microbalance (Ohaus Corporation N30330). *S. littoralis* performance was measured similarly to *S. frugiperda* performance 9 days after infestation as described above (n = 7 - 9). *D. balteata* performance was determined by placing six pre-weighed second instar *D. balteata* larvae in 5 cm deep holes in the soil. After 6 days, all larvae were collected and weighed to determine average weight gain (n = 8).

For *S. exigua* growth assays, NILs containing either the Oh43 or the B73 allele at *Bx13* were planted in 1.5 cm deep in 200 cm^3 plastic pots filled with moistened maize mix [produced by combining 0.16 m^3 Metro-Mix 360 (Scotts), 0.45 kg finely ground lime, 0.45 kg Peters Unimix (Scotts), 68 kg Turface MVP (Profile Products), 23 kg coarse quartz sand and 0.018 m^3 pasteurized field soil]. Plants were grown in a growth chamber (Conviron) under a 16:8 h light:dark photoperiod and 180 mmol photons/m^2/s light intensity at constant 23°C and 60% relative humidity. Neonate larvae were confined on individual maize plants with perforated polypropylene bags (15 cm x 61 cm; http://www.pjpmarketplace.com). After 10 days, *S. exigua* larvae were harvested, lyophilized, and weighed (n = 38 - 52).

For measurements of aphid reproduction, ten adult *R. maidis* from B73 plants were confined on two-week-old *Bx13*NIL-Oh43 and *Bx13*NIL-B73 plants (grown as described above for *S. exigua* experiments) using perforated polypropylene bags. Experimental plants with aphids were placed in the same growth room as the aphid colony. Seven days after infestation, the remaining adults and progeny were counted. As it was not possible to determine whether missing adult aphids had died, absconded, or were otherwise not found, aphid fecundity was calculated as progeny per adult aphid remaining at the end of the experiment. This experiment was independently replicated twice with comparable results.

Statistical analysis

Statistical significance was tested using analysis of variance in SigmaPlot 11.0 for Windows (Systat Software Inc., 2008). Whenever necessary, the data were *In* transformed to meet statistical assumptions, such as normality and homogeneity of variances.

Accession numbers

Sequence data from this article can be found in GenBank/EMBL data libraries under the accession numbers: *Bx6,* AY104457; *Bx7*-CI31A, NM_001127247; *Bx10*-B73, AGS16666; *Bx11*-B73, AGS16667; *Bx12*-CML322, AGS16668; *Bx13*-P39, KU521787*, Bx13*-Oh43, KU521786; *Bx14*-B73, KU521788; *Bx14*-Il14H, KU521789; OMT1-B73*,* ABQ58826*; Zrp4*, NM_001112219.

SUPPLEMENTAL DATA

The following materials are available in the online version of this article.

Supplemental Figure 0.

Herbivory-induced changes in HDM$_2$BOA-Glc and DIM$_2$BOA-Glc are restricted to the wound site.

Supplemental Figure 1.

LC-MS/MS fragmentation patterns of DIMBOA-Glc and TRIMBOA-Glc.

Supplemental Figure 2.

Substrate specificity of the 2-oxoglutarate-dependent dioxygenases BX6 and BX13.

Supplemental Figure 3.

Nucleic acid alignment of *Bx13*-P39 and *Bx13*-Oh43.

Supplemental Figure 4.

Amino acid alignment of 2-oxoglutarate-dependent dioxygenases.

Supplemental Figure 5.

A mutated start codon in *Bx13*.

Supplemental Figure 6.

Generation of *Bx13* near isogenic lines for the *Bx13* locus on chromosome 2.

Supplemental Figure 7.

Enzymatic activity of *O*-methyltransferases similar to BX7 towards TRIMBOA-Glc. The intensities of the specific LC-MS/MS transitions are shown.

Supplemental Figure 8.

Enzymatic activity of *O*-methyltransferases similar to BX7 towards DIMBOA-Glc and DIM$_2$BOA-Glc.

Supplemental Figure 9.

Nucleic acid alignment of *Bx14*-B73 and *Bx14*-Il14H.

Supplemental Figure 10.

*In vitro a*ctivity of *Bx14*-Il14H and the presence/absence of an 30 bp-in frame insertion in *Bx14* within the NAM population.

Supplemental Figure 11.

Effect of BX13 on benzoxazinoid accumulation and hydrolysis.

Supplemental figure 12.

BX13 decreases aphid performance (2nd independent experiment).

Supplemental Figure 13.

Codon-optimized gene sequences of *Bx6*-CI31A and Bx7-CI31A for expression in *Escherichia coli*.

Supplemental Table 1.

Concentrations of DIM_2BOA-Glc in undamaged controls and *Spodoptera exigua*-treated maize leaf samples.

Supplemental Table 2.

Concentrations of HDM_2BOA-Glc in undamaged controls and *Spodoptera exigua*-treated maize leaf samples.

Supplemental Table 3.

Estimates of the additive allelic effect under the hypotheses H1, with the additive allelic effect, a, distinguishable from zero and the dominance deviation equal to zero.

Supplemental Table 4.

Primers for open reading frame amplification of investigated genes.

Supplemental Table 5.

^{1}H- and ^{13}C NMR data of TRIMBOA-Glc (700.45 MHz for ^{1}H and 176.13 MHz for ^{13}C, MeOH-d_4)

Supplemental Table 6. *P*-values of two-way repeated measures analyses of variance (ANOVA) to test for genotype and genotype*time effects in the *Bx13* NILs.

Supplemental Table 7.

qRT-PCR Primers used to determine expression levels of *Bx7*, *Bx13,* and *Bx14* and primers for the detection of SNP markers.

Supplemental Table 8.

Annotation of benzoxazinoid derivatives by t_R and their fragmentation patterns.

Supplemental Table 9.

LC-MS/MS settings used for the analysis of benzoxazinoids.

Supplemental Table 10.

List of RILs used for mapping in this study.

Supplemental Dataset 1.

FASTA file of the alignment of maize *2ODD* genes similar to *Bx6*-B73.

Supplemental Dataset 2.

FASTA file of the alignment of maize *OMT* genes similar to *Bx7*.

ACKNOWLEDGEMENTS

AUTHOR CONTRIBUTIONS

VH, CAMR, ESB, JG, GJ, ME, and TGK designed the research. VH, CAMR, RARM, ME, ERM, GJ, and JNC carried out the experimental work. VH, CAMR, RARM, WB, ERM, GJ, BS, and ME analyzed data. ESB contributed essential research materials. VH, CAMR, GJ, ME, and TGK wrote the paper. All authors read and approved the final manuscript. VH and CAMR contributed equally to the study and share first authorship. GJ, ME, and TGK contributed equally to the study and share senior authorship.

REFERENCES

Ahmad, S., Veyrat, N., Gordon-Weeks, R., Zhang, Y., Martin, J., Smart, L., Glauser, G., Erb, M., Flors, V., Frey, M., and Ton, J. (2011). Benzoxazinoid metabolites regulate innate immunity against aphids and fungi in maize. Plant Physiol. **157**: 317–327.

Babcock, G.D. and Esen, A. (1994). Substrate specificity of maize β-glucosidase. Plant Sci. **101**: 31–39.

Berim, A., Kim, M.-J., and Gang, D.R. (2014). Identification of a unique 2-oxoglutarate-dependent flavone 7-O-demethylase completes the elucidation of the lipophilic flavone network in basil. Plant Cell Physiol. **56**: 126–136.

Betsiashvili, M., Ahern, K.R., and Jander, G. (2015). Additive effects of two quantitative trait loci that confer *Rhopalosiphum maidis* (corn leaf aphid) resistance in maize inbred line Mo17. J. Exp. Bot. **66**: 571–578.

Bukowski, R. et al. (2015). Construction of the third generation *Zea mays* haplotype map. bioRxiv: doi.org/10.1101/026963.

Cambier, V., Hance, T., and de Hoffmann, E. (1999). Non-injured maize contains several 1,4-benzoxazin-3-one related compounds but only as glucoconjugates. Phytochem. Anal. **10**: 119–126.

Cambier, V., Hance, T., and de Hoffmann, E. (2000). Variation of DIMBOA and related compounds content in relation to the age and plant organ in maize. Phytochemistry **53**: 223–229.

Cingolani, P., Platts, A., Wang, L.L., Coon, M., Nguyen, T., Wang, L., Land, S.J., Lu, X., and Ruden, D.M. (2012). A program for annotating and predicting the effects of single nucleotide polymorphisms, SnpEff: SNPs in the genome of *Drosophila melanogaster* strain w1118 ; iso-2; iso-3. Fly (Austin). **6**: 80–92.

Czjzek, M., Cicek, M., Zamboni, V., Bevan, D.R., Henrissat, B., and Esen, A. (2000). The mechanism of substrate (aglycone) specificity in beta-glucosidases is revealed by crystal structures of mutant maize β-glucosidase-DIMBOA, -DIMBOAGlc, and -dhurrin complexes. Proc. Natl. Acad. Sci. U. S. A. **97**: 13555–13560.

Dafoe, N.J., Huffaker, A., Vaughan, M.M., Duehl, A.J., Teal, P.E., and Schmelz, E.A. (2011). Rapidly induced chemical defenses in maize stems and their effects on short-term growth of *Ostrinia nubilalis*. J. Chem. Ecol. **37**: 984–991.

Erb, M., Balmer, D., de Lange, E.S., von Merey, G., Planchamp, C., Robert, C.A.M., Röder, G., Sobhy, I., Zwahlen, C., Mauch-Mani, B., and Turlings, T.C.J. (2011). Synergies and trade-offs between insect and pathogen resistance in maize leaves and roots. Plant, Cell Environ. **34**: 1088–1103.

Erb, M., Flors, V., Karlen, D., de Lange, E., Planchamp, C., D'Alessandro, M., Turlings, T.C.J., and Ton, J. (2009). Signal signature of aboveground-induced resistance upon belowground herbivory in maize. Plant J. **59**: 292–302.

Flint-Garcia, S.A., Thuillet, A.-C., Yu, J., Pressoir, G., Romero, S.M., Mitchell, S.E., Doebley, J., Kresovich, S., Goodman, M.M., and Buckler, E.S. (2005). Maize association population: A high-resolution platform for quantitative trait locus dissection. Plant J. **44**: 1054–1064.

Frey, M., Chomet, P., Glawischnig, E., Stettner, C., Grün, S., Winklmair, A., Eisenreich, W., Bacher, A., Meeley, R.B., Briggs, S.P., Simcox, K., and Gierl, A. (1997). Analysis of a chemical plant defense mechanism in grasses. Science **277**: 696–699.

Frey, M., Schullehner, K., Dick, R., Fiesselmann, A., and Gierl, A. (2009). Benzoxazinoid biosynthesis, a model for evolution of secondary metabolic pathways in plants. Phytochemistry **70**: 1645–1651.

Ganal, M.W. et al. (2011). A large maize (*Zea mays* L.) SNP genotyping array: Development and germplasm genotyping, and genetic mapping to compare with the B73 reference genome. PLoS One **6**: e28334.

Gierl, A. and Frey, M. (2001). Evolution of benzoxazinone biosynthesis and indole production in maize. Planta **213**: 493–498.

Glauser, G., Marti, G., Villard, N., Doyen, G.A., Wolfender, J.-L., Turlings, T.C.J., and Erb, M. (2011). Induction and detoxification of maize 1,4-benzoxazin-3-ones by insect herbivores. Plant J. **68**: 901–911.

Goodwin, T.W. and Mercer, E.I. (1983). Introduction to plant biochemistry. Oxford, UK Pergamon Press.

Hagel, J.M. and Facchini, P.J. (2010). Dioxygenases catalyze the *O*-demethylation steps of morphine biosynthesis in opium poppy. Nat. Chem. Biol. **6**: 273–275.

He, P. and Moran, G.R. (2009). We two alone will sing: The two-substrate alpha-keto acid-dependent oxygenases. Curr. Opin. Chem. Biol. **13**: 443–450.

Ibrahim, R.K. (1997). Plant *O*-methyltransferase signatures. Trends Plant Sci. **2**: 249–250.

Jaganaman, S., Pinto, A., Tarasev, M., and Ballou, D.P. (2007). High levels of expression of the iron-sulfur proteins phthalate dioxygenase and phthalate dioxygenase reductase in *Escherichia coli*. Protein Expr. Purif. **52**: 273–279.

Jonczyk, R., Schmidt, H., Osterrieder, A., Fiesselmann, A., Schullehner, K., Haslbeck, M., Sicker, D., Hofmann, D., Yalpani, N., Simmons, C., Frey, M., and Gierl, A. (2008). Elucidation of the final reactions of DIMBOA-glucoside biosynthesis in maize: Characterization of *Bx6* and *Bx7*. Plant Physiol. **146**: 1053–1063.

Kawai, Y., Ono, E., and Mizutani, M. (2014). Evolution and diversity of the 2-oxoglutarate-dependent dioxygenase superfamily in plants. Plant J. **78**: 328–343.

Köhler, A., Maag, D., Veyrat, N., Glauser, G., Wolfender, J.-L., Turlings, T.C.J., and Erb, M. (2015). Within-plant distribution of 1,4-benzoxazin-3-ones contributes to herbivore niche differentiation in maize. Plant. Cell Environ. **38**: 1081–1093.

Lee, M., Sharopova, N., Beavis, W.D.G.D., Katt, M., Blaie, D., and Hallauer, A. (2002). Expanding the genetic map of maize with the intemated B73×Mo17 (IBM) population. Plant Mol. Biol. **48**: 453–461.

Maag, D., Dalvit, C., Thevenet, D., Köhler, A., Wouters, F.C., Vassão, D.G., Gershenzon, J., Wolfender, J.L., Turlings, T.C.J., Erb, M., and Glauser, G. (2014). 3-*β*-d-Glucopyranosyl-6-methoxy-2-benzoxazolinone (MBOA-*N*-Glc) is an insect detoxification product of maize 1,4-benzoxazin-3-ones. Phytochemistry **102**: 97–105.

Maresh, J., Zhang, J., and Lynn, D.G. (2006). The innate immunity of maize and the dynamic chemical strategies regulating two-component signal transduction in *Agrobacterium tumefaciens*. ACS Chem. Biol. **1**: 165–175.

Marti, G., Erb, M., Boccard, J., Glauser, G., Doyen, G.R., Villard, N., Robert, C.A.M., Turlings, T.C.J., Rudaz, S., and Wolfender, J.-L. (2013). Metabolomics reveals herbivore-induced metabolites of resistance and susceptibility in maize leaves and roots. Plant, Cell Environ. **36**: 621–639.

McMullen, M.D. et al. (2009). Genetic properties of the maize nested association mapping population. Science **325**: 737–740.

Meihls, L.N., Handrick, V., Glauser, G., Barbier, H., Kaur, H., Haribal, M.M., Lipka, A.E., Gershenzon, J., Buckler, E.S., Erb, M., Köllner, T.G., and Jander, G. (2013). Natural variation in maize aphid resistance is associated with 2,4-dihydroxy-7-methoxy-1,4-benzoxazin-3-one glucoside methyltransferase activity. Plant Cell **25**: 2341–2355.

Mijares, V., Meihls, L.N., Jander, G., and Tzin, V. (2013). Near-isogenic lines for measuring phenotypic effects of DIMBOA-Glc methyltransferase activity in maize. Plant Signal. Behav. **8**: e26779.

Niemeyer, H.M. (2009). Hydroxamic acids derived from 2-hydroxy-2H-1,4-benzoxazin-3(*4H*)-one: Key defense chemicals of cereals. J. Agric. Food Chem. **57**: 1677–1696.

Nishida, R. (2014). Chemical ecology of insect–plant interactions: Ecological significance of plant secondary metabolites. Biosci. Biotechnol. Biochem. **78**: 1–13.

Oikawa, A., Ishihara, A., Tanaka, C., Mori, N., Tsuda, M., and Iwamura, H. (2004). Accumulation of HDMBOA-Glc is induced by biotic stresses prior to the release of MBOA in maize leaves. Phytochemistry **65**: 2995–3001.

Osbourn, A. (2010). Gene clusters for secondary metabolic pathways: An emerging theme in plant biology. Plant Physiol. **154**: 531–535.

Rad, U. von, Hüttl, R., Lottspeich, F., Gierl, A., and Frey, M. (2001). Two glucosyltransferases are involved in detoxification of benzoxazinoids in maize. Plant J. **28**: 633–642.

Raspail, C., Graindorge, M., Moreau, Y., Crouzy, S., Lefebvre, B., Robin, A.Y., Dumas, R., and Matringe, M. (2011). 4-Hydroxyphenylpyruvate dioxygenase catalysis. J. Biol. Chem. **286**: 26061–26070.

Rimmer, A., Phan, H., Mathieson, I., Iqbal, Z., Twigg, S.R.F., Wilkie, A.O.M., McVean, G., and Lunter, G. (2014). Integrating mapping-, assembly- and haplotype-based approaches for calling variants in clinical sequencing applications. Nat. Genet. **46**: 912–918.

Robert, C.A.M. et al. (2012). A specialist root herbivore exploits defensive metabolites to locate nutritious tissues. Ecol. Lett. **15**: 55–64.

Rostás, M. (2007). The effects of 2,4-dihydroxy-7-methoxy-1,4-benzoxazin-3-one on two species of *Spodoptera* and the growth of *Setosphaeria turcica* in vitro. J. Pest Sci. (2004). **80**: 35–41.

Sasai, H., Ishida, M., Murakami, K., Tadokoro, N., Ishihara, A., Nishida, R., and Mori, N. (2009). Species-specific glucosylation of DIMBOA in larvae of the rice armyworm. Biosci. Biotechnol. Biochem. **73**: 1333–1338.

Schnable, P.S. et al. (2009). The B73 maize genome: Complexity, diversity, and dynamics. Science **326**: 1112–1115.

Schofield, C.J. and Zhang, Z. (1999). Structural and mechanistic studies on 2-oxoglutarate-dependent oxygenases and related enzymes. Curr. Opin. Struct. Biol. **9**: 722–731.

Søltoft, M., Jørgensen, L.N., Svensmark, B., and Fomsgaard, I.S. (2008). Benzoxazinoid concentrations show correlation with Fusarium Head Blight resistance in Danish wheat varieties. Biochem. Syst. Ecol. **36**: 245–259.

Tamura, K., Peterson, D., Peterson, N., Stecher, G., Nei, M., and Kumar, S. (2011). MEGA5: Molecular evolutionary genetics analysis using maximum likelihood, evolutioanry distance, and maximum parsimony methods. Mol. Biol. Evol. **28**: 2731–2739.

Tuinstra, M.R., Ejeta, G., and Goldsbrough, P.B. (1997). Heterogeneous inbred family (HIF) analysis: A method for developing near-isogenic lines that differ at quantitative trait loci. Theor. Appl. Genet. **95**: 1005–1011.

Tzin, V., Lindsay, P.L., Christensen, S. A., Meihls, L.N., Blue, L.B., and Jander, G. (2015). Genetic mapping shows intraspecific variation and transgressive segregation for caterpillar-induced aphid resistance in maize. Mol. Ecol. **24**: 5739–5750.

Wei, F. et al. (2009). The physical and genetic framework of the maize B73 genome. PLoS Genet. **5**: e1000715.

Wouters, F.C., Reichelt, M., Glauser, G., Bauer, E., Erb, M., Gershenzon, J., and Vassão, D.G. (2014). Reglucosylation of the benzoxazinoid DIMBOA with inversion of stereochemical configuration is a detoxification strategy in lepidopteran herbivores. Angew. Chem. Int. Ed. Engl. **53**: 11320–11324.

Yu, J., Holland, J.B., McMullen, M.D., and Buckler, E.S. (2008). Genetic design and statistical power of nested association mapping in maize. Genetics **178**: 539–551.

Zhou, J.-M., Fukushi, Y., Wollenweber, E., and Ibrahim, R.K. (2008). Characterization of two *O*-methyltransferase-like genes in barley and maize. Pharm. Biol. **46**: 26–34.

Zhou, S. et al. (2009). A single molecule scaffold for the maize genome. PLoS Genet. **5: e1000711..Zubieta, C., He, X.Z., Dixon, R.A., and Noel, J.P.** (2001). Structures of two natural product methyltransferases reveal the basis for substrate specificity in plant *O*-methyltransferases. Nat. Struct. Biol. **8**: 271–279.

4 Discussion

In my doctoral thesis I investigated the biosynthesis of induced nitrogenous defense compounds in maize – benzoxazinoids and aldoximes. I identified and characterized enzymes producing 4- and 8-*O*-methylated benzoxazinoid derivatives, and discovered that these compounds function in plant defense as toxins as well as signals. Furthermore, I characterized a cytochrome P450 enzyme catalyzing the formation of aldoximes in maize and obtained evidence for the function of the enzymatic products. The produced aldoximes may act as defense compounds or serve as precursors for plant hormones.

I will now discuss the findings we obtained for the biosynthesis of nitrogen-containing defense compounds and their properties in maize from a broader perspective, and provide further data and insights about their formation, function and evolution.

4.1 The biosynthesis of benzoxazinoids in maize – the current state of knowledge

The biosynthesis of benzoxazinoids including all the known hydroxamic acids has now been fully elucidated in maize (Figure 4) (Frey et al., 1997; Rad et al., 2001; Jonczyk et al., 2008; Manuscript I, Manuscript III). This work describes the identification and characterization of the 4-*O*-methyltransferases (BX10, BX11, BX12, and BX14) that catalyze the formation of the methylated hydroxamic acids HDMBOA-Glc and HDM_2BOA-Glc (Manuscript I; Manuscript III). The characterization of the 2-oxoglutarate/Fe(II)-dependent dioxygenase BX13 adds another biosynthetic branch to the benzoxazinoid pathway (Figure 4) (Manuscript III). Furthermore, we have shown that BX7 methylates additionally the BX13 product, TRIMBOA-Glc, at position 7, which is highly uncommon in such a linear pathway (Manuscript III). Remarkably within the linear benzoxazinoid pathway, BX7 is involved in the formation of two major benzoxazinoids, DIMBOA-Glc and DIM_2BOA-Glc, which have been demonstrated to contribute to maize resistance

(Niemeyer, 2009) to herbivores, bacteria and fungi (Corcuera et al., 1978; Sahi et al., 1990; Søltoft et al., 2008). Thus, differences in regulation or sequence modifications at *Bx*7 might have major consequences for maize innate immunity. Changes in *Bx*7 expression and sequence polymorphisms, for instance, can potentially influence the accumulation of benzoxazinoids and consequently affect protection against attackers (Manuscript III).

We have shown that the identified biosynthetic enzymes BX10, BX11, BX12, BX13, and BX14 determine the composition and ratio of the complex benzoxazinoid mixture in maize. For example, a transposon insertion in *Bx*12 significantly reduced the HDMBOA-Glc formation and a natural occurring mutation in *Bx*13 resulted in the absence of DIM_2BOA-Glc while all other BXD compounds were not influenced (Manuscript III). The absence of DIM_2BOA-Glc in two near isogenic lines comprising either a functional or mutated inactive *Bx*13 allele strengthens our findings. However, these near isogenic lines differed not only in their *Bx*13 alleles, which opens some room for interpretation (Manuscript III). RNAi-mediated knock-down of target genes may give final proof for their role in the biosynthesis of benzoxazinoids.

Although the biosynthesis of hydroxamic acid benzoxazinoid derivatives in maize is now completely solved, the biosynthesis of benzoxazinoid lactams is still unclear (Figure 4). It is likely that enzymes catalyzing the formation of hydroxamic acid derivatives also take part in the formation of the structurally closely-related lactams since we have not found any homologs to the characterized enzymes that might catalyze the formation of the corresponding lactams. More insights in the biosynthesis of benzoxazinoids will help to understand the biological impact and function of individual benzoxazinoid derivatives.

In addition to the work presented in this thesis, we created transgenic plants overexpressing *Bx*12 to study the biological and physiological impact of methylated benzoxazinoids. I designed constructs for the overexpression of *Bx*12 in wheat and maize. Positive transformation events have already been selected, which now have to be back-crossed to achieve homozygous plants. Similarly, a *Bx*11 150 bp-fragment, which shares the highest identity with sequences of the homologs *Bx*10, *Bx*12 and *Bx*14 (90–99%), has been chosen to try to silence all characterized 4-*O*-methyltransferases in maize. The resulting transgenic plants will provide further insights about the role of 4-*O*-methylated benzoxazinoid derivatives in chemical defense in grasses.

While DIBOA-Glc and DIMBOA-Glc as products of the core BXD pathway are produced in nearly all investigated grass species, the methylated compounds HDMBOA-Glc, DIM_2BOA-Glc, and HDM_2BOA-Glc have only been described in a
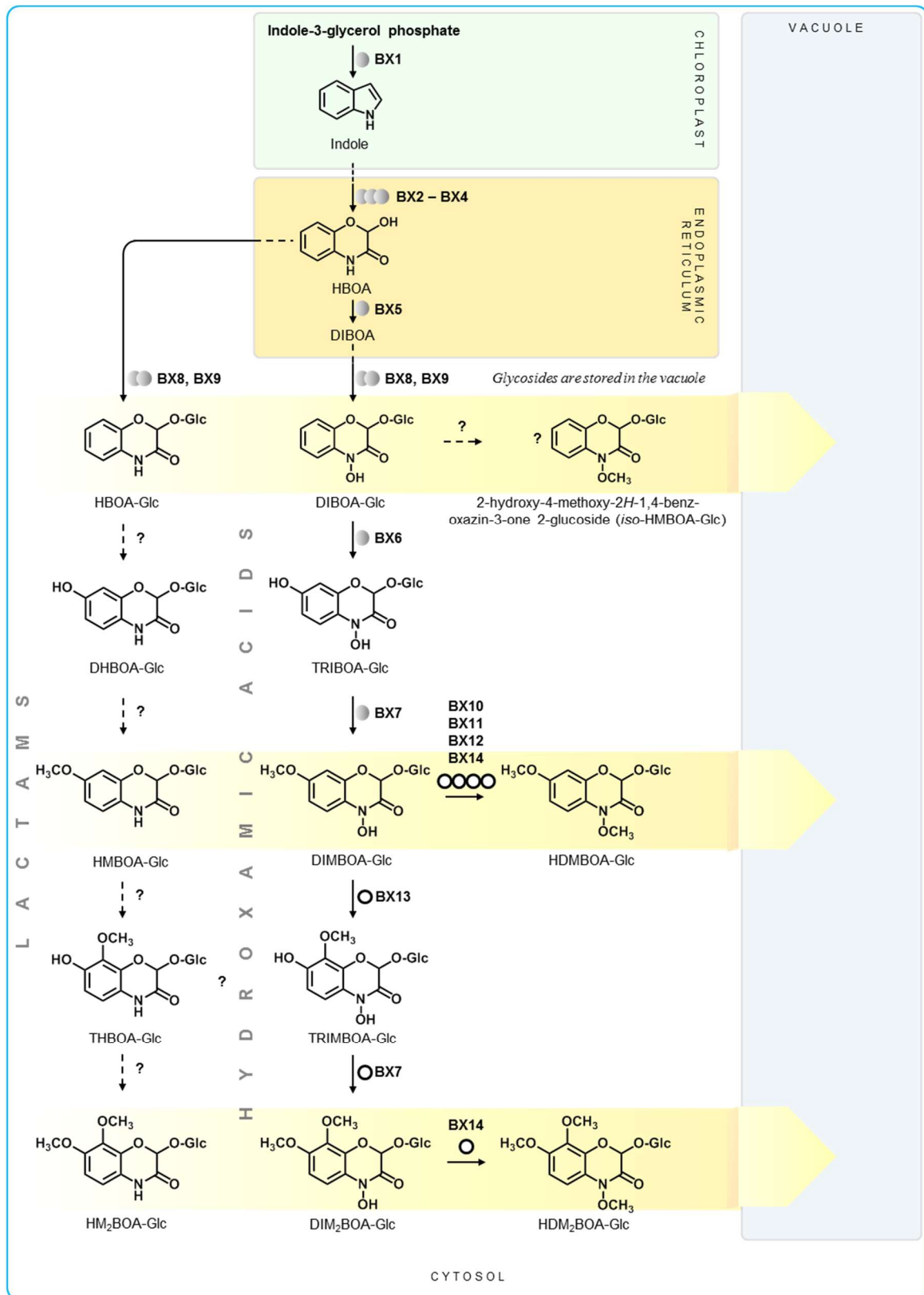
Figure 4. Current state of benzoxazinoid biosynthesis in maize.
Enzymes which have been characterized in the present study are marked with black lined spheres (○). The biosynthesis of HMBOA-Glc, HM2BOA-Glc and the presence and formation of a HMBOA-Glc isomer (2-hydroxy-4-methoxy-2H-1,4-benzoxazin-3-one 2-glucoside) remains unknown. The biosynthetic steps which might lead to the mentioned benzoxazinoids are indicated (- - -).

few grasses such as wheat and maize (Hofman and Masojidková, 1973; Sicker and Schulz, 2002, Søltoft et al., 2008). This suggests that the ability to synthesize the methylated benzoxazinoids is a unique and recent evolutionary adaptation. However it is still unclear whether the biosynthetic genes involved in HDMBOA-Glc, DIM_2BOA-Glc, and HDM_2BOA-Glc formation are of the same origin in wheat and maize or whether they evolved independently.

Increased pest density in monocultures and artificial selection might have influenced the evolution of plant defenses in crops (Andow, 1991; Zhang et al., 2002; Tian et al., 2009). The selection of disease-related alleles has been found to pass through episodic laps, presumably influenced by pathogen availability and specificity (Tiffin and Gaut, 2001; Zhang et al., 2002). Approximately 1200 genes throughout the maize genome have been affected by artificial selection (Wright et al., 2005). The *Bx*1 allele (Accession No. AY104439) is one of the top-ranked candidates, and was likely affected by selection during domestication (Wright et al., 2005). Additionally, it has been shown that the genetic variation at *Bx*1, supposedly affected by breeding, controls benzoxazinoid biosynthesis in maize (Butrón et al., 2010). Other benzoxazinoid biosynthetic genes have not been found to be affected by breeding (Wright et al., 2005). However, this study surveyed only a limited number of inbred lines (14 maize inbred lines and 16 inbred teosintes, the maize ancestors) (Wright et al., 2005), meaning that it cannot be excluded that maize breeding, which has yielded hundreds of diverse maize inbred lines, broadly influenced benzoxazinoid biosynthesis.

4.2 Genetic mapping of biosynthetic genes responsible for defense compound formation in maize

To identify genes involved in benzoxazinoid formation, we combined homology-based sequence analysis and genetic mapping. The mapping provides additional proof for the biosynthesis of benzoxazinoids in planta. This is of significance as the standard approach to validate *in-vitro* enzyme characterization, the Agrobacterium-mediated overexpression or knock-out of genes, is neither as routine nor as reproducible in maize as in dicotyledonous plants (Potrykus, 1989; Songstad, 2010).

We used a genome-wide association mapping approach to identify genes responsible for benzoxazinoid production in maize. The genetic mapping of certain chemical traits in maize including DIMBOA-Glc, maysin, and chlorogenic acid content has been conducted before (Guo et al., 2001; Butrón et al., 2010; Widstrom et al., 2003) and previously characterized genes were assigned to mapped quantitative trait loci (QTL). For instance, chalcone isomerase genes were

associated with maysin biosynthesis QTLs and the location of *Bx* genes was consistent with a DIMBOA-Glc biosynthesis QTL on the tip of chromosome 4 (Meihls et al., 2012). However mapped candidate genes with unknown function have rarely been characterized in maize.

Genetic mapping of the formation of HDMBOA-Glc, DIM_2BOA-Glc and HDM_2BOA-Glc revealed a total of four QTLs on chromosomes 1, 2, and 4 (bin1.04, bin2.05, bin2.09, and bin4.03, respectively) (Manuscript I; Manuscript III). At the same time, benzoxazinoid content mapped in root and shoot tissues of varying recombinant inbred line (RIL) populations yielded the same specific QTLs (Manuscript III). Although each mapped QTL comprises a few hundred genes, we were able to limit potential candidate genes to a manageable number. Key to this was making basic assumptions about the enzyme class that might catalyze the reaction under consideration, and using the annotated maize genome (Schnable et al., 2009). Heterologous expression of candidate genes and subsequent activity assays with purified enzymes resulted in the identification of benzoxazinoid biosynthetic enzymes (Manuscript I; Manuscript III). Near isogenic inbred lines provided further evidence that the characterized enzymes are responsible for the formation of benzoxazinoid derivatives in maize (Manuscript III).

The applied genetic mapping approach for HDMBOA-Glc, DIM_2BOA-Glc and HDM_2BOA-Glc contents turned out to be robust due to the high sensitivity and resolution of the chemical analysis and use of both targeted und untargeted metabolomics approaches. In combination with genetic background information (Flint-Garcia et al., 2005; Yu et al., 2008; McMullen et al., 2009; Schnable et al., 2009; Wei et al., 2009; Zhou et al., 2009; Ganal et al., 2011), metabolomics data can provide tremendous information about biosynthetic pathways of natural plant products. Untargeted metabolic analysis of maize tissues might be especially of value in future pathway discovery. Making such metabolomics data accessible to the public can lead to advances in maize research in many different areas.

4.3 The origin and activity of benzoxazinoid *O*-methyltrans-ferases

It has already been stated that the 7-*O*-methyltransferase BX7 is related to flavonoid 7-*O*-methyltransferases based on sequence identity (Jonczyk et al., 2008). In many cases, substrates of related *O*-methyltransferases have been found to share structural features (Lam et al., 2007). The overall chemical skeleton of flavonoids in fact resembles that of benzoxazinoids. Both are
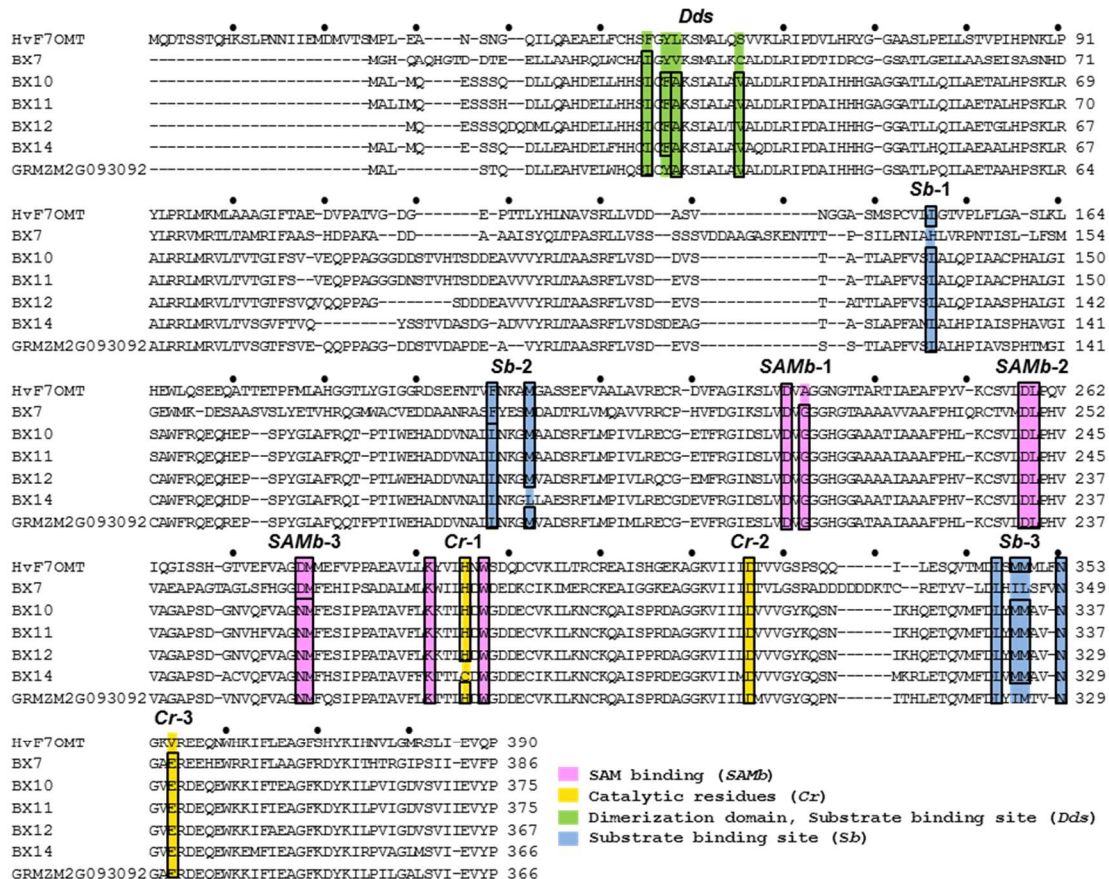
A

B

GRMZM2G093092
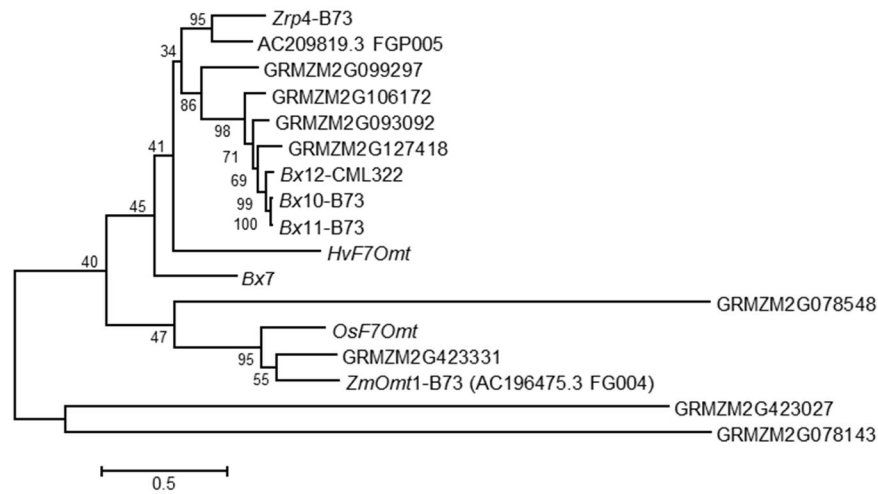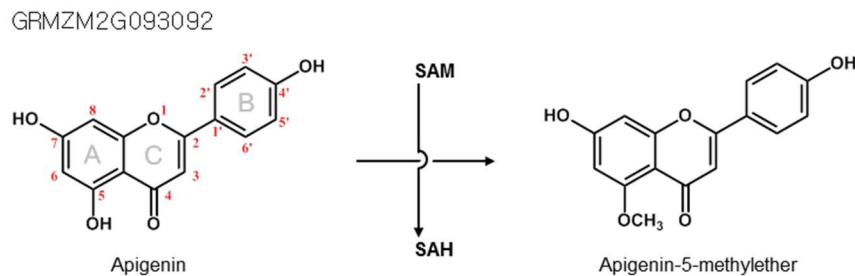
C

◄ **Figure 5**. Rooted phylogenetic tree of grass *O*-methyltransferases, a novel 5-*O*-methyltransferase enzyme activity in grasses found in maize, and an alignment of characterized grass *O*-methyltransferases.
(A) The tree was inferred using the maximum likelihood method and n = 1000 replicates for bootstrapping. Bootstrap values are shown next to each node. The tree is drawn to scale, with branch lengths measured in the number of substitutions per site. (B) Enzyme activity of GRMZM2G093092: Purified recombinant GRMZM2G093092 as well as the empty vector control were incubated with Apigenin and the *S*-adenosyl-L-methionine. Product formation was analyzed by LC-MS/MS. The chemical structure of the methylation product, Apingenin-5-methylether, has been obtained by NMR. (C) Sequence alignment of seven characterized plant *O*-methyltransferases. The numbering of each protein is in parentheses, with every 10th position dotted. Residues involved in SAM/SAH binding (pink), substrate binding (blue), substrate binding in trans from the dyad related polypeptide (green), and catalysis (yellow) are highlighted. Modified from Zubieta et al., 2001.

composed of two six-membered rings and a heterocycle; however the origin, the type and number of functional groups, and the stereochemistry differ (Figure 5B). Flavonoids are ancient and widespread specialized compounds, ubiquitously found in plants (Winkel-Shirley, 2002). It might be possible that the benzoxazinoid enzymes characterized in this study originate from enzymes from the older flavonoid pathway or share at least a common evolutionary history.

Table 1. Enzyme activities of related maize *O*-methyltransferases (OMTs).
The examined OMTs form a cluster in a phylogenetic analysis of maize OMT sequences. Activity with DIMBOA-Glc and various flavonoids is indicated by black spheres (●). A lack of activity is indicated by a cross (X). Enzymes with a higher relative activity are labeled with two spheres. Product formation was analyzed by LC-MS/MS.

	O-METHYLTRANSFERASES FROM *Zea mays*						
SUBSTRATE	BX10	BX11	BX12	BX14[a]	GRMZM2G093092[a]	GRMZM2G106172	GRMZM2G099297
DIMBOA-Glc	●	●	●	●	X	X	X
Naringenin	X	X	X	X	●●	●	X
Apigenin	X	X	X	X	●●	●	X
Kaempferol	X	X	X	X	●●	●	X

[a]Amino acid sequences of BX14 and GRMZM2G093092 share 81% identity.

In a phylogenetic analysis, *Bx*7 clusters with flavonoid 7-*O*-methyltransferases from rice (OsF7OMT) and barley (HvF7OMT) (Figure 5A). Applying findings from

the crystallization of plant OMTs, the catalytic residues of the 7-*O*-methyltransferases BX7 and HvF7OMT match each other quite well among the conserved regions (Zubieta et al., 2001). BX7 and HvF7OMT share 14 out of 22 catalytic residues responsible for substrate binding, co-factor binding and residues involved in the transfer of the activated methyl group (Figure 5C). Six of the varying amino acid side chains belong to regions assigned to substrate binding and substrate pocket assembly (Zubieta et al., 2001), which might explain why BX7 does not utilize flavonoids (Jonczyk et al., 2008).

Between benzoxazinoid 4-*O*-methyltransferases and flavonoid 7-*O*-methyltransferases many catalytic residues are also shared (Figure 5C). However, the characterized benzoxazinoid 4-OMTs do not utilize flavonoids based on recent data I obtained that are not included in the rest of the thesis (Table 1). I further performed enzyme assays with the maize *O*-methyltransferases GRMZM2G093092 and GRMZM2G106172, which are closely related to BX10, BX11, BX12, and Bx14 (Figure 5A). These assays revealed that GRMZM2G093092 and GRMZM2G106172 methylate various flavonoids (Table 1). Interestingly, GRMZM2G093092 and GRMZM2G106172 were not able to methylate the benzoxazinoid DIMBOA-Glc (Table 1), although they are highly homologous to BX10, BX11, BX12, and BX14 (81– 85%).

For flavonoids, a number of hydroxyl groups are potential sites of *O*-methylation. NMR analysis of the purified apigenin GRMZM2G093092 methylation product revealed the methylation site to be at position 5 (Figure 5B). The apigenin-5-methylether has been described from tropical oleander (Voigtländer and Balsam, 1970), but has not been found in maize or other grasses before. I found apigenin-5-methylether in maize and sorghum. Maize produces apigenin-5-methylether in response to *Bipolaris maydis* infection (data not shown). *Bipolaris maydis*, a fungal pathogen, can cause yield losses up to 70% in a tropical climate.

The distinct substrate specificity of BX14 and GRMZM2G093092 could be explained by differing residues in the dimerization domain, the catalytic domain, and the substrate binding domain (Figure 5C). *In vitro* mutagenesis may help to identify amino acid side chains that maintain the catalytic properties.

Both the phylogenetic analysis and the characterization of GRMZM2G093092 and GRMZM2G106172 as flavonoid *O*-methyltransferases give first indications that *O*-methyltransferase genes of the benzoxazinoid pathway evolved from flavonoid *O*-methyltransferases. However, the exact evolutionary history of benzoxazinoid *O*-methyltransferase genes in grasses is still unclear (Dutartre et al., 2012). As an example for the evolution of resistance genes, our growing knowledge about plant OMTs will allow us to understand how novel and beneficial enzyme activities evolved in grasses.

4.4 Benzoxazinoid dioxygenases: Enzyme activity and evolution

Similar to benzoxazinoid *O*-methyltransferases, the evolution of the dioxygenase genes *Bx*6 and *Bx*13 is still unclear (Dutartre et al., 2012). In maize, the most related gene to *Bx*6 and *Bx*13 is the dioxygenase Flavone synthase I (*Fsn*I), which shares 60% sequence identity with *Bx*6/13. Analogous to the *O*-methyltransferases, the benzoxazinoid dioxygenases may have evolved from an ancestor accepting flavonoids as substrates.
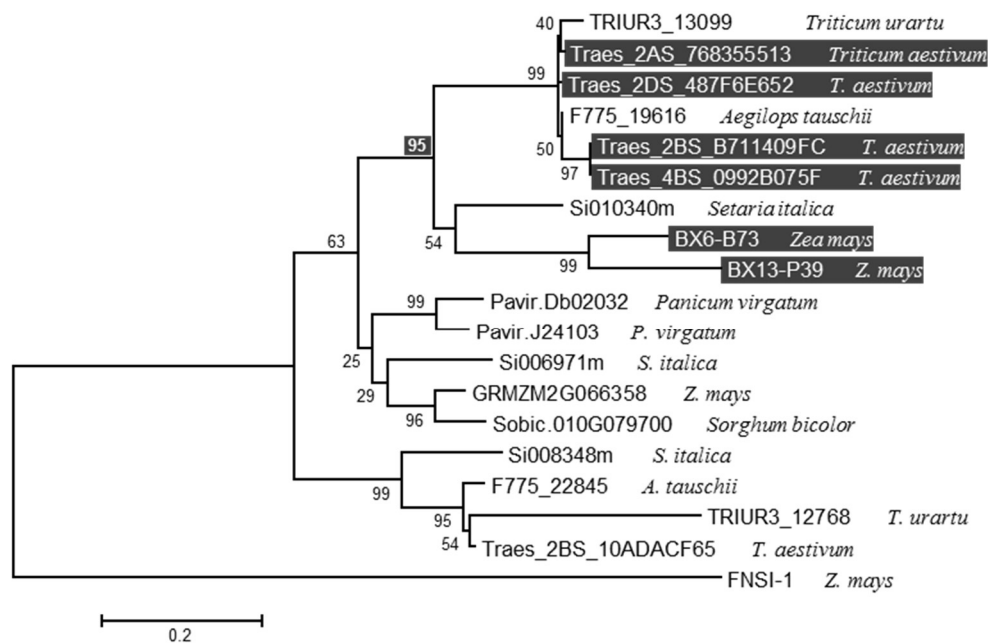

Figure 6. Rooted phylogenetic tree of maize 2-ODD amino acid sequences similar to BX13-P39. The tree was inferred using the maximum likelihood method and n = 1000 replicates for bootstrapping. Bootstrap values are shown next to each node. The tree is drawn to scale, with branch lengths measured in the number of substitutions per site. The originating genus and species for each sequence are indicated. BX6 and BX13 from *Zea mays* and the BX6/BX13-homologs from *Triticum aestivum* are marked black.

The wheat genome comprises genes homologous to both maize benzoxazinoid dioxygenases *Bx*6 and *Bx*13 (http://www.gramene.org; Traes_2AS_768355513, Traes_2DS_487F6E652, Traes_2BS_B711409FC, and Traes_4BS_0992B075F; Figure 6). In addition, wheat is also known to produce the respective enzymatic products, DIMBOA-Glc and DIM_2BOA-Glc (Hofman and Masojidková, 1973; Sicker and Schulz, 2002, Søltoft et al., 2008). However, wheat and maize BX6/BX13-like dioxygenase sequences are surprisingly well separated in phylogenetic analysis according to plant species and not separated in a distinct BX6- and a BX13-cluster as expected (Figure 6). This suggests that maize BX13 and the wheat BX13-like enzyme evolved independently in maize and wheat by duplication of their respective *Bx*6(-like) ancestors, demonstrating convergent evolution. A consequence of convergence could be that there re differences in the

reaction mechanism of BX13 between wheat and maize. Contrary to the catalytic mechanism of the maize BX13 (Manuscript III), the homologous dioxygenase from wheat may directly catalyze the hydroxylation at position 8 of DIMBOA-Glc, which would confirm an independent evolution of DIM_2BOA-Glc formation in wheat and maize.

4.5 Second Messengers: Parallels in signaling properties of benzoxazinoid and glucosinolate aglucones

Well-known plant defense chemicals have been discovered to function not only as direct weapons against enemies, but also additionally as signals in inducing defense pathways (Maag et al., 2014). For instance, glucosinolates have been found to be required for callose deposition after treatment with the main component of bacterial flagellum, flagellin, microbial pathogens, and aphids (Clay et al., 2009; Bednarek et al., 2009; Pfalz et al., 2009). Glucosinolates show many parallels to benzoxazinoids, e.g. in terms of activation and mode of action (Halkier and Gershenzon, 2006). Maize lines mutated in indole-3-glycerol phosphate lyase (*Bx*1) have diminished benzoxazinoid concentrations and were impaired in callose deposition triggered by the fungal polysaccharide chitosan (Ahmad et al., 2011). However, application of the benzoxazinoid aglucone DIMBOA restored callose deposition in the benzoxazinoid deficient maize mutant in a dose-dependent manner (Ahmad et al., 2011). Application of a solution containing 20 µg mL^{-1} DIMBOA induced the deposition of approximately 4 times more callose than a solution containing 4 µg mL^{-1} of DIMBOA (Ahmad et al, 2011). Therefore, accumulation of DIMBOA glucoside in maize organs positively influenced defense against aphids, because of the increased potential for callose formation.

An inactivating transposon insertion in the 4-*O*-methyltransferase *Bx*12, which uses DIMBOA-Glc as substrate, significantly affected the DIMBOA-Glc concentration in leaves (Manuscript I). Maize lines of the NAM population with this *Bx*12-insertion were found to produce significantly more DIMBOA-Glc than lines with an active *Bx*12. The varying DIMBOA-Glc concentrations also positively correlate with altered callose deposition upon leaf aphid infestation, indicating a signaling function for DIMBOA-Glc (Manuscript I).

Structurally related to benzoxazinoids, indole-derived glucosinolate aglucones have also been identified to influence callose deposition (Clay et al., 2009; Bednarek et al., 2009; Pfalz et al., 2009). The plant hormone indole-3-acetic acid has been shown to affect the callose deposition by influencing glucan synthase like 8 (GLS8) in Arabidopsis, which is involved in callose synthesis (Han et al., 2014). Hypothetically, the mechanism which leads to callose deposition by glucosinolates

and benzoxazinoid aglucones might be similar to the mechanism by which auxin accomplishes this, with the difference that higher concentrations are necessary in order to achieve the same effect e.g. due to lower binding affinities to receptors. It is feasible that the second messenger effect of glucosinolates and benzoxazinoids is based on the same or a modulated signaling pathway normally triggered by phytohormones. Therefore these recently discovered signaling functions of indolic glucosinolates and indole-derived benzoxazinoids may have also coexisted with the direct effects of these compounds towards plant attackers. Modulations of the system such as the transposon insertion in *Bx*12 might be an adaptation to the specific selection pressure of a pathogen or an aphid species (Manuscript I).

Another group of maize nitrogenous metabolites studied, the aldoximes, may also participate in signaling serving as potential precursors for phytohormones. We characterized the maize cytochrome P450 enzyme CYP79A61 which catalyzes the formation of (*E/Z*)-phenylacetaldoxime and (*E/Z*)-indole-3-acetaldoxime (Manuscript II). It has already been discussed that both compounds might be transformed to the phytohormones, phenylacetic acid and indole-3-acetic acid, respectively. We found that CYP79A61 gene expression and the enzyme products (*E/Z*)-phenylacetaldoxime and (*E/Z*)-indole-3-acetaldoxime were induced upon herbivory, corresponding well with elevated levels of phenylacetic acid and indole-3-acetic acid in herbivore-damaged plants (Manuscript II). Thus for the induction of phenylacetic acid and indole-3-acetic acid in maize, CYP79A61 activity is decisive. Aldoximes have also been shown to contribute to direct and indirect plant defense (Irmisch et at., 2013; McCormick et al., 2014), and furthermore intermediates in indole-3-acetic biosynthesis were found to be toxic (Pedras et al., 2002), illustrating that aldoximes may play multiple roles in plant defense responses.

4.6 Outlook

In this thesis, I have not only filled in most of the gaps in the biosynthetic pathway for benzoxazinoid formation, but also obtained the first indications of the evolutionary history of some of the genes characterized. The benzoxazinoid 4-*O*-methyltransferses seem to have been recruited from flavonoid *O*-methyltransferases, while the benzoxazinoid 2-oxoglutarate/Fe(II)-dependent dioxygenases seem to have arisen independently in wheat and maize, despite the close relationship of these two grasses. The results shed light on some of the mechanisms that have created the biosynthetic machinery producing the enormous variety of plant natural products.

5 Summary

The aim of this work was to identify enzymes responsible for the formation of induced nitrogenous defence compounds in maize. Benzoxazinoids represent the major class of defence compounds in maize and other grass species. The biosynthetic pathway leading to the main benzoxazinoid in maize, DIMBOA-Glc, has been unravelled before. However, upon herbivory or pathogen infestation, DIMBOA-Glc can be converted into a mixture of methylated benzoxazinoids including HDMBOA-Glc, DIM_2BOA-Glc, and HDM_2BOA-Glc. The aglucons of these compounds are more toxic than DIMBOA, suggesting that this conversion is part of a plant defense reaction. However, the biosynthesis as well as the exact biological functions of these compounds in maize were unknown.

A genome-wide association mapping approach was used to identify genes associated with the formation of methylated benzoxazinoids. In total, we identified five *O*-methyltransferase genes and a single 2-oxoglutarete/Fe(II)-dependent dioxygenase gene. Candidate genes were heterologously expressed in *Escherichia coli*. In activity assays, the candidates were shown to specifically catalyze the formation of HDMBOA-Glc, DIM_2BOA-Glc and HDM_2BOA-Glc. The *O*-methyltransferases BX10, BX11, BX12, and BX14 methylate DIMBOA-Glc which results in HDMBOA-Glc formation. The dioxygenase BX13 hydroxylates DIMBOA-Glc. The hydroxylation product, TRIMBOA-Glc, is subsequently methylated by the *O*-methyltransferase BX7 which leads to DIM_2BOA-Glc. DIM_2BOA-Glc is a substrate for the *O*-methyltransferase BX14 yielding HDM_2BOA-Glc. We have found natural occurring mutations and a transposon insertion in the identified biosynthetic genes causing diminished concentrations or a lack of the considered benzoxazinoids in the respective maize lines.

Further we discovered that an inactivating transposon insertion in *Bx*12 modulates the ratio of the BX12 substrate DIMBOA-Glc and the methylation product. Maize inbred lines harbouring the transposon insertion were found to produce elevated levels of DIMBOA-Glc which correlated with a decreased susceptibility towards maize leaf aphids. This is attributed to signalling properties of DIMBOA-Glc or its aglucone, which cause callose formation, a known defence trait against sucking insects. The indole-derived DIMBOA-Glc presumably triggers signalling components that are also mediated by phytohormones such as indole-3-acetic acid (IAA). We characterized cytochrome P450 enzymes, which catalyze the formation of (*E/Z*)-phenylacetaldoxime and (*E/Z*)-indole-3-acetaldoxime from L-tryptophan und L-phenylalanine, respectively. There is evidence that auxins are potentially synthesized from these aldoximes.

6 Zusammenfassung

Ziel der Arbeit war es Enzyme zu identifizieren, welche die Biosynthese von induzierten, stickstoffhaltigen Pflanzenabwehrstoffen in Mais katalysieren – namentlich von Benzoxazinoiden und Aldoximen. Benzoxazinoide sind Substanzen, die überwiegend in Süßgräsern auftreten. Viele Süßgräser, zu denen auch Nutzpflanzen wie Mais, Roggen oder Weizen gehören, akkumulieren die Benz-oxazinoide DI-BOA-Glc oder DIMBOA-Glc. Nach Insektenbefall oder auch Pilzbefall werden vermehrt die methylierten Benzoxazinoide HDMBOA-Glc, DIM$_2$BOA-Glc und HDM$_2$BOA-Glc gebildet, deren Aglukon meist reaktiver sind als deren chemische Vorläufer. Die Biosynthese und die genaue Funktion dieser, nach Befall durch Schädlinge induzierten Benzoxazinoide, waren jedoch unbekannt.

Basierend auf genetischen Kartierungen identifizierten wir Kandidatengene, die für fünf O-Methyltransferasen und für eine 2-oxoglutarate/Fe(II)-abhängige Dioxygenase kodieren. In Aktivitätsassays konnte ich nachweisen, dass die heterolog exprimierten Enzyme die Synthese von HDMBOA-Glc, DIM$_2$BOA-Glc und HDM$_2$BOA-Glc katalysieren. Die O-Methyltransferasen BX10, BX11, BX12 und BX14 methylieren DIMBOA-Glc, wodurch direkt HDMBOA-Glc gebildet wird. DIM$_2$BOA-Glc wird in zwei aufeinanderfolgenden enzymatischen Schritten synthetisiert: DIMBOA-Glc wird zunächst durch die 2-oxoglutarate/Fe(II)-abhängige Dioxygenase BX13 hydroxyliert. Die O-Methyltransferase BX7 setzt dann das Hydroxylierungsprodukt TRIMBOA-Glc um und gibt schließlich DIM$_2$BOA-Glc frei. DIM$_2$BOA-Glc dient als Substrat für die O-Methyltransferasen BX14, welche HDM$_2$BOA-Glc bildet. Maisinzuchtlinien, die Mutationen oder Transposoninsertionen in den identifizierten Biosynthesegenen tragen, sind nicht oder nur begrenzt in der Lage das entsprechende Benzoxazinoid zu bilden.

Wir konnten zeigen, dass DIMBOA-Glc oder deren Aglukon neben toxischen Eigenschaften auch Signaleigenschaften in Mais besitzt und in Folge von Blattlausbefall die Synthese von Callose beeinflusst. Das von Indol abstammende DIMBOA-Glc nutzt dabei möglicherweise Strukturen, die auch von Pflanzenhormonen wie z.B. Indol-3-essigsäure (IAA) angesprochen werden. In einer weiteren Studie konnten wir ein Cytochrom-P450 abhängiges Enzym identifizieren, das aus L-Tryptophan und L-Phenylalanin die entsprechenden Aldoxime herstellt. Die Synthese der Aldoxime wird durch Insektenbefall induziert. Diese Aldoxime fungieren möglicherweise direkt als Abwehrstoffe oder werden als Vorläufer für die Synthese von Pflanzenhormone wie IAA benötigt, die ihrerseits Abwehrreaktionen auslösen können.

7 References

Ahmad, S., Veyrat, N., Gordon-Weeks, R., Zhang, Y., Martin, J., Smart, L., Glauser, G., Erb, M., Flors, V., Frey, M., and Ton, J. (2011). Benzoxazinoid metabolites regulate innate immunity against aphids and fungi in maize. Plant Physiol. **157**: 317–327.

Andow, D.A. (1991). Vegetational Diversity and Arthropod Population Response. Rev . Entomol **36**: 561–86.

Atkinson, J., Morand, P., and Arnason, J.T. (1991). Analogues of the cyclic hydroxamic acid 2,4-dihydroxy-7-methoxy-2H-1,4-benzoxazin-3-one: Decomposition to benzoxazolinones and reaction with β-mercaptoethanol. J. Org. Chem. **56**: 1788–1800.

Bak, S. et al. (2006). Cyanogenic glycosides: A case study for evolution and application of cytochromes P450. Phytochem. Rev. **5**: 309–329.

Beck, D.L., Dunn, G.M., Routley, D.G., and Bowman, J.S. (1983). Biochemical basis of resistance in corn to the corn leaf aphid. Crop Sci **23**: 995–998.

Bednarek, P., Pišlewska-Bednarek, M., Svatoš, A., Schneider, B., Doubský, J., Mansurova, M., Humphry, M., Consonni, C., Panstruga, R., Sanchez-Vallet, A., Molina, A., and Schulze-Lefert, P. (2009). A Glucosinolate Metabolism Pathway in Living Cells Mediates Broad-Spectrum Antifungal Defense. Science (80-.). **323**: 101–106.

Bjarnholt, N. and Møller, B.L. (2008). Hydroxynitrile glucosides. Phytochemistry **69**: 1947–1961.

Boerjan, W., Ralph, J., and Baucher, M. (2003). Lignin biosynthesis. Annu. Rev. Plant Biol. **54**: 519–546.

Bones, A.M. and Rossiter, J.T. (1996). The myrosinase-glucosinolate system, its organisation and biochemistry. Physiol. Plant. **97**: 194–208.

Britsch, L. (1990). Purification and characterization of flavone synthase I, a 2-oxoglutarate-dependent desaturase. Arch. Biochem. Biophys. **282**: 152–160.

Bushman, B.S., Snook, M.E., Gerke, J.P., Szalma, S.J., Berhow, M.A., Houchins, K.E., and McMullen, M.D. (2002). Two loci exert major effects on chlorogenic acid synthesis in maize silks. Crop Sci. **42**: 1669–1678.

Butrón, A., Chen, Y.C., Rottinghaus, G.E., and McMullen, M.D. (2010). Genetic variation at bx1 controls DIMBOA content in maize. Theor Appl Genet **120**: 721–34.

Cambier, V., Hance, T., and De Hoffmann, E. (2000). Variation of DIMBOA and related compounds content in relation to the age and plant organ in maize. Phytochemistry **53**: 223–229.

Chini, A., Fonseca, S., Fernández, G., Adie, B., Chico, J.M., Lorenzo, O., García-Casado, G., López-Vidriero, I., Lozano, F.M., Ponce, M.R., Micol, J.L., and Solano, R. (2007). The JAZ family of repressors is the missing link in jasmonate signalling. Nature **448**: 666–671.

Chiron, H., Drouet, A., Claudot, A.C., Eckerskorn, C., Trost, M., Heller, W., Ernst, D., and Sandermann, H. (2000). Molecular cloning and functional expression of a stress-induced multifunctional O-methyltransferase with pinosylvin methyltransferase activity from scots pine (*Pinus sylvestris* L.). Plant Mol. Biol. **44**: 733–745.

Cho, J.N., Ryu, J.Y., Jeong, Y.M., Park, J., Song, J.J., Amasino, R.M., Noh, B., and Noh, Y.S.

(2012). Control of seed germination by light-induced histone arginine demethylation activity. Dev. Cell **22**: 736–748.

Clavijo McCormick, A., Irmisch, S., Reinecke, A., Boeckler, G.A., Veit, D., Reichelt, M., Hansson, B.S., Gershenzon, J., Köllner, T.G., and Unsicker, S.B. (2014). Herbivore-induced volatile emission in black poplar: Regulation and role in attracting herbivore enemies. Plant, Cell Environ. **37**: 1909–1923.

Clay, N.K., Adio, A.M., Denoux, C., Jander, G., and Ausubel, F.M. (2009). Glucosinolate metabolites required for an Arabidopsis innate immune response. Science **323**: 95–101.

Corcuera, L.J., Woodward, M.D., Helgeson, J.P., Kelman, A., and Upper, C.D. (1978). 2,4-Dihydroxy-7-methoxy-2H-1,4-benzoxazin-3(4H)-one, an inhibitor from *Zea mays* with differential activity against soft rotting *Erwinia* species. Plant Physiol. **61**: 791–795.

Cuevas, L., Niemeyer, H.M., and Pérez, F.J. (1990). Reaction of DIMBOA, a resistance factor from cereals with α-chymotrypsin. Phytochemistry **29**: 1429–1432.

Dafoe, N.J., Huffaker, A., Vaughan, M.M., Duehl, A.J., Teal, P.E., and Schmelz, E.A. (2011). Rapidly induced chemical defenses in maize stems and their effects on short-term growth of *Ostrinia nubilalis*. J. Chem. Ecol. **37**: 984–991.

Dixon, R.A (2001). Natural products and plant disease resistance. Nature **411**: 843–847.

Dixon, R.A. and Strack, D. (2003). Phytochemistry meets genome analysis, and beyond ... Phytochemistry **62**: 815–816.

Dixon, R.A. and Paiva, N.L. (1995). Stress-induced phenylpropanoid metabolism. Plant Cell **7**: 1085–97.

Dutartre, L., Hilliou, F., and Feyereisen, R. (2012). Phylogenomics of the benzoxazinoid biosynthetic pathway of Poaceae: Gene duplications and origin of the Bx cluster. BMC Evol. Biol. **12**: 64.

Elliger, C.A., Chan, B.G., Waiss Jr., A.C., Lundin, R.E., and Haddon, W.F. (1980). C-glycosylflavones from *Zea mays* that inhibit insect development. Phytochemistry **19**: 293–297.

Falcone Ferreyra, M.L., Emiliani, J., Rodriguez, E.J., Campos-Bermudez, V.A., Grotewold, E., and Casati, P. (2015). The Identification of maize and Arabidopsis type I FLAVONE SYNTHASEs links flavones with hormones and biotic interactions. Plant Physiol. **169**: 1090–1107.

Farrow, S.C. and Facchini, P.J. (2014). Functional diversity of 2-oxoglutarate/Fe(II)-dependent dioxygenases in plant metabolism. Front. Plant Sci. **5**: 1–15.

Flint-Garcia, S.A., Thuillet, A.-C., Yu, J., Pressoir, G., Romero, S.M., Mitchell, S.E., Doebley, J., Kresovich, S., Goodman, M.M., and Buckler, E.S. (2005). Maize association population: A high-resolution platform for quantitative trait locus dissection. Plant J. **44**: 1054–1064.

Frey, M., Chomet, P., Glawischnig, E., Stettner, C., Grün, S., Winklmair, A., Eisenreich, W., Bacher, A., Meeley, R.B., Briggs, S.P., Simcox, K., and Gierl, A. (1997). Analysis of a chemical plant defense mechanism in grasses. Science **277**: 696–699.

Frey, M., Huber, K., Park, W.J., Sicker, D., Lindberg, P., Meeley, R.B., Simmons, C.R., Yalpani, N., and Gierl, A. (2003). A 2-oxoglutarate-dependent dioxygenase is integrated in DIMBOA-biosynthesis. Phytochemistry **62**: 371–376.

Frey, M., Schullehner, K., Dick, R., Fiesselmann, A., and Gierl, A. (2009). Benzoxazinoid

biosynthesis, a model for evolution of secondary metabolic pathways in plants. Phytochemistry **70**: 1645–1651.

Frick, S. and Kutchan, T.M. (1999). Molecular cloning and functional expression of *O*-methyltransferases common to isoquinoline alkaloid and phenylpropanoid biosynthesis. Plant J. **17**: 329–339.

Ganal, M.W. et al. (2011). A large maize (*Zea mays* L.) SNP genotyping array: Development and germplasm genotyping, and genetic mapping to compare with the B73 reference genome. PLoS One **6**: e28334.

Gardiner, J.M., Coe, E.H., Melia-Hancock, S., Hoisington, D.A., and Chao, S. (1993). Development of a core RFLP map in maize using an immortalized F_2 population. Genetics **134**: 917–930.

Gauthier, A., Gulick, P.J., and Ibrahim, R.K. (1996). cDNA cloning and characterization of 3'/5'-*O*-methyltransferase for partially methylated flavonols from *Chrysosplenium americanum*. Plant Mol. Biol. **32**: 1163–1169.

Gierl, A. and Frey, M. (2001). Evolution of benzoxazinone biosynthesis and indole production in maize. Planta **213**: 493–498.

Glauser, G., Marti, G., Villard, N., Doyen, G.A., Wolfender, J.-L., Turlings, T.C.J., and Erb, M. (2011). Induction and detoxification of maize 1,4-benzoxazin-3-ones by insect herbivores. Plant J. **68**: 901–911.

Guo, B.Z., Zhang, Z.J., Li, R.G., Widstrom, N.W., Snook, M.E., Lynch, R.E., and Plaisted, D. (2001). Restriction fragment length polymorphism markers associated with silk maysin, antibiosis to corn earworm (Lepidoptera: Noctuidae) larvae, in a dent and sweet corn cross. J. Econ. Entomol. **94**: 564–71.

Hahlbrock, K. and Scheel, D. (1989). Physiology and molecular biology of phenylpropanoid metabolism. Annu. Rev. Plant Physiol. Plant Mol. Biol. **40**: 347–369.

Halkier, B.A. and Gershenzon, J. (2006). Biology and biochemistry of glucosinolates. Annu. Rev. Plant Biol. **57**: 303–333.

Hamberger, B. and Bak, S. (2013). Plant P450s as versatile drivers for evolution of species-specific chemical diversity. Philos. Trans. R. Soc. Lond. B. Biol. Sci. **368**: 20120426.

Han, X., Hyun, T., Zhang, M., Kumar, R., Koh, E. ji, Kang, B.H., Lucas, W., and Kim, J.Y. (2014). Auxin-Callose-Mediated Plasmodesmal Gating Is Essential for Tropic Auxin Gradient Formation and Signaling. Dev. Cell **28**: 132–146.

Hangasky, J.A., Taabazuing, C.Y., Valliere, M.A., and Knapp, M.J. (2013). Imposing function down a (cupin)-barrel: Secondary structure and metal stereochemistry in the αKG-dependent oxygenases. Metallomics **5**: 287–301.

Hansen, B.G., Kerwin, R.E., Ober, J.A., Lambrix, V.M., Mitchell-Olds, T., Gershenzon, J., Halkier, B.A., and Kliebenstein, D.J. (2008). A novel 2-oxoacid-dependent dioxygenase involved in the formation of the goiterogenic 2-hydroxybut-3-enyl glucosinolate and generalist insect resistance in Arabidopsis. Plant Physiol. **148**: 2096–2108.

Hashimoto, T. and Yamada, Y. (1987). Purification and characterization of hyoscyamine 6b-hydroxylase from root cultures of *Hyoscyamus niger* L. Eur. J. Biochem. **164**: 277–285.

Hegg, E.L. and Que, L. (1997). The 2-His-1-carboxylate facial triad - an emerging structural motif

in mononuclear non-heme iron(II) enzymes. Eur. J. Biochem. **250**: 625–629.

Hewitson, K.S., Granatino, N., Welford, R.W.D., McDonough, M.A, and Schofield, C.J. (2005). Oxidation by 2-oxoglutarate oxygenases: Non-haem iron systems in catalysis and signalling. Philos. Trans. A. Math. Phys. Eng. Sci. **363**: 807–828.

Hofman, J. and Masojídková, M. (1973). 1,4-Benzoxazine glucosides from *Zea mays*. Phytochemistry **12**: 207–208.

Houseman, J.G., Campos, F., Thie, N.M.R., Philogene, B.J.R., Atkinson, J., Morand, P., and Arnason, J.T. (1992). Effect of the maize-derived compounds DIMBOA and MBOA on growth and digestive processes of European corn-borer (Lepidoptera, Pyralidae). J. Econ. Entomol. **85**: 669–674.

Huffaker, A., Dafoe, N.J., and Schmelz, E.A. (2011). ZmPep1, an ortholog of Arabidopsis elicitor peptide 1, regulates maize innate immunity and enhances disease resistance. Plant Physiol. **155**: 1325–1338.

Hutton, J.J., Tappel Jr., A.L., and Udenfriend, S. (1967). Cofactor and substrate requirements of collagen proline hydroxylase. Arch. Biochem. Biophys. **118**: 231–240.

Ibrahim, R.K., De Luca, V., Khouri, H., Latchinian, L., Brisson, L., and Charest, P.M. (1987). Enzymology and compartmentation of polymethylated flavonol glycosides in *Chrysosplenium americanum*. Phytochemistry **26**: 1237–1245.

Ibrahim, R.K. (1997). Plant *O*-methyltransferase signatures. Trends Plant Sci. **2**: 249–250.

Ibrahim, R.K., Bruneau, A., and Bantignies, B. (1998). Plant *O*-methyltransferases: Molecular analysis, common signature and classification. Plant Mol. Biol. **36**: 1–10.

Irmisch, S., Clavijo McCormick, A., Boeckler, G.A., Schmidt, A., Reichelt, M., Schneider, B., Block, K., Schnitzler, J.-P., Gershenzon, J., Unsicker, S.B., and Kollner, T.G. (2013). Two herbivore-induced cytochrome P450 enzymes CYP79D6 and CYP79D7 catalyze the formation of volatile aldoximes involved in poplar defense. Plant Cell **25**: 4737–4754.

Isman, M.B. and Duffey, S.S. (1982). Toxicity of tomato phenolic compounds to the fruitworm, *Heliothis zea*. Entomol. Exp. Appl. **31**: 370–376.

Jayaraman, D., Gilroy, S., and Ané, J.-M. (2014). Staying in touch: Mechanical signals in plant–microbe interactions. Curr. Opin. Plant Biol. **20**: 104–109.

Jeworutzki, E., Roelfsema, M.R.G., Anschütz, U., Krol, E., Elzenga, J.T.M., Felix, G., Boller, T., Hedrich, R., and Becker, D. (2010). Early signaling through the Arabidopsis pattern recognition receptors FLS2 and EFR involves Ca^{2+}-associated opening of plasma membrane anion channels. Plant J. **62**: 367–378.

Jonczyk, R., Schmidt, H., Osterrieder, A., Fiesselmann, A., Schullehner, K., Haslbeck, M., Sicker, D., Hofmann, D., Yalpani, N., Simmons, C., Frey, M., and Gierl, A. (2008). Elucidation of the final reactions of DIMBOA-glucoside biosynthesis in maize: Characterization of *Bx*6 and *Bx*7. Plant Physiol. **146**: 1053–1063.

Kai, K., Mizutani, M., Kawamura, N., Yamamoto, R., Tamai, M., Yamaguchi, H., Sakata, K., and Shimizu, B.I. (2008). Scopoletin is biosynthesized via ortho-hydroxylation of feruloyl CoA by a 2-oxoglutarate-dependent dioxygenase in *Arabidopsis thaliana*. Plant J. **55**: 989–999.

Karban, R., Agrawal, A. a, and Mangel, M. (1997). The Benefits of induced defenses against herbivores. Ecology **78**: 1351–1355.

Kawai, Y., Ono, E., and Mizutani, M. (2014). Evolution and diversity of the 2-oxoglutarate-dependent dioxygenase superfamily in plants. Plant J. **78**: 328–343.

Kessler, A. and Baldwin, I.T. (2001). Defensive function of herbivore-induced plant volatile emissions in nature. Science **291**: 2141–2144.

Kliebenstein, D.J., Lambrix, V.M., Reichelt, M., Gershenzon, J., and Mitchell-Olds, T. (2001). Gene duplication in the diversification of secondary metabolism: Tandem 2-oxoglutarate-dependent dioxygenases control glucosinolate biosynthesis in Arabidopsis. Plant Cell **13**: 681–693.

Klun, J.A., Guthrie, W.D., Hallauer, AR, and Russell, W.A. (1970). Genetic nature of the concentration of 2,4-dihydroxy-7-methoxy-2H-1,4-benzoxazin-3(4H)-one and resistance to the European corn borer in a diallel set of eleven maize inbreds. Crop Sci **10**: 87–90.

Koch, B., Sibbesen, O., Halkier, B.A., Svendsen, I., and Møller, B.L. (1995). The primary sequence of cytochrome P-450$_{TYR}$, the multifunctional *N*-hydroxylase catalyzing the conversion of L-tyrosine to p-hydroxyphenylacetaldehyde oxime in the biosynthesis of the cyanogenic glucoside dhurrin in *Sorghum bicolor* (L.) Moench. J. Biol. Chem. **323**: 177–186.

Köhler, A., Maag, D., Veyrat, N., Glauser, G., Wolfender, J.-L., Turlings, T.C.J., and Erb, M. (2015). Within-plant distribution of 1,4-benzoxazin-3-ones contributes to herbivore niche differentiation in maize. Plant. Cell Environ. **38**: 1081–1093.

Koornneef, A. and Pieterse, C.M.J. (2008). Cross talk in defense signaling. Plant Physiol. **146**: 839–844.

Lam, K.C., Ibrahim, R.K., Behdad, B., and Dayanandan, S. (2007). Structure, function, and evolution of plant *O*-Methyltransferases. Genome **50**: 1001–1013.

LaPorte, D.C., Walsh, K., and Koshland, D.E. (1984). The branch point effect. J. Biol. Chem. **259**: 14068–14075.

Lawrence, S.D., Novak, N.G., Kayal, W. El, Ju, C.J.-T., and Cooke, J.E.K. (2012). Root herbivory: Molecular analysis of the maize transcriptome upon infestation by Southern corn rootworm, *Diabrotica undecimpunctata howardi*. Physiol. Plant. **144**: 303–319.

Lunter, G. and Goodson, M. (2011). Stampy: A statistical algorithm for sensitive and fast mapping of Illumina sequence reads. Genome Res. **21**: 936–939.

Maag, D., Dalvit, C., Thevenet, D., Köhler, A., Wouters, F.C., Vassão, D.G., Gershenzon, J., Wolfender, J.L., Turlings, T.C.J., Erb, M., and Glauser, G. (2014). 3-β-d-Glucopyranosyl-6-methoxy-2-benzoxazolinone (MBOA-N-Glc) is an insect detoxification product of maize 1,4-benzoxazin-3-ones. Phytochemistry **102**: 97–105.

Maffei, M.E., Arimura, G.-I., and Mithöfer, A. (2012). Natural elicitors, effectors and modulators of plant responses. Nat. Prod. Rep. **29**: 1288 –1303.

Makowska, B., Bakera, B., and Rakoczy-Trojanowska, M. (2015). The genetic background of benzoxazinoid biosynthesis in cereals. Acta Physiol. Plant. **37**: 176.

Marti, G., Erb, M., Boccard, J., Glauser, G., Doyen, G.R., Villard, N., Robert, C.A.M., Turlings, T.C.J., Rudaz, S., and Wolfender, J.-L. (2013). Metabolomics reveals herbivore-induced metabolites of resistance and susceptibility in maize leaves and roots. Plant, Cell Environ. **36**: 621–639.

Clavijo Mccormick, A., Irmisch, S., Reinecke, A., Boeckler, G.A., Veit, D., Reichelt, M., Hansson, B.S., Gershenzon, J., Köllner, T.G., and Unsicker, S.B. (2014). Herbivore-induced volatile

emission in black poplar: Regulation and role in attracting herbivore enemies. Plant, Cell Environ. **37**: 1909–1923.

McMullen, M.D. et al. (2009). Genetic properties of the maize nested association mapping population. Science **325**: 737–740.

Meihls, L.N., Kaur, H., and Jander, G. (2012). Natural variation in maize defense against insect herbivores. Cold Spring Harb. Symp. Quant. Biol. **77**: 269–283.

Mithöfer, A. and Boland, W. (2012). Plant defense against herbivores: Chemical aspects. Annu. Rev. Plant Biol. **63**: 431–450.

Mukanganyama, S., Figueroa, C.C., Hasler, J.A., and Niemeyer, H.M. (2003). Effects of DIMBOA on detoxification enzymes of the aphid *Rhopalosiphum padi* (Homoptera: Aphididae). J. Insect Physiol. **49**: 223–229.

Nafisi, M., Sønderby, I.E., Hansen, B.G., Geu-Flores, F., Nour-Eldin, H.H., Nørholm, M.H.H., Jensen, N.B., Li, J., and Halkier, B.A. (2006). Cytochromes P450 in the biosynthesis of glucosinolates and indole alkaloids. Phytochem. Rev. **5**: 331–346.

Nelson, D. and Werck-Reichhart, D. (2011). A P450-centric view of plant evolution. Plant J. **66**: 194–211.

Niemeyer, H.M. (2009). Hydroxamic acids derived from 2-hydroxy-2*H*-1,4-benzoxazin-3(4*H*)-one: Key defense chemicals of cereals. J. Agric. Food Chem. **57**: 1677–1696.

Normanly, J., Grisafi, P., Fink, G.R., and Bartel, B. (1997). Arabidopsis mutants resistant to the auxin effects of indole-3-acetonitrile are defective in the nitrilase encoded by the NIT1 gene. Plant Cell **9**: 1781–1790.

Novák, O., Hényková, E., Sairanen, I., Kowalczyk, M., Pospíšil, T., and Ljung, K. (2012). Tissue-specific profiling of the *Arabidopsis thaliana* auxin metabolome. Plant J. **72**: 523–536.

Oikawa, A., Ishihara, A., and Iwamura, H. (2002). Induction of HDMBOA-Glc accumulation and DIMBOA-Glc 4-*O*-methyltransferase by jasmonic acid in poaceous plants. Phytochemistry **61**: 331–337.

Oikawa, A., Ishihara, A., Tanaka, C., Mori, N., Tsuda, M., and Iwamura, H. (2004). Accumulation of HDMBOA-Glc is induced by biotic stresses prior to the release of MBOA in maize leaves. Phytochemistry **65**: 2995–3001.

Osbourn, A. (2010). Gene clusters for secondary metabolic pathways: An emerging theme in plant biology. Plant Physiol. **154**: 531–535.

Park, W.J., Kriechbaumer, V., Müller, A., Piotrowski, M., Meeley, R.B., Gierl, A., and Glawischnig, E. (2003). The nitrilase ZmNIT2 converts indole-3-acetonitrile to indole-3-acetic acid. Plant Physiol. **133**: 794–802.

Pechan, T., Ye, L., Chang, Y., Mitra, A., Lin, L., Davis, F.M., Williams, W.P., and Luthe, D.S. (2000). A unique 33-kD cysteine proteinase accumulates in response to larval feeding in maize genotypes resistant to fall armyworm and other lepidoptera. Plant Cell **12**: 1031–1041.

Pedras, M.S.C., Nycholat, C.M., Montaut, S., Xu, Y., and Khan, A.Q. (2002). Chemical defenses of crucifers: Elicitation and metabolism of phytoalexins and indole-3-acetonitrile in brown mustard and turnip. Phytochemistry **59**: 611–625.

Pfalz, M., Vogel, H., and Kroymann, J. (2009). The gene controlling the indole glucosinolate modifier1 quantitative trait locus alters indole glucosinolate structures and aphid resistance

in Arabidopsis. Plant Cell **21**: 985–999.

Pichersky, E. and Lewinsohn, E. (2011). Convergent evolution in plant specialized metabolism. Annu. Rev. Plant Biol. **62**: 549–566.

Potrykus, I. (1989). Gene transfer to cereals: An assessment[Review] . Trends Biotechnol. **7**: 269–272.

Preisig, C.L., Matthews, D.E., and VanEtten, H.D. (1989). Purification and characterization of a S-adenosyl-L-methionine:6a-hydroxymaackiain 3-*O*-methyltransferase from *Pisum sativum*. Plant Physiol. **91**: 559–66.

Preisser, E.L., Gibson, S.E., Adler, L.S., and Lewis, E.E. (2007). Underground herbivory and the costs of constitutive defense in tobacco. Acta Oecologica **31**: 210–215.

Rad, U. von, Hüttl, R., Lottspeich, F., Gierl, A., and Frey, M. (2001). Two glucosyltransferases are involved in detoxification of benzoxazinoids in maize. Plant J. **28**: 633–642.

Rasmann, S., Köllner, T.G., Degenhardt, J., Hiltpold, I., Toepfer, S., Kuhlmann, U., Gershenzon, J., and Turlings, T.C. (2005). Recruitment of entomopathogenic nematodes by insect-damaged maize roots. Nature **434**: 732–737.

Rector, B.G., Liang, G., and Guo, Y. (2003). Effect of Maysin on wild-type, deltamethrin-resistant, and Bt-resistant *Helicoverpa armigera* (Lepidoptera: Noctuidae). J. Econ. Entomol. **96**: 909–913.

Rivas, S. (2012). Nuclear dynamics during plant innate immunity. Plant Physiol. **158**: 87–94.

Sahi, S. V, Chilton, M.D., and Chilton, W.S. (1990). Corn metabolites affect growth and virulence of *Agrobacterium tumefaciens*. Proc. Natl. Acad. Sci. U. S. A. **87**: 3879–3883.

Sato, F., Hashimoto, T., Hachiya, A., Tamura, K., Choi, K.B., Morishige, T., Fujimoto, H., and Yamada, Y. (2001). Metabolic engineering of plant alkaloid biosynthesis. Proc. Natl. Acad. Sci. USA **98**: 367–372.

Schnable, P.S. et al. (2009). The B73 maize genome: Complexity, diversity, and dynamics. Science **326**: 1112–1115.

Sibbesen, O., Koch, B., Halkier, B.A., and Møller, B.L. (1995). Cytochrome P-450$_{TYR}$ is a multifunctional heme-thiolate enzyme catalyzing the conversion of L-tyrosine to p-hydroxyphenylacetaldehyde oxime in the biosynthesis of the cyanogenic glucoside Dhurrin in *Sorghum bicolor* (L.) Moench. J. Biol. Chem. **270**: 3506–3511.

Sicker, D. and Schulz, M. (2002). Benzoxazinones in plants: Occurrence synthetic access, and biological activity. Stud. Nat. Prod. Chem. **27**: 185–232.

Siqueira, J.O., Safir, G.R., and Nair, M.G. (1991). Stimulation of vesicular-arbuscular mycorrhiza formation and growth of white clover by flavonoid compounds. New Phytol. **118**: 87–93.

Smirnova, N.A., Hushpulian, D.M., Speer, R.E., Gaisina, I.N., Ratan, R.R., and Gazaryan, I.G. (2012). Catalytic mechanism and substrate specificity of HIF prolyl hydroxylases. Biochem. **77**: 1108–1119.

Snook, M.E., Gueldner, R.C., Widstrom, N.W., Wiseman, B.R., Himmelsbach, D.S., Harwood, J.S., and Costello, C.E. (1993). Levels of Maysin and Maysin analogues in silks of maize germplasm. J. Agric. Food Chem. **41**: 1481–1485.

Søltoft, M., Jørgensen, L.N., Svensmark, B., and Fomsgaard, I.S. (2008). Benzoxazinoid

concentrations show correlation with Fusarium head blight resistance in Danish wheat varieties. Biochem. Syst. Ecol. **36**: 245–259.

Somerville, C. and Somerville, S. (1999). Plant functional genomics. Science **285**: 380–383.

Songstad, D.D. (2010). Genetic Modification of Plants, Ch. 18: Maize. In Biotechnology in Agriculture and Forestry, pp. 349–367.

Strable, J. and Scanlon, M.J. (2009). Maize (*Zea mays*): A model organism for basic and applied research in plant biology. Cold Spring Harb. Protoc. **4**: 1–10.

Sugawara, S., Hishiyama, S., Jikumaru, Y., Hanada, A., Nishimura, T., Koshiba, T., Zhao, Y., Kamiya, Y., and Kasahara, H. (2009). Biochemical analyses of indole-3-acetaldoxime-dependent auxin biosynthesis in Arabidopsis. Proc. Natl. Acad. Sci. U. S. A. **106**: 5430–5435.

Tamayo, M.C., Rufat, M., Bravo, J.M., and San Segundo, B. (2000). Accumulation of a maize proteinase inhibitor in response to wounding and insect feeding, and characterization of its activity toward digestive proteinases of *Spodoptera littoralis* larvae. Planta **211**: 62–71.

Tena, G., Boudsocq, M., and Sheen, J. (2011). Protein kinase signaling networks in plant innate immunity. Curr. Opin. Plant Biol. **14**: 519–529.

Tian, F., Stevens, N.M., and Buckler, E.S. (2009). Tracking footprints of maize domestication and evidence for a massive selective sweep on chromosome 10. Proc. Natl. Acad. Sci. U. S. A. **106 Suppl**: 9979–86.

Tiffin, P. and Gaut, B.S. (2001). Molecular Evolution of the Wound-Induced Serine Protease Inhibitor *wip1* in Zea and Related Genera. Mol. Biol. Evol. **18**: 2092–2101.

Vidgren, J., Svensson, L.A., and Liljas, A. (1994). Crystal structure of catechol *O*-methyltransferase. Nature **368**: 354–57.

Vigani, G., Morandini, P., and Murgia, I. (2013). Searching iron sensors in plants by exploring the link among 2'-OG-dependent dioxygenases, the iron deficiency response and metabolic adjustments occurring under iron deficiency. Front. Plant Sci. **4**: 169.

Voigtländer, H. and Balsam, G. (1970). Apigenin-5-methyläther, ein neues Flavon aus *Thevetia peruviana*. Arch Pharm Ber Dtsch Pharm Ges **303**: 782–7.

Wasternack, C. and Hause, B. (2013). Jasmonates: An update on biosynthesis, signal transduction and action in plant stress response, growth and development. Ann Bot. **111**: 1021–1058.

Wei, F. et al. (2009). The physical and genetic framework of the maize B73 genome. PLoS Genet. **5**: e1000715.

Weinhold, A. and Baldwin, I.T. (2011). Trichome-derived *O*-acyl sugars are a first meal for caterpillars that tags them for predation. Proc. Natl. Acad. Sci. U. S. A. **108**: 7855–7859.

Werck-Reichhart, D. and Feyereisen, R. (2000). Cytochromes P450: A success story. Genome Biol. **1**: reviews3003.1–3003.9.

Widstrom, N.W., Butron, A., Guo, B.Z., Wilson, D.M., Snook, M.E., Cleveland, T.E., and Lynch, R.E. (2003). Control of preharvest aflatoxin contamination in maize by pyramiding QTL involved in resistance to ear-feeding insects and invasion by *Aspergillus* spp. Eur. J. Agron. **19**: 563–572.

Winkel-Shirley, B. (2002). Biosynthesis of flavonoids and effects of stress biosynthesis of flavonoids and effects of stress. Curr. Opin. Plant Biol. **5**: 218–223.

Wright, S.I., Bi, I.V., Schroeder, S.G., Yamasaki, M., Doebley, J.F., McMullen, M.D., and Gaut,

B.S. (2005). The effects of artificial selection on the maize genome. Science **308**: 1312–1314.

Xu, L., Liu, F., Lechner, E., Genschik, P., Crosby, W.L., Ma, H., Peng, W., Huang, D., and Xie, D. (2002). The SCF(COI1) ubiquitin-ligase complexes are required for jasmonate response in Arabidopsis. Plant Cell **14**: 1919–1935.

Yu, J., Holland, J.B., McMullen, M.D., and Buckler, E.S. (2008). Genetic design and statistical power of nested association mapping in maize. Genetics **178**: 539–551.

Zhang, L., Peek, A.S., Dunams, D., and Gaut, B.S. (2002). Population Genetics of Duplicate Disease-Defense Genes, hm1 and hm2, in Maize (*Zea mays* ssp. *mays* L.) and Its Wild Ancestor (*Zea mays* ssp. *parviglumis*). Genetics **162**: 851–860.

Zheng, L., McMullen, M.D., Bauer, E., Schön, C.C., Gierl, A., and Frey, M. (2015). Prolonged expression of the BX1 signature enzyme is associated with a recombination hotspot in the benzoxazinoid gene cluster in *Zea mays*. J. Exp. Bot. **66**: 3917–3930.

Zhou, S. et al. (2009). A single molecule scaffold for the maize genome. PLoS Genet. **5**: e1000711.

Zubieta, C., He, X.Z., Dixon, R.A., and Noel, J.P. (2001). Structures of two natural product methyltransferases reveal the basis for substrate specificity in plant *O*-methyltransferases. Nat. Struct. Biol. **8**: 271–279.

8 Danksagung

Viele haben zum Gelingen dieser Arbeit beigetragen. Ich möchte mich dafür an dieser Stelle herzlich bedanken. Ich habe sehr vom intensiven Austausch, dem Enthusiasmus, der Energie und der Unterstützung der Beteiligten profitiert.

Ich möchte mich allen voran bei Dr. Tobias G. Köllner bedanken, der mich in all den Jahren betreut, unterrichtet, mich in Zeiten des Misserfolgs bestärkt, mich gefordert und aber vor allem gefördert hat. Mir hat es Freude bereitet gemeinsam nachzudenken, um Schritt für Schritt der Lösung näher zu kommen.

Prof. Dr. Jonathan Gershenzon möchte ich für seinen Rat, seine umfangreiche Hilfe, sein immerwährendes Interesse und seine Begeisterung an meiner Arbeit danken.

Ebenso danke ich Prof. Dr. Matthias Erb, Dr. Christelle A. M. Robert und Prof. Dr. Georg Jander, die die gemeinsamen Projekte mit ermöglicht und vorangetrieben haben, die ich stets um Rat fragen konnte, und die mir bereitwillig geholfen haben.

Vielen Dank der *Kuchen Gruppe* für die vielen süßen Speisen, das schöne Beisammensein und das gute Miteinander. Der gesamten Abteilung *Gershenzon* danke ich für ihre Unterstützung, durch die so manches so viel einfacher war.

Ich bedanke mich bei den Gutachtern für die Beurteilung der Arbeit.

Dank gilt meinen Eltern, meinen Geschwistern und ihren Familien, die mich begleitet und die mich jederzeit unterstützt haben.

Ich bin froh und dankbar, dass ich die Aufs und Abs mit meinen Freunden Teilen konnte.

Ich danke Dir liebe Anke für Deine Unterstützung in kleinen und großen Dingen, Dein Zureden, Aufbauen, das Teilen von Kummer, das Feiern von Erfolgen und Dein großes Zutrauen in mich.
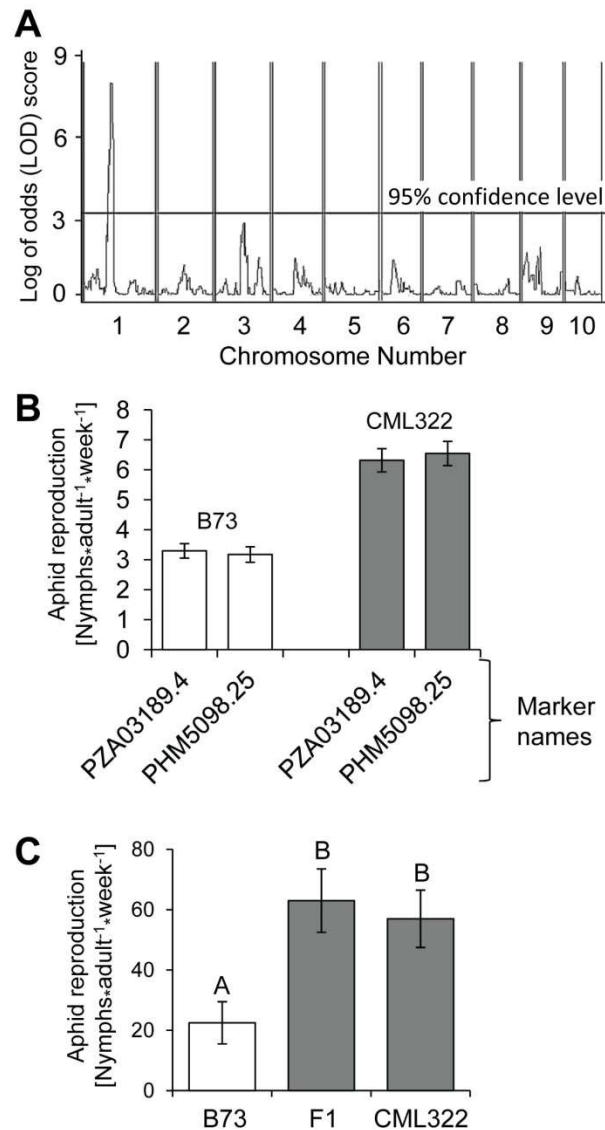
9 Supplemental Material

9.1 Supplemental Material Manuscript I

Natural Variation in Maize Aphid Resistance is Associated with 2,4-Dihydroxy-7-Methoxy-1,4-Benzoxazin-3-One Glucoside Methyltransferase Activity°

Supplemental Figure 1. Aphid susceptibility is caused by a dominant allele on CML322 chromosome 1. (A) Location of QTL for aphid progeny production. (B) Aphid reproduction on B73 x CML322 recombinant inbred lines. Lines that are homozygous for B73 or CML322 alleles, respectively, at molecular markers flanking the QTL shown in panel A are grouped together (Mean ± s.e.; n = 68 for B73, n = 61 for CML322). (C) Number of progeny produced by 10 aphids over 7 days on B73, CML322, and F1 progeny from a cross (Mean ± s.e.; n = 10). Different letters indicate significant differences between lines (*$P < 0.05$; Tukey's HSD).
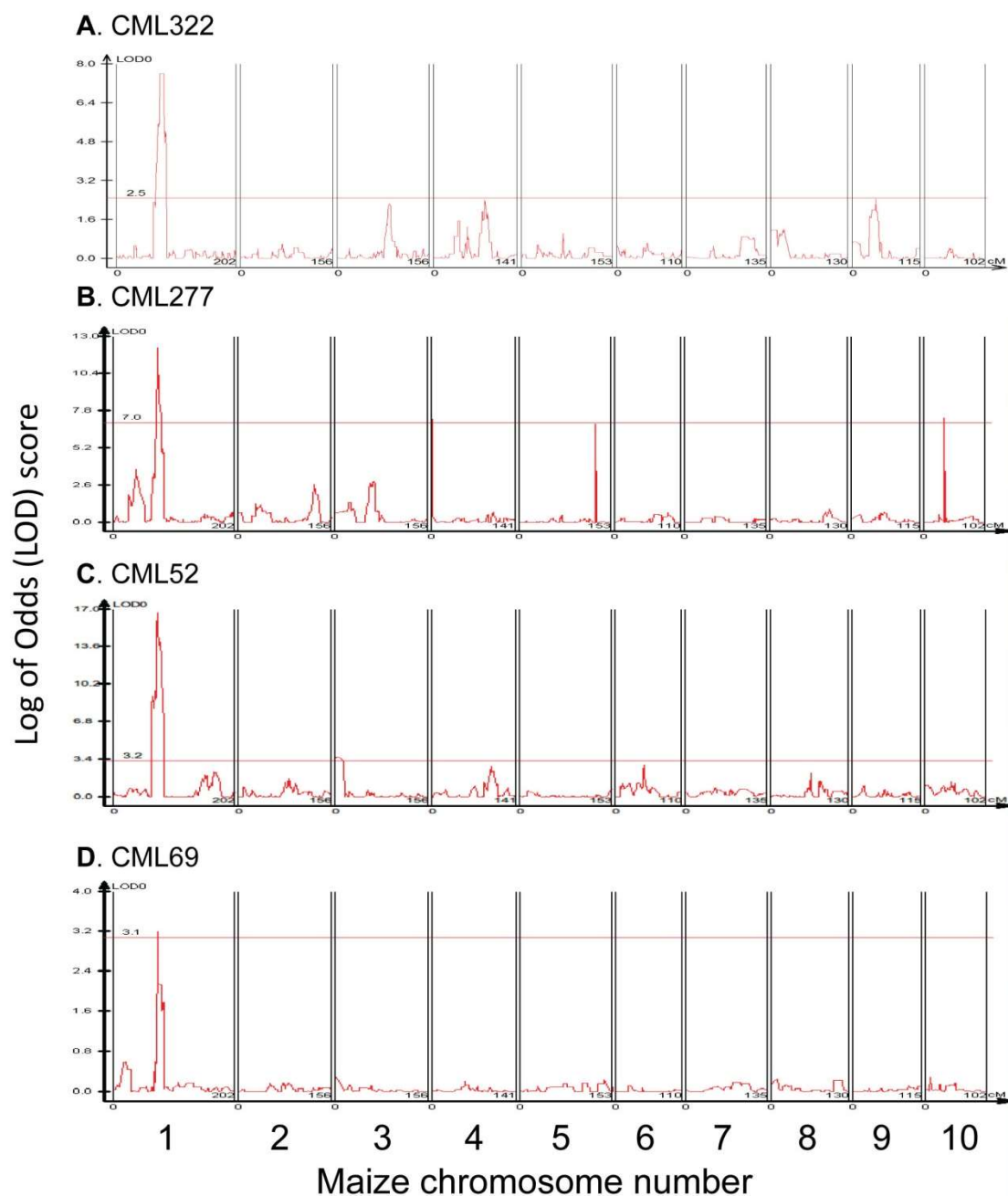
Supplemental Figure 2. Maize chromosome LOD plots showing location of aphid resistance QTL. (A-D) B73 x CML322, B73 x CML277, B73 x CML52, and B73 x CML52 recombinant inbred lines. Horizontal lines within in the figures show the 95% confidence level.
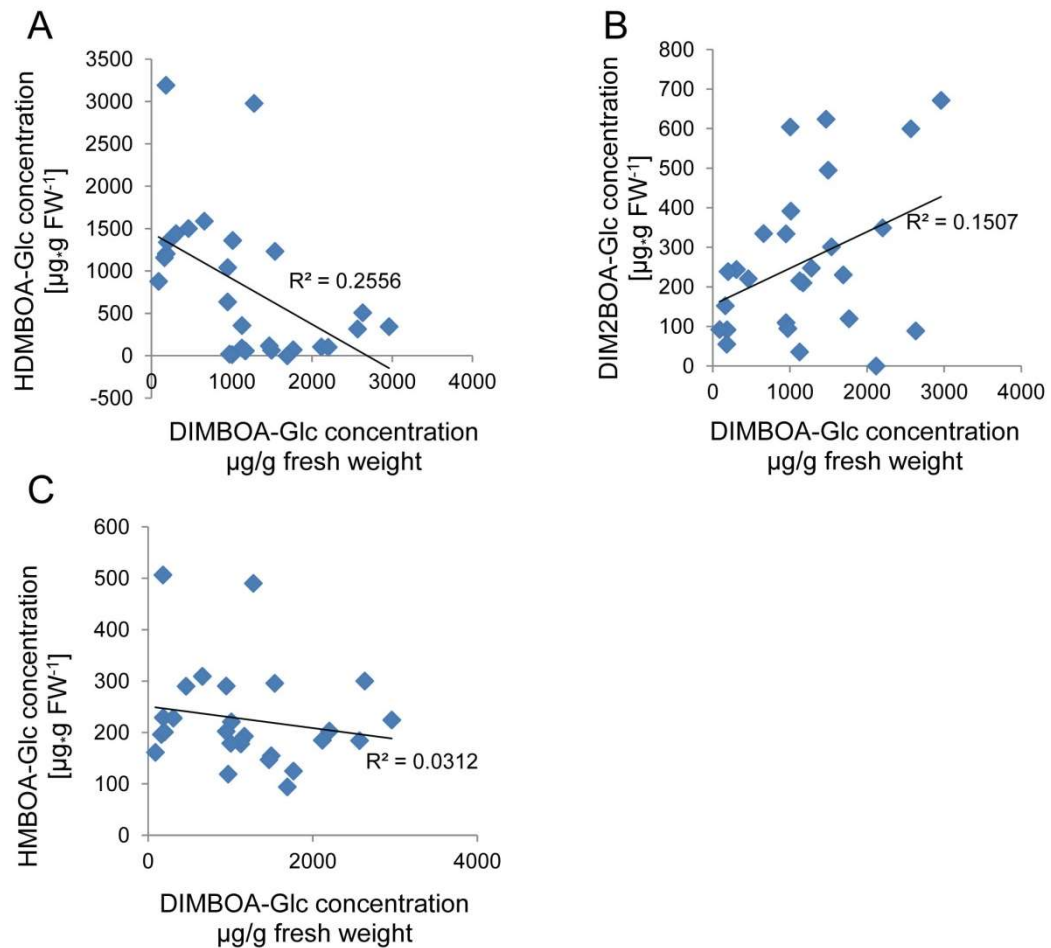
Supplemental Figure 3. Correlation of DIMBOA-Glc content with other benzoxazinoids in parental lines of the NAM population. (A) DIMBOA-Glc concentrations were compared to HDMBOA-Glc ($r = -0.51$; $P < 0.01$, Student's t-distribution). (B) DIMBOA-Glc concentrations were compared to DIM2BOA-Glc ($r = 0.39$; $P < 0.05$, Student's t-distribution). (C) DIMBOA-Glc concentrations were compared to HMBOA-Glc ($r = 0.18$; $P > 0.05$, Student's t-distribution). Data for the correlation analyses are from Figure 2.
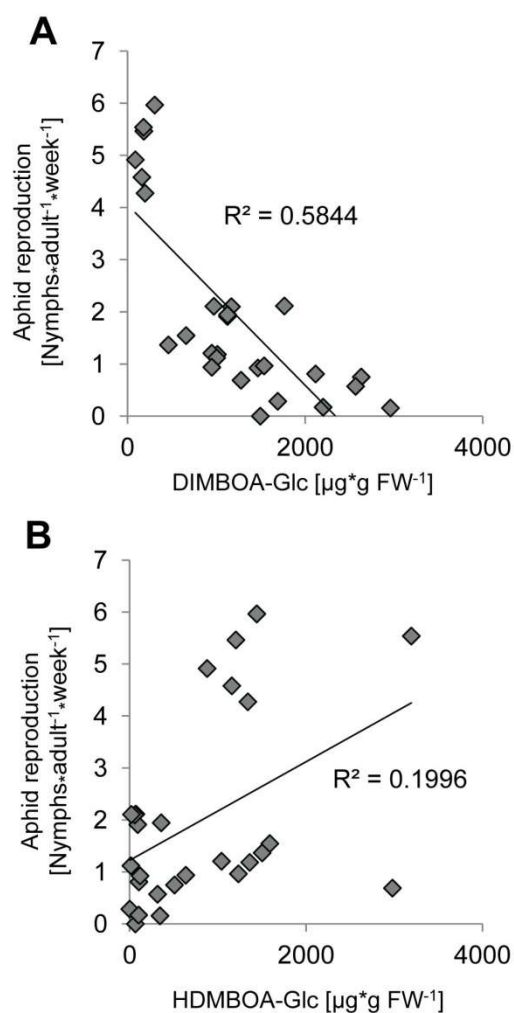
Supplemental Figure 4. Correlation of aphid resistance and benzoxazinoid content of maize leaves (A) Correlation between DIMBOA-Glc and aphid reproduction on parental lines of the maize NAM population. (r = 0.76; *P* < 0.001, Student's t-distribution). (B) Correlation between HDMBOA-Glc content and aphid reproduction on parental lines of the maize NAM population. Data points represent means from datasets depicted in Figure 2. (r = 0.45; *P* < 0.05, Student's t-distribution)
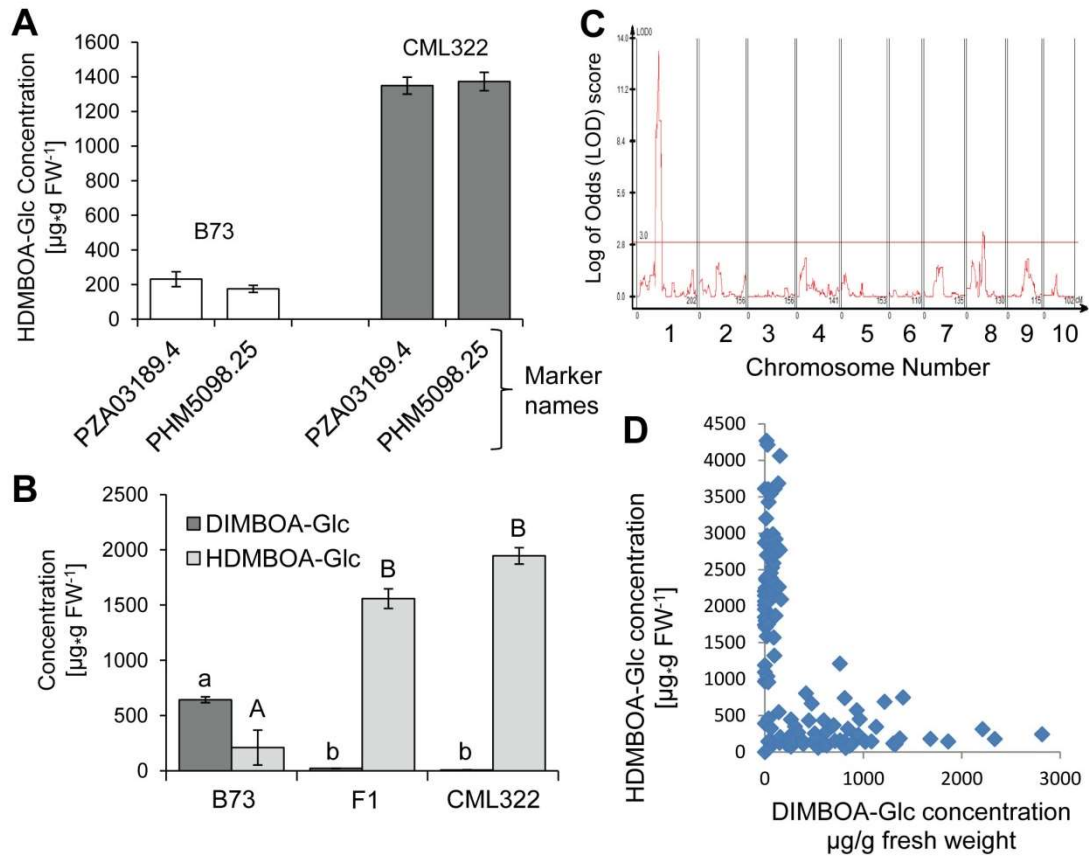
Supplemental Figure 5. High HDMBOA-Glc accumulation is caused by a dominant allele on CML322 chromosome 1. (A) HDMBOA-Glc content in B73 x CML322 RILs. Lines that are homozygous for B73 or CML322 alleles, respectively, at molecular markers flanking the QTL shown in panel A are grouped together (Mean ± s.e.; n = 68 for B73, n = 61 for CML322). (B) Constitutive DIMBOA-Glc and HDMBOA-Glc concentrations of B73, CML322, and B73 x CML322 F1 progeny. (Mean ± s.e.; n = 9). Different letters indicate significant differences between lines (*P < 0.05; Tukey's HSD). (C) LOD plot showing the location of QTL for DIMBOA-Glc content in the maize genome. The 95% significance level is shown as a horizontal line. (D) Comparison of DIMBOA-Glc and HDMBOA-Glc content in 128 B73 x CML322 recombinant inbred lines.

Supplemental data. Meihls et al. (2013). Plant Cell 10.1105/tpc.113.112409
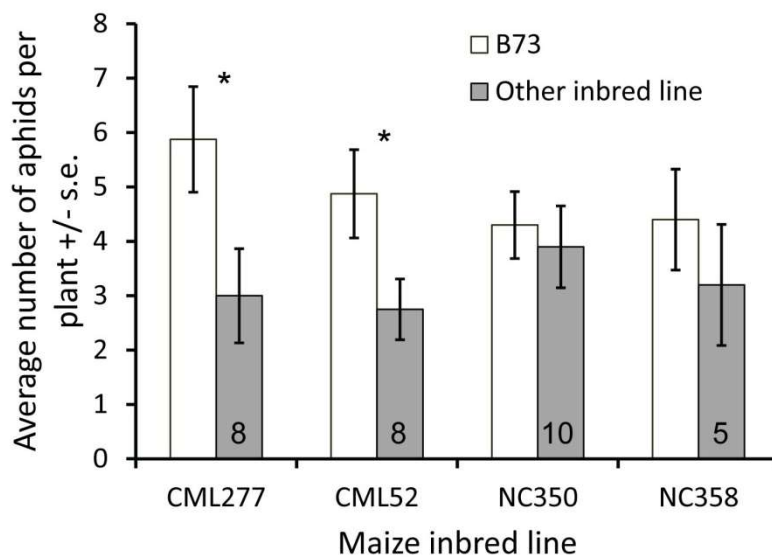
Supplemental Figure 6. Aphid choice experiments, comparing B73 to more susceptible inbred lines. Ten adult aphids were place between two two-week-old maize plants. After 24 hours the number of aphids on each plant was counted. Mean +/- s.e.; numbers in bars indicate the number of replicates for each experiment; *P < 0.05, two-tailed *t*-test.

Supplemental data. Meihls et al. (2013). Plant Cell 10.1105/tpc.113.112409

Supplemental Table 1. Predicted B73 genes in the area of the bin 1.04 R. maidis resistance QTL, mapped with four sets of recombinant inbred lines: B73 x CML322, B73 x CML277, B73 x CML52 and B73 x CML69. DIMBOA-Glc methyltransferase genes *Bx10a* (GRMZM2G311036), *Bx10b* (GRMZM2G336824), and *Bx10c* (GRMZM2G023325) are marked in red.

| Gene ID	Description	Start of gene (base pairs on chromosome 1)
GRMZM2G107196_T03	Protein kinase isozyme 4 n=5 (Andropogoneae) Exp=0; maizesequence.org: Uniprot/S	64,004,698
GRMZM2G084407_T01	Cytochrome P450 CYP709H1 n=2 (Andropogoneae) Exp=0; maizesequence.org: Uniprot/S	64,148,065
GRMZM2G147698_T01	Myb-related protein Hv33 n=2 (Zea mays) Exp=4e-170; maizesequence.org: Uniprot/S	64,237,900
GRMZM2G063498_T01	Low temperature viability protein n=1 (Zea mays) Exp=0	64,540,771
GRMZM2G015902_T01	Hepatocellular carcinoma-associated antigen 59 family protein n=2 (Andropogoneae	64,598,032
GRMZM2G001361_T01	Ortholog; UniRef90: Q6ZFN3_ORYSJ (Rice Genome Annotation Project) CSLE2 - cellul	64,672,346
GRMZM2G301271_T01	Cationic amino acid transporter n=1 (Zea mays) Exp=0; maizesequence.org: Uniprot	64,719,329
GRMZM2G127138_T01	Cationic amino acid transporter n=2 (Andropogoneae) Exp=1e-173; maizesequence.or	64,964,613
GRMZM2G127150_T01	Cationic amino acid transporter n=2 (Andropogoneae) Exp=0; maizesequence.org: Un	64,969,310
GRMZM2G075153_T01	Cystathionine gamma-synthase n=2 (Zea mays) Exp=2e-99; maizesequence.org: UniGen	65,036,541
GRMZM2G042683_T01	Ribonucleoprotein A n=3 (Andropogoneae) Exp=3e-99; maizesequence.org: Uniprot/SP	65,086,182
GRMZM2G097426_T01	Q75M66_ORYSJ Os03g0381200 protein n=4 (Poaceae) Exp=1e-88; maizesequence.org: U	65,618,360
GRMZM2G097426_T02	Q75M66_ORYSJ Os03g0381200 protein n=4 (Poaceae) Exp=1e-88; maizesequence.org: U	65,618,602
GRMZM2G097426_T03	Q75M66_ORYSJ Os03g0381200 protein n=4 (Poaceae) Exp=1e-53; maizesequence.org: G	65,618,602
GRMZM2G350312_T01	Amelogenin like protein n=2 (Zea mays) Exp=1e-146; maizesequence.org: Uniprot/SP	65,657,063
GRMZM2G051836_T01	Ribosomal protein S9-2 n=1 (Arabidopsis thaliana) Exp=1e-36; maizesequence.org:	65,679,752
GRMZM2G100452_T01	Aldose 1-epimerase n=1 (Zea mays) Exp=0; maizesequence.org: Uniprot/SPTREMBL:B6T	65,729,353
GRMZM2G100497_T01	Pseudouridylate synthase n=2 (Zea mays) Exp=0; maizesequence.org: Uniprot/SPTREM	65,731,126
GRMZM2G004298_T01	Rhicadhesin receptor n=6 (Zea mays) Exp=5e-110; maizesequence.org: Uniprot/SPTRE	65,994,545
GRMZM2G311036_T01	O-methyltransferase ZRP4 n=3 (Zea mays) Exp=0; maizesequence.org: Uniprot/SPTREM	66,304,872
GRMZM2G336824_T01	O-methyltransferase ZRP4 n=3 (Zea mays) Exp=0; maizesequence.org: Uniprot/SPTREM	66,387,644
GRMZM2G023325_T01	O-methyltransferase ZRP4 n=3 (Zea mays) Exp=1e-97; maizesequence.org: UniGene:Zm	66,500,692
GRMZM2G113139_T01	Domain containing protein expressed n=3 (Oryza sativa) Exp=1e-175; maizesequence	66,575,918
GRMZM2G003138_T01	Acyltransferase n=3 (Zea mays) Exp=0; maizesequence.org: GO:0016020; membrane		66,670,982
GRMZM2G152925_T01	Cytochrome c oxidase subunit n=4 (Zea mays) Exp=4e-70; maizesequence.org: Unipro	66,948,065
GRMZM2G120069_T01	LOL3 n=2 (Andropogoneae) Exp=0; maizesequence.org: Uniprot/SPTREMBL:B6UDT2; LOL	67,055,552
GRMZM2G120079_T01	LOL3 n=2 (Zea mays) Exp=0; maizesequence.org: Uniprot/SPTREMBL:C0HFB8; Putative	67,077,443
GRMZM2G125314_T01	LOL3 n=1 (Zea mays) Exp=0; maizesequence.org: Uniprot/SPTREMBL:B6SUK0; LOL3	Un	67,128,996
GRMZM2G104353_T01	Splicing factor arginine/serine-rich 2 n=1 (Zea mays) Exp=1e-86; maizesequence.o	67,248,423
GRMZM2G051879_T01	A8MRL0_ARATH Histone H3 n=3 (Embryophyta) Exp=3e-71; maizesequence.org: Uniprot/	67,644,786
GRMZM2G056151_T01	Putative RING-H2 zinc finger protein n=1 (Oryza sativa subsp. japonica) Exp=1e-4	67,648,529

Supplemental Table 2. Primers used in this study.

Name	Sequence (5' – 3')	Function
OMT1fwd	ATGGTAGGTCTCAGCGCATGGCCCTCAT GCAGGAGAGTA	Cloning of *Bx10a* into pASK-IBA37plus
OMT1rev	ATGGTAGGTCTCATATCAAGGATAGACCT CGATGATGACCG	
OMT2fwd	ATGGTAGGTCTCAGCGCATGGCACTCAT CATGCAGGAGAG	Cloning of *Bx10b* into pASK-IBA37plus
OMT2rev	ATGGTAGGTCTCATATCAAGGATAGACCT CGATGATGACTG	
OMT3fwd	ATGGTAGGTCTCAGCGCATGGCACTCAT GCAAGAGAGCAG	Cloning of *Bx10c* into pASK-IBA37plus
OMT3rev	ATGGTAGGTCTCATATCAAGGATAGACCT CGATGATGACCG	
OMT3-UTRfwd	TATACGTTGGCACGCACGAATAC	Amplification of *Bx10c*
OMT3-UTRrev	AATTAGGCGCCCTTTATTATTCAC	
TPA1	AGCACGGCAACAACCTTGG	Transposon analysis
TPA2	CGCGGTGGTGAGAACCGTTT	
TPA3	AAGTGCACGTTGCCATCAGATGGAG	
Actinfwd	CCATGAGGCCACGTACAACT	qRT-PCR of *actin*
Actinrev	GGTAAAACCCCACTGAGGA	
Bx10a,bfwd	CAGCAGGTGGTGGTGATAAT	qRT-PCR of *Bx10a* and *Bx10b*
Bx10a,brev	AGCGCCAGACTCACAAAGG	
Bx10cfwd	GCCCACCCAAGTAAGCTTCG	qRT-PCR of *Bx10c*
Bx10crev	AGAGACAGCGATAGGATGGA	

9.2 Supplemental Material Manuscript II

The maize cytochrome P450 CYP79A61 produces
phenylacetaldoxime and indole-3-acetaldoxime in heterologous
systems and might contribute to plant defense and auxin formation
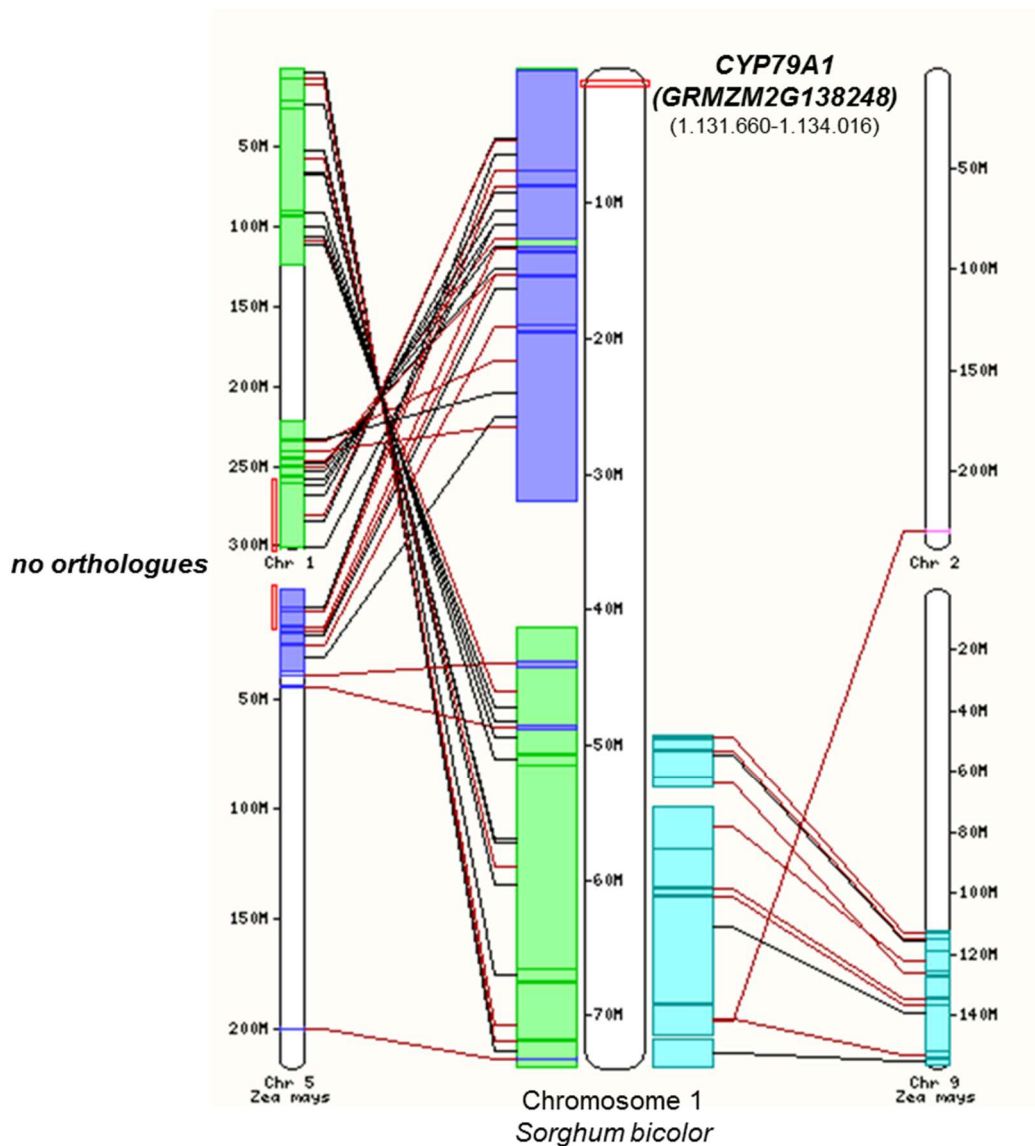
Supplemental Figure 1. Comparative genomic analysis of *Sorghum bicolor* chromosome 1 with maize chromosomes 1, 2, 5, and 9. The analysis was done using the web server http://www.plants.ensembl.org.
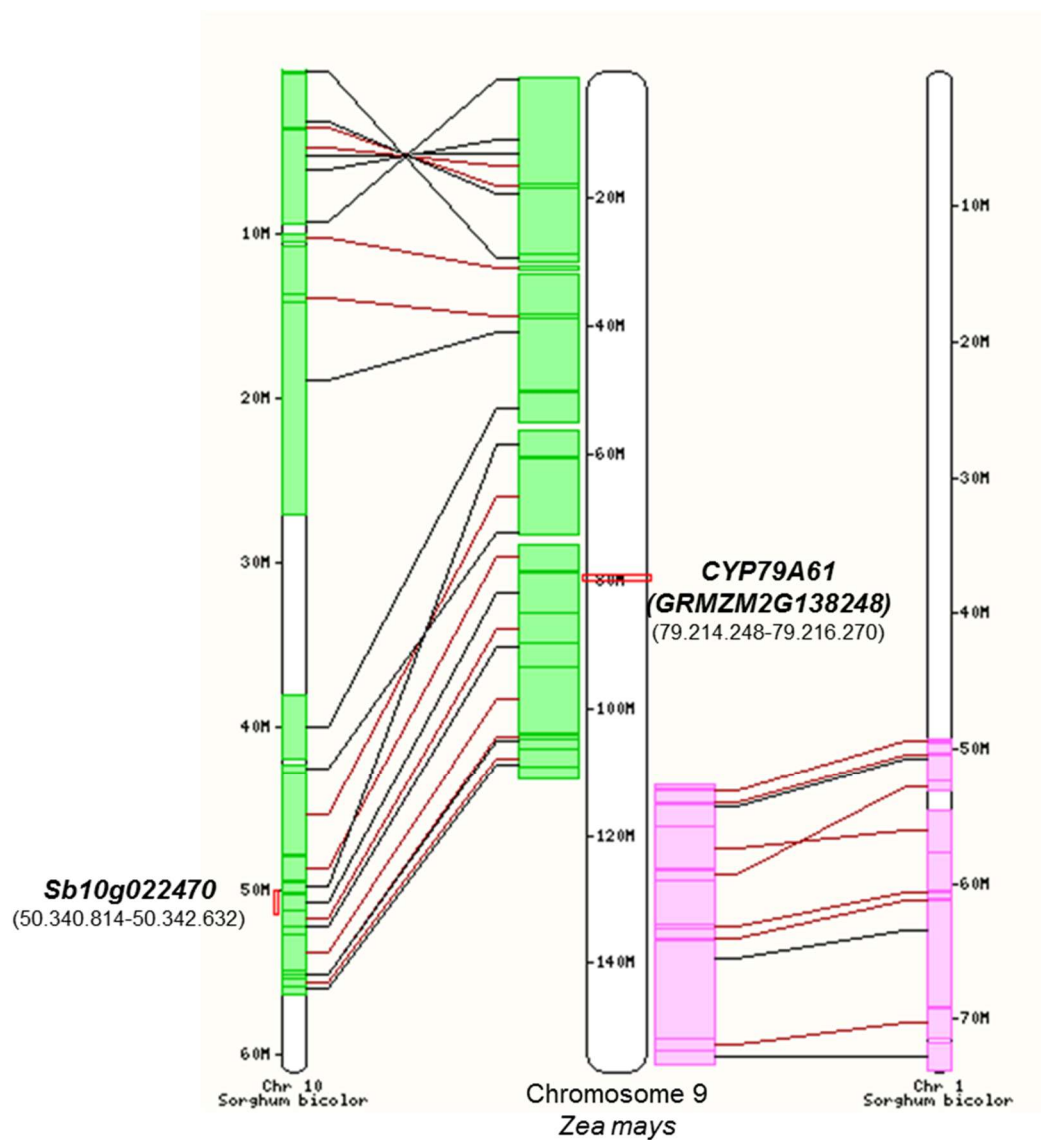
Supplemental Figure 2. Comparative genomic analysis of *Zea mays* chromosome 9 with *Sorghum bicolor* chromosomes 1 and 10. The analysis was done using the web server http://www.plants.ensembl.org.
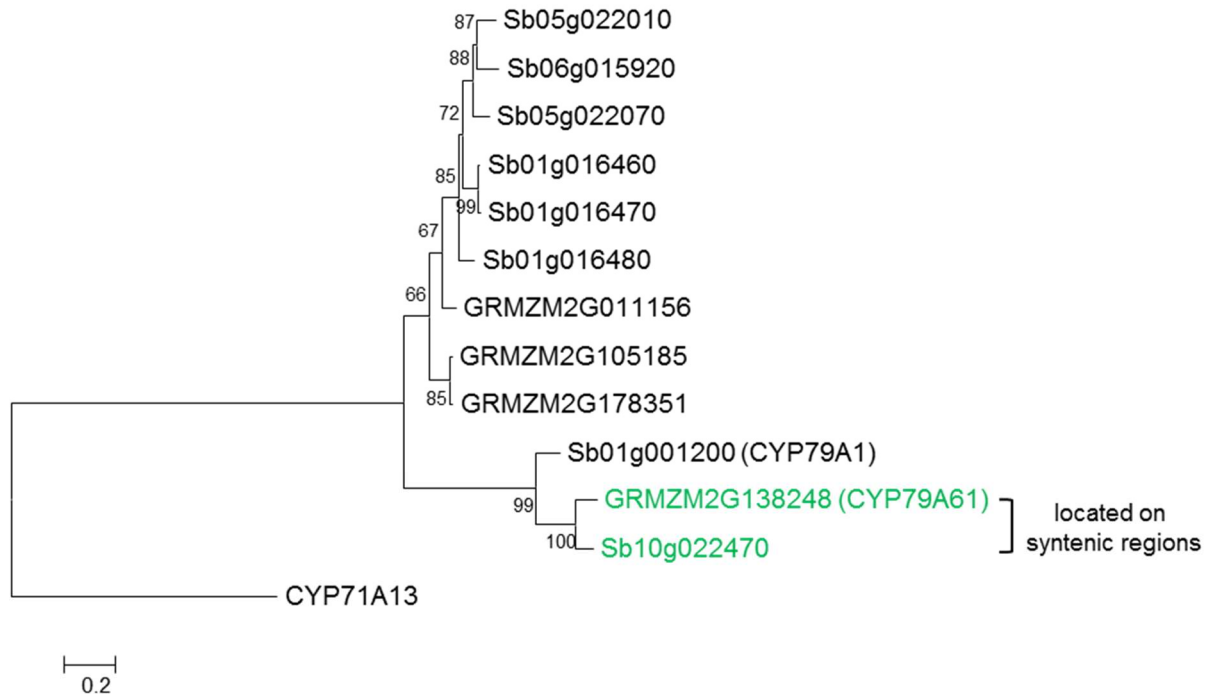
Supplemental Figure 3. Phylogenetic tree of CYP79 sequences from maize and *Sorghum bicolor*. The rooted tree was inferred with the neighbor-joining method and n = 1000 replicates for bootstrapping. Bootstrap values are shown next to each node. As an outgroup, CYP71A13 from *Arabidopsis thaliana* was chosen.
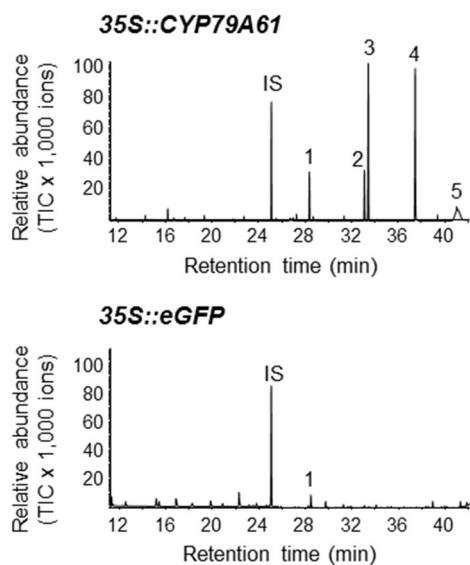
1, 5-*epi*-aristolochene; 2, 2-phenylethanol; 3, benzyl cyanide; 4, 2-phenylnitroethane; 5, phenylacetaldoxime; IS, internal standard

Supplemental Figure 4. Volatiles released from transgenic *Nicotiana benthamiana* plants transiently overexpressing either a *35S::eGFP* construct or a *35S::CYP79A61* construct. Volatiles were collected three days after *Agrobacterium tumefaciens* infiltration and analyzed using GC-MS. 1, 5-epi-aristolochene; 2, 2-phenylethanol; 3, benzyl cyanide; 4, 2-phenylnitroethane; 5, phenylacetaldoxime; IS, internal standard.
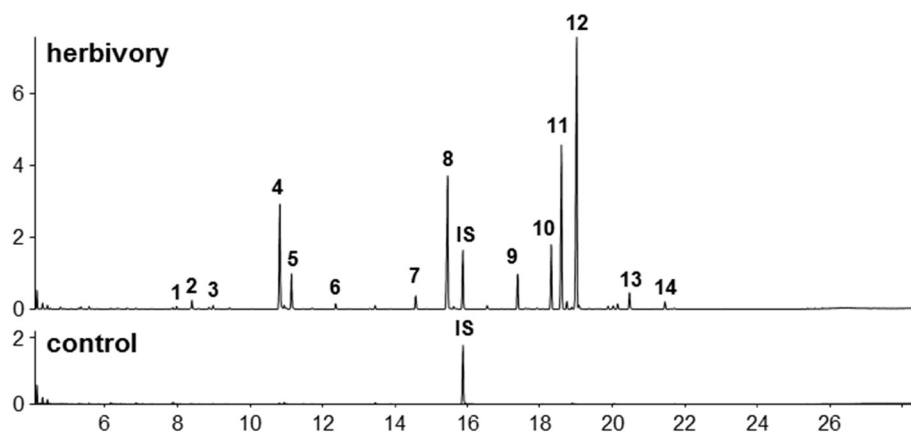
Supplemental Figure 5. Volatiles released from undamaged 10 day-old *Zea mays* (cultivar Delprim) seedlings (control) and seedlings treated with caterpillar oral secretion (herbivory). Volatiles were collected and analyzed using GC-MS. 1, β-myrcene; 2, 3-hexen-1-ol acetate; 3, limonene; 4, linalool; 5, (*E*)-4,8-dimethyl-1,3,7-nonatriene; 6, phenylmethyl acetate; 7, 2-phenylethyl acetate; 8, indole; 9, geranyl acetate; 10, (*E*)-β-caryophyllene; 11, (*E*)-α-bergamotene; 12, (*E*)-β-farnesene; 13, β-sesquiphellandrene; 14, 4,8,12-trimethyltrideca-1,3,7,11-tetraene; IS, internal standard.
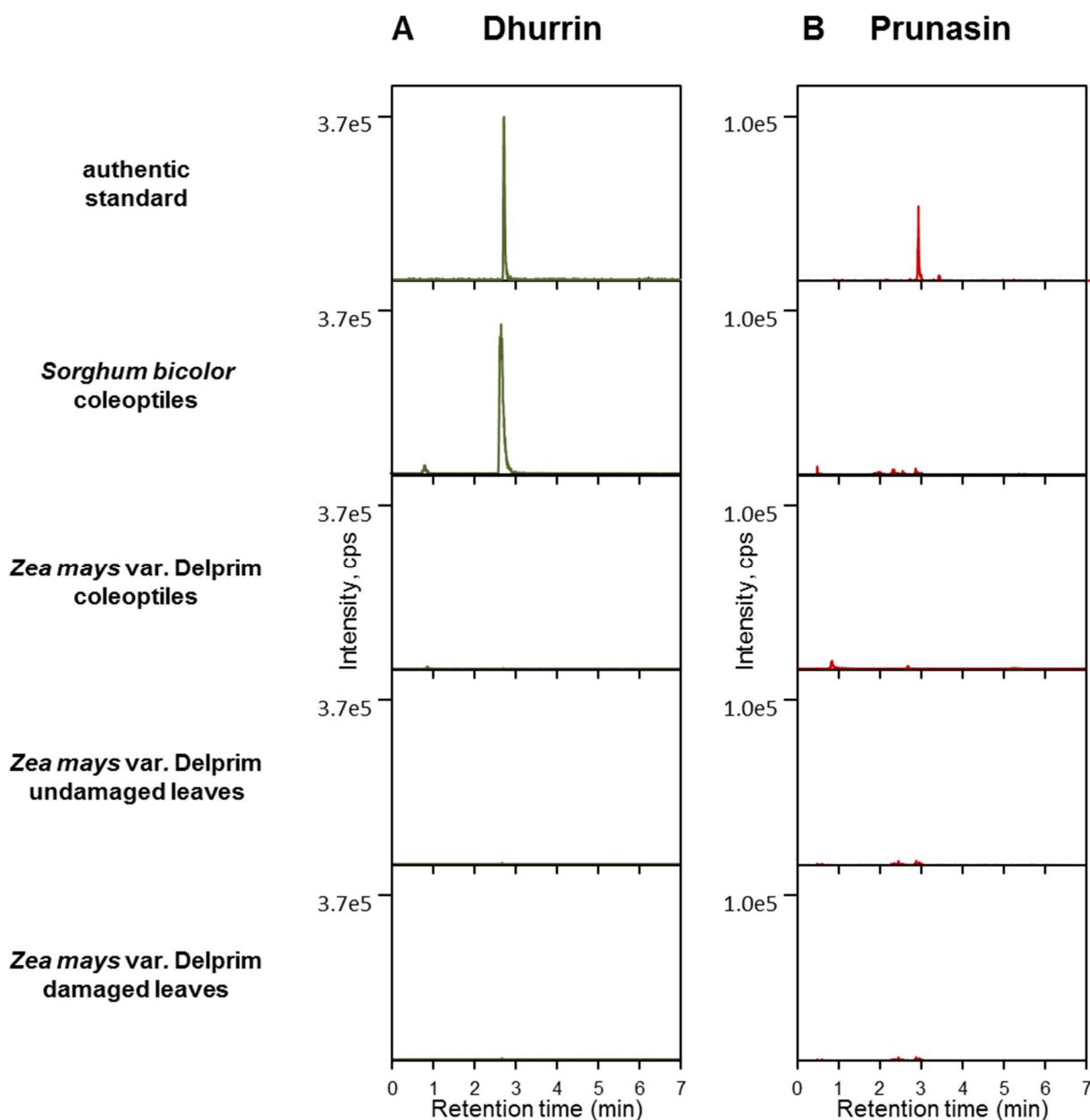
Supplemental Figure 6. Accumulation of cyanogenic glycosides in maize and sorghum. Maize and sorghum coleoptiles were harvested three days after germination. Undamaged maize leaves and caterpillar oral secretion-treated maize leaves were obtained as described in the Methods section. Glycosylated compounds were extracted with methanol and cyanogenic glycosides were analyzed using LC-MS/MS with multiple reaction monitoring (MRM). MRMs for dhurrin, prunasin, and amygdalin were established using authentic standards obtained from SIGMA-Aldrich (http://www.sigmaaldrich.com) (dhurrin) or prepared from bitter almonds (prunasin, amygdalin) and MRMs for lotaustralin and linamarin were calculated from those of dhurrin and prunasin. Amygdalin, lotaustralin and linamarin could not be detected in maize and sorghum (data not shown).

Supplemental Table 1. Oligonucleotides used in this study.

	primer	purpose
138248_fwd	ATGGTTTCCTCTCCGCAAGCA	GRMZM2G138248 cloning
138248_rev	CTACTTACAAAGCAAGATCCCG	GRMZM2G138248 cloning
Del-CYP79-USER-fwd	GGCTTAAUATGGTTTCCTCTCCGCAAGCAA	pCAMBiA
Del-CYP79-USER-rev	GGTTTAAUCTACTTACAAAGCAAGATCCCGG	pCAMBiA
CYP79-NotI fwd	AAGCGGCCGCAATGGTTTCCTCTCCGCAAGCAAAT	pESC-Leu2d
CYP79-BglII rev	TTAGATCTCTACTTACAAAGCAAGATCCCGG	pESC-Leu2d
HG-LUG fwd	TCCAGTGCTACAGGGAAGGT	qRT-PCR
HG-LUG rev	GTTAGTTCTTGAGCCCACGC	qRT-PCR
CYP79-QRT1	TACTGCGGGAATGTCGTC	qRT-PCR
CYP79-QRT2	GGAGACACAGAAGGAGTAGAG	qRT-PCR
SPI1-fwd5	GGTCAGCCTGGATTTGTGCC	qRT-PCR
SPI1-rev5	AACGTCGAGAGACCCAGCAT	qRT-PCR

9.3 Supplemental Material Manuscript III

Biosynthesis of 8-*O*-Methylated Benzoxazinoid Defense Compounds in Maize°
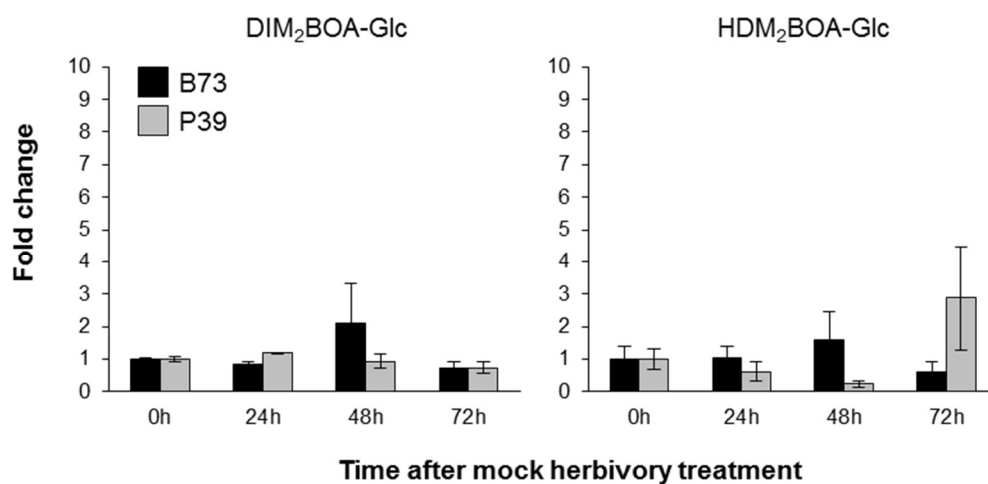
Supplemental Figure 0. Herbivory-induced changes in HDM$_2$BOA-Glc and DIM$_2$BOA-Glc are restricted to the wound site. Induction of DIM$_2$BOA-Glc and HDM$_2$BOA-Glc in the systemic parts of leaves of the lines B73 and P39 at different time points is shown. Herbivory was mimicked by wounding and application of *Spodoptera exigua* regurgitant on one side of the midrib of a maize leaf. Systemic induction was measured on the other side of the midrib. Fold changes are expressed compared to non-elicited controls. No significant induction was detected for the different genotypes at the different time points (Two-way ANOVAs, *P* > 0.05)

Supplemental Figure 1. LC-MS/MS fragmentation patterns of DIMBOA-Glc and TRIMBOA-Glc. (A) LC-MS/MS chromatogram of DIMBOA-Glc eluting at 9.4 min under conditions described in the methods section. Prominent fragments are marked with *F1 – F4*. (B) LC-MS/MS chromatogram of the BX13 DIMBOA-Glc oxidation product, TRIMBOA-Glc, at 4.2 min. The structure of the product was confirmed by NMR. Fragments related to *F1 – F4* are indicated.
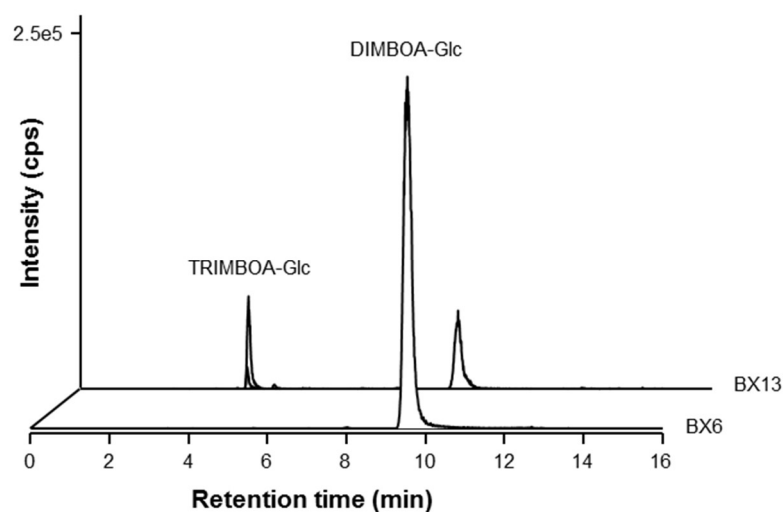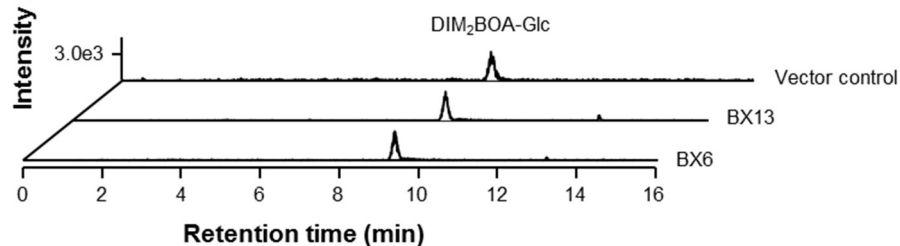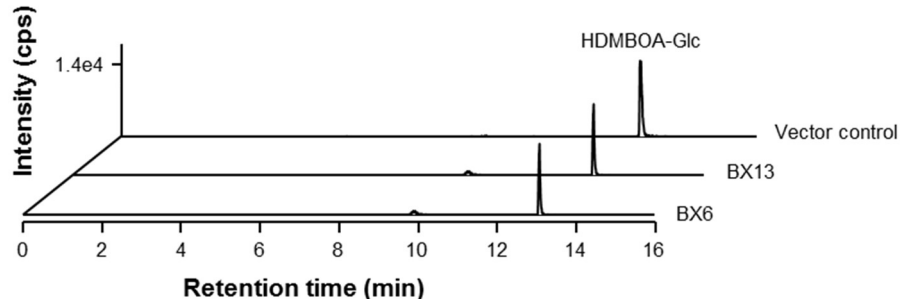
Supplemental Figure 2. Substrate specificity of the 2-oxoglutarate-dependent dioxygenases BX6 and BX13. Activity assays of purified enzymes were incubated with (A) DIMBOA-Glc, (B) DIM$_2$BOA-Glc, and (C) HDMBOA-Glc in the presence of the cofactors Fe(II), and 2-oxoglutarate. The intensities of the specific LC-MS/MS transitions are shown. Assays were repeated at least three times.

```
Bx13-P39    ATGGCTCCGACCGCCGCCAAGGACAGTGGCTCCGCCGACCGCTGGCGCGA
Bx13-Oh43   TTGGCTCCGACCACCGCCAAGGACAGTGGCTCCGCCGATCGATGGCGCGA

Bx13-P39    GGTGCAGGCGTTCGAGGACAGCAAGCTGGGTGTGAAGGGCCTGGTCGACT
Bx13-Oh43   GGTGCAGGCGTTCGAGGACAGCAAGCTGGGTGTGAAGGGCCTGGTCGACT

Bx13-P39    CCGGCGTCAAGTCCATCCCGGCCATGTTCCACCACCCGCCGGAGTCCCTC
Bx13-Oh43   CCGGCGTCAAGTCCATCCCGGCCATGTTCCACCACCCGCCGGAGTCCCTC

Bx13-P39    AAGGATGTCATTTCTCCACCAGCTCTGCCCTCCTCCGACGATGCGCCGGC
Bx13-Oh43   AAGGATGTCATTTCTCCACCAGCTCTGCCCTCCTCCGACGATGCGCCGGC

Bx13-P39    CATCCCAGTGGTGGACCTGTCGGTCGCGCGGCGCGAGGATCTGGTGGCCC
Bx13-Oh43   CATCCCAGTGGTGGACCTGTCCGTGGCGCGGCGCGAGGATCTGGTGGCCC

Bx13-P39    AGGTGAAGCACGCGGCCGGGACGGTGGGCTTCTTCTGGGTGGTGAACCAC
Bx13-Oh43   AGGTGAAGCACGCGGCCGGGACGGTGGGCTTCTTCTGGGTGGTGAACCAC

Bx13-P39    GGCGTGCCGGAGGAGCTGATGGCCAGCATGCTCAGCGGGGTGCGCCAGTT
Bx13-Oh43   GGCGTGCCGGAGGAGCTGATGGCCAGCATGCTCAGCGGGGTGCGCCAGTT

Bx13-P39    CAACGAGGGCTCTCTGGAGGCCAAGCAGGCGCTCTACTCACGGGACCCCG
Bx13-Oh43   CAACGAGGGCTCTCTGGAGGCCAAGCAGGCGCTCTACTCACGGGACCCTG

Bx13-P39    CTCG---------CAACGTGCGCTTCGCTTCCAACTTCGACCTCTTCGAG
Bx13-Oh43   CTCGGAGTGCTCGCAACGTGCGCTTCGCTTCCAACTTCGACCTCTTCGAG

Bx13-P39    TCCGCGGCGGCCGACTGGCGCGACACGCTCTACTGCAAGATTGCGCCGGA
Bx13-Oh43   TCCGCGGCGGCCGACTGGCGCGACACGCTCTACTGCAAGATTGCGCCGGA

Bx13-P39    TCCGGCGCCGCGGGAGCTCGTGCCGGAGCCTCTCCGGAACGTGATGATGG
Bx13-Oh43   TCCGGCGCCGCGGGAGCTCGTGCCGGAGCCTCTCCGGAACGTGATGATGG

Bx13-P39    AATACGGCGAGGAACTGACGAAGCTGGCGCGGTCCATGTTCGAGCTGCTG
Bx13-Oh43   AATACGGCGAGGAACTGACGAAGCTGGCGCGGTCCATGTTCGAGCTGCTG

Bx13-P39    TCGGAGTCCCTCGGCATGCCCAGCGACCACCTGCACAAGATGGAGTGCAT
Bx13-Oh43   TCGGAGTCCCTCGGCATGCCCAGCGACCACCTGCACAAGATGGAGTGCAT

Bx13-P39    GCAGCAGCTCCACATCGTGTGCCAGTACTACCCGCCATGCCCGGAGCCGC
Bx13-Oh43   GCAGCAGCTCCACATCGTGTGCCAGTACTACCCGCCATGCCCGGAGCCGC

Bx13-P39    ACCTCACCATGGGCGTCAGGAAGCACTCGGACACTGGTTTCTTCACCATC
Bx13-Oh43   ACCTCACCATGGGCGTCAGGAAGCACTCGGACACCGGTTTCTTCACCATC

Bx13-P39    CTCCTGCAGGACGGCATGGGCGGCCTGCAGGTGCTAGTCGATCGCGGAGG
Bx13-Oh43   CTCCTGCAGGACGGCATGGGCGGCCTGCAGGTGCTAGTTGATCGCGGAGG

Bx13-P39    CGGCCGCCAGACGTGGGTGGACGTCACTCCCCGACCTGGGGCACTCATGG
Bx13-Oh43   CGGCCGCCAGACGTGGGTGGACGTCACTCCCCGACCTGGGGCACTCATGG

Bx13-P39    TCAACATGGGCAGCTTTCTTCAGCTTGTGACGAATGACCGGTACAAGAGC
Bx13-Oh43   TCAACATGGGCAGCTTTCTTCAGCTTGTGACGAATGACCGGTACAAGAGC

Bx13-P39    GTGGATCACCGGGTGCCGGCTAACAAGAGCAGTGACACGGCGAGGGTCTC
Bx13-Oh43   GTGGATCACCGGGTGCCGGCTAACAAGAGCAGTGACACGGCGAGGGTCTC

Bx13-P39    GGTAGCTGCCTTCTTCAACCCCGACGAGAAGAGAACCGAGAGGCTGTATG
Bx13-Oh43   GGTAGCTGCCTTCTTCAACCCCGACGAGAAGAGAACCGAGAGGCTGTATG

Bx13-P39    GCCCAATTCCAGACCCCAGCAAGCCTCCGCTGTACAGGAGCGTCACGTTC
Bx13-Oh43   GCCCCATTCCAGACCCCAGCAAGCCTCCGCTGTACAGGAGCGTCACGTTC

Bx13-P39    CCGGACTTCATCGCCAAGTTCAACAGCATCGGACTGGACGGTCGCGTGCT
Bx13-Oh43   CCGGACTTCATCGCCAAGTTCAACAGCATCGGACTGGACGGCCGCGTGCT

Bx13-P39    CGACCACTTCCGGTTGGAGGACGACGGCCCTACTCCTCTTGCTGCTCCTG
Bx13-Oh43   CGACCACTTCCGGTTGGAGGACGACGGCCCTACTCGTCTTGCTGCTGCTG

Bx13-P39    CACACCACGTCTAG
Bx13-Oh43   CACACCACGTCTAG
```

Supplemental Figure 3. Nucleic acid alignment of *Bx13*-P39 and *Bx13*-Oh43.
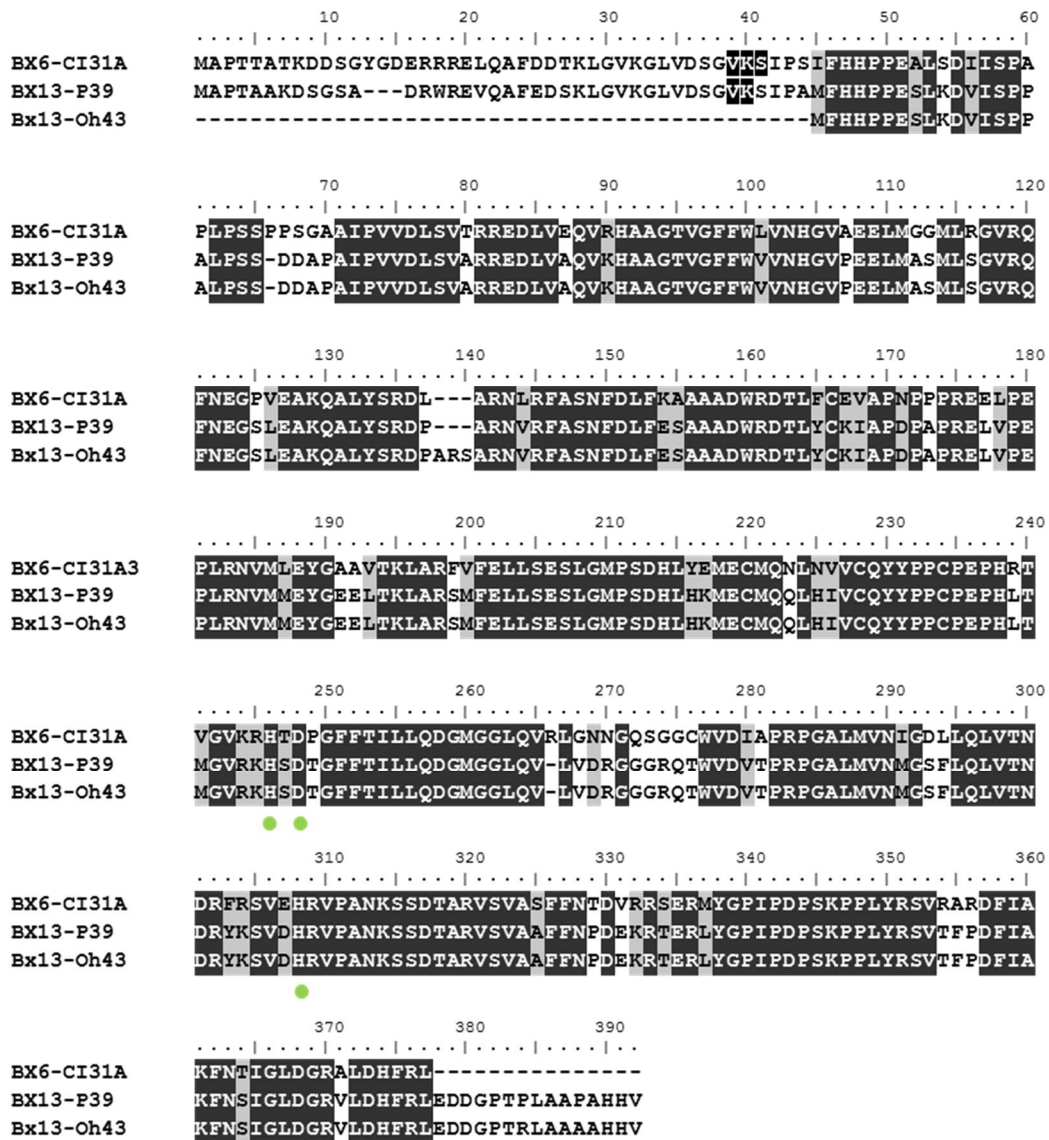
Supplemental Figure 4. Amino acid alignment of 2-oxoglutarate-dependent dioxygenases. Alignment of BX6-CI31A, BX13-P39 and BX13-Oh43. Identical amino acid are colored in black and similar amino acids in grey. Conserved residues of the active center are marker by green dots.

A

Bx13 translation start site

```
B73   CAAGCTAGCAATTGAAAAAAAAAACAGGCAAGGAAAATGGCTCCGACCGCCGCCAAGGAC
W22   CAAGCTAGCAATTGAAAAAAAAAACAGGCAAGGAAAATGGCTCCGACCGCCGCCAAGGAC
Oh43  CAAGCTAGCAATTGAAAAAAAA-------------TTGGCTCCGACCACCGCCAAGGAC
LH38  CAAGCTAGCAATTGAAAAAAAA-------------TTGGCTCCGACCACCGCCAAGGAC
LH39  CAAGCTAGCAATTGAAAAAAAA-------------TTGGCTCCGACCACCGCCAAGGAC
```

B

Maize inbred line	BXD content in untreated leaves, µg g_{FW}^{-1} (Mean ± s.e.)			
	DIMBOA-Glc	HDMBOA-Glc	DIM_2BOA-Glc	HDM_2BOA-Glc
B73	1971.7 ± 618.3	321.2 ± 81.0	37.7 ± 4.7	6.3 ± 1.8
Oh43	2041.8 ± 518.1	231.7 ± 42.4	n.d.	n.d.
LH38	249.5 ± 5.8	88.1 ± 0.1	n.d.	n.d.
LH39	285.5 ± 1.3	40.9 ± 0.01	n.d.	n.d.

Supplemental Figure 5. Some *Bx13* alleles contain a mutated start codon. (A) Alignment of chromosomal DNA sequences in the area of the *Bx13* translation start site, showing mutation of the start codon from ATG to TTG in maize inbred lines Oh43, LH38, and LH39. (B) Benzoxazinoid concentrations of untreated maize leaves of 10 day-old inbred lines different in the *Bx13* translation start site (n ≥ 3).
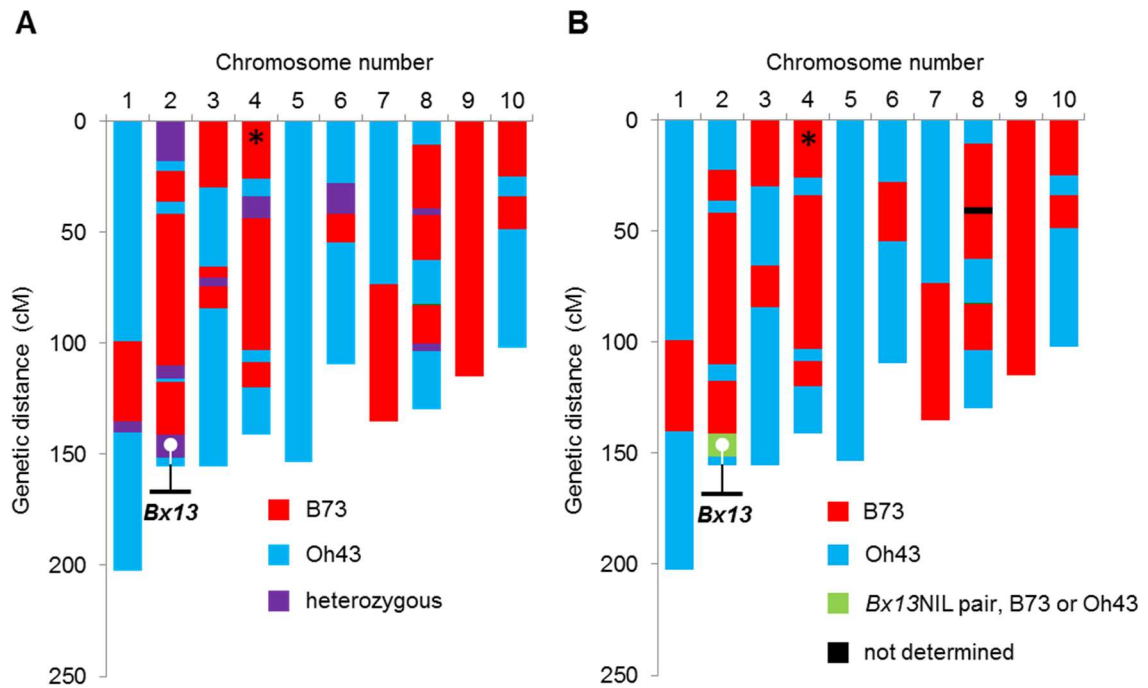
Supplemental Figure 6. Generation of *Bx13* near isogenic lines for the *Bx13* locus on chromosome 2. (A) Genotype of recombinant inbred line Z022E0081, as downloaded from www.panzea.org. Plants used to generate NILs were selfed for two generations after the original genotyping and were homozygous for the originally heterozygous (purple color) segments on chromosomes 1, 3, 6, and the lower segment on chromosome 8. The area of heterozygosity containing *Bx13* is indicated with an white dot. (B) Genotype of near-isogenic lines with the B73 or the Oh43 genotype at the *Bx13* locus. An asterisk (*) represents the approximate location of other benzoxazinoid biosynthesis genes on the short arm of chromosome 4 (*Bx6*, 1.1 Mbp; *Bx3*, 3.0 Mbp; *Bx4/Bx5*, 3.1 Mbp; *Bx8*, 3.2 Mbp; *Bx1/Bx2*, 3.3 Mbp; *Bx7*, 18.2 Mbp).
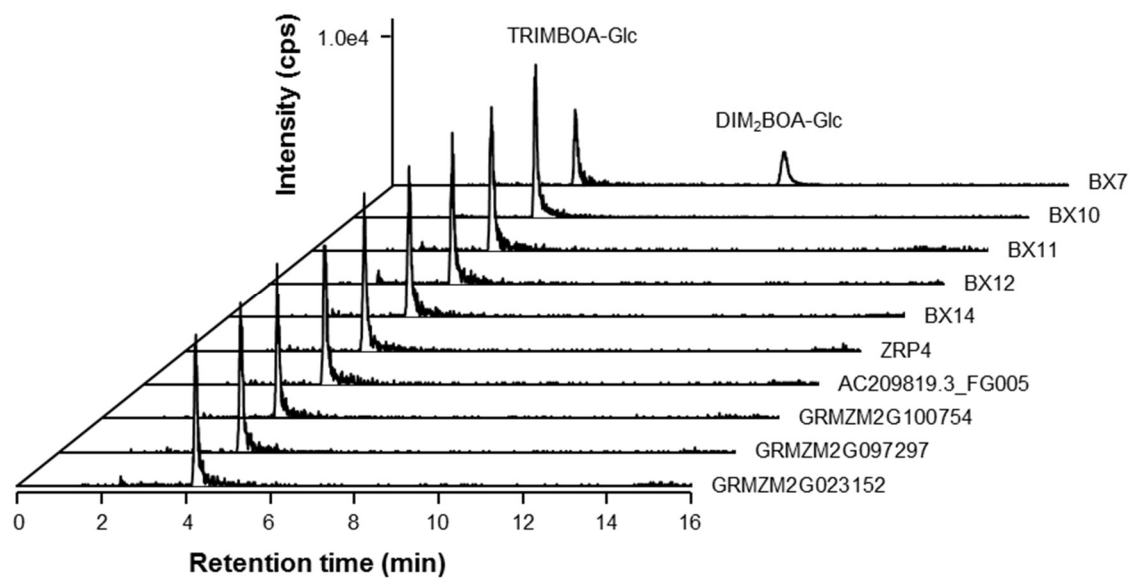
Supplemental Figure 7. Enzymatic activity of *O*-methyltransferases similar to BX7 towards TRIMBOA-Glc. The intensities of the specific LC-MS/MS transitions are shown. Assays were repeated at least three times.
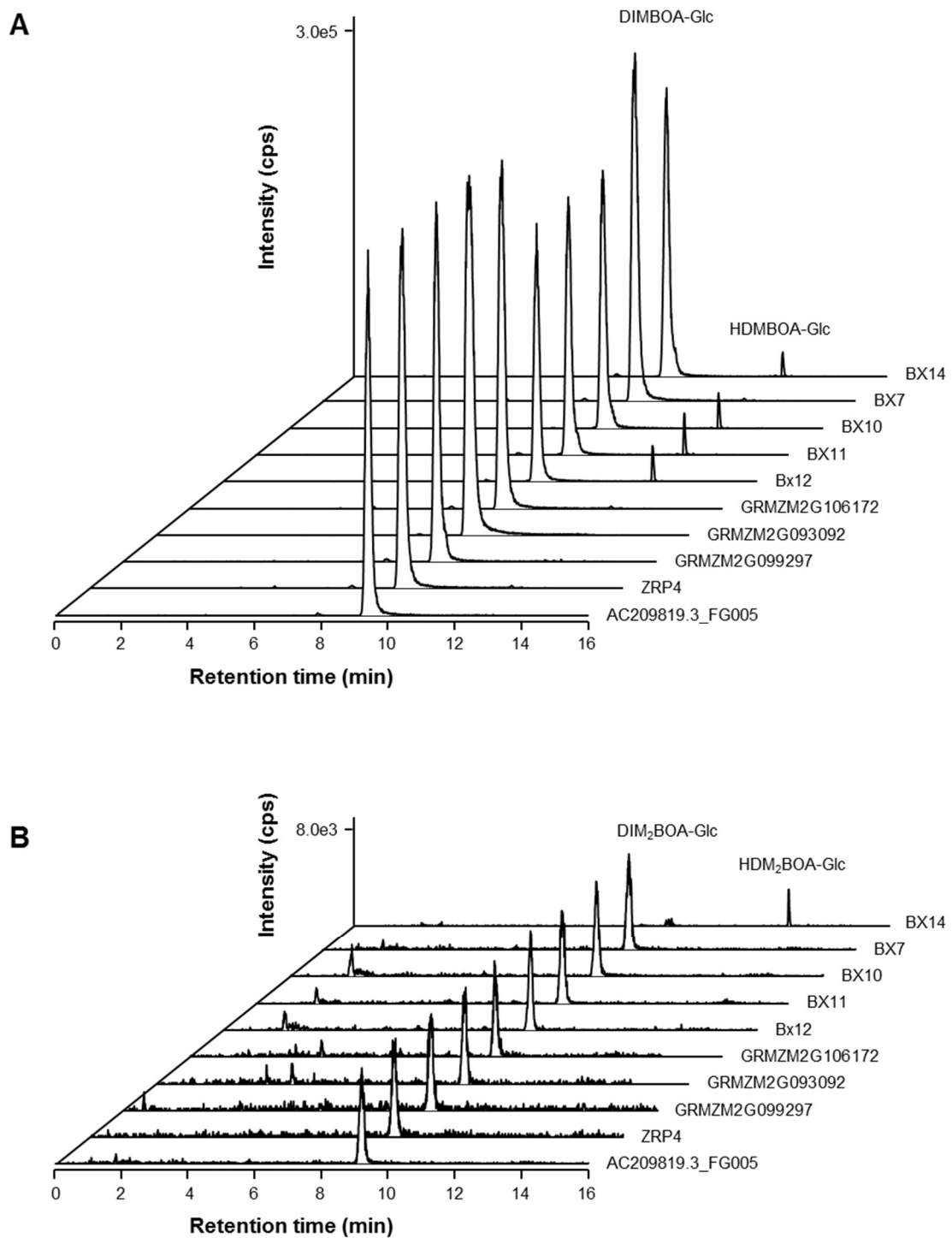
Supplemental Figure 8. Enzymatic activity of *O*-methyltransferases similar to BX7 towards DIMBOA-Glc and DIM$_2$BOA-Glc. Activity assays of purified enzymes incubated with (A) DIMBOA-Glc and (B) DIM$_2$BOA-Glc and the co-factor *S*-adenosyl-L-methionine. The intensities of the specific LC-MS/MS transitions are shown. Assays were repeated at least three times.

```
ZmBx14-B73     ATGGCACTCATGCAGGAGAGCAGCCAGGACTTGCTCGAAGCGCACGACGAGCTCTTCCAC
ZmBx14-Il14H   ATGGCACTCATGCAGGAGAGCAGCCAGGACTTGCTCGAAGCGCACGACGAGCTCTTCCAC

ZmBx14-B73     CACTGCCTGTGCTTCGCCAAATCGCTCGCGCTCGCCGTGGCGCAGGACCTCCGCATCCCC
ZmBx14-Il14H   CACTGCCTGTGCTTCGCCAAATCGCTCGCGCTCGCCGTGGCGCAGGACCTCCGCATCCCC

ZmBx14-B73     GACGCGATCCACCACCACGGAGGCGGCGCCACCCTCCACCAGATCCTCGCCGAGGCCGCG
ZmBx14-Il14H   GACGCGATCCACCACCACGGAGGCGGCGCCACCCTCCCCCAGATCCTCGCCGAGACCGCG

ZmBx14-B73     CTCCACCCAAGCAAGCTTCGCGCCCTACGCCGCCTGATGCGCGTGCTCACCGTCTCGGGC
ZmBx14-Il14H   CTCCACCCAAGCAAGCTTCGCGCCCTACGCCGCCTGATGCGCGTGCTCACCGTCTCGGGC

ZmBx14-B73     GTCTTCACCGTCCAGTA----------------------------------TTCTTCAACC
ZmBx14-Il14H   GTCTTCACCGTCCAGCAGGAGCAATCACCAGACGGTGGTGGTGGTGCTGATTCTTCAACC

ZmBx14-B73     GTCGACGCGTCGGACGGAGCTGATGTCGTCTACAGGCTGACGGCAGCCTCCCGCTTCCTC
ZmBx14-Il14H   GTCGACGCGTCGGACGGAGCTGATGTCGTCTACAGGCTGACGGCAGCCTCCCGCTTCCTC

ZmBx14-B73     GTCAGCGATAGCGACGAGGCGGGCACGGCGTCCTTGGCTCCCTTTGCGAACCTGGCGCTC
ZmBx14-Il14H   GTCAGCGATAACGACGAGGCGAGCACGGCGTCCTTGGCTCCCTTTGCGAGGCTGGCGCTC

ZmBx14-B73     CACCCTATCGCCATCTCCCCGCACGCCGTGGGCATCTGCGCGTGGTTCCGGCAGGAGCAG
ZmBx14-Il14H   CACCCTATCGCCATCTCCCCGCACGCCGTGGGCATCTGCGCGTGGTTCCGGCAGGAGCAG

ZmBx14-B73     CACGACCCGTCCCCGTACGGCCTGGCGTTCCGCCAGATCCCGACCATCTGGGAGCATGCT
ZmBx14-Il14H   CACGACCCGTCCCCGTACGGTCTGGCGTTCCGCCAGATCCCGACCATCTGGGAGCACGCT

ZmBx14-B73     GACAACGTAAACGCCCTACTGAACAAAGGCTTGCTCGCGGAAAGCCGCTTCTTGATGCCA
ZmBx14-Il14H   GACAACGTAAACGCCCTACTGAACAAAGGCTTGCTCGCGGAAAGCCGCTTCTTGATGCCA

ZmBx14-B73     ATCGTACTCAGGGAGTGCGGAGACGAGGTGTTCCGTGGGATCGACTCGTTGGTCGACGTC
ZmBx14-Il14H   ATCGTACTCAGGGAGTGCGGAGACGAGGTGTTCCGTGGGATCGACTCGTTGGTCGACGTC

ZmBx14-B73     GGCGGTGGGCACGGTGGCGCCGCCGCCACCATCGCCGCCGCATTCCCGCACGTCAAGTGC
ZmBx14-Il14H   GGCGGTGGGCACGGNGGCGCCGCCGCCACCATCGCCGCCGCATTCCCGCACGTCAAGTGC

ZmBx14-B73     AGCGTGCTTGACCTCCCGCACGTTGTCGCCGGTGCTCCATCCGATGCCTGCGTGCAGTTC
ZmBx14-Il14H   AGCGTGCTTGACCTCCCGCACGTTGTCGCCGGTGCTCCATCCGATGCCGGCGTGCACTTC

ZmBx14-B73     GTTGCGGGCAATATGTTCCACAGTATTCCACCTGCAACCGCCGTTTTCTTCAAGACAACT
ZmBx14-Il14H   GTTGCGGGCAATATGTTCCACAGTATTCCACCTGCAACCGCCGTTTTCTTCAAGACAACT

ZmBx14-B73     CTATGTGACTGGGGTGACGACGAGTGCATCAAGATATTGAAGAATTGCAAGCAAGCCATA
ZmBx14-Il14H   CTATGTGACTGGGGTGACGACGAGTGCATCAAGATATTGAAGAATTGCAAGCAAGCCATA

ZmBx14-B73     TCTCCACGGGATGAGGGTGGGAAGGTGATAATCATGGACGTGGTAGTCGGGTATGGGCAG
ZmBx14-Il14H   TCTCCACGGGACGCGGGTGGGAAGGTGATAATCATGGACGTGGTAGTCGGGCATGGGCAG

ZmBx14-B73     TCAAACATGAAGCGCCTAGAGACACAAGTTATGTTTGATTTGGTTATGATGGCGGTCAAT
ZmBx14-Il14H   TCAAACATGAAGCGCCTAGAGACACAAGTTATGTTTGATTTGGTTATGATGGCGGTCAAT

ZmBx14-B73     GGAGTCGAGCGCGACGAGCAAGAGTGGAAGGAGATGTTCATTGAAGCTGGATTCAAAGAC
ZmBx14-Il14H   GGAGTCGAGCGCGACGAGCAAGAGTGGAAGGAGATGTTCATTGAAGCTGGATTCAAAGAC

ZmBx14-B73     TACAAAATCCGACCAGTAGCTGGCCTCATGTCGGTCATCGAGGTCTATCCATGA
ZmBx14-Il14H   TACAAAATCCGACCAGTAGCTGGCCTCATGTCGGTCATCGAGGTCTATCCATGA
```

Supplemental Figure 9. Nucleic acid alignment of *Bx14*-B73 and *Bx14*-Il14H.
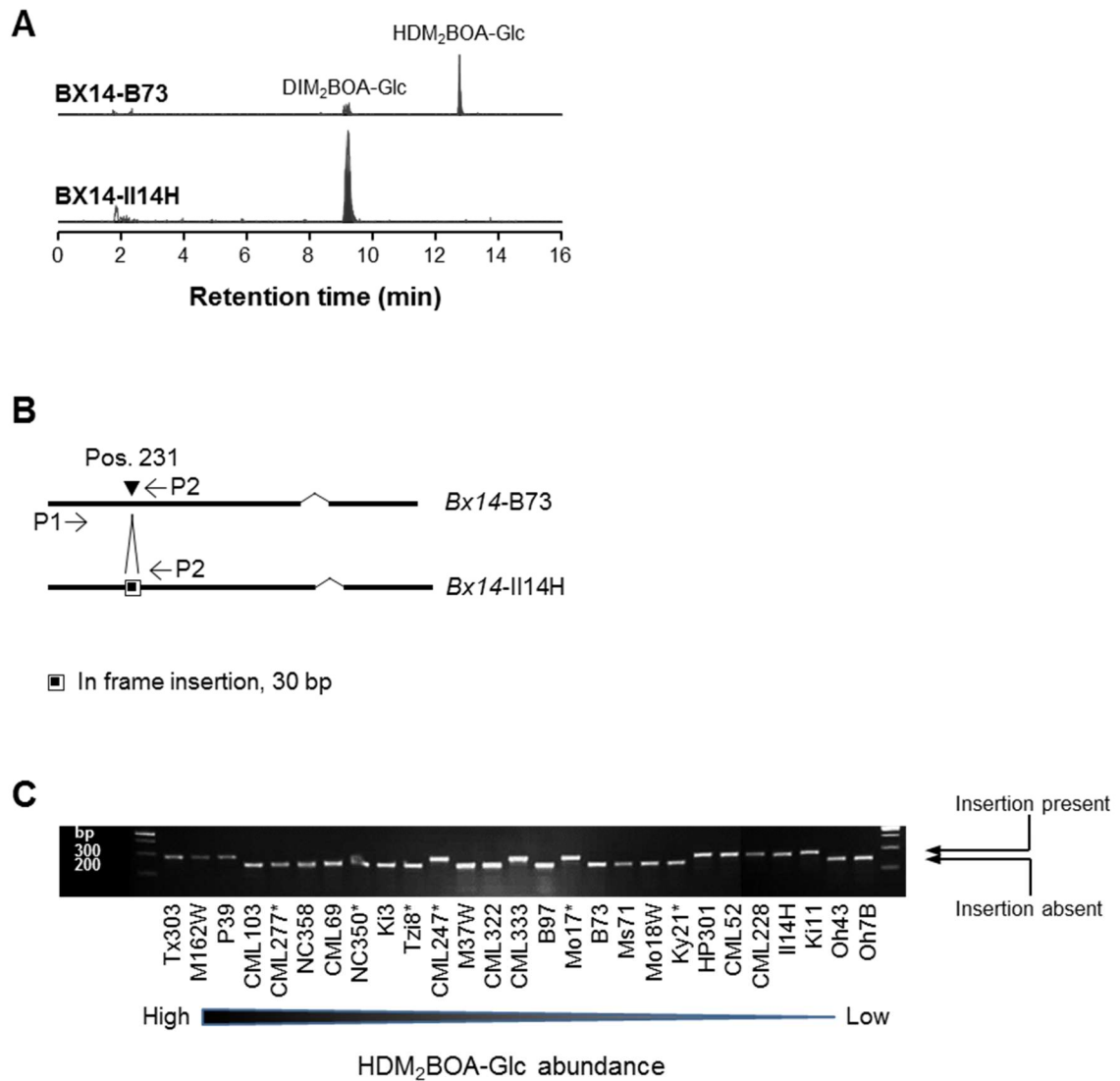
Supplemental Figure 10. *In vitro a*ctivity of *Bx14*-Il14H and the presence/absence of an 30 bp-in frame insertion in *Bx14* within the NAM population. (A) Activity assays of purified recombinant enzymes incubated with the respective substrate and the co-substrate *S*-adenosyl-L-methionine. The relative intensities of the specific LC-MS/MS transitions are shown. (B) Genomic structure of *Bx14*-B73 and *Bx14*-Il14H with an 30 bp-in frame insertion in the Il14H allele. (C) Presence/absence of the 30 bp in-frame insertion within the NAM line population. Lines are sorted according to HDM$_2$BOA-Glc concentrations in leaves from high to low abundance.
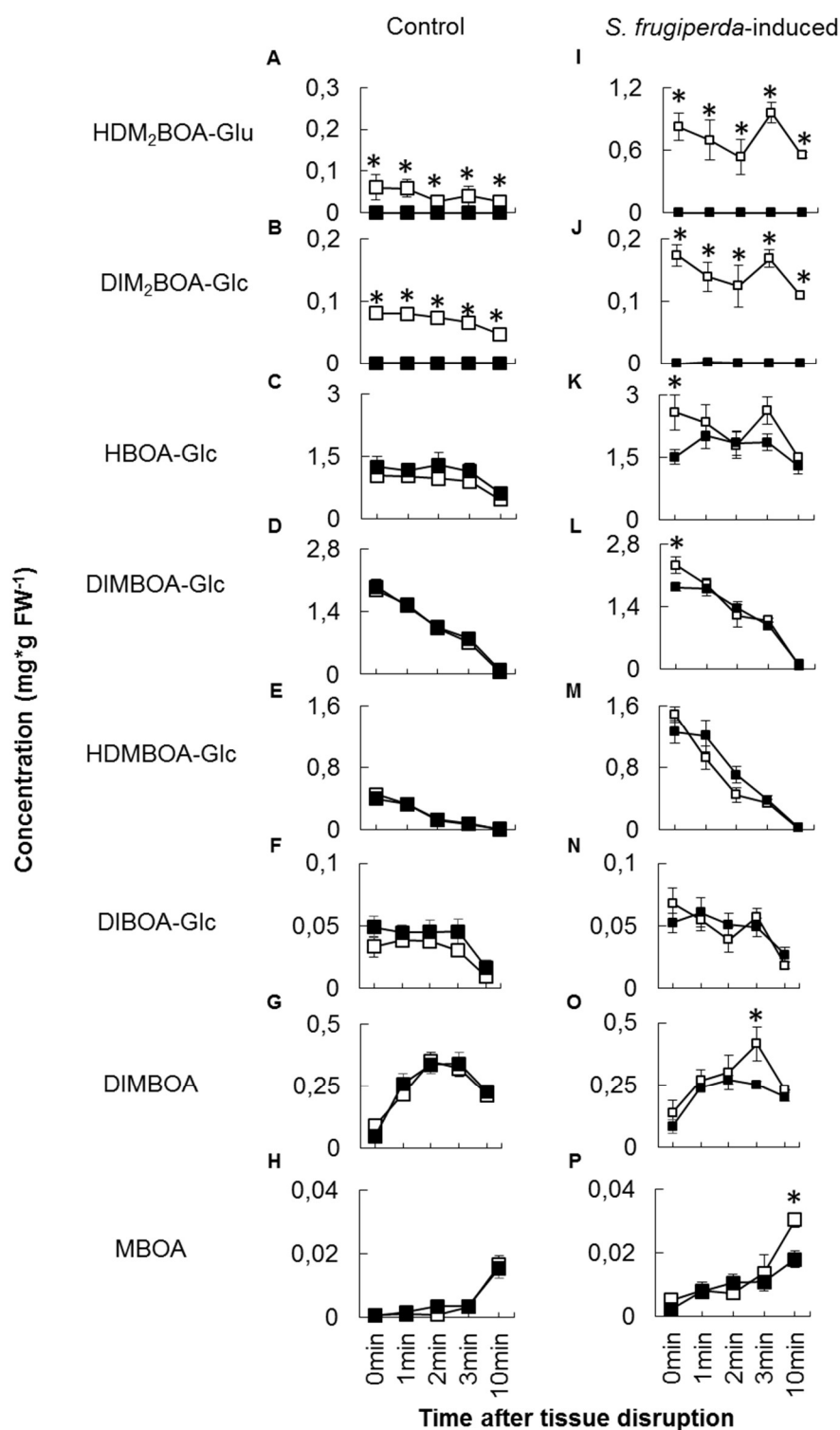
Supplemental Figure 11. Effect of BX13 on benzoxazinoid accumulation and hydrolysis. Accumulation and deglycosylation of constitutive (A-G) and induced (I-N) benzoxazinoids 0-10 min after mechanical tissue disruption. Stars indicate significant differences between genotypes within time points (Holm-Sidak post-hoc tests, $P < 0.05$). Two-way repeated ANOVAs did not show any differences between genotypes apart from HDM_2BOA-Glc and DIM_2BOA-Glc (Supplemental table 6). n = 4.
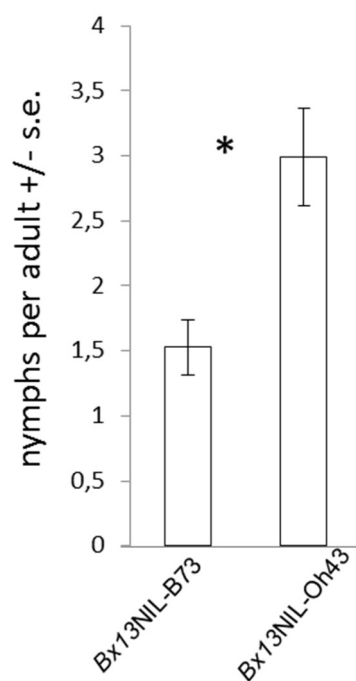
Supplemental Figure 12. BX13 decreases aphid performance (2nd independent experiment). The number of nymphs per adult on the *Bx13* mutant (*Bx13*NIL-Oh43) and its near-isogenic wild type line (*Bx13*NIL-B73) is shown (n = 36). The asterisk indicates a significant differences between genotypes ($P < 0.01$, Student's *t*-test).

```
Bx6-optimized
ATG GCG CCC ACA ACG GCC ACG AAA GAT GAT AGC GGT TAT GGC GAT
GAA CGT CGG CGC GAG CTT CAA GCT TTC GAC GAC ACC AAA CTG GGC
GTG AAA GGA CTG GTC GAT AGT GGT GTG AAA AGC ATT CCT AGT ATC
TTT CAC CAT CCT CCG GAA GCG TTG TCG GAC ATC ATC AGT CCG GCA
CCG TTA CCA AGC AGT CCG CCG TCT GGC GCT GCC ATT CCG GTG GTG
GAT CTG TCC GTT ACT CGC CGC GAA GAT TTA GTC GAA CAG GTA CGC
CAT GCA GCC GGT ACC GTG GGT TTC TTC TGG TTG GTC AAC CAT GGT
GTT GCC GAA GAG TTA ATG GGC GGC ATG TTG CGC GGT GTA CGC CAG
TTT AAC GAA GGG CCA GTT GAG GCA AAA CAG GCG CTG TAT TCC CGT
GAT CTG GCG CGT AAC CTT CGG TTT GCG TCG AAT TTC GAC CTG TTT
AAA GCC GCA GCT GCG GAT TGG CGC GAT ACC CTG TTT TGC GAG GTA
GCG CCG AAT CCA CCG CCT CGC GAG GAA TTA CCC GAA CCT TTG CGC
AAT GTG ATG CTG GAA TAT GGT GCA GCG GTT ACC AAG CTG GCC CGT
TTT GTC TTT GAA CTG CTG TCA GAA AGC CTG GGT ATG CCG AGC GAC
CAC CTC TAC GAG ATG GAG TGC ATG CAG AAC CTC AAT GTG GTT TGC
CAG TAC TAT CCG CCA TGT CCG GAA CCG CAT CGT ACG GTG GGC GTT
AAA CGC CAT ACG GAT CCA GGG TTC TTC ACC ATT CTG CTG CAG GAT
GGC ATG GGT GGC CTC CAA GTC CGT CTG GGC AAC AAT GGG CAA AGC
GGC GGT TGT TGG GTG GAT ATT GCA CCC CGT CCT GGG GCT CTG ATG
GTA AAT ATC GGA GAC TTA CTC CAG CTT GTC ACC AAT GAT CGC TTT
CGC TCC GTG GAA CAC CGT GTT CCG GCT AAC AAG AGC TCT GAC ACT
GCG CGC GTT TCG GTC GCG TCA TTC TTT AAC ACA GAT GTA CGC CGC
TCA GAA CGG ATG TAC GGA CCA ATT CCG GAT CCG TCG AAA CCG CCC
CTG TAT CGC TCT GTG CGT GCC CGT GAC TTC ATC GCG AAG TTT AAC
ACC ATT GGC CTG GAT GGC CGT GCC CTT GAC CAC TTT CGT CTG TAA

Bx7-optimized
ATG GGT CAT CAA GCC CAG CAT GGT ACG GAT GAC ACC GAA GAA CTG
TTG GCT GCG CAT CGT CAG CTT TGG TGT CAT GCC TTG GGA TAT GTG
AAA AGC ATG GCT CTG AAA TGC GCA CTG GAT CTG CGC ATT CCG GAC
ACC ATT GAT CGC TGT GGT GGC AGT GCG ACG TTA GGC GAA TTG CTG
GCA GCA AGC GAA ATT TCC GCG TCC AAC CAC GAT TAT CTT CGC CGT
GTT ATG CGG ACC TTA ACT GCC ATG CGG ATT TTC GCA GCC AGT CAT
GAT CCT GCC AAA GCT GAT GAT GCC GCC GCG ATT TCG TAC CAG CTC
ACC CCA GCG TCA CGT TTG CTG GTG AGC AGC TCC TCT AGC GTG GAT
GAT GCG GCC GGA GCA TCG AAA GAG AAC ACC ACA ACC CCG TCC ATT
CTG CCC AAT ATC GCG CAC CTG GTA CGC CCG AAC ACC ATT TCT CTG
CTG TTT TCG ATG GGC GAG TGG ATG AAA GAC GAA AGT GCA GCC TCT
GTT AGT CTG TAT GAG ACA GTC CAT CGT CAG GGT ATG TGG GCG TGT
GTG GAA GAT GAT GCG GCG AAT CGC GCT TCA TTC TAC GAA AGC ATG
GAC GCG GAT ACT CGC TTA GTC ATG CAA GCG GTT GTC CGT CGT TGC
CCT CAC GTG TTC GAC GGG ATT AAG AGC CTG GTT GAC GTA GGT GGA
GGT CGT GGT ACC GCT GCA GCC GCC GTT GTT GCG GCG TTT CCC CAT
ATC CAG CGC TGC ACG GTA ATG GAT CTT CCG CAT GTG GTA GCG GAA
GCA CCG GCT GGG ACT GCT GGC CTG TCT TTT CAT GGC GGG GAT ATG
TTT GAA CAC ATC CCA TCG GCG GAT GCT CTG ATG CTG AAA TGG ATC
CTC CAT GAT TGG GAT GAG GAT AAA TGC ATC AAG ATC ATG GAA CGC
TGC AAA GAA GCC ATT GGC GGT AAA GAA GCC GGC GGC AAA GTC ATC
ATC ATC GAC ACA GTC CTC GGG TCA CGC GCG GAT GAT GAC GAC GAC
GAC AAA ACG TGT CGT GAA ACG TAT GTG CTG GAT CTC CAC ATT CTG
AGC TTC GTG AAT GGC GCA GAA CGT GAG GAG CAC GAA TGG CGC CGC
ATT TTC TTA GCA GCG GGC TTT CGC GAC TAC AAG ATT ACG CAC ACC
CGC GGT ATT CCG TCA ATC ATT GAG GTG TTT CCG TAA
```

Supplemental Figure 13. Codon-optimized gene sequences of *Bx6*-CI31A and Bx7-CI31A for expression in *Escherichia coli*.

Supplemental Table 1. Concentrations of DIM$_2$BOA-Glc in undamaged controls and *Spodoptera exigua*-treated maize leaf samples.

Maize inbred line	Control	S. exigua	t Statistic	Prob>|t|	DF
	µg g$_{FW}^{-1}$, Mean ± s.e.	µg g$_{FW}^{-1}$, Mean ± s.e.			
P39	596.6 ± 174.1	633.8 ± 213.9	-0.135	0.896	8
M37W	515.7 ± 167.6	615.1 ± 192.9	-0.389	0.717	4
M162W	360.5 ± 66.5	600.2 ± 52.2	-2.824	<u>0.030</u>	6
Ki3	323.8 ± 34.8	212.3 ± 34.2	2.268	<u>0.050</u>	9
Tx303	270.6 ± 38.5	268.7 ± 59.9	0.027	0.979	10
B96	258.0 ± 66.0	628.6 ± 93.1	-3.247	<u>0.018</u>	6
CML103	243.3 ± 124.5	67.6 ± 21.7	1.390	0.214	6
Tzi8	235.8 ± 42.2	147.9 ± 52.0	1.245	0.253	7
CML247	209.3 ± 96.6	62.2 ± 12.4	1.511	0.181	6
Il14H	203.0 ± 79.6	90.1 ± 71.7	1.040	0.339	6
Mo18W	196.8 ± 70.3	128.2 ± 26.8	0.825	0.436	7
Mo17	189.9 ± 104.7	352.5 ± 31.8	-1.485	0.188	6
Ki11	174.1 ± 45.7	90.6 ± 33.0	1.480	0.189	6
CML228	172.0 ± 95.9	127.9 ± 44.3	0.449	0.667	7
CML333	171.3 ± 36.9	194.6 ± 93.0	-0.278	0.790	6
Oh7B	156.5 ± 101.5	236.6 ± 33.1	-0.712	0.497	8
CML52	153.9 ± 38.6	186.8 ± 27.7	0.397	0.705	6
MS71[a]	151.2 ± 51.8	125.1 ± 40.4	---	---	---
NC350[a]	84.3 ± 27.7	27.5 ± 5.2	---	---	---
CML69	84.0 ± 40.8	87.6 ± 34.3	-0.060	0.954	6
NC358	75.9 ± 23.3	148.1 ± 28.1	-1.871	0.120	5
HP301	56.1 ± 8.5	57.0 ± 32.6	-0.032	0.975	7
CML322	47.1 ± 14.7	7.3 ± 2.4	3.016	<u>0.019</u>	7
B73	37.7 ± 4.7	30.2 ± 4.0	1.219	0.262	7
Ky21	32.1 ± 6.8	29.4 ± 4.4	0.337	0.748	6
CML227	17.6 ± 7.2	1.9 ± 0.9	1.671	0.156	5
Oh43	n.d.	n.d.	---	---	---

[a] No statistics available due to low number of replicates for the *S. exigua* treatment.

Underlined probabilities indicate that at the 0.05 level, the difference of the population means is significantly different from zero.

Supplemental Table 2. Concentrations of HDM$_2$BOA-Glc in undamaged controls and *Spodoptera exigua*-treated maize leaf samples.

Maize inbred line	Control μg g$_{FW}$$^{-1}$, Mean ± s.e.	S. exigua μg g$_{FW}$$^{-1}$, Mean ± s.e.	t Statistic	Prob>|t|	DF
M162W	34.7 ± 11.1	65.6 ± 11.1	-1.786	0.117	7
P39	34.4 ± 4.6	132.9 ± 63.8	-1.540	0.162	8
CML103	32.7 ± 17.1	34.1 ± 26.3	-0.045	0.965	6
Tx303	31.6 ± 25.5	9.4 ± 2.6	1.082	0.329	5
CML69	22.2 ± 7.8	24.1 ± 4.1	-0.216	0.836	6
NC350[a]	21.3 ± 3.5	74.6 ± 2.2	---	---	---
M37W	20.9 ± 2.7	20.5 ± 7.1	-1.030	0.361	4
CML227	18.7 ± 5.7	4.8 ± 1.7	2.429	0.045	7
NC358	16.8 ± 15.1	151.5 ± 43.2	-2.365	0.064	5
CML322	15.7 ± 8.2	16.5 ± 3.9	-0.701	0.506	7
CML247	14.4 ± 4.8	90.4 ± 22.9	-3.250	0.017	6
Tzi8	12.3 ± 7.0	67.7 ± 20.4	-3.287	0.013	7
CML333	11.8 ± 3.7	38.1 ± 22.9	-1.545	0.173	6
Ki3	11.3 ± 9.2	31.3 ± 7.9	-2.001	0.076	9
B97	10.0 ± 1.9	39.7 ± 19.4	-1.525	0.178	6
MS71[a]	9.0 ± 5.3	58.3 ± 6.2	---	---	---
Mo17	8.2 ± 4.0	21.3 ± 2.2	-3.010	0.020	7
B73	8.1 ± 1.2	16.9 ± 11.5	-0.616	0.555	8
Mo18W	5.5 ± 1.1	72.9 ± 39.3	-1.970	0.090	7
HP301	3.0 ± 1.1	49.0 ± 41.9	-1.264	0.247	7
Ky21	2.8 ± 1.4	22.9 ± 7.0	-2.365	0.050	7
CML52	1.1 ± 0.8	27.2 ± 11.8	-3.753	0.013	5
CML228	n.d.	n.d.	---	---	---
Il14H	n.d.	n.d.	---	---	---
Ki11	n.d.	n.d.	---	---	---
Oh43	n.d.	n.d.	---	---	---
Oh7B	n.d.	n.d.	---	---	---

[a] No statistics available due to low number of replicates for the *S. exigua* treatment.

Underlined probabilities indicate that at the 0.05 level, the difference of the population means is significantly different from zero.

Supplemental Table 3. Estimates of the additive allelic effect under the hypotheses H1, with the additive allelic effect, a, distinguishable from zero and the dominance deviation equal to zero. Values are listed for the benzoxazinoid biosynthesis QTLs *Bb1 – Bb3* obtained in the different mapping experiments described in the main text. In addition, broad-sense heritability values are given for B73 x Oh43 and B73 x Mo17 mapping populations. Heritability for the B73 x P39 population could not be estimated since we had not enough data to calculate environmental variation for this population. n.d., not determined.

Mapping	Estimate of the additive allelic effect (µg / g fresh weight) under H1 a(H1)			broad-sense heritability
	QTL *Bb1*	QTL *Bb2*	QTL *Bb3*	
Constitutive DIM$_2$BOA-Glc (B73 x P39, leaves)	-2.8	+11.5	+3.2	n.d.
Constitutive HDM$_2$BOA-Glc (B73 x P39, leaves)	-0.4	+0.4	---	n.d.
Constitutive DIM$_2$BOA-Glc (B73 x Oh43, leaves)	---	+0.4	---	0.78
Constitutive DIM$_2$BOA-Glc (B73 x Mo17, roots)	---	-0.1	---	0.65
Constitutive HDM$_2$BOA-Glc (B73 x Mo17, roots)	-0.3	-0.3	---	0.95
Induced HDM$_2$BOA-Glc (B73 x P39, leaves)	---	+1.2	---	n.d.

Supplemental Table 4 . Primers for open reading frame amplification of investigated genes.

Abbreviation	Targeted Gene (Accession No.)	Primer Sequence (5' → 3')
ORF amplification		
Bx6.fwd	*Bx6*-CI31A	CACCATGGCGCCCACAACGGCCACGAAAG
Bx6.rev		TTACAGACGAAAGTGGTCAAGGGCACGGC
Bx7.fwd	*Bx7*-CI31A	CACCATGGGTCATCAAGCCCAGCATGGTACG
Bx7.rev		TTACGGAAACACCTCAATG
Bx10.fwd	*Bx10*-B73	CACCATGGCCCTCATGCAGGAGAGTAG
Bx10.rev		TCAAGGATAGACCTCGATGATGA
Bx11.fwd	*Bx11*-B73	CACCATGGCACTCATCATGCAGGAGAGT
Bx11.rev		TCAAGGATAGACCTCGATGATGAC
Bx12.fwd	*Bx12*-CML322	CACCATGGCACTCATGCAAGAGAGCAG
Bx12.rev		TCAAGGATAGACCTCGATGATGA
Zrp4.fwd	*Zrp4*-P39	CACCATGGAGCTCAGCCCCAACAAC
Zrp4.rev		TTATGGATAGACCTCGATTATAG
Bx13.fwd	AC148152.3_FG005	CACCATGGCTCCGACCGCCGCCAAGGA
Bx13.rev		CTAGACGTGGTGTGCAGGAGCAGC
Bx13.short.fwd	AC148152.3_FG005	CACCATGTTCCACCACCCGCCGGAG
Bx13.short.rev		CTAGACGTGGTGTGCAGGAGCAGC
Bx13+UTR.fwd	AC148152.3_FG005	TCGATGAGCTAGGTCGTCATTAATTC
Bx13+UTR.rev		AAGAGACGACGACGAGAACTG
Bx14.fwd	GRMZM2G127418	CACCATGGCACTCATGCAGGAGAGCAG
Bx14.rev		TGATGGATAGACCTCGATGACCG
Zrp4-like.fwd	AC209819.3_FG005	CACCATGGCACTCGCCGGCATCACCAAC
Zrp4-like-rev		TCAAGGGTACACCTCGATGATG
Bx14.llike-1.fwd	GRMZM2G093092	CACCATGGCACTCAGCACTCAGGACTT
Bx14.like-1.rev		TCATGGATAGACCTCGATGACTTAG
Bx14.like-2.fwd	GRMZM2G106172	CACCATGGCATTCACAGAGGAGAGTAG
Bx14.like-2.rev		TTATGGATAGACCTCGATGACTG
Bx14.like-3.fwd	GRMZM2G099297	CACCATGGCGTTGCTCGGCGAGTAC
Bx14.like-3.rev		TTAATTAGGATAGAGCTCGATGAT
unkwnOmt1.fwd	GRMZM2G100754	CACCATGGCGCTCAGCAAGGAGCAA
unkwnOmt1.rev		CTATGGGCAGACTTCAATTATGG
unkwnOmt2.fwd	GRMZM2G097297	CACCATGGCGCTCAGCAAGGAGCAA
unkwnOmt2.rev		CTATGGGCAGACTTCAATTATGG
unkwnOmt3.fwd	GRMZM2G023152	CACCATGCGGCGGCATATGGC
unkwnOmt3.rev		CTATAGGCAGATTTCAATTATGG
unkwnOmt4.fwd	GRMZM2G102863	CACCATGGCGCCCGCCAACGTGCAAC
unkwnOmt4.rev		TCATGGGTAGACCTCGATTAT
unkwnOmt5.fwd	GRMZM2G141026	CACCATGGCGCCCGCCAAAG
unkwnOmt5.rev		CTACGGGTAGACCTCTATG

Supplemental Table 5. ^{1}H- and ^{13}C NMR data of TRIMBOA-Glc (700.45 MHz for ^{1}H and 176.13 MHz for ^{13}C, MeOH-d_4)

Position	δ_H, mult, J (Hz)	$\delta_C{}^1$
2	5.96, s	98.1
3		157.1
5	6.96, d, 8.9	109.1
6	6.63, d, 8.9	110.9
7		148.9
8		138.1
9		136.3
10		122.7
1'	4.71, d, 7.9	104.3
2'	3.20, dd, 8.8, 7.9	74.7
3'	3.36, overlap	77.9
4'	3.24, dd, 9.2, 9.2	71.1
5'	3.34, overlap	78.2
6'a	3.85, dd, 12.0, 2.0	62.7
6'b	3.64, dd, 12.0, 6.1	
8-OCH$_3$	3.90, s	61.4

$^{1)}$ ^{13}C NMR chemical shifts from HSQC and HMBC.

Supplemental Table 6. *P*-values of two-way repeated measures analyses of variance (ANOVA) to test for genotype and genotype*time effects in the BX13 NILs in the experiment shown in Supplementary Figure 11.

Metabolite	Factor	Control	*S. frugiperda*
HDM$_2$BOA-Glu	Genotype	**0.019**	**<0.001**
	Time	0.079	0.118
	Time*Genotype	0.813	0.119
DIM$_2$BOA-Glc	Genotype	**<0.001**	**<0.001**
	Time	**0.017**	0.112
	Time*Genotype	0.251	0.104
HBOA-Glc	Genotype	0.323	0.218
	Time	**<0.001**	**0.004**
	Time*Genotype	0.858	0.24
DIMBOA-Glc	Genotype	0.758	0.316
	Time	**<0.001**	**<0.001**
	Time*Genotype	0.799	0.361
HDMBOA-Glc	Genotype	0.627	0.49
	Time	**<0.001**	**<0.001**
	Time*Genotype	0.904	0.325
DIBOA-Glc	Genotype	0.273	0.976
	Time	**<0.001**	**<0.001**
	Time*Genotype	0.444	0.161
DIMBOA	Genotype	0.93	0.131
	Time	**<0.001**	**<0.001**
	Time*Genotype	0.472	0.335
MBOA	Genotype	0.841	0.149
	Time	**<0.001**	**<0.001**
	Time*Genotype	0.915	0.185

Supplemental Table 7. qRT-PCR Primers used to determine expression levels of *Bx7*, *Bx13,* and *Bx14* and primers for the detection of SNP markers.

Abbreviation	Targeted Gene (Accession No.)	Primer Sequence (5' → 3')
qRT-PCR		
qPCR.Bx7-fwd	Bx7	TCGACCGCTGCGGCGGGAGC
qPCR.Bx7-rev		ATGCTCTCGTAGAAGCTGGCCCT
qPCR.Bx13-fwd	Bx13	CATCGTGTGCCAGTACTACC
qPCR.Bx13-rev		ACCGGTCATTCGTCACAAGC
qPCR.Bx14-fwd	Bx14	AACTGCAGGAAGGCCATCCC
qPCR.Bx14-rev		TGACTCTGTAGTCGGTGAAC
Bx14-insert.fwd	Bx14	TAGACGACATCAGCTCCGTCCG
Bx14-insert.rev		TCCACCACTGCCTGTGCTTC
Primer for SNP detection	**SNP marker / SNP coordinate**	
PZA02081.1-fwd	PZA02081.1 Chr2: 5,925,823	ATGAGAGTTTGCGTCTTCATC
PZA02081.1´-rev		ATGAATTCCCACTCCCTTATC
zfl2.9-fwd	zfl2.9 Chr2: 12,644,166	GTGTGCGTACCTTGGTAGGGG
zfl2.9-rev		CTTCCACACCGGGAGCACATT
PZB00772.7-fwd	PZB00772.7 Chr2: 211,400,204	AGCAATGCTTCTGCTTGTACT
PZB00772.7-rev		CTCCTCCTCTCGTACTCCATT
PZB02179.1-fwd	PZB02179.1 Chr3: 158,890,320	TCTTCACTAACTACCGGATGC
PZB02179.1-rev		AGGAACACTCCCTAGGATAGC
PZA02385.6-fwd	PZA02385.6 Chr4: 15,299,213	TCATGCAGCTACAGATGGGCG
PZA02385.6-rev		CCGGGGTGGTACGATGTGATG
PHM1978.111-fwd	PHM1978.111 Chr8: 21,824,853	CATGGCACTAGACTTTCATCC
PHM1978.111-rev		GGCAAAAGATGTCAGGTAAGA
PHM934.19-fwd	PHM934.19 Chr8: 118,191,641	CGAGTGGACATCCAAAGTATC
PHM934.19-rev		ATTCCTTACTGCTGGAAACCT
PZA00904.1-fwd	PZA00904.1 Chr8: 167,092,992	TGTGCACACTTCAGCATAGTT
PZA00904.1-rev		AGCATATAAGGCCATGTTCAG

Supplemental Table 8. Annotation of benzoxazinoid derivatives by t_R and their fragmentation patterns.

Benzoaxozinoid derivate	t_R (min)	[M-H]⁻ (m/z_{obs})	Fragments (m/z) (intensity (%))[a]
DIMBOA-Glc (Standard)	9.1	372.2	164.0 (100), 194.1 (42), 191.8 (24), 210.1 (18), 372.2 (49)
TRIMBOA-Glc (Enzymatic product)[b]	4.3	387.9	152.2 (16), 165.1 (22), 168.2 (11), 180.1 (80), 192.2 (7), 207.6 (100), 222.0 (32), 225.7 (5), 341.9 (34), 369.9 (17), 387.9 (25)
DIM₂BOA-Glc (Std.)	8.5	402.2	164.2 (5), 179.1 (53), 194.4 (100), 222 (12), 240 (19), 356.3 (28), 402.2 (27)
DIM₂BOA-Glc (Enz. product)	8.5	402.6	179.4 (8), 194.1 (100), 356.4 (100), 402.6 (5)
HDMBOA-Glc (Std.)	12.7	385.8	112.6 (25), 164.4 (19), 183.2 (19), 194.1 (12), 223.4 (100), 318.1 (19), 385.8 (44)
HDMBOA-Glc (Enz. product)	12.7	386.2	112.9 (29), 183.1 (18), 194.1 (43), 224.1 (27), 386.2 (100)
HDM₂BOA-Glc (Std.)	12.5	462.2 [M+FA-H]⁻	163.5 (21), 176.0 (61), 193.1 (100), 210.5 (19), 224.5 (28), 260.4 (30), 277.1 (21), 361.5 (41), 416.3 (7)
HDM₂BOA-Glc (Enz. product)	12.5	461.9 [M+FA-H]⁻	163.2 (100), 175.9 (56), 193.5 (87.5), 210.5 (19), 260.4 (38), 277.3 (24), 361.5 (38)

Supplemental Table 9. LC-MS/MS settings used for the analysis of benzoxazinoids.

Turbospray ion source settings (operated in negative ionization mode)

Ion spray voltage:	-4500 eV
Turbo gas temp:	500°C
Nebulizing gas:	260 psi
Curtain gas:	5 psi
Heating gas:	60 psi
Collision gas:	5 psi

Mass analyzer settings

Benzoaxozinoid derivate	MRM Transition (m/z)	CE (V)[a]	DP (V)[b]	EP (V)[c]	CXP (V)[d]
TRIMBOA-Glc	388.0 [M-H]⁻ > 207.0	-20	-30	-4	-3
DIMBOA-Glc	418.0 [M+FA-H]⁻ > 372.0	-18	-22	-4	-5
DIM$_2$BOA-Glc	448.0 [M+FA-H]⁻ > 402.0	-16	-22	-4	-4
HDMBOA-Glc	432.0 [M+FA-H]⁻ > 356.0	-20	-30	-4	-3
HDM$_2$BOA-Glc	462.0 [M+FA-H]⁻ > 194.0	-25	-30	-4	-4

[a] Collision energy

[b] Declustering potential

[c] Entrance potential

[d] Collision cell exit potential

Both Q1 and Q3 quadrupoles were maintained at unit resolution.

Analyst 1.5 software (Applied Biosystems) was used for data acquisition and processing.

Supplemental Table 10. List of RILs used for mapping in this study.

B73 x P39		B73 x Oh43				B73 x Mo17	
Z024E0001	Z024E0105	Z006E0001	Z006E0050	Z006E0103	Z006E0155	MO001	MO229
Z024E0004	Z024E0108	Z006E0004	Z006E0053	Z006E0105	Z006E0156	MO005	MO235
Z024E0010	Z024E0112	Z006E0005	Z006E0055	Z006E0107	Z006E0157	MO008	MO248
Z024E0013	Z024E0115	Z006E0006	Z006E0056	Z006E0108	Z006E0158	MO010	MO256
Z024E0014	Z024E0117	Z006E0009	Z006E0057	Z006E0109	Z006E0159	MO014	MO262
Z024E0016	Z024E0119	Z006E0010	Z006E0058	Z006E0110	Z006E0160	MO019	MO263
Z024E0019	Z024E0120	Z006E0011	Z006E0060	Z006E0111	Z006E0161	MO021	MO265
Z024E0020	Z024E0122	Z006E0012	Z006E0061	Z006E0112	Z006E0162	MO022	MO266
Z024E0021	Z024E0123	Z006E0013	Z006E0062	Z006E0113	Z006E0164	MO027	MO268
Z024E0022	Z024E0124	Z006E0014	Z006E0063	Z006E0114	Z006E0165	MO028	MO269
Z024E0024	Z024E0126	Z006E0015	Z006E0064	Z006E0115	Z006E0166	MO030	MO272
Z024E0025	Z024E0127	Z006E0016	Z006E0065	Z006E0116	Z006E0167	MO036	MO274
Z024E0027	Z024E0128	Z006E0017	Z006E0068	Z006E0117	Z006E0168	MO038	MO276
Z024E0030	Z024E0129	Z006E0018	Z006E0069	Z006E0119	Z006E0169	MO042	MO277
Z024E0033	Z024E0130	Z006E0019	Z006E0070	Z006E0120	Z006E0170	MO055	MO286
Z024E0039	Z024E0132	Z006E0020	Z006E0071	Z006E0121	Z006E0171	MO057	MO292
Z024E0041	Z024E0133	Z006E0021	Z006E0072	Z006E0122	Z006E0172	MO058	MO297
Z024E0042	Z024E0135	Z006E0022	Z006E0073	Z006E0123	Z006E0173	MO060	MO305
Z024E0045	Z024E0136	Z006E0023	Z006E0075	Z006E0124	Z006E0174	MO074	MO308
Z024E0047	Z024E0137	Z006E0024	Z006E0076	Z006E0125	Z006E0177	MO075	MO309
Z024E0048	Z024E0138	Z006E0025	Z006E0077	Z006E0126	Z006E0179	MO088	MO311
Z024E0049	Z024E0141	Z006E0026	Z006E0079	Z006E0127	Z006E0180	MO093	MO315
Z024E0051	Z024E0142	Z006E0027	Z006E0080	Z006E0130	Z006E0181	MO098	MO321
Z024E0054	Z024E0146	Z006E0028	Z006E0081	Z006E0131	Z006E0182	MO106	MO322
Z024E0060	Z024E0147	Z006E0029	Z006E0082	Z006E0133	Z006E0183	MO116	MO328
Z024E0062	Z024E0148	Z006E0031	Z006E0083	Z006E0134	Z006E0184	MO123	MO335
Z024E0063	Z024E0151	Z006E0032	Z006E0084	Z006E0135	Z006E0185	MO136	MO341
Z024E0071	Z024E0152	Z006E0033	Z006E0085	Z006E0136	Z006E0187	MO141	MO351
Z024E0076	Z024E0153	Z006E0034	Z006E0086	Z006E0137	Z006E0189	MO151	MO352
Z024E0079	Z024E0157	Z006E0035	Z006E0087	Z006E0140	Z006E0190	MO154	MO354
Z024E0080	Z024E0158	Z006E0036	Z006E0088	Z006E0141	Z006E0191	MO162	MO356
Z024E0083	Z024E0161	Z006E0037	Z006E0089	Z006E0142	Z006E0192	MO169	MO357
Z024E0085	Z024E0163	Z006E0038	Z006E0090	Z006E0143	Z006E0193	MO172	MO360
Z024E0088	Z024E0167	Z006E0039	Z006E0091	Z006E0144	Z006E0194	MO181	MO361
Z024E0089	Z024E0168	Z006E0040	Z006E0092	Z006E0145	Z006E0196	MO185	MO368
Z024E0091	Z024E0172	Z006E0042	Z006E0094	Z006E0146	Z006E0197	MO188	MO369
Z024E0095	Z024E0178	Z006E0043	Z006E0095	Z006E0147	Z006E0198	MO190	MO373
Z024E0096	Z024E0180	Z006E0044	Z006E0096	Z006E0148	Z006E0200	MO192	MO378
Z024E0097	Z024E0184	Z006E0045	Z006E0097	Z006E0149		MO214	MO379
Z024E0098	Z024E0188	Z006E0046	Z006E0099	Z006E0150		MO218	MO383
Z024E0099	Z024E0200	Z006E0047	Z006E0100	Z006E0151		MO219	
Z024E0102		Z006E0048	Z006E0101	Z006E0152		MO225	
Z024E0104		Z006E0049	Z006E0102	Z006E0153		MO228	

11 Curriculum Vitae

Personal

Last Name	**Handrick**
First Name	**Vinzenz**
Place of Birth	**Bautzen, Germany**
Date of Birth	**November 10, 1985**
Address	**John Innes Centre**
	Cell and Developmental Biology
	Norwich Research Park, Colney Ln, Norwich NR4 7UH, UK
E-mail	**vinzenz.handrick@jic.ac.uk**
Citizenship	**German**

Education & Qualifications

Dec. 2011 – Dec. 2016	Max Planck Institute for Chemical Ecology, Department of Biochemistry, Jena, Germany	**Doctoral student** THESIS TITLE *"Biosynthesis and biological relevance of herbivore-induced nitrogenous defense compounds in Maize"*
April 2011 – July 2011	Copenhagen University, Faculty of Life Science, Centre for Synthetic Biology	**Scholar**, supported by a Leonardo Da Vinci Mobility Grand
Jan. 2010 – Nov. 2010	Leibniz Institute of Plant Biochemistry, Department of Secondary Metabolism, Halle (Saale), Germany	**Diploma thesis** THESIS TITLE *"Biochemical characterization of pollen walls of Arabidopsis thaliana"* GRADE 1.3
Oct. 2005 – Nov. 2010	Martin-Luther-University Halle-Wittenberg, Halle (Saale), Germany	**Diplom in Biochemistry** GRADE 1.6
Aug. 1998 – June 2004	Sorbisches Gymnasium, Bautzen, Germany	**Abitur** GRADE 1.8

Publications

| 2016

1 Handrick, V.°, Robert, C. A. M.°, Ahern, K. R., Zhou, S., Machado, R. A. R., Maag, D., Glauser, G., Fernandez-Penny, F. E., Chandran, J. N., Rodgers-Melnik, E., Schneider, B., Buckler, E. S., Boland, W., Gershenzon, J., Jander, G., Erb, M., Köllner T. G. (2016). Biosynthesis of 8-*O*-methylated benzoxazinoid defense compounds in maize. **Plant Cell**, 28(7):1682-700. doi: 10.1105/tpc.16.00065.

| 2015

1 Irmisch, S., Zeltner, P., Handrick, V., Gershenzon, J., Köllner, T. G. (2015). The maize cytochrome P450 CYP79A61 produces phenylacetaldoxime and indole-3-acetaldoxime in heterologous systems and might contribute to plant defense and auxin formation. **BMC Plant Biology**, 15: 128. doi:10.1186/s12870-015-0526-1.

| 2013

1 Meihls, L. N.°, Handrick, V.°, Glauser, G., Barbier, H., Kaur, H., Haribal, M., Lipka, A., Gershenzon, J., Buckler, E., Erb, M., Köllner, T. G., Jander, G. (2013). Natural variation in maize aphid resistance is associated with 2,4-dihydroxy-7-methoxy-1,4-benzoxazin-3-one glucoside methyltransferase activity. **The Plant Cell**, 25: 2341-2355. doi:10.1105/tpc.113.112409.

| 2012

1 Balcke, G.°, Handrick, V.°, Bergau, N., Fichtner, M., Henning, A., Stellmach, H., Tissier, A., Hause, B., Frolov, A. (2012). An UPLC-MS/MS method for highly sensitive high-throughput analysis of phytohormones in plant tissues. **Plant Methods**, 8: 47. doi:10.1186/1746-4811-8-47.

2 Fellenberg, C., van Ohlen, M., Handrick, V., Vogt, T. (2012). The role of CCoAOMT1 and COMT1 in Arabidopsis anthers. **Planta**, 236: 51-61. doi:10.1007/s00425-011-1586-6.

3 Fellenberg, C., Ziegler, J., Handrick, V., Vogt, T. (2012). Polyamine homeostasis in wild type and phenolamide deficient *Arabidopsis thaliana* stamens. **Frontiers Plant Science**, 3: 180. doi:10.3389/fpls.2012.00180.

| 2010

1 Handrick, V., Vogt, T., Frolov, A. (2010). Profiling of hydroxycinnamic acid amides in *Arabidopsis thaliana* pollen by tandem mass spectrometry. **Analytical and Bioanalytical Chemistry**, 398: 2789-2801. doi:10.1007/s00216-010-4129-2.

° Authors contributed equally to this work and share first authorship

Oral Presentations

| 2015

1 Handrick V. (2015). Elucidation of the final steps of benzoxazinoid formation in maize. Talk presented at 57th Annual Maize Genetics Conference, St. Charles, Illinois, US

| 2014

1 Handrick V. (2014). Benzoxazinoids: Biosynthesis and function of major defense compounds in maize. Talk presented at SIP 15 - Symposium on Insect-Plant Interactions, University of Neuchâtel, Neuchâtel, CH

2 Handrick V. (2014). Benzoxazinoids: Biosynthesis and function of major defense compounds in maize. Talk presented at Banff Conference on Plant Metabolism, Alberta, CA

3 Handrick V. (2014). Tracking the benzoxazinoid pathway in maize. Talk presented at 13th IMPRS Symposium, MPI for Chemical Ecology, Dornburg, DE

| 2013

1 Handrick V. (2013). Biosynthesis of induced defense compounds in corn: Methylation of DIMBOA-Glc. Talk presented at 9th Plant Science Student Conference - PSSC 2013, Halle (Saale), DE

Poster Presentations

| 2015

1 Handrick V., Meihls L., Glauser G., Gershenzon J., Erb M., Jander G., Köllner T. (2015). Benzoxazinoids: Biosynthesis and function of major defense compounds in maize. Poster presented at 14th IMPRS Symposium, MPI for Chemical Ecology, Dornburg, DE

| 2014

1 Köllner T., Gershenzon J., Irmisch S., Handrick V., Günther J., Stödtler H.J. (2014). The metabolism and biological roles of nitrogenous defense compounds in trees and grasses. Poster presented at SAB Meeting 2014, MPI for Chemical Ecology, Jena, DE

| 2013

1 Handrick V., Meihls L., Gershenzon J., Jander G., Erb M., Köllner T. (2013). An O-Methyltransferase Activity Causes Variation in Maize Aphid Resistance. Poster presented at ICE Symposium, MPI for Chemical Ecology, Jena, DE

2 Handrick V. (2013). Induced defense compounds in corn: Methylation of DIMBOA-Glc. Poster presented at 12th IMPRS Symposium, MPI for Chemical Ecology, Jena, DE

3 Maag D., Erb M., Handrick V., Köllner T., Wolfender J.L., Turlings T., Glauser G. (2013). Local induction of chemical defences in maize: spatio-temporal aspects of benzoxazinone metabolism. Poster presented at NCCR Plant Survival Final Conference: "Plant Survival: a story of sex, violence and light", NCCR (National Centre of Competence in Research) Plant Survival, Université de Neuchâtel, CH
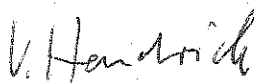
1 Handrick, V., Vogt, T., Frolov, A., (2010). LC-MS/MS based analysis of phenylpropane spermi-
dine conjugates in pollen of *Arabidopsis thaliana*. Poster presented at the 43th Annual Meeting
of the German Society for Mass Spectrometry.

Award

Student Travel Award (4th Banff Conference on Plant Metabolism 2014)
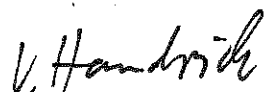
Norwich,   March 1, 2017

V. Handrich

(Vinzenz Handrick)

11 Eigenständigkeitserklärung

Hiermit erkläre ich, entsprechend der zur Zeit gültigen Promotionsordnung der Biologisch-Pharmazeutischen Fakultät der Friedrich-Schiller-Universität Jena, dass ich die vorliegende Promotionsarbeit selbstständig und nur unter Verwendung der angegebenen Hilfsmittel und Quellen angefertigt habe. Personen, die einen Beitrag zu dieser Arbeit geleistet haben, sind in Kapitel 2 aufgeführt bzw. in den Manuskripten und in der Danksagung erwähnt. Die Hilfe eines Promotionsberaters wurde nicht in Anspruch genommen, noch haben Dritte geldwerte Leistungen für Arbeiten im Zusammenhang mit der vorliegenden Dissertation erhalten. Zu keinem früheren Zeitpunkt wurde die vorgelegte Dissertationsarbeit, eine in wesentlichen Teilen ähnliche Arbeit oder eine andere Arbeit an der Friedrich-Schiller-Universität Jena oder einer anderen Hochschule eingereicht.

Norwich, den   1. März 2017

V. Handrick

(Vinzenz Handrick)